

THE SORPTION AND PERMEATION OF MOISTURE IN MOISTURE BARRIER POLYMER FILM COATINGS



A Ph.D Thesis

BY

Enosh Mwesigwa B. Pharm, MSc

**THE SCHOOL OF PHARMACY
UNIVERSITY OF LONDON**

MARCH 2006



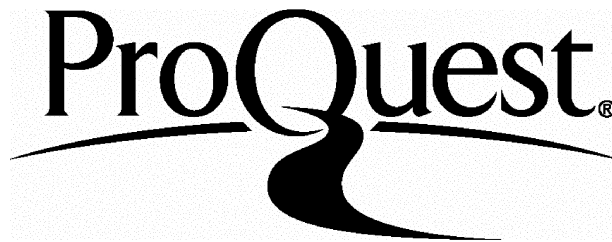
ProQuest Number: 10104806

All rights reserved

INFORMATION TO ALL USERS

The quality of this reproduction is dependent upon the quality of the copy submitted.

In the unlikely event that the author did not send a complete manuscript and there are missing pages, these will be noted. Also, if material had to be removed, a note will indicate the deletion.



ProQuest 10104806

Published by ProQuest LLC(2016). Copyright of the Dissertation is held by the Author.

All rights reserved.

This work is protected against unauthorized copying under Title 17, United States Code.
Microform Edition © ProQuest LLC.

ProQuest LLC
789 East Eisenhower Parkway
P.O. Box 1346
Ann Arbor, MI 48106-1346

DECLARATION AS TO ORIGINALITY OF THESIS

This thesis describes research conducted in the School of Pharmacy, University of London between 2002 and 2005 under the joint supervision of Professor Graham Buckton and Dr. Abdul W Basit. I certify that the research described is original and that any parts of the work that have been conducted by collaboration are clearly indicated. I also certify that I have written all the text herein and have clearly indicated by suitable citation any part of this thesis that has already appeared in publication.

Signed  Date: 12.06.06

“Those who judge us would do well to consider not where we have reached but how far we have come” Osagyefo Kwame Nkrumah (1902-1972)

ABSTRACT

Several moisture barrier coatings for use as barriers to moisture uptake into solid dosage forms of moisture-sensitive drug substances are commercially available. The aim of this study was to investigate the moisture sorption and permeation characteristics of four moisture barrier coatings, formulated from the following polymers, i.e., ethyl methacrylate copolymer (Eudragit L30 D-55®), aminobutyl methacrylate copolymer (Eudragit EPO®), poly(vinyl alcohol) (Opadry AMB®) and hypromellose system (Sepifilm LP 10®).

The gravimetric vapour sorption technique, utilising a dynamic vapour sorption apparatus (Surface Measurement Systems, UK), was the main method used to determine the extent of moisture sorption and desorption. Cast free films of the moisture barrier coatings, and uncoated and coated model tablet cores were investigated. The model tablet cores were designed to exhibit hygroscopic, non-hygroscopic or waxy characteristics. Additional tests with near-infrared spectroscopy, thermogravimetric analysis and dissolution testing were done to ascertain the hydration characteristics and/or the water-coating interactions.

Sepifilm LP and Opadry AMB films sorbed comparatively more moisture than the Eudragit L30 D-55 and Eudragit EPO films. Differences in hygroscopicity of the films were attributed to differences in the hydrophilicity of the constitutive polymers. Analysis of sorption-desorption kinetics showed that all the film samples exhibited non-Fickian kinetics. The calculated permeability coefficients for moisture in the films were of the order of 10^{-6} to 10^{-7} cm^3 [(STP) cm/cm^2 s cmHg]. Thus, the moisture barrier coatings were comparatively inferior to conventional barriers like high density polyethylene or polyvinylidene (cling film), with reported permeabilities of the order of 10^{-10} to 10^{-11} [(STP) cm/cm^2 s cmHg]. Application of the moisture barrier coatings onto the model tablet cores resulted in a net reduction in the extent of sorption over the uncoated cores only for the hygroscopic cores. Thus, there was no benefit of applying a moisture barrier coating to the waxy or non-hygroscopic tablet formulations. Results obtained from the stability profile of aspirin used as a model moisture-sensitive compound in the tablet cores confirmed this outcome. However, when the barrier coatings were applied onto the aspirin model cores, the coated samples exhibited higher degradation than the uncoated samples. No correlation between the degradation of aspirin in the cores and the permeability of the films was established.

As the moisture barrier coatings were not able to completely seal the tablet cores from moisture uptake, it was speculated the sorbed moisture decreased the adhesion of the coatings to the underlying cores. This facilitated the collection of water at the coating-core boundary, from where aspirin hydrolysis could have taken place. Therefore, if moisture barrier coatings are to protect moisture sensitive compounds in tablet cores, the ability to prevent hydrolysis at the coating-core boundary is deemed essential.

DEDICATION

In gracious memory of a much loved father and a much loved sister

ACKNOWLEDGEMENTS

I would like to sincerely thank my joint supervisors, Professor Graham Buckton and Dr. Abdul W Basit, for their help, counsel and constant support with this project. Without their keenness and enthusiasm, this project would have never materialised.

The help from the technical and secretarial staff of the Department of Pharmaceutics at The School of Pharmacy, University of London, in particular, Mr. Keith Barnes, is greatly acknowledged. I also wish to appreciate the assistance from Dr. Hardyal Gill with HPLC method development and assay.

My gratitude is also conveyed to the Registry staff (Margaret Stone and Sudershina Dave) at The School of Pharmacy for their helpfulness and willingness to listen.

My appreciation also goes to all the technical staff at Colorcon UK Ltd, Rohm Pharma (Darmstadt, Germany) and Seppic UK Ltd for help with samples and literature.

Thanks also to all my friends in Lab 342 and 343, and all the other friends in the Department of Pharmaceutics for their companionship.

This project would not have come to fruition without the financial assistance of the Commonwealth Scholarship Commission of the United Kingdom. I am for ever grateful to Her Majesty's Government for the continued commitment to the Commonwealth in general and the Scholarship scheme in particular. I would also like to pay special tribute to the wonderful people at the Association of Commonwealth Universities, and The British Council, Manchester, for taking care of me and my family so well during my stay in the UK.

The financial support from Makerere University is also acknowledged.

To my dear family, firstly my beloved father and mum who gave me all the guidance throughout my early years and encouraged me to pursue a science career. To my sisters and brother for being so loving and supportive throughout. Dad, though you are departed from me, I still cherish your great wisdom and insight. I know you would have loved every moment of this accomplishment.

Finally to my wonderful wife, Kate, for your support, understanding and much love, and my two boys Walter and Jerry, for being so understanding while I was away in "Yandan".

"It was the best of times; it was the worst of times"
Charles Dickens

TABLE OF CONTENTS

DECLARATION AS TO ORIGINALITY OF THESIS	1
ABSTRACT	3
DEDICATION	4
ACKNOWLEDGEMENTS.....	5
TABLE OF CONTENTS	6
LIST OF FIGURES.....	15
LIST OF TABLES.....	21
ABBREVIATIONS, CONSTANTS, FORMULAE AND NOMENCLATURE	23
CHAPTER ONE	30
1.0 GENERAL INTRODUCTION	30
1.1 BACKGROUND.....	30
1.2 ROLE OF WATER IN DRUG STABILITY	31
1.3 MOISTURE BARRIER COATINGS BROADLY DEFINED	32
1.4 FILM COATING OF DOSAGE FORMS	34
1.4.1 Introduction	34
1.4.2 Film Coating Materials.....	36
1.4.2.1 Polymers	36
1.4.2.1.1 Polymers used in conventional film coatings.....	36
1.4.2.1.2 Polymers used in delayed release film coatings.....	36
1.4.2.1.3 Polymers used in extended/sustained-release film coatings	36
1.4.2.2 Plasticizers	36
1.4.2.3 Miscellaneous additives.....	37
1.4.2.4 Solvents.....	37
1.5 PRINCIPLES OF PERMEATION IN POLYMERS.....	37
1.5.1 Introduction	37
1.5.2 Mechanisms of Permeation in Polymer Membranes.....	40
1.6 THE SOLUTION-DIFFUSION THEORY	40
1.6.1 Introduction	40
1.6.2 Sorption and Desorption in Polymers	42
1.6.2.1 Principles and Definitions	42
1.6.2.2 Sorption Isotherms	43
1.6.2.3 Sorption Theories	45
1.6.2.3.1 Langmuir's model	45
1.6.2.3.2 Brunauer, Emmet and Teller (BET) model	46

1.6.2.3.3	Guggenheim Anderson de Boer (GAB) model	47
1.6.2.3.4	Flory-Huggins model.....	47
1.6.2.3.5	Dual-Mode sorption model.....	48
1.6.2.3.6	Novel Theories	50
1.6.2.4	Typical Water-Polymer Equilibrium Sorption Characteristics....	50
1.6.3	Diffusion in Polymers	53
1.6.3.1	Definition	53
1.6.3.2	Theories of Diffusion in Polymers	53
1.6.3.3	Fickian Diffusion Analysis	54
1.6.3.3.1	Fick's First Law of Diffusion	55
1.6.3.3.2	Fick's Second Law of Diffusion	55
1.7	FACTORS AFFECTING PERMEATION IN POLYMERS	56
1.7.1	Introduction	56
1.7.2	Nature of the Membrane	56
1.7.2.1	Chemical Nature of the Polymer	57
1.7.2.2	Membrane Composition.....	58
1.7.2.3	Physical State of the Polymer	60
1.7.2.4	Membrane Thickness	60
1.7.3	Nature and State of the Penetrant.....	60
1.7.4	Environmental Conditions	61
1.7.4.1	Temperature.....	61
1.7.4.2	Pressure.....	62
1.7.4.3	Presence of Water in the Membrane	62
1.7.5	Summary.....	63
1.8	THESIS PHILOSOPHY	63
1.8.1	Problem Statement and Justification of this Study.....	63
1.8.2	Research Questions.....	65
1.8.3	Aims and Objectives	66
CHAPTER TWO.....		68
2.0	MOISTURE SORPTION/DESORPTION BY CAST POLYMER FILMS	68
2.1	INTRODUCTION	68
2.2	SPECIFIC OBJECTIVES	70
2.2	MATERIALS AND METHODS	70
2.2.1	Materials	70

2.2.1.1	Polymers for Preparing Coating Dispersions	70
2.2.1.1.1	Eudragit L30 D-55	71
2.2.1.1.2	Eudragit EPO	71
2.2.1.1.3	Shin-Etsu Aqoat.....	71
2.2.1.1.4	Opadry AMB Coating System	71
2.2.1.1.5	Sepifilm LP Coating System	72
2.2.1.1.6	Sureteric Coating System	72
2.2.1.2	Other coating formulation additives.....	72
2.2.1.2.1	Triethyl citrate	72
2.2.1.2.2	Carboxymethylcellulose sodium	73
2.2.1.2.3	Polyethylene glycol.....	73
2.2.1.2.4	Talc.....	73
2.2.1.2.5	Magnesium stearate	73
2.2.1.2.6	Stearic acid	74
2.2.1.2.7	Sodium lauryl sulphate	74
2.2.1.2.8	Titanium dioxide	74
2.2.2	Methods	75
2.2.2.1	Preparation of Coating Dispersions	75
2.2.2.1.1	Eudragit L 30 D-55	75
2.2.2.1.2	Eudragit EPO	76
2.2.2.1.3	Shin-Etsu Aqoat (Hypromellose acetate succinate)	77
2.2.2.1.4	Opadry AMB, Sepifilm LP and Sureteric	77
2.2.2.2	Preparation of Free Films	78
2.2.2.3	Scanning Electron Microscopy Studies.....	79
2.2.2.4	Gravimetric Moisture Sorption and Desorption Studies.....	79
2.2.2.4.1	Description of technique	79
2.2.2.4.2	Experimental procedure.....	81
2.2.2.5	Measurement of Moisture Vapour Transmission Rate	81
2.2.2.5.1	Description of the technique	81
2.2.2.5.2	Experimental procedure.....	83
2.2.2.6	Thermogravimetric Analysis.....	83
2.2.2.6.1	Description of technique	83
2.2.2.6.2	Experimental procedure.....	84
2.2.2.7	Near Infrared Spectroscopy	84

2.2.2.7.1	Description of technique	84
2.2.2.7.2	Experimental Procedure	85
2.4.	RESULTS	86
2.4.1	Film Appearance and Characteristics	86
2.4.2	Moisture Sorption-Desorption Profiles	88
2.4.3	Measurement of Moisture Vapour Transmission Rates	94
2.4.4	Thermogravimetric Analysis of Moisture in Films.....	100
2.4.5.	Near infrared spectroscopy studies	104
2.5.	DISCUSSION	112
2.5.1	Introduction	112
2.5.2	Moisture Sorption-Desorption Characteristics	112
2.5.3	Moisture Vapour Transmission Rates (MVTR)	119
2.5.4	Water-Polymer Interactions	121
2.6	CONCLUSIONS	124
2.6.1	Introduction	124
2.6.2	Effect of Film Type	124
2.6.3	Effect of RH and Temperature on Moisture Sorption	124
2.6.5	Moisture Vapour Transmission Rates.....	125
2.6.4	Nature of Water-Polymer Interactions	125
CHAPTER 3	127
3.0	MOISTURE PERMEATION IN CAST POLYMER FILMS.....	127
3.1	INTRODUCTION	127
3.1.1	Measurement of Sorption Isotherms.....	128
3.1.2	Methods for Measurement of Diffusion Coefficients	129
3.1.2.1	Permeation through a Membrane (Constant Volume)	130
3.1.2.2	Permeation through a Membrane (Constant Pressure).....	131
3.1.2.3	Gravimetric Sorption-Desorption Techniques	132
3.2.	SPECIFIC OBJECTIVES	133
3.3.	MATERIALS AND METHODS	134
3.3.1	Materials	134
3.3.2	Methods	134
3.3.2.1	Equilibrium Moisture Sorption-Desorption Studies	134
3.3.2.2	Determination of Film Density.....	134
3.3.2.2	Model Fitting.....	134
3.4.	RESULTS	135

3.4.1	Introduction	135
3.4.2	Equilibrium Moisture Sorption-Desorption Studies.....	135
3.4.2.1	Equilibrium Sorption-Desorption Profiles.....	135
3.4.2.2	Equilibrium Sorption-Desorption Isotherms.....	138
3.4.2.3	Moisture Solubility Coefficients	144
3.4.3	Modelling of Sorption-Desorption Isotherm Data	146
3.4.3.1	BET model.....	146
3.4.3.2	Zimm and Lundberg Clustering Function (G/v)	151
3.4.4.	Equilibrium Sorption-Desorption Kinetics	155
3.4.4.1	Sorption-Desorption Profiles	155
3.4.4.2	Calculation of Diffusion Coefficients.....	158
3.4.5	Calculation of Permeability Coefficients	166
3.5	DISCUSSION	168
3.5.1	Introduction	168
3.5.2	Equilibrium Moisture Sorption-Desorption Characteristics	168
3.5.2.1	Isotherms.....	168
3.5.2.2	Sorption Hysteresis	170
3.5.2.3	Solubility Coefficients.....	171
3.5.2.3.1	Effect of Temperature	172
3.5.2.3.2	Effect of RH	173
3.5.3	Isotherm Modelling.....	174
3.5.3.1	BET Isotherm Model	174
3.5.3.2	Clustering Function (G/v).....	176
3.5.6	Sorption-Desorption Kinetics	177
3.5.6.1	Sorption-Desorption Kinetics	177
3.5.6.2	Diffusion Coefficients.....	179
3.5.6	Permeability Coefficients.....	180
3.6	CONCLUSIONS	184
3.6.1	Introduction	184
3.6.2	Moisture Sorption-Desorption Isotherms	184
3.6.3	Theoretical Analysis of Isotherms.....	184
3.6.4	Sorption-Desorption Kinetics	185
3.6.5	Permeability Coefficients.....	185
CHAPTER 4	187

4.0	MOISTURE SORPTION AND DESORPTION BY TABLET CORES OF DISSIMILAR HYGROSCOPICITY	187
4.1	INTRODUCTION	187
4.2	SPECIFIC OBJECTIVES	189
4.3	MATERIALS AND METHODS	189
4.3.1	Materials	189
4.3.1.1	Lactose.....	190
4.3.1.2	Microcrystalline cellulose	190
4.3.1.3	Calcium dihydrogen Phosphate	190
4.3.1.4	Starch.....	190
4.3.1.5	Carnauba wax	191
4.3.1.6	Colloidal silicon dioxide.....	191
4.3.1.7	Model Drug Substance (Diltiazem HCl)	191
4.3.1.8	Coating materials.....	192
4.3.2	Methods	192
4.3.2.1	Tablet Formulation and Manufacture	192
4.3.2.2	Tablet Coating	193
4.3.2.3	Evaluation of Uncoated and Coated Tablets.....	195
4.3.2.3.1	Uniformity of Weight	195
4.3.2.3.2	Tablet dimensions	195
4.3.2.3.3	Tablet breaking strength and friability	195
4.3.2.3.4	Tablet disintegration	195
4.3.2.3.5	Tablet dissolution studies	195
4.3.2.3.6	Calibration and validation of UV spectrometry	196
4.3.2.3.7	Scanning Electron Microscopy.....	196
4.3.2.4	Moisture Sorption and Desorption Studies.....	196
4.4	RESULTS.....	197
4.4.1	General Characteristics of Manufactured Tablet Cores	197
4.4.1.1	Uniformity of weight.....	197
4.4.1.2	Tablet Strength.....	197
4.4.1.3	Tablet disintegration	198
4.4.1.4	Tablet Coating	199
4.4.1.5	Dissolution Test Profiles	201

4.4.1.6	Mean Dissolution Time	203
4.4.2	Moisture Sorption-Desorption Profiles of Tablet Cores	204
4.4.2.1	Uncoated Tablet Cores	204
4.4.2.2	Coated Hygroscopic Tablet Cores	206
4.4.2.2.1	Hygroscopic cores coated with moisture barrier coatings	206
4.4.2.2.2	Hygroscopic cores coated with enteric polymers	208
4.4.2.3	Coated Non-Hygroscopic Tablet Cores.....	210
4.4.2.4	Coated Waxy Tablet Cores.....	211
4.4.3	Effect of Weight Gain on Moisture Uptake/Dissolution.....	213
4.4.3.1	Moisture Sorption-Desorption Profiles	213
4.4.3.2	Dissolution Profiles	217
4.4.4	Equilibrium Sorption Profiles of Tablet Cores	221
4.5	DISCUSSION	223
4.5.1	Introduction	223
4.5.2	Tablet Core Formulation.....	223
4.5.4	Moisture Sorption-Desorption Characteristics of Tablet Cores	224
4.5.5.2	Relationship Between Dissolution and Moisture Sorption	229
4.6	CONCLUSIONS	232
4.6.1	Introduction	232
4.6.2	Effect of Tablet Core Hygroscopicity on Sorption-Desorption	232
4.6.3	Effect of Increasing Weight Gain on Moisture Sorption-Desorption and Dissolution Characteristics	233
4.6.4	Distribution of Water Between the Core and the Coating.....	233
CHAPTER 5	235
5.1	INTRODUCTION	235
5.2	SPECIFIC OBJECTIVES	236
5.3	MATERIALS AND METHODS	236
5.3.1	Materials	236
5.3.1.1	Aspirin	236
5.3.1.2	Salicylic acid	237
5.3.1.3	Reagents and Solvents.....	237
5.3.2.	Methods	238
5.3.2.1	Manufacture and Coating of Conventional Tablet Cores	238
5.3.2.2	Manufacture and Coating of Powder-Layered Tablet Cores... ..	239

5.3.2.3	Stability Testing Conditions and Sampling	239
5.3.2.4	Assay Method	240
5.3.2.4.1	Sample preparation	240
5.3.2.4.2	Sample analysis	241
5.3.2.4.3	Chromatographic conditions	241
5.3.2.4.4	Calibration of HPLC assay method	241
5.3.2.4.4	Validation of HPLC assay method	241
5.3.2.5	Statistical Analysis	242
5.4	RESULTS	243
5.4.1	HPLC Assay Validation	243
5.4.2	Results for Conventional Tablet Cores	245
5.4.2.1	Physical Characteristics of Uncoated Tablet Cores	245
5.4.2.2	Aspirin Hydrolysis in Uncoated Tablet Cores After Exposure to 75% RH/25 °C	245
5.4.2.3	Coated Conventional Tablet Cores	247
5.4.2.3.1	Influence of coating process on aspirin hydrolysis	248
5.4.2.3.2	Aspirin hydrolysis in coated tablet cores after exposure to 75% RH/25 °C	248
5.4.3	Powder-Layered Tablet Cores	251
5.4.3.1	Physical Characteristics of Uncoated Powder-Layered Tablet Cores	251
5.4.3.2	Aspirin Hydrolysis in Powder-Layered Tablet Cores Coated with Moisture Barrier Coatings and Exposed to 75 %RH/25 °C	251
5.5	DISCUSSION	254
5.5.1	Introduction	254
5.5.2	Uncoated Conventional Cores	254
5.5.3	Application of Moisture Barrier Coatings	256
5.6	CONCLUSIONS	261
5.6.1	Introduction	261
5.6.2	Role of Tablet Core Hygroscopicity	261
5.6.3	Effect of Application of Moisture Barrier Coatings	261
CHAPTER 6	263
6.0	GENERAL CONCLUSIONS AND SUGGESTED FUTURE WORK	263
6.1	GENERAL CONCLUSIONS	263
6.1.1	Moisture Barrier Polymer Films	263

6.1.1.1 Sorption-Desorption Characteristics of Cast Polymer Films...	263
6.1.1.2 Permeability Characteristics of Cast Polymer Films	264
6.1.2 Moisture Sorption-Desorption Characteristics of Tablet Cores	264
6.1.3 Aspirin Hydrolysis in Tablet Cores.....	265
6.1.4 Conclusion	265
6.2 SUGGESTED FUTURE WORK.....	266
REFERENCES.....	268
APPENDICES	288
APPENDIX 1	289
APPENDIX 2	290
APPENDIX 3	298
APPENDIX 4	298
APPENDIX 4	300

LIST OF FIGURES

Chapter One

Figure 1-1	Illustration of Permeation Across a Membrane	38
Figure 1-2	Illustration of the Solution–Diffusion Theory	41
Figure 1-3	Schematic Illustration of Henry's Law Isotherm	44
Figure 1-4	The BET Classification of Isotherms	44
Figure 1-5	Schematic Illustration of the Dual-Sorption Theory	49
Figure 1-6	Schematic of the Dual-Mode Sorption Isotherm	49
Figure 1-7	Isotherm Representations for Water-Polymer Systems	50

Chapter Two

Figure 2-1	Schematic Illustration of the Main Parts of a Dynamic Vapour Sorption (DVS) Apparatus/System	80
Figure 2-2	Schematic Flow Diagram of a WPA-100 Permeability Analyser Apparatus	82
Figure 2-3	Schematic Illustration of a Thermogravimetric Analysis (TGA) Apparatus	83
Figure 2-4	Scanning Electron Micrograph (SEM) of a Typical Hypromellose-Based Cast Film	86
Figure 2-5	Fixed-Time Moisture Sorption-Desorption Profiles of Moisture Barrier Films Exposed to 0-50-0-50-0 % RH Cycle (25 °C)	88
Figure 2-6	Fixed-Time Moisture Sorption-Desorption Profiles of Moisture Barrier Films Exposed to 0-75-0-75-0 % RH Cycle (25 °C)	89
Figure 2-7	Fixed-Time Moisture Sorption-Desorption Profiles of Moisture Barrier Films Exposed to 0-90-0-90-0 % RH Cycle (25 °C)	89
Figure 2-8	Fixed-Time Moisture Sorption-Desorption Profiles of Moisture Barrier Films Exposed to 0-75-0-75-0 %RH Cycle (40 °C)	90
Figure 2-9	Fixed-Time Moisture Sorption-Desorption Profiles of Enteric Polymer Films Exposed to 0-90-0-90-0 %RH Cycle (25 °C)	91
Figure 2-10	MVTR, Wet and Dry RH Versus Elapsed Time Plot for Eudragit L30 D-55 Film at 0-75 % RH Gradient (25 °C)	95
Figure 2-11	MVTR, Wet-Side and Dry-Side RH Versus Elapsed Time plot for Amino butyl methacrylate Film at 0-75 % RH Gradient (25 °C)	95
Figure 2-12	MVTR, Wet-Side and Dry-Side RH Versus Elapsed Time Plot for Opadry AMB Film at 0-75 % RH Gradient (25 °C)	96

Figure 2-13	MVTR, Wet-Side and Dry-Side RH Versus Elapsed Time Plot for Sepifilm LP Film at 0-75 % RH Gradient (25 °C)	96
Figure 2-14	Schematic Diagram of an MVTR Permeation Cell	98
Figure 2-15	Thermogravimetric Curve and Derivatogram of Water Sorbed in Eudragit L30 D-55 Film Post Exposure to 75% RH (25 °C)	100
Figure 2-16	Thermogravimetric Curve and Derivatogram of Water Sorbed in Opadry AMB Film Post Exposure to 75% RH (25 °C)	101
Figure 2-17	Thermogravimetric Curve and Derivatogram of Water Sorbed in Hypromellose Film Post Exposure to 75% RH (25 °C)	101
Figure 2-18a	NIR Spectra [Absorbance Versus Wavelength (nm)] for Eudragit L30 D-55 Film Collected During Exposure to the 0-75-0-75-0 % RH (25 °C) Cycle	105
Figure 2-18b	NIR Spectra [Absorbance Versus Wavelength (nm)] for Amino butyl methacrylate Film Collected During Exposure to the 0-75-0-75-0 % RH (25 °C) Cycle	105
Figure 2-18c	NIR Spectra [Absorbance Versus Wavelength (nm)] for Opadry AMB Film Collected During Exposure to the 0-75-0-75-0 % RH (25 °C) Cycle	106
Figure 2-18d	NIR Spectra [Absorbance Versus Wavelength (nm)] for Hypromellose Film Collected During Exposure to the 0-75-0-75-0 % RH (25 °C) Cycle	106
Figure 2-19	SNV-2 nd Derivative Spectra of Moisture Barrier Films in the 2200-1100 nm Wavelength Region. The Spectra Shown Were Collected at t=300 min Following Exposure in the DVS to the 0-75-0-75-0 % RH (25 °C) Cycle	107
Figure 2-20a	SNV-2 nd Derivative Spectra (1960-1820nm) for Eudragit L30 D-55 Film	105
Figure 2-20b	SNV-2 nd Derivative Spectra (1960-1800nm) for Amino butyl methacrylate Film	108
Figure 2-20c	SNV-2 nd Derivative Spectra (1980-1820nm) for Opadry AMB Film	109
Figure 2-20d	SNV-2 nd Derivative Spectra (1990-1800nm) for Hypromellose Film	110
Figure 2-21.	Schematic Diagram Illustrating How Polymer Chains of a Hypothetical Polymer Result into (a) Crystalline (b) Amorphous Morphology	112
Figure 2-22.	Structural Formulas of Hypromellose, Opadry AMB, Amino butyl methacrylate and Ethyl methacrylate monomer units	114
Figure 2-23.	Structural Formulas of Hypromellose acetate succinate and Poly(vinyl acetate phthalate)	118
Figure 2-24.	Sketch Diagram Illustrating the Transport of Vapour Through a Film	119

Chapter Three

Figure 3-1	Time Dependence of Permeation	131
Figure 3-2	Equilibrium Moisture Sorption-Desorption Profile of Eudragit L30 D-55 Film Exposed to 0-10-25-35-50-65-75-90-75-65-50-35-25-10-0 % RH Cycle (25 °C)	136
Figure 3-3	Equilibrium Moisture Sorption-Desorption Profile of Amino butyl methacrylate Film Exposed to 0-10-25-35-50-65-75-90-75-65-50-35-25-10-0 % RH Cycle (25 °C)	136
Figure 3-4	Equilibrium Moisture Sorption-Desorption Profile of Opadry AMB Film Exposed to 0-10-25-35-50-65-75-90-75-65-50-35-25-10-0 % RH Cycle (25 °C)	137
Figure 3-5	Equilibrium Moisture Sorption-Desorption Profile of Hypromellose Film Exposed to 0-10-25-35-50-65-75-90-75-65-50-35-25-10-0 % RH Cycle (25 °C)	137
Figure 3-6	Moisture Sorption-Desorption Isotherms of Eudragit L30 D-55, Amino butyl methacrylate, Opadry AMB and Hypromellose Films Measured at 25 °C	138
Figure 3-7	Moisture Sorption-Desorption Isotherms of Eudragit L30 D-55, Amino butyl methacrylate, Opadry AMB and Hypromellose Films Measured at 30 °C	141
Figure 3-8	Moisture Sorption-Desorption Isotherms of Eudragit L30 D-55, Amino butyl methacrylate, Opadry AMB and Hypromellose Measured at 40 °C	141
Figure 3-9	BET Isotherm Model Linearization Plot of the Equilibrium Moisture Sorption-Desorption Data for Ethyl methacrylate Film	148
Figure 3-10	BET Isotherm Model Linearization Plot of the Equilibrium Moisture Sorption-Desorption Data for Amino butyl methacrylate Film	148
Figure 3-11	BET Isotherm Model Linearization Plot of the Equilibrium Moisture Sorption-Desorption Data for Opadry AMB Film	149
Figure 3-12	BET Isotherm Model Linearization Plot of the Equilibrium Moisture Sorption-Desorption Data for Hypromellose Film	149
Figure 3-13	Regression Plots of Sorbed Water Volume-Fraction-Activity-Coefficient Versus Activity for the Equilibrium Moisture Sorption Data for Moisture Barrier Films	152
Figure 3-14	Stepwise Equilibrium Moisture Sorption-Desorption Profile of Ethyl methacrylate Film Exposed to 0-25-0-50-0-75-0-90-0 % RH Cycle (25.0 °C)	155
Figure 3-15	Stepwise Equilibrium Moisture Sorption-Desorption Profile of Amino butyl methacrylate Film Exposed to 0-25-0-50-0-75-0-90-0 % RH Cycle (25.0 °C)	156
Figure 3-16	Stepwise Equilibrium Moisture Sorption-Desorption Profile of	156

	Opadry AMB Film Exposed to 0-25-0-50-0-75-0-90-0 % RH Cycle (25.0 °C)	
Figure 3-17	Stepwise Equilibrium Moisture Sorption-Desorption Profile of Hypromellose Film Exposed to 0-25-0-50-0-75-0-90-0 % RH Cycle (25.0 °C)	157
Figure 3-18	Fractional Moisture Uptake-Loss (M_t/M_∞) Data Versus Reduced Time ($\sqrt{t/l}$) for Eudragit L30 D-55 Film. Data Obtained at 25 °C	158
Figure 3-19	Fractional Moisture Uptake-Loss (M_t/M_∞) Data Versus Reduced Time ($\sqrt{t/l}$) for Amino butyl methacrylate Film. Data Obtained at 25 °C	159
Figure 3-20	Fractional Moisture Uptake-Loss (M_t/M_∞) Data Versus Reduced Time ($\sqrt{t/l}$) for Opadry AMB Film. Data Obtained at 25 °C	159
Figure 3-21	Fractional Moisture Uptake-Loss (M_t/M_∞) Data Versus Reduced Time ($\sqrt{t/l}$) for Hypromellose Film. Data Obtained at 25 °C	160
Figure 3-22	Early Time Linearization of Fractional Moisture Uptake-Loss (M_t/M_∞) Versus Reduced Time ($\sqrt{t/l}$) for the Eudragit L30 D-55 Film (Sorption Cycles)	161
Figure 3-23	Early Time Linearization of Fractional Moisture Uptake-Loss (M_t/M_∞) Versus Reduced Time ($\sqrt{t/l}$) for the Eudragit L30 D-55 Film (Desorption Cycles)	162
Figure 3-24	Illustration of the Influence of C_B on the Moisture Sorption profile	176
Figure 3-25	Typical Fractional Mass Uptake-Loss (M_t/M_∞) Versus Reduced Time ($\sqrt{t/L}$) Curves for Different Transport Mechanisms	178

Chapter Four

Figure 4-1	Schematic Illustration of a Fluidized Bed Coater	189
Figure 4-2a	Scanning Electron Micrograph of a Hygroscopic Tablet Core Coated With Hypromellose-Based Coating.	200
Figure 4-2b	Scanning Electron Micrograph of the Surface of a Hygroscopic Tablet Core Coated With Hypromellose-Based Coating	201
Figure 4-3	Dissolution Profiles of Diltiazem From Uncoated and Coated Hygroscopic Tablet Cores. Dissolution Testing was Undertaken in Distilled Water	201
Figure 4-4	Fixed-Time Moisture Sorption-Desorption Profiles of Uncoated Hygroscopic, Non-hygroscopic and Waxy Tablet Cores Exposed to 0-90-0-90-0 % RH Cycle (25 °C)	205
Figure 4-5	Fixed-Time Moisture Sorption-Desorption Profiles of Hygroscopic Tablet Cores Coated with Moisture Barrier Films and Exposed to 0-90-0-90-0 % RH Cycle (25 °C)	206
Figure 4-6	Fixed-Time Moisture Sorption-Desorption Profiles of Hygroscopic Tablet Cores Coated with Enteric Polymer Films and Exposed to 0-90-0-90-0 % RH Cycle (25 °C)	207

Figure 4-7	Fixed-Time Moisture Sorption-Desorption Profiles of Non-hygroscopic Tablet Cores Coated with Moisture Barrier Films and Exposed to 0-90-0-90-0 % RH Cycle (25 °C)	210
Figure 4-8	Fixed-Time Moisture Sorption-Desorption Profiles of Waxy Tablet Cores Coated with Moisture Barrier Films and Exposed to 0-90-0-90-0 % RH Cycle (25 °C)	211
Figure 4-9	Fixed-Time Moisture Sorption-Desorption Profiles of Hygroscopic Tablet Cores Coated with Ethyl methacrylate Film at Increasing Weight Gain. Samples were Exposed to 0-90-0-90-0 % RH Cycle (25 °C)	213
Figure 4-10	Fixed-Time Moisture Sorption-Desorption Profiles of Hygroscopic Tablet Cores Coated with Amino butyl methacrylate Film at Increasing Weight Gain. Samples were Exposed to 0-90-0-90-0 % RH Cycle (25 °C)	214
Figure 4-11	Fixed-Time Moisture Sorption-Desorption Profiles of Hygroscopic Tablet Cores Coated with Opadry AMB Film at Increasing Weight Gain. Samples were Exposed to 0-90-0-90-0 % RH Cycle (25 °C)	214
Figure 4-12	Fixed-Time Moisture Sorption-Desorption Profiles of Hygroscopic Tablet Cores Coated with Hypromellose Film at Increasing Weight Gain. Samples were Exposed to 0-90-0-90-0 % RH Cycle (25 °C)	215
Figure 4-13	Fixed-Time Moisture Sorption-Desorption Profiles of Hygroscopic Tablet Cores Coated with Shin-Etsu Aqoat Film at Increasing Weight Gain. Samples were Exposed to 0-90-0-90-0 % RH Cycle (25 °C)	215
Figure 4-14	Fixed-Time Moisture Sorption-Desorption Profiles of Hygroscopic Tablet Cores Coated with Sureteric Film at Increasing Weight Gain. Samples were Exposed to 0-90-0-90-0 % RH Cycle (25 °C)	216
Figure 4-15	Dissolution Profiles of Diltiazem From Hygroscopic Tablet Cores Coated with Eudragit L30 D-55 Film at Increasing Weight Gain	217
Figure 4-16	Dissolution Profiles of Diltiazem From Hygroscopic Tablet Cores Coated with Amino butyl methacrylate Film at Increasing Weight Gain	218
Figure 4-17	Dissolution Profiles of Diltiazem From Hygroscopic Tablet Cores Coated with Opadry AMB Film at Increasing Weight Gain	218
Figure 4-18	Dissolution Profiles of Diltiazem From Hygroscopic Tablet Cores Coated with Hypromellose Film at Increasing Weight Gain	218
Figure 4-19	Dissolution Profiles of Diltiazem From Hygroscopic Tablet Cores Coated with Shin-Etsu Aqoat Film at Increasing Weight Gain	219
Figure 4-20	Dissolution Profiles of Diltiazem From Hygroscopic Tablet Cores Coated with Sureteric Film at Increasing Weight Gain	220
Figure 4-21	Equilibrium Moisture Sorption Profiles of Uncoated and Coated Hygroscopic Tablet Cores Following Exposure to 0-90 % RH Cycle (25 °C) in the DVS	221

Chapter Five

Figure 5-1	Typical Chromatograms of Aspirin and Salicylic acid in the Extraction Solvent	243
Figure 5-2:	Typical Chromatograms of Aspirin and Salicylic acid in the Mobile phase	244
Figure 5-3	Aspirin Hydrolysis in Uncoated Hygroscopic, Non-hygroscopic and Waxy Tablet Cores Exposed to 75 % RH/25 °C for Three months	246
Figure 5-4.	Salicylic acid Generated in Uncoated Hygroscopic, Non-Hygroscopic and Waxy Tablet Cores exposed to 75 % RH/25 °C	246
Figure 5-5	Aspirin Hydrolysis in Uncoated and Coated Hygroscopic Tablet Cores. Samples Exposed to 75 % RH/25 °C for Three months	249
Figure 5-6:	Aspirin Hydrolysis in Uncoated and Coated Non-hygroscopic Tablet Cores. Samples Exposed to 75 % RH/25 °C for Three months	249
Figure 5-7	Aspirin Hydrolysis in Uncoated and Coated Waxy Tablet Cores Exposed to 75 % RH/25 °C. Samples Exposed to 75 % RH/25 °C for Three months	250
Figure 5-8	Aspirin Hydrolysis in Powder Layered Coated Tablet Cores to which Moisture Barrier Films were Applied. Samples Exposed to 75 % RH/25 °C for Three months	252
Figure 5-9:	Schematic Diagram Depicting the Film Coating-Core Boundary as a Moisture-Rich Region for Aspirin Hydrolysis	258
Figure 5-10:	Photographs of Amino butyl methacrylate Coated Hygroscopic Tablets: (a) Coating Without Magnesium stearate (b) Coating with Magnesium stearate	259

Appendices

Appendix 1:	Moisture sorption-desorption profile of xanthan gum exposed to 0-75-0-75-0 %RH Cycle.	289
Appendix 2:	Typical equilibrium and Step-wise moisture sorption-desorption profiles of moisture barrier films obtained at 30 and 40 °C	290-297
Appendix 3:	Calibration Curve for the Quantitative Determination of Diltiazem HCl by UV-Visible Spectroscopy	298
Appendix 4:	Calibration Curve for the Quantitative Analysis of Aspirin and Salicylic acid by HPLC	299
Appendix 4:	Copy of Article (Mwesigwa et al., 2005) in which part of this work appears in publication	300

LIST OF TABLES

Chapter One

Table 1.1	Effect of Functional Groups on Oxygen Permeability. Reference Permeability = $0.038 \text{ cm}^3 \text{ mm/m}^2 \text{ 24h atm at } 23 \text{ }^\circ\text{C}$ and 0 % RH	57
-----------	---	----

Chapter Two

Table 2-1	Formula Used to Prepare Ethyl methacrylate Dispersion	75
Table 2-2	Formula Used to Prepare Amino butyl methacrylate Dispersion	76
Table 2-3	Formula for Used to Prepare Shin-Etsu Aqoat Dispersion	77
Table 2-4	Qualitative Formulas for Opadry AMB, Hypromellose, and Sureteric Systems	78
Table 2-5	Summary of Moisture Vapour Transmission Rates (MVTR) [g (H ₂ O)/day/100 sq. inch) (\pm Std. Dev, n=3) Data for Barrier Films measured with the wpa-100 equipment at 0-50, 0-75 and 0-90 RH gradients (25 $^\circ\text{C}$)	97
Table 2-6	Mean Specific Moisture Vapour Transmission Rates (MVTR) [g (H ₂ O) cm /min. cm ²] (\pm Std.Dev, n=3) Data for Moisture Barrier Films	97

Chapter Three

Table 3-1	Mean Equilibrium Sorption-Desorption Moisture Content of Eudragit L30 D-55, Amino butyl methacrylate, Opadry AMB and Hypromellose Films at 0, 10, 25, 35, 50, 65, 75, 90 % RH. Data shown are (\pm Std.Dev, n=3). Measurements Undertaken at 25, 30 and 40 $^\circ\text{C}$	139
Table 3-2	Calculated Mean Moisture Solubility Coefficients [(cm ³ (STP)/cm ³ polymer. cm Hg) for Moisture Barrier Films in the 10-90 % RH Range at 25, 30 and 40 $^\circ\text{C}$. Measurements Undertaken at 25, 30 and 40 $^\circ\text{C}$	144
Table 3-3	Calculated BET Model Constants M_{0B} (mg H ₂ O/mg film) and C_B (Dimensionless) for Moisture Barrier Films	147
Table 3-4	Calculated Clustering Function (G/v) Values for Moisture Barrier Films	151
Table 3-5	Mean Moisture Diffusion Coefficients (cm ² /s, $\times 10^{-8}$) for Moisture Barrier Film Samples	163
Table 3-6	Calculated Mean (n=3) Permeability Coefficients [(cm ³ (STP) cm)/(cm ² s, cm Hg)] for Moisture Barrier Films	166

Chapter Four

Table 4-1	Comparative Properties of Some Tablet Fillers Graded on a Scale of 5 (Good/High) to 1 (Poor/Low). 0 Means None	188
Table 4-2	Details of Tablet Core Formulations	192
Table 4-3	Tablet Coating Conditions Used for Different Polymer Coatings	194
Table 4-4	Results of the Assessment of Tablet Weight Uniformity.	197
Table 4-5	Results of the Tablet Breaking Force (N)	198
Table 4-6	Results of the Tablet Disintegration Time (min)	198
Table 4-7	Dry Weight Gain (%) of Coated Tablet Cores	199
Table 4-8:	Mean Dissolution Time (MDT) (min) and Area Under the Curve (AUC) (%.min) for Coated Tablet Cores.	204
Table 4-9	Summary of DVS Moisture Uptake/Loss Data for Uncoated Hygroscopic, Non-hygroscopic and Waxy (at 25°C)	205
Table 4-10	Summary of DVS Moisture Uptake/Loss Data for Uncoated and Coated Hygroscopic Tablet Cores (at 25°C)	206
Table 4-11	Summary of DVS Moisture Uptake/Loss Data for Uncoated and Coated Non-hygroscopic Tablet Cores (at 25°C)	211
Table 4-12	Summary of DVS Moisture Uptake/Loss Data for Uncoated and Coated Waxy Tablet Cores (at 25°C)	212

Chapter Five

Table 5-1	Details for Aspirin Tablet Core Formulations	238
Table 5-2	Physical Characteristics of Aspirin Tablets	245
Table 5-3	Mean Amount of Aspirin (mg) Remaining in Tablet Cores Following Coating with Different Moisture Barrier Films	248
Table 5-4	Physical Characteristics of Powder Layered Tablet Cores	251
Table 5-5	Mean Amount of Aspirin Remaining in Powder-Layered Tablet Cores Following Coating with Moisture Barrier Films	252
Table 5-6	Aspirin decomposition, moisture sorbed (at 75 % RH/25 °C) and mean tablet breaking force of uncoated cores.	255

ABBREVIATIONS, CONSTANTS, FORMULAE AND NOMENCLATURE

GREEK ALPHABET

α	Alpha
β	Beta
γ	Gamma
δ	Delta
ϵ	Epilson
ι	Iota
θ	Theta
κ	Kappa
λ	Lambda
μ	Mu
ν	Nu
π	Pi
ρ	Rho
σ	Sigma
φ	Phi
χ	Chi
ψ	Psi
ω	Omega

PHYSICAL CONSTANTS

Constant	Other units	SI units
Acceleration of gravity, g	980.665 cm / sec ²	9.80665 m / s ²
Avogadro's number, N	6.0221 x 10 ²³ / mole	6.0221 x 10 ²³ / mole
1 calorie (gram calorie)	4.1840 x 10 ⁷ erg	4.1840 J
Gas constant, R	1.9872 cal/deg/mol	8.3143 J/ K mole
1 litre atmosphere	24.22 cal	
1 atmosphere	760 mm Hg	101 325 N/m ²
1 bar	0.987 atm	100 000 N/m ²
Ideal gas volume (STP)	22.414 litre/mole	

$$\ln (\log_e) = \log_{10} \times 2.303$$

$$\text{Ice point (0 }^\circ\text{C)} = 273.15 \text{ K}$$

$$\pi = 3.14159$$

DIMENSIONS AND UNITS

Dimension	Symbol	Other units	SI units
Length	l	centimetre (cm)	meter (m ²)
Mass	M	gram (g)	kilogram (kg)
Time	t	minute (min)	Second (s)

DERIVED DIMENSIONS AND UNITS

Dimension	Symbol	Other units	SI units
Area (A)	l ²	cm ²	m ²
Volume (V)	l ³	cm ³	m ³
Mass (M)	M	g	kg
Density (ρ)	M/l ³	G / cm ³	kg / m ³
Velocity (v)	l/t	cm/s	m/s
Acceleration (a)	l/t ²	cm/s ²	m/s ²
Force (F)	Ml/t ²	-	N
Pressure (p)	M/lt ²	-	N/m ² = Pa
Energy (E)	Ml ² /t ²	-	N m = J

FRACTIONS AND MULTIPLES OF UNITS

Multiple	Prefix	Symbol
10 ⁻³	milli	m
10 ⁻⁶	micro	μ
10 ⁻⁹	nano	n

STANDARD FORMULAS

Density $M = \rho V$

Mean $\bar{X} = \frac{\sum(X_i)}{n}$

Standard Deviation $= \sqrt{\text{var}} = \sqrt{\frac{\sum(X - \bar{X})^2}{n-1}}$

NOMECLATURE

A	Area
ABMC	Amino butyl methacrylate copolymer
ASTM	American Society for Testing and Materials
AUC	Area Under the Curve
a_w	Water activity
b	Langmuir's hole affinity constant
B.E.T	Branauer, Emmett and Teller
BP	British Pharmacopoeia
C	concentration
C_B	Energy constant (BET Model)
C_G	Energy constant (GAB Model)
C_d	Henry's Law sorption concentration
C_H	Langmuir sorption concentration
C'_H	Langmuir's capacity
-CH ₃	Methyl
Cl	Chloride
-CN	Nitrile
c_r	Critical radius
D	Diffusion coefficient
db	Dry basis
DSC	Differential Scanning Calorimetry
DVS	Dynamic Vapour Sorption
E	Energy
EMAC	Ethyl methacrylate copolymer
EMC	Equilibrium Moisture Content
ENSIC	Engaged Species Induced Clustering
f	Flow rate
F	Function
FOC	Free of Charge
g	gram
GAB	Guggenheim-Anderson-de Boer
G/v	Zimm and Lundberg Clustering Function
-H	Hydrogen
H ₂ O	Water
H	Heat (Enthalpy)
h	height (tablet)

HCl	Hydrochloric acid
HDPE	High Density Polyethylene
HPLC	High performance liquid chromatography
HPMC	Hypromellose (Hydroxy propyl methyl cellulose)
hr	Hour
IUPAC	International Union of Pure and Applied Chemistry
J	Flux
K(k)	Constant
K _D	Henry's Law solubility coefficient
k _G	GAB model third constant
k _L	Equilibrium constant (Langmuir's model)
l	Thickness
LiCl	Lithium chloride
M	Mass
MCC	Microcrystalline cellulose
MDT	Mean Dissolution Time
M _{Eq}	Equilibrium moisture content
mg	milligram
min	Minute
ml	milli litre
M _o	Monolayer moisture content
M _{oB}	Monolayer moisture content (BET model)
M _{oG}	Monolayer moisture content (GAB model)
M _{oL}	Langmuir's amount
MVTR	Moisture Vapour Transmission Rate
MW	Molecular Weight
N	Newton
N ₂	Nitrogen
NaCl	Sodium chloride
NIR	Near Infra-red Spectrometry
nm	nanometer
NMR	Nuclear Magnetic Resonance
-OH	Hydroxyl
p	Partial pressure
P	Permeability
PEG	Polyethylene glycol
PVAP	Poly(vinyl acetate phthalate)
Q	Quantity

r	radius
R ²	Square of the Correlation Coefficient
RH	Relative Humidity
s	Second
S	Solubility coefficient
Sq	Squared
SEM	Scanning Electron Microscopy
Std. Dev.	Standard Deviation
STP	Standard Temperature and Pressure
t	Time
T _g	Glass transition Temperature
TGA	Thermogravimetric Analysis
UNIQUAC	Univeral Quasi Chemical
USP	United States Pharmacopoeia
V(v)	Volume
V _p	Volume of polymer
V _w	Volume of water
wg	Weight gain
x	Distance/Position
γ	Volume fraction activity coefficient
Δ/σ	Infinitesimal change
ΔH	Heat/Enthalpy change
θ	Fractional coverage
λ	% Polymer requirement
μl	micro litre
μm	micro metre
ρ	density
φ	Volume fraction
χ	Flory-Huggins Interaction Parameter

SUBSCRIPTS

D	Diffusion
Eff.	Effective
Eq.	Equilibrium
n	nth
o	Pre
P	Permeation
p	Polymer
s	Sorption

t after time t
w Water

MISCELLANEOUS SYMBOLS

% Per cent
≈ Approximately
≡ Identical to
≤ Less than or equal to
≥ Greater than or equal
© Copy right
∞ Infinity (maximum)
°C degree Celsius
TM Registered Trademark

CHAPTER ONE

Chapter One

1.0 GENERAL INTRODUCTION

Outline of Chapter One

1.1	Background
1.2	Role of Water in Drug Stability
1.3	Moisture Barrier Coatings Broadly Defined
1.4	Film Coating of Solid Dosage Forms
1.5	Principles of Permeation in Polymers: Fundamental Theories
1.6	The Solution-Diffusion Theory
1.7	Factors Affecting Permeation in Polymers
1.8	Thesis Philosophy

1.1 BACKGROUND

The majority of drug products deteriorate during the course of time because of the influence of environmental stresses like temperature, humidity or light. The Federal Drug Administration (FDA) Guidelines on Stability Testing (FDA, 1998) define stability as the ability of the active drug substance or other ingredients in the drug product to remain within the set limits for identity, strength or purity for a specified period of time.

Drug product stability is a function of parameters related to the product and the external environment. During the development of new drug products, stability testing is undertaken to determine how the quality of the active drug substance or other ingredients in the product may vary with time under the influence of the environmental stress factors outlined above. This helps to establish the shelf life and also the optimum storage conditions of the product (Pope, 1980; Richards and Aulton, 1988).

Nowadays, the majority of active drug substances are obtained by synthetic, semi-synthetic or biotechnological methods. They, thus, tend to be chemically very complex. Today's pharmaceutical formulators not only have to grapple with the difficulties of optimising drug bioavailability, they also have to contend with the need to ensure that the formulations they have developed are stable. This is because any mass exchange between the drug products with stress substances from the external environment can trigger changes in chemical and/or physical properties of the product.

Thus, the prevailing interest in solid-state chemistry of drug substances arises not only because solid dosage forms are the most commonly used form of drug administration but also because understanding stability in solid state facilitates the selection of solids with the most suitable physical and chemical characteristics.

1.2 ROLE OF WATER IN DRUG STABILITY

Water is probably the most important factor for drug deterioration. There exists a direct relationship between drug product stability and its water content (Ahlneck and Zografi, 1990; Waterman et al., 2002). For solid dosage forms, water may originate from processing, e.g., granulation if the moisture is not sufficiently driven off during the drying stage. However, the main source of residual moisture is exposure to the external environment. Depending on the product, the moisture in the product can instigate hydrolysis of chemical bonds, polymorphic changes, or changes in the dissolution properties (Byrn, 1982; Zografi, 1988). Water is additionally important to drug stability due to its low molecular mass; hence, the presence of even small amounts is significant in terms of molar reactivity. Crucially, due to the ubiquitous nature and ability of water to exist in vapour form, avoiding moisture can be difficult task (Franks, 1997).

For moisture sensitive products, uptake of moisture into the solid dosage form must therefore be prevented or at least minimized. This can be achieved by several ways; categorised here as formulation-related and packaging-related. Formulation-related approaches mainly involve the selection of excipients likely to improve the solid state stability of the drug. In this case, the excipient not only functions as an inert diluent (to facilitate manufacturability or enable convenience of administration), it also functions as an adjuvant, that is, facilitates the active ingredient to function by providing the required “environment” within the product. Packaging, on the other hand, although primarily aims to contain, deliver and market the said product, it can be used to provide the protection element to the product (Dean, 1988; Allinson et al., 2001).

Generally, the above-mentioned approaches are, to different degrees, capable of reducing moisture ingress into drug products sensitive to moisture (Lehto and Lankinen, 2004). However, they are likely to add expense to the process of producing drug products and may not guarantee that during the life of the product, moisture sorption will be completely prevented. Therefore, for certain formulations of solid dosage forms, application of a coating with moisture-barrier properties to individual dosage units has been considered (Prinderre, 1997; Campbell and Sackett, 1999; Pearnchob et al, 2003). Here, the moisture barrier coating is intended to slow moisture entry into the primary dosage form units (and may thereby contribute to improving the overall stability of the product). As a result, this approach is increasingly becoming popular. A recent patent search by the author on the US Patent and Trademark Office portal (<http://portal.uspto.gov/external/portal/home>) yielded 17 patents for moisture barrier coatings for the pharmaceutical and nutraceutical sectors.

1.3 MOISTURE BARRIER COATINGS BROADLY DEFINED

At this point, it is worthwhile to explore what constitutes a “moisture barrier” coating. In the current pharmaceutical literature, moisture barrier coatings are categorised as conventional coatings, by which it is implied that the coating performs an auxiliary role and does not contribute to the functionality of the dosage form. This is usually contrasted with the so-called functional coatings, comprising delayed (enteric) and extended/sustained release coatings. These mainly aim to control the rate of drug release from the dosage form. There is, however, no comprehensive definition of a moisture barrier coating in the current literature. Therefore, in the following paragraphs, definitions of the terms coating, barrier and moisture are given in order to build a clearer picture of what constitutes a moisture barrier coating.

The term *coating* usually implies a membrane formed directly on a substrate. It separates two phases between which fluids (gases, vapours or liquids) may be exchanged. It is distinguished from *film*, a term often used interchangeably with *coating*, which, however, refers to a preformed stand-alone membrane (a film becomes a coating when applied onto a substrate). Pharmaceutical coatings are usually dense, non-porous films obtained from polymeric substances and are typically $\leq 100 \mu\text{m}$ thick (Hogan, 1995), although films with much higher thickness are not atypical.

The term *barrier* describes a region that offers resistance to passage of a diffusant, such as a gas, a vapour or a liquid (Flynn et al, 1974; Martin, 1993). Barrier action may be achieved by physical means, where by the barrier material physically obstructs the path of the diffusant, or by chemical means, whereby the barrier acts to neutralise the diffusant, such as by binding or confining it in some way or form. Barriers can be fabricated from all sorts of materials, including plastic films and sheeting, wood laminates, metallic foils, and even paper.

The term *moisture* can have different meanings. It is often used non-specifically to describe water existing either in the form of small droplets (e.g., mist or damp). In the scientific literature, moisture refers to water existing in vapour form. The vapour phase corresponds to isolated water molecules which are highly random in space, akin to a gas. Such molecules have had enough energy to overcome forces of attraction holding them as a liquid (or as a solid, in the case of ice). Although they do not possess a shape or volume, vapour molecules are capable of exerting a pressure due to collisions with the walls of the container which they occupy. In this thesis, the terms moisture and water vapour are used interchangeably. By implication, therefore, a moisture barrier is a material that resists the passage or transfer of moisture across two phases.

Moisture barrier coatings are not limited to the pharmaceutical industry. Actually, pharmaceutical use represents only a small portion of this type of technology. They are widely used in many other different fields of technology, sometimes with slightly different principles of operation, each, of course, with different formulation constraints (McGinnis, 1996): In the food industry, for instance, they are used to protect foodstuffs against desiccation, and are commonly referred to as edible films (Donhowe and Fennema, 1994). In the steel industry, moisture barrier coatings are used to coat steel in order to prevent corrosion (Klages et al, 1996). In the electronic industry, they are employed to protect high precision instruments against moisture (Vogt and Hauptmann, 1995). In the construction field, damp proof-course, vanishes and emulsion paint, are the more familiar uses of this technology. Regardless of the field of application, however, the essence of a good moisture barrier coating is the same, i.e., the barrier material must possess a low water permeability (Koros, 1990; Vieth, 1991).

An issue of interest to the present work relates to the definition of “low water permeability” as far as pharmaceutical moisture barrier coatings are concerned. Since, strictly speaking, it is (environmental) moisture that is the more important stress rather than liquid water, pharmaceutical moisture barrier coatings should, in effect, be able to resist the passage of water vapour from the environment but not necessarily liquid water. Low permeability to liquid water would render the coating less ideal for use as a conventional coating as this would deter solubility or disintegration in gastric fluids. However, by rendering the barrier coating attractive to liquid water (due to the need for hydrophilicity or water solubility to facilitate wetting/disintegration), there is a possibility that the balance may somehow tip against the propensity for low affinity to the vapour form of water. It must be remembered that liquid water and water vapour are essentially the same compound. Given the knowledge that a water soluble polymer that is also a good water vapour barrier has yet to be discovered (Guilbert (1986), pharmaceutical moisture barrier coatings, therefore, constitute a formulation paradox.

It would appear therefore that the approach used currently in the development of pharmaceutical barrier coatings is to obtain a compromise by fabricating a system that combines elements of hydrophilicity (e.g., incorporating a water soluble polymer as the film former) and hydrophobicity (achieved by incorporation of materials with moisture repellent or scavenging properties) (Guilbert and Biquet, 2000) rather than utilise structures that are 100 % water proof to the liquid and vapour forms of water. The current approach, however, renders the barrier coating somewhat inferior to conventional packaging materials like high density polyethylene (HDPE). However, it is

reported that useful barrier coatings can still be achieved provided the coating is dense, is free from defects, has good adhesion to the substrate, possesses good thermal stability, and is of a uniform thickness (Banker, 1966; Koros, 1990; Bauer et al., 1998; Barranco et al., 2004). Adhesion is widely acknowledged in parallel applications of moisture barrier coatings but its significance has yet to be demonstrated in pharmaceutical applications.

Finally, it is necessary to explore potential advantages of moisture barrier coatings, especially in comparison to alternative approaches for attaining product stability:

(i). Coatings generally confer other desirable properties to the dosage form, such as enhanced strength due to the ability of polymeric materials to form membranes that are mechanically strong, improvement of the aesthetics, enhancement of swallowability, and lately, as a way for fighting against counterfeit medicines.

(ii). Also, it may be possible to use a sustained release coating that also possesses moisture barrier functionality, thus giving the formulator additional flexibility and or dual functionality with one technology.

(iii). Also, the ability to offer protection to individual dose units is very appealing. So even when the tablets are taken out their primary container, the barrier coating may still be able to offer protection against the elements.

(iv). Lastly, since these coatings are edible, there would be no issues arising with regard to disposal and the associated environmental effects, as is the case with aluminium foil, plastic or glass. This, probably, represents the strongest case for the use of moisture barrier coatings in the pharmaceutical sector.

1.4 FILM COATING OF DOSAGE FORMS

1.4.1 Introduction

Coating (of solid dosage forms, mainly tablets) is a very old practice and has been undertaken for many centuries. The modern operation utilizing polymers, however, can be traced to the period between 1930 and 1950 during which Abbott Laboratories of the USA introduced a cellulosic coating polymer (Ellis et al., 1970). This set a precedent for further introduction of polymers as materials for pharmaceutical coating. The current usage of polymer coatings can be broadly categorized into three groups based on their functional roles, i.e., (1) conventional coatings; (2) delayed release (e.g., enteric) coatings; and (3) sustained/extended release coatings.

Conventional coatings are the most commonly encountered type of coating. They are sometimes known as non-functional coatings. As already mentioned in section 1.2, moisture barrier coatings broadly belong to this category. Generally, conventional coatings are designed to dissolve rapidly in the gastrointestinal tract. This ensures that they exert minimum effect on the drug release properties of the uncoated core. Conventional coatings mainly serve protective, aesthetic or other functions, such as masking taste or odours, improving mechanical strength of the core, facilitation of handling, reduction of the risk of interaction between incompatible components or reduction of dust and the associated explosion hazards. The main requirement for conventional coatings is pH independent solubility, as mentioned above, so as to have a minimum influence on drug release of the core (Ellis et al., 1970).

Delayed release coatings are mainly exemplified by enteric polymer coatings. There are many reasons why an enteric coating may be applied to solid dosage forms: Firstly, they may be utilised to protect certain drug substances which are hydrolysed in the stomach by gastric secretions (e.g., acids and enzymes), perhaps to prevent gastric distress associated with acidic drugs (e.g., aspirin), to deliver drugs intended for local action in the intestines, e.g., intestinal antiseptics, to deliver drugs that are optimally absorbed in the intestines to their prime absorption site, or to effect a delayed response to the dosage form (Baudoux et al., 1990). Therefore, the ideal enteric-coating should be impermeable to gastric juices but easily susceptible to intestinal juices. The majority of enteric polymers are polyacids with carboxyl ionizable groups. When placed in acid media, the acid groups become protonated (and insoluble) but form salts in alkaline pH enabling them to dissolve in the intestinal juices (Baudoux et al., 1990).

The third category covers coatings used to control the rate of release of drugs from a dosage form, usually by a diffusion process to provide release behaviour, e.g., zero-order kinetics, pulsatile or sigmoid patterns (Van Savage and Rhodes, 1995; Rhodes and Porter, 1998) although other mechanisms are utilised. Controlled release coatings serve a variety of purposes. They are used to achieve more effective therapy while eliminating the potential for both under- and overdosing. Controlled release coatings are also used to achieve the slow release of highly soluble and or permeable drugs, fast release of low-solubility drugs, or delivery of drugs to specific sites, such as the colon (Basit, 2005). Lastly, it is not uncommon that drug manufacturers make use of controlled release technologies, including application of controlled release coatings, as a way of achieving brand line extension to an already existing conventional product line or, in other cases, to add marketing depth to an already existing brand.

1.4.2 Film Coating Materials

Film coatings are fabricated from a variety of materials that include a polymer, a plasticizer, and several other (miscellaneous) additives (Rowe, 1984; 1985). Some of the materials incorporated into film coatings are reviewed below:

1.4.2.1 Polymers

In a film coating formulation, the polymer is usually the film former and the main component on the formulation (Ellis et al., 1970). The ideal polymer is one capable of producing smooth, thin films that are reproducible under routine coating conditions. The range of materials that can be used as film formers is very wide and covers materials that may be natural, synthetic or semi-synthetic. Examples of polymers used in coatings are given in the paragraphs that follow.

1.4.2.1.1 Polymers used in conventional film coatings

This category includes cellulose ether derivatives, e.g., hypromellose (also called hydroxypropyl methylcellulose), methylcellulose, hydroxypropylcellulose and sodium carboxy methylcellulose; vinyl polymers, e.g., poly(vinyl alcohol); and polymethacrylates, mainly copolymers of butylmethacrylate, (2-dimethylaminoethyl) methacrylate and methylmethacrylate (Hogan, 1995; Bauer et al., 1998b).

1.4.2.1.2 Polymers used in delayed release film coatings

This category, mainly enteric polymers, includes polymethacrylate derivatives (e.g., ethylmethacrylate copolymer); polyvinyl acetate derivatives, e.g., poly(vinyl acetate phthalate) and cellulose derivatives, e.g., cellulose acetate phthalate, cellulose acetate trimellitate, hydroxypropyl methylcellulose acetate phthalate, and hydroxypropyl methylcellulose acetate succinate (Bauer et al, 1998b).

1.4.2.1.3 Polymers used in extended/sustained-release film coatings

This category includes the following compounds: cellulosic derivatives, e.g., ethylcellulose and cellulose acetate, polyacrylates, such as Eudragit R series of polymers; and polylactides, poly(lactide-co-glycolides and polyorthoesters (Li and Peck, 1989; Bauer et al, 1998; Rhodes and Porter, 1998).

1.4.2.2 Plasticizers

Plasticizers are low molecular weight organic esters added to coatings to facilitate processing (Nielsen, 1974). They modify generic properties of the polymer rendering

them easy to process and or to perform as membranes. Although many compounds, covering diverse functions like phthalates, aliphatics, epoxides (vegetable oils), etc., and even polymers, possess plasticizing properties, only few are approved for pharmaceutical use. These include polyols such as glycerol, propylene glycol and polyethylene glycols, organic esters such as phthalates, dibutyl sebacate, and triacetin, vegetable oils/glycerides such as castor oil (Hogan, 1995).

1.4.2.3 Miscellaneous additives

Additives serve a variety of purposes: Colorants are used for individualization of the product by colour. They may be pigments, e.g., amaranth and γ -carotene, or dyes such as lakes of aluminium or iron oxides. Opacifiers are used to impart opacity. For this purpose, talc and titanium dioxide are the mainly used opacifiers. Fillers and anti-tack agents are used to provide coating solids to the formulation and to reduce tackiness. They include talc, microcrystalline cellulose, glyceryl monostearate, stearic acid, magnesium stearate, to mention just a few (Hogan, 1995; Petereit et al., 1995).

1.4.2.4 Solvents

Solvents permit uniform film formation and application over the entire substrate. Those which have been used for film coating include water, ethanol, ethanol/water, and various other solvent/solvent mixtures. Their selection is based on the following criteria: (i) empirically; according to the "like dissolves like" rule; (ii) qualitatively, based on the assessment of intermolecular forces; and (iii) quantitatively, based on solubility parameters (Bauer et al., 1998). Up to the early 1970s, organic solvents were the main stay of film-coating applications. However, due to increasing costs, concerns about toxicity and effects on the environment, a move to aqueous based systems was prompted. As such, water is the current preferred coating medium (Pickard and Rees, 1974; Hogan, 1982).

1.5 PRINCIPLES OF PERMEATION IN POLYMERS

1.5.1 Introduction

Most barrier coatings regulate mass exchange by controlling a process known as permeation. Permeation, as applied to the transport of gases, vapours or liquids, is a process of mass transfer that occurs by simple molecular transport or by movement through pores and channels. This transport process is quantitatively defined in terms of permeability (Petropolous, 1994). Permeability, a term very closely associated with permeation, is defined as the mass of material transferred in unit time, area and driving

force (Koros, 1990). The driving force for the mass transfer may be a difference partial pressure or concentration in which case, the mass transfer is due to diffusion. If the driving force is a difference in total pressure rather than partial pressure, the mass transfer results from a flow (Koros, 1990; Petropoulos, 1994).

Figure 1.1 below depicts a membrane of sectional area A and thickness l . Initially it is subjected to a permeant of partial pressure p_0 , volume v_0 and concentration c_0 . After a time t , an amount of permeant corresponding to partial pressure of p_t , volume v_t and concentration c_t is transmitted across the membrane.

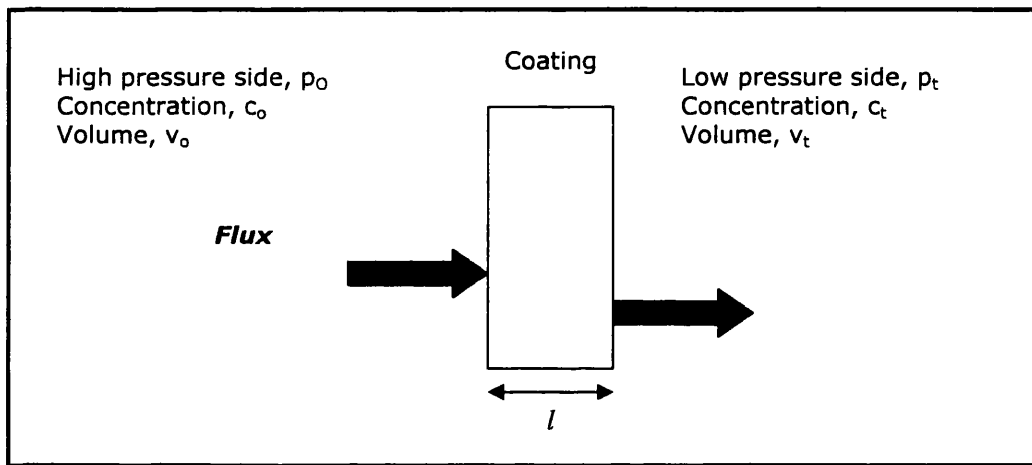


Figure 1-1. Illustration of Permeation Across a Membrane (Koros, 1990)

The volume V of permeant that penetrates the membrane is given by (Koros, 1990):

$$V = \frac{A \cdot P \cdot \Delta p \cdot t}{l} \quad \text{Equation 1-1}$$

where Δp is the normalized partial pressure differential of the penetrant ($p_1 - p_2$) and P the permeability of the barrier. It can be seen from Equation 1-1 above that the volume of a permeant penetrating a barrier is proportional to the cross sectional area, the permeability of the barrier, the partial pressure differential of the penetrant and the time of exposure but inversely proportional to the barrier thickness.

Permeability can be further defined in terms of a state flux. This is illustrated by the following relationship in Equation 1.2, i.e:

$$P = \frac{(Flux)}{\Delta p / l} \quad \text{Equation 1.2}$$

The steady state flux in *Equation 1.2* above can be defined as the quantity of permeant (Q) flowing through the barrier of unit area in unit time. It follows that permeability of a membrane is the amount of material that traverses a membrane in unit time, area and flux (Units: g/m.s. Pa or cm³ (STP) cm/cm. s. cmHg). Mathematically,

$$P = \frac{Q}{A.t.\Delta p/l} \quad \text{Equation 1.3}$$

In an ideal membrane (i.e., a homogeneous polymer membrane without defects, and where no interaction occurs between the polymer and the permeant) the permeability is constant and independent of the environmental conditions, mainly the pressure exerted by the permeant. As it will be discussed later, this is not always the case with many polymer membranes encountered in practice. For this reason, a description of the permeability for most barrier membranes requires information about the dependence of the permeability on partial pressure to be specified.

The following general trends are reported in the literature: Permanent gases, like Nitrogen, exhibit permeabilities that are independent of their partial pressures in polymer membranes that are above their glass transition temperature, T_g (such polymers systems are also known as “rubbery”). Condensable gases (e.g., water vapour), and in many instances, carbon dioxide, which have a high propensity for interaction with the polymer, exhibit upwardly inflecting permeabilities, which are a function of the prevailing partial pressure. However, the permeability of most gases in polymers below their T_g (such systems are also known as “glassy”) decreases with the prevailing partial pressure (Koros and Chern, 1987).

Finally, it may be more convenient to measure the weight rather than the pressure of the permeant across a unit area of barrier in unit time, for instance, in the case of water vapour. *Equation 1-1* may be modified by the introduction of another parameter, the moisture vapour transmission rate, VTR (g/m².s) to obtain:

$$\frac{Q}{A.t} = VTR = \frac{P.\Delta p}{l} \quad \text{Equation 1.4}$$

The American Society for Testing and Materials, ASTM (e.g., ASTM 1980) specifies another parameter, the Permeance, which equals the VTR divided by the the normalized partial pressure differential of the penetrant. It is not difficult to deduce that the permeability is equal to permeance multiplied by thickness of the membrane.

1.5.2 Mechanisms of Permeation in Polymer Membranes

The mechanisms for permeation of gaseous and vapour permeants in polymer membranes appear to be dependent on the structure of the membrane in question:

The first mechanism to consider is the permeation process in membranes with pores, cracks or other defects in their structure. For these, transport of penetrants occurs primarily by viscous or pipe flow. In this case, the penetrant fills the conduit during the permeation process. The driving force for this kind of flow is the applied pressure. Such flow may be further described as laminar, turbulent or transitional. The transport process is characterized by ordinary (Brownian diffusion) diffusion. Viscous flow is thought to be the main way by which liquids are transported through barriers.

The second mechanism to consider is when the diameter of the pores in the membrane is much smaller than the mean free path of the gas molecules. Here, the molecules of the penetrating gas almost certainly have a higher probability to collide with the pore walls rather than with other penetrant molecules. In this case, another form of diffusion, i.e., Knudsen diffusion, controls the transport process (Kast and Hohenthanner, 2000).

The third mechanism applies to dense, non porous membranes. The transport is thought to be of the activated-diffusion type, i.e., the internal energy of the molecules provides the force for diffusion. The permeation process then occurs as a result of the penetrant molecules sorbing at the upstream side of the membrane, diffusing through the membrane under a concentration gradient and subsequently desorbing at the down stream side of the membrane (Vieth, 1991; Kesting and Fritzche, 1993). The quantitative analysis for this type of permeation has been undertaken on the basis of three models, i.e., the non-equilibrium thermodynamics model (Baranowski, 1991), the pore flow model (Okada et al., 1991) and the solution diffusion model (Merten, 1966; Paul et al., 1976; Stern and Frisch, 1981). Of the three models above for permeation in dense membranes, the solution-diffusion model is the most widely used model to describe permeation through barriers (Wijmans and Baker, 1995).

1.6 THE SOLUTION-DIFFUSION THEORY

1.6.1 Introduction

The solution diffusion-mechanism is attributed to Sir Thomas Graham (1805-1869), who is also one of the first people to qualitatively describe permeation of gases through polymer membranes. Between 1828 and 1833 Graham postulated the well known Graham's law. In 1866, he formulated the "solution diffusion process" theory by

suggesting that the permeation process in rubber involved the dissolution of the gas followed by transmission of the dissolved molecules through the membrane (Stannett, 1978). Thus, contrary to the pore flow model above, the molecules in Graham's solution-diffusion model, are not convected through pores but preferentially dissolve in the membrane, where they diffuse through the membrane down a concentration gradient. This model has been verified theoretically and experimental by several workers, notably Merten (1966) and Paul (Paul et al., 1976).

To put it more clearly, the solution diffusion mechanism proposes that permeation through a membrane proceeds via a series of steps, i.e., sorption and solution of the permeant molecules at the upstream side of polymer membrane, activated diffusion of the permeant molecules along the thickness of the polymer in response to a concentration gradient; and desorption from the downstream side of the membrane. This mechanism is schematically illustrated in Figure 1-2 below. Furthermore, the pressure in the membrane is assumed uniform and the diffusant species on either membrane interface are in equilibrium. There is, as a result, a continuous gradient of chemical potential from one side of the membrane to the other side. Also, sorption at the membrane surfaces is spontaneous; the rate of which is much higher than that of diffusion, the latter process being dependent on the internal energy of the molecules, and is, hence, the rate limiting step in the permeation process.

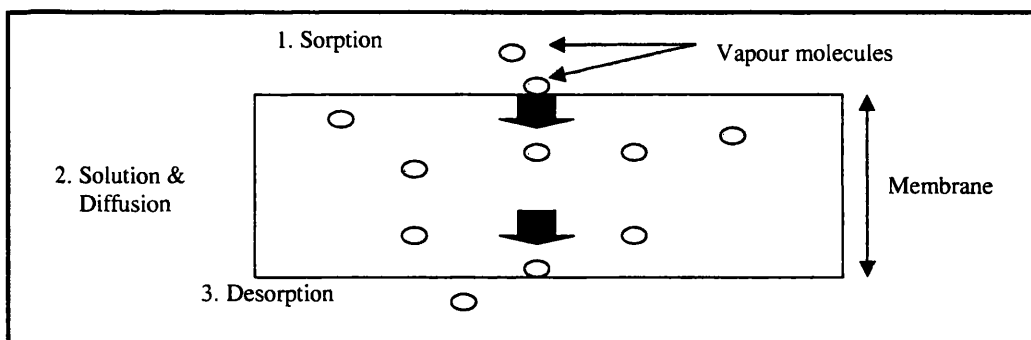


Figure 1-2. Illustration of the Solution–Diffusion Theory (Tsujita, 2003)

In 1855, Adolph Eugene Fick (1829-1901) published two laws for the quantitative description of diffusion. He proposed that the driving force for the net mass transfer was the concentration gradient. His description of diffusion required the definition and use of the diffusion coefficient, D . In 1870, Stefan and Exner showed that permeation was proportional to the product of a thermodynamic factor, the solubility or sorption coefficient (S) and Fick's diffusion coefficient (D), a kinetic parameter. This was later

used by Wroblewski and others to present a solution to Graham's solution-diffusion theory in the form (Stannett, 1978; Stannett et al., 1979):

$$P = [S] \cdot [D] \quad \text{Equation 1-5}$$

where P is the permeability, otherwise known as the permeability coefficient. The solubility coefficient S is based on Henry's Law of solubility and relates the concentration c of the gas dissolved in the solution to the partial pressure p above the solution, i.e.:

$$c = S \cdot p \quad \text{Equation 1-6}$$

The solubility coefficient is shown to be dependent on the condensability of the penetrant and the extent of the polymer-penetrant interactions while the diffusion coefficient denotes the ability of the permeant to move in the membrane.

In summary, the solution-diffusion model above considers the permeation process in polymer membranes as consisting of sorption at the surface of the membrane, (Fickian) diffusion through the membrane, and desorption the downstream side of the membrane. It follows that an understanding of both sorption and diffusion processes is necessary if the permeation in polymer membranes is to be fully comprehended. Therefore, in the following sections, a detailed description of both sorption and diffusion phenomena in polymer membranes is presented.

1.6.2 Sorption and Desorption in Polymers

1.6.2.1 Principles and Definitions

Sorption is simply the process whereby one substance takes up another. Sorption occurs because the molecules of the gas or vapour strike the surface of the solid phase as they wander randomly in space. If the conditions at the surface of the solid are ideal, the gas or vapour molecules may be retained by the solid phase. The solid phase is referred to as the sorbent while the sorbed molecules of the gas or vapour are the sorbate phase. The terms absorption and adsorption, which are often used interchangeably with sorption, refer to, respectively an internal phenomenon within the solid phase or a surface phenomenon on the solid phase. When sorption is used, it is non-specific for both adsorption and absorption (de Boer, 1968).

The sorption process is a thermodynamic in nature. A thermodynamic process is defined as the energetic evolution of a system proceeding from an initial state to a final state (Smith, 1984). This essentially means that during the sorption, the system's

energetic quantities, i.e., internal energy, U , enthalpy, H , Gibb's free energy, G , etc., being measures of the internal energy of the sorption system, change from an initial state to a final state, depending on the constraints of the system, i.e., whether temperature, pressure or volume, etc., are held constant. It will become clear that this is the reason why sorption is equilibrium driven.

During the sorption process, the sorbent and sorbate molecules continuously exchange energy through collisions. If this energy is large enough, the sorbate molecules may pick up enough momentum enabling them to leave the solid. This phenomenon is the opposite of sorption and is commonly known as desorption. With time, a stage may be reached when the number of molecules being sorbed equals the number desorbed. This constitutes a state of thermodynamic equilibrium. The net increase in the number of molecules sorbed is zero. At this state, the energy per molecule or the chemical potential, of the sorbate and sorbent are the same (de Boer, 1968).

1.6.2.2 Sorption Isotherms

The amount of gas or vapour material sorbed by the solid phase depends on the partial pressure exerted by the gas, the temperature and the (physical and chemical) nature of both the sorbent and sorbate (Ruthven, 1984). This amount can be determined from the fall in pressure by application of universal gas laws if the volume of the vessel and the solid are known, or it may be calculated directly from the increase in weight of the solid material following a period of sorbate activity. The relationship between the amount sorbed (at equilibrium) and the partial pressure of the sorbate above the solid at fixed temperature is known as the isotherm.

When the sorbate concentrations on the sorbent phase are low, the molecules of the sorbate phase on the sorbent are isolated from their neighbours. The isotherm obtained for this type of sorption for a uniform surface is found to be linear (Langmuir, 1918). This isotherm is analogous to Henry's Law (*Equation 1-6*). Hence, this type of isotherm is sometimes called Henry's Law isotherm.

For sorption in polymeric materials, Henry's Law isotherm, the shape of which is schematically illustrated in *Figure 1-3* below, has been shown to be valid only for permanent gases or other low molecular weight gases sorbed in rubbery polymers (i.e., polymers that are above their glass transition temperature, T_g). As can be seen in *Figure 1-3* below, this isotherm describes the partitioning of the penetrant in the polymer, which is taken to behave as a liquid. The slope of the curve is the partition coefficient otherwise known as Henry's Law coefficient, S .

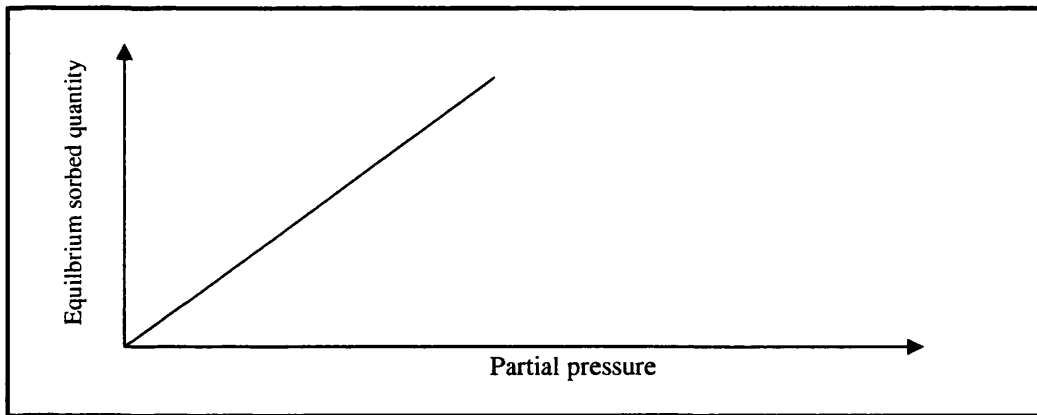


Figure 1-3. Schematic Illustration of Henry's Law Isotherm (Vieth, 1966)

There are recorded in the literature on this subject several hundred isotherms for a variety of materials; nevertheless, the majority can be grouped into five classes—the classification originally proposed by Brunauer, Deming, Deming and Teller and nowadays simply known as the B.E.T classification (Brunauer et al., 1938). The five classes of isotherm are schematically illustrated in *Figure 1-4* below.

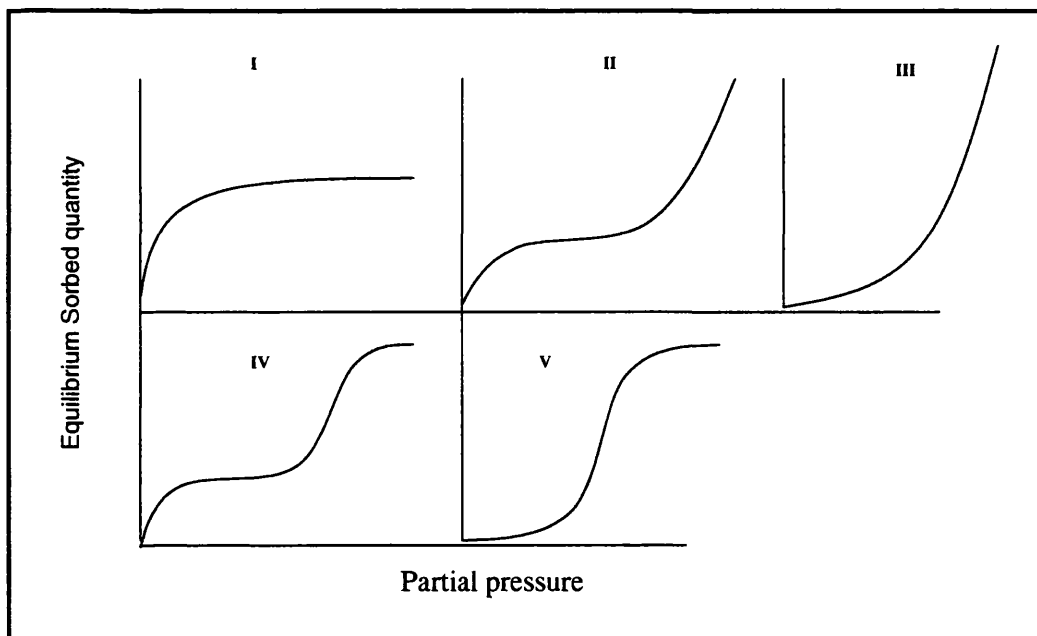


Figure 1-4. The BET Classification of Isotherms (Brunauer et al, 1940)

-Type I isotherm is known as the Langmuir isotherm. Materials exhibiting this behaviour usually sorb materials onto specific sites with a high binding energy and or into a network of non-swelling capillaries (Bell and Labuza, 1984). The material holds a large amount of the sorbent at low sorbate activities.

-Type II isotherms exhibit features of Henry's Law isotherm and Type I isotherm described above. They are thought to be caused by a combination of colligative effects, capillary effects or surface interactions (de Boer, 1968). The two bends in the curve result from differences in the interaction between the sorbate and the sorbent. Type II isotherms have been reported in water-polymer systems (Bell and Labuza, 1984; Hancock and Zografis, 1993; Stubberud et al, 1996).

-Type III isotherm has been described in crystalline substances like lactose (Buckton and Darcy, 1995) as well some synthetic methacrylate polymers (Bravo-Osuna, 2005). Such materials exhibit little uptake until a critical activity has been reached. The main type of interaction is thought to be by hydrogen bonding (Ruthven, 1984). Further increase in the activity results in a decrease in sorbate-polymer interactions while sorbate-sorbate interactions increase. This leads to a dramatic increase in sorption, manifesting as the large upturn in the isotherm.

-Type IV and V isotherms are respectively similar to type II and III but exhibit inflection points. Both type of isotherm have been reported in very hydrophilic polymers (e.g., cellulose and silk) or microporous solid systems (van der Wel and Adan, 1998).

1.6.2.3 Sorption Theories

Several theories have been proposed for the quantitative interpretation of sorption isotherms. Broadly, they can be divided into three groups, i.e., localised sorption theories, dissolution theories and novel theories. Localised sorption theories consider the sorbate to be bound at specific sites in the sorbent, e.g., in cracks and pores, or other specific sites on the polymer segments, such as polar groups, if present. The well known Langmuir's sorption theory, the BET isotherm model, and the dual mode sorption theory are typical examples of models in this category. Dissolution theories, on the other hand, assume homogeneous dissolution of sorbate in the sorbent, akin to the mixing of a solute in a solvent, and are exemplified by the Flory and Huggins theory. Novel theories, which neither belong to the localised nor dissolution categories, have been proposed, and include the ENSIC model, and UNIQUAC models (Favre, 1996a; van der Wel and Adan, 1998). These theories are briefly reviewed below:

1.6.2.3.1 Langmuir's model

For a surface on which a certain number of molecules are present, impinging molecules may not strike an empty surface but could instead strike the top of already sorbed molecules. Molecules hitting the top of those already sorbed either reflect or

reside for short periods of time but do not contribute to sorption (Langmuir, 1918). Langmuir used this picture as the basis for his model. He proposed that the monolayer amount was the limit for sorption and corresponded to the point when the surface was covered with a layer of molecules. Also, molecules were sorbed at a fixed number of well-defined localized sites, with each site holding one molecule. The most common mathematical representation of Langmuir's model is as shown:

$$\theta = \frac{M_{\infty}}{M_{oL}} = \frac{k_L p}{1 + k_L p} \quad \text{Equation 1-7}$$

where θ is the fractional coverage, being equal to the amount of sorbate M_{∞} sorbed at equilibrium divided by the Langmuir amount M_{oL} , k_L is equilibrium constant equal to the ratio of rate constants for sorption and desorption (this is related to the affinity of the sorbate for the sorbent) and p is the partial pressure of sorbate above the sorbent (Ruthven, 1984). A plot of M_{∞} against p yields a straight line from which M_{oL} , k_L can be computed. This isotherm is of the correct form to represent a Type I isotherm shown above (BET Classification). When applied to other types of isotherm, derived constants for the experimental data over the entire concentration range do not bear physical meaning (Ruthven, 1984).

1.6.2.3.2 Brunauer, Emmet and Teller (BET) model

Brunauer, Emmet and Teller (1938) derived a model for multilayer adsorption by assuming that the incident sorbate molecules become attracted to those molecules already sorbed on the surface of the sorbent when they strike the surface, and contrary to Langmuir, their time of sorption was not negligible. Each molecule in the first sorbed layer provided one site for the second and the subsequent layers. The molecules in subsequent layers, which were in direct contact with other sorbed molecules but not the surface of the sorbent, behaved as a saturated liquid. Mathematically, this model is expressed as:

$$M_{Eq} = \frac{M_{oB} C_B a_w}{[(1 - a_w)(1 + (C_B - 1)a_w)]} \quad \text{Equation 1-8}$$

where M_{Eq} is the equilibrium amount of sorbate sorbed by a unit weight of sorbent at sorbate activity a_w , M_{oB} is the monolayer moisture content and C_B the BET energy constant, which is related to the difference of the energy (enthalpy) of the sorbate molecules in the pure liquid and in the monolayer. M_{oB} and C_B can be obtained from the linearized BET equation of the form:

$$F(BET) \equiv \frac{a_w}{(1-a_w)M_{EMC}} = \frac{1}{M_{oB}C_B} + \frac{C_B-1}{C_B M_{oB}} a_w \quad \text{Equation 1-9}$$

Thus, a plot of $F(BET)$ versus a_w in the appropriate a_w range is linear but at higher activities, an upward curvature is noticed at which point the model ceases to apply. M_{oB} and C_B can then be obtained from the slope and intercept of the linear part (Bell and Labuza, 1984). The BET model has the general form of a Type II isotherm and provides good representation of experimental sorption isotherms in a limited sorbate activity range, usually $0.05 < a_w < 0.3-0.5$. Despite this limitation, the BET equation is the most widely used model to calculate isotherm constants. It is routinely used in the calculation of specific surface area and is recommended by IUPAC.

1.6.2.3.3 Guggenheim Anderson de Boer (GAB) model

The GAB model is a three-parameter model and is an extension of the BET theory (Anderson, 1946; Guggenheim, 1966; de Boer, 1968). Unlike the BET model, the GAB model has a wider activity range applicability (typically, $0.05 < a_w < 0.8-0.9$). A modified form of this model is as follows:

$$M_{Eq} = \frac{M_{oG} C_G k_G a_w}{[(1 - k_G a_w)(1 + (C - 1)k_G a_w)]} \quad \text{Equation 1-10}$$

The M_{oG} and C_G are related to the BET constants M_{oB} and C_B . The constant, k_G , is related to the difference in the enthalpy of the sorbate molecules in layers beyond the monolayer and the pure liquid and is assumed to be less than 1. A simple way of calculating GAB equation constants is the so-called method of the transformed form of the GAB isotherm (Equation 1-11) (Labuza, 1984; Timmermann, 2003):

$$\frac{a_w}{M_{Eq}} = \alpha + \beta(a_w) + \gamma(a_w)^2 \quad \text{Equation 1-11}$$

This second order polynomial can be analysed using non-linear regression, from which the constants α , β and γ are obtained, and hence the GAB constants.

1.6.2.3.4 Flory-Huggins model

In the early 1940s, Flory (1941) and Huggins (1942) independently presented a theory for describing sorption based on the entropy of mixing small molecules and polymers. Maurice L Huggins and Paul Flory independently presented a mathematic model for describing sorption based on the entropy of mixing small molecules in polymer

solutions. Taking into account the similarity in molecular sizes, the Flory-Huggins theory makes a statistical calculation of the different configurations of a polymer/solvent system using a lattice concept. The modelling of the polymer behaviour was achieved by using a single parameter, the Flory-Huggins Interaction Parameter, χ , according to the following equation below:

$$\ln a = 1 - \phi + \ln \phi + \chi (1 - \phi)^2 \quad \text{Equation 1-12}$$

where χ (dimensionless) is the Flory-Huggins interaction factor, which is adapted to measure data as a constant or as a function of the volume fraction ϕ of sorbate. χ also expresses the compatibility of polymer and penetrant. A lower value implies higher affinity between the sorbate and polymer and hence greater sorption. The χ , parameter is a reflection of the polymer-sorbate affinity, where a low value describes the highest sorption and hence, the best affinities.

1.6.2.3.5 Dual-Mode sorption model

The dual-mode sorption model, as the name suggests, proposes that sorbed molecules in a polymer exist in two populations. The basic assumption of this theory is the existence of microcavities within the matrix of the polymer (Vieth, 1988). Thus, the two populations of the sorbate are distributed as follows: the first population is dissolved by an ordinary dissolution process and obeys Henry's Law isotherm, while the second is bound at high energy sites at the periphery of or inside the hypothetical microcavities, and corresponds to the Langmuir sorption isotherm. The environment corresponding to the Henry's Law mode has a relaxed, quasi-liquid structure, while the environment of the population corresponding to the Langmuir mode is formed within packets of un-relaxed, disordered polymer chains.

In the dual mode theory, the amount of sorbate sorbed by the polymer, is expressed in terms of the total concentration C , which is the sum of Henry's Law sorption C_D and Langmuir sorption C_H , i.e.:

$$C = C_D + C_H = k_D p + \frac{b C_H^0 p}{1 + bp} \quad \text{Equation 1-13}$$

where p is the vapour pressure of the sorbate, k_D is the Henry's Law solubility coefficient, C_H^0 is the Langmuir capacity, b is the Langmuir's affinity constant. The dual sorption equation is linear against vapour pressure only in the high pressure region. In this region, the slope corresponds to the Henry's solubility coefficient. A strong argument which is believed to support the dual mode theory is the fact that the

volumetric volume of the polymer can actually be predicted from the sorption experiment (El-Hibri and Paul, 1985). Thus, the volume of the polymer should increase only linearly with the pressure because only molecules sorbed in the Henry's Law mode swell while the Langmurian mode is trapped in the cavities without disturbing the polymer matrix. *Figures 1-5 and 1-6* below are schematic illustrations of both the dual mode sorption theory, demonstrating the two hypothetical locations, and the accompanying isotherm (Stern and Trohalaki, 1990):

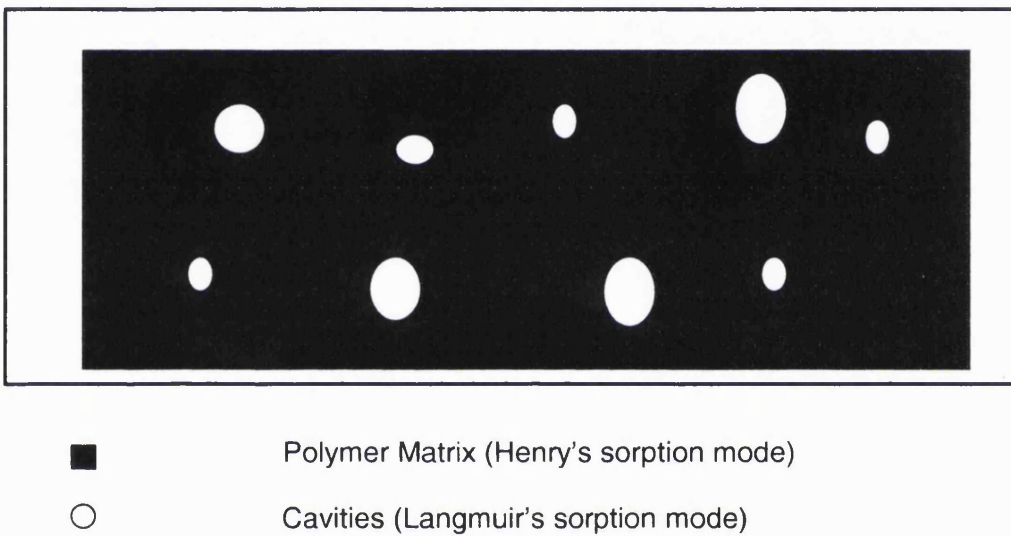


Figure 1-5. Schematic Illustration of the Dual-Mode Sorption Theory

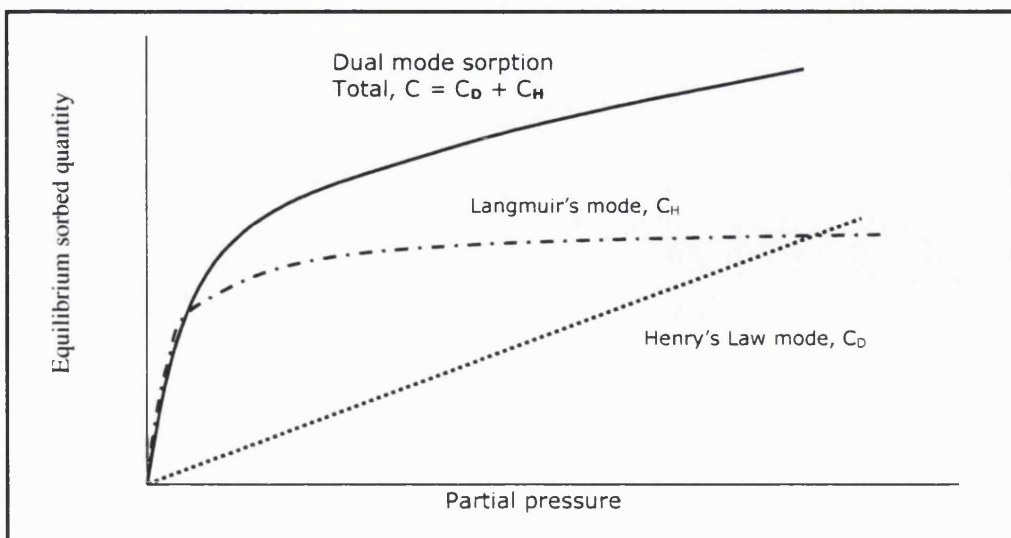


Figure 1-6. Illustration of the Dual-Mode Sorption Isotherm

1.6.2.3.6 Novel Theories

Novel theories include the UNIQUAC (Universal Quasi Chemical) model and its modifications (Abrams and Prausnitz, 1975; Freundslund et al, 1975; Jonquières, et al., 1998) and the ENSIC (Engaged Species Induced Clustering) model (Favre et al, 1996a). Although claimed to successfully predict sorption in a wide range of polymer systems, their applicability to pharmaceutical systems is not reported.

1.6.2.4 Typical Water-Polymer Equilibrium Sorption Characteristics

Equilibrium sorption characteristics of water vapour in polymers have been widely reported. Surveys of the literature indicate four main types of sorption isotherms, i.e., Henry's Law sorption, Type II (Langmuir) and Type III sorption and in some cases Flory-Huggins type of isotherms (Kyritsis et al, 1995; Favre et al, 1996b; van der Wel, 1999; Rutherford, 2001; Ismael and Lorna, 2002; Tsujita, 2003). These isotherms are schematically shown in Figure 1-7 below:

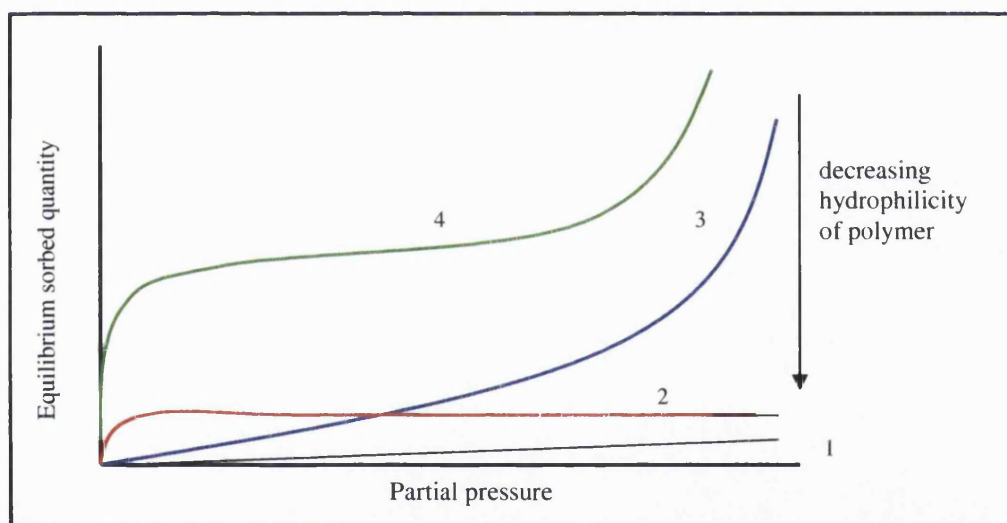


Figure 1-7. Isotherm Representations for Water-Polymer Systems

Henrian sorption behaviour (indicated by isotherm 1) is an example of ideal sorption. The amount of sorbed water in the polymer is very small and this amount varies linearly with respect to the applied pressure. Henrian behaviour has been observed for the sorption of water vapour by highly hydrophobic polymers (Legras et al, 2002).

Type I sorption isotherms (indicated by isotherm 2) are explained in terms of the Langmuir sorption, that is, the sorption of water to specific hydrophilic functions in the

polymer. This is thought to lead to a non-random distribution of water in the polymer which results in a relatively high amounts of being taken up at low pressure (Detallante et al, 2001; Stroeks and Dijkstra, 2001; Legras et al, 2002).

Type III and II sorption isotherms (indicated by isotherms 3 and 4, respectively) have been reported in the more hydrophilic polymers (Stroeks and Dijkstra, 2001). In both cases, the sorbed water is thought to interact with the polymer, mainly via hydrogen bonding. The amount of sorbed water is directly correlated to the number of polar groups in the polymers. These isotherms have been interpreted quantitatively in terms of the BET, GAB and Flory-Huggins models. In Type II isotherms, the chemisorption of water molecules leads to non-random distribution of water molecules in the polymer, thus, the characteristic high extents of sorption at low vapour pressures.

On the other hand, the convex nature of the isotherm in Type III isotherm has been explained in terms of the Flory-Huggins sorption theory, which implies a random distribution of the water molecules within the polymer. Where a weak convex behaviour of the isotherm is obtained, usually a concentration-dependent Flory-Huggins interaction parameter is anticipated. A stronger convex isotherm (characterised by a large degree upturn in the sorption isotherm at high sorbate activities, also as seen in Type II-V isotherms) has been explained by the phenomenon of cluster formation. This concept is based on the idea that the water molecules sorbed in the polymer materials are not sorbed as single molecules but as clusters, i.e., aggregated water molecules. Moreover, the extent of cluster formation in polymer has been shown to depend, not only on the type of polar group in the chains but also their position (Hancock and Zografis, 1993; Harnandez and Gavara, 1994; Stroeks and Dijkstra, 2001).

Cluster formation, when present, can significantly affect the sorption, diffusion and permeation properties of polymers (Favre et al., 1994). It is also reported by the same authors that clusters introduce big errors during the measurement of the Flory-Huggins interaction parameter. Consequently, it is important that clustering is characterized. This, however, is very complicated. Spectroscopic techniques like FT-IR, Raman and NMR, as well as DSC, have been employed. DSC may detect the ice melting peak or crystallization peaks, from which the extent of clustering is indirectly deduced. X-ray diffraction can detect crystals of water directly. However, none of these techniques can enable the direct estimation of cluster size or the tendency to cluster. One of the more successful ways of estimating clustering in polymers is the theory of Zimm and Lundberg (Zimm and Lundberg, 1956; Lundberg, 1972). The authors proposed a function G/v defined as:

$$\frac{G}{v} = -(1 - \phi) \left[\frac{\partial(\gamma)}{\partial a} \right]_{p,T} - 1$$

Equation 1-14

where G/v is the cluster function, based on the statistical distribution of the penetrant in the polymer, a is the activity of the penetrant, ϕ is the volume fraction of the penetrant and γ is the volume fraction activity coefficient (a/ϕ). A G/v value of -1 signifies ideal sorption. The penetrant dissolves in the polymer randomly. Higher values signify a tendency to cluster (Lundberg, 1972). Non-random aggregation originate from water molecules sorbed in Langmuirian sites (qv Dual-mode sorption model).

Penetrant-induced plasticization is frequently associated with water sorption in polymers. However, unlike clustering, this phenomenon is less well understood even though many plasticization-induced effects in polymers are well characterized (e.g., Sanders, 1988; Wessling et al, 1991; Petropoulos, 1989; Bos et al, 1998, Thrasher and Rezac, 2004, etc). There is still no consensus on the description of plasticization or a method to predict whether a material will be plasticized or not. It is known, however, that plasticization arises because the relatively small molecules of the penetrant interpose between the polymer chains and effectively reduce polymer-polymer interactions (Hoy, 1973; Kesting and Fritzsche, 1993; Hancock, and Zografi, 1994; Stading et al., 2001). On a macro scale, this manifests as increased softness and a depression of the T_g , while on a micro scale, it leads to increased chain mobility, increased free volume fraction and permeability. In many polymers, it has been demonstrated that plasticization by sorbed water manifests as non-ideal sorption, showing a characteristic increase in permeation at high RH (Huvarud et al., 1980).

In consideration of the above two phenomenon, water molecules sorbed in polymers exist in three thermodynamically distinct states, i.e., as single water molecules, which neither show significant interactions with other water molecules nor with their immediate environment; or as aggregated water molecules, which interact with other water molecules to form clusters. Such clusters are not large enough to resemble bulk water and may therefore present with properties of state that are different from liquid bulk water (Higuchi et al., 1985). The other state is the water that is in close association with the polymer segment. This water fraction is further differentiated as non-freezing water, i.e., the water that is strongly bound to polar groups, and freezable bound water that is weakly bound to the polymer or to the water clusters (Higuchi et al., 1985; Quinn et al., 1988; Hatakeyama and Hatakeyama, 1998). The different water fractions exhibit differences in transition enthalpies enabling them to be identified calorimetrically or by spectroscopy (Fukuda et al., 1990; Hatakayama and Hatakayama, 1998).

1.6.3 Diffusion in Polymers

1.6.3.1 Definition

Diffusion, is the other phenomenon in the solution-diffusion model. It is defined as the process whereby one substance (called the diffusant) becomes redistributed between different parts of another as a result of thermal motion of the diffusant molecules (Knight, 1981). It is essentially kinetic in nature, and leads to the homogenisation of components in the phase. Two types of diffusion can be distinguished, i.e., inter-diffusion (commonly called diffusion), and self diffusion. The former occurs when a concentration gradient exists and is characterised by the diffusant flowing in the direction of diminishing concentration. Self diffusion, on the other hand, occurs in the absence of a concentration gradient. The displacement of the substance is chaotic and the total diffusive flux is zero (Chalykh, 1983).

1.6.3.2 Theories of Diffusion in Polymers

Diffusion in polymers is thought to occur as a result of the random motion of molecules driven by the concentration difference between the two phases. It is, however, a function of the polymer and the diffusant (Felder and Huvad, 1980; Van Krevelen, 1990). During this process (i.e., diffusion), polymer chains are perturbed which allows the diffusant molecules to reside between the chains of the polymer. When sufficiently energized, diffusing molecules develop a location that is favourable to make a diffusive jump (Stern and Troahaliki, 1990). The diffusion coefficient, D , expresses the frequency at which a location appears next to the diffusant for it to make a diffusive jump.

It is widely acknowledged that the diffusion process can be affected by the state of the polymer, as reflected by the dependence of the diffusion coefficients on the partial pressure and the temperature in rubbery and glassy polymers. Thus, in rubbery polymers, for example, diffusion coefficients of non-condensable gases are independent of concentration. For such gases, equilibrium sorption is low and interactions with the polymer are minimal. By contrast, the diffusion coefficients for the same gases in glassy polymers are highly nonlinear and increase with increasing concentration due to the fact that above T_g , polymers respond rapidly to changes in their physical condition (Crank, 1975; Stern and Frisch, 1981). Below T_g , the motions of polymer chains are not rapid to homogenise the penetrant's environment, i.e., the polymer does not attain equilibrium in the timescale of diffusion (Vieth et al, 1991).

In general, it is found that the diffusion process in polymers is much more complex than the sorption process. For this reason, several theories have been proposed in an

attempt to explain how diffusion in polymers takes place, but as yet, there is no unified theory to explain this phenomenon. The different theories advanced to account for diffusion may be categorised into three broad groups, i.e., macroscopic theories, microscopic theories and atomistic theories.

Macroscopic theories relate the rate of diffusion to the concentration gradients responsible for the net mass transfer. These theories are essentially phenomenological, i.e., describe a physical effect (which, in this case, is diffusion) purely on the basis of observing it without claiming that it derives from some deeper understanding or a more basic precept. These theories are exemplified by the theories based on Fickian diffusional analysis.

Microscopic theories attempt to link experimental results, e.g., the dependence of diffusion coefficients on temperature, nature of the penetrant and its concentration in the polymer, etc., with structural or energy parameters of the polymer. They are further subdivided into two groups, i.e., molecular theories (Meares, 1954; DiBenedetto and Paul, 1964; Pace and Datyner, 1979) and free volume theories (Fujita, 1961, Vrentas and Duda, 1977). The theoretical basis and applicability of these theories has been extensively reviewed in the literature (e.g., Stannett et al, 1979, Frisch and Stern, 1981; Vieth, 1991; Mercea, 2000).

Atomistic theories are computer generated simulations of penetrant migration in the polymer matrix based on local parameters such as the dimensions of the atoms and molecules, molecular chain angles, the potential fields acting on the atoms and molecules. The beauty of these models is that they do not make ad hoc assumptions about the behaviour of the system (i.e., the polymer) (Catlow et al, 1990; Roe, 1991; Theodorou, 1996). With the advance of super computers, atomistic theories have been shown to offer a more accurate prediction of diffusion compared to microscopic or macroscopic theories. Although attractive in this sense, their practical achievement is very complex (Mercea, 2000).

1.6.3.3 Fickian Diffusion Analysis

For most practical purposes, diffusion in polymers can be described by Fick's two laws of diffusion (Stern and Trohalaki, 1990). These laws are represented by the following two equations, commonly referred to as Fick's First Law and Fick's Second Law, for the isothermal diffusion in a sufficiently large area. The relevance of these laws to permeation in polymers is further elaborated in the sections that follow:

1.6.3.3.1 Fick's First Law of Diffusion

Fick's First Law relates the net diffusion of a gas across a membrane to the partial pressure of the gas, and the area and thickness of the membrane. The amount Q of a gas or vapour flowing through a barrier of unit cross sectional area A in unit time t is known as the flux, J . Mathematically,

$$J = \frac{1}{A} \frac{\partial Q}{\partial t} \quad \text{Equation 1-15}$$

Fick's First Law is based on the hypothesis that at steady state, the diffusive flux J is proportional to the concentration gradient dC/dx measured normal to the section.

$$J = -D \frac{\partial C}{\partial x} \quad \text{Equation 1-16}$$

where D is the diffusion coefficient (cm^2/s). The negative sign indicates that diffusant flows in the direction of lower concentration.

1.6.3.3.2 Fick's Second Law of Diffusion

Fick derived an equation for mass transport that describes the change in concentration with time at a definite location rather than the mass diffusing across a unit area. Thus,

$$\frac{\partial C}{\partial t} = D \frac{\partial^2 C}{\partial x^2} \quad \text{Equation 1-17}$$

Equation 1-17 is a fundamental equation for one-dimensional diffusion in an isotropic medium and shows that under non-steady state flow, the gradient and local concentration of the penetrant decrease with time. The concentration gradient with respect to time is equal to the gradient of the flux, J , with respect to position, x . Being a differential equation, an analytical solution must be obtained for D by assuming some boundary conditions. Several such solutions are discussed in the literature (e.g., by Stern and Trohalaki, 1990; Vieth, 1991; Piringer, 2000).

Diffusion in and permeation through non-isotropic (non-homogeneous) polymers is more complex, but has been considered by several investigators (e.g., Rogers, 1965; Barrer, 1968; Barrer, 1975). The treatment becomes even more complex where the polymer is plasticized by the penetrant. In this case, the diffusion coefficient varies not only with time but also with "history". These cases are discussed by Stannett et al. (1970, 1972, 1978).

In his seminal work, Crank (1975) proposed a classical solution for Fick's Second Law for a one-dimensional diffusion process for a planar sheet. The diffusion coefficient was presumed constant. Taking the initial and boundary conditions for a membrane of thickness $2l$ exposed to an infinite reservoir of penetrant were $C=C_0$ at $0 < x < l$, $t=0$; $C=C_1$ at $x=l$, $t \geq 0$; and $\delta C / \delta x = 0$ at $x=0$, $t \geq 0$, where C is the concentration.

A series solution for these boundary conditions obtained by the separation of variables method is as shown in *Equation 1-18* below:

$$\frac{C - C_0}{C_1 - C_0} = 1 - \frac{4}{\pi} \sum_{n=0}^{\infty} \frac{(-1)^n}{2n+1} \exp\left(\frac{-D(2n+1)^2 \pi^2 t}{4l^2}\right) \cos\left[\frac{(2n+1)\pi x}{2l}\right] \quad \text{Equation 1-18}$$

In hydrophilic polymers, some of the diffusing molecules may be immobilized either as a result of penetrant-polymer interactions or through cluster formation. The diffusion coefficient is essentially an effective diffusion coefficient (D_{eff}) related to the diffusion coefficient of free vapour and the mobile fraction (Vieth, 1991).

1.7 FACTORS AFFECTING PERMEATION IN POLYMERS

1.7.1 Introduction

Permeation of gases and vapours through polymers is influenced by a number of factors, some of which have been already elaborated. These can be categorised into three main groups, i.e., factors related to the nature of the polymer membrane, factors related to the nature and state of the penetrant, and factors related to the external environment. Although a generalised discussion is presented here, for all purposes many concepts apply to the permeation of water through polymers as well.

1.7.2 Nature of the Membrane

On the basis of the introductory concepts hitherto discussed, diffusion, and hence, permeation, should demonstrate a dependence on the existence of cavities and the ease with which they are formed within the polymeric membrane. The nature of the polymeric material has a profound influence on the formation of these cavities and therefore on the rate of diffusion. In this respect, factors inherent to the polymer membrane that are known to affect diffusion can be classified as chemical nature of the polymer; composition of the membrane; polymer's physical state and structural properties. These are discussed below:

1.7.2.1 Chemical Nature of the Polymer

Permeation properties of polymers depend on the chemical structure of the constituent units, and the length and conformation of the polymer segments. By chemical nature is meant the molecular weight, degree of polymerization, presence of hydrophilic or hydrophobic groups, length of the chains, density, lateral chains, double bonds, etc. The effect of the chemical structure on permeability can be observed in Table 1-1 below for the permeability to oxygen in a polymer whose repeating unit is $[-CH_2-CHX-]_n$ where X is a varying functional group (Pascat, 1984).

X	Permeability
-OH (Hydroxyl)	1 [§]
-CN (Nitrile)	4
-Cl (Chloride)	800
-F (Fluoride)	1500
-Acryl	1700
-CH ₃ (Methyl)	15000
-Phenyl	42000
-H (Hydrogen)	48000

Table 1.1. Effect of functional groups on oxygen permeability. [§]Reference permeability = 0.038 [cm³.mm/m² day. Atm] at 23 °C and 0 % RH (Pascat, 1984)

Other polymer properties that directly relate to chemical nature include molecular weight, symmetry, degree of saturation and polarity (Berens and Hopfenberg, 1982; Salame, 1986; Jones, 1994; Soney and Sabu, 2001). It is noted that an increase in molecular weight results in a decrease in permeability. For instance, Berens and Hopfenberg (1982) showed that for a series of polystyrenes, the diffusivity of a range of organic vapours decreased by a factor of almost ten as the molecular weight was increased from 10,000 to 300,000.

The degree of polymerization, presence and nature of side groups, cross-linking, and extent of unsaturation, etc., are also known to affect chain mobility and packing, and thus the amount of free volume available for diffusion. It is reported that polymers with simple linear polymer chains, e.g., high density polyethylene, pack tightly, and as a consequence, exhibit much lower permeability compared polymers with bulky side-groups (Aguilar-Vega and Paul, 1993; Zimmerman and Koros, 1999; El-Shafee and Naguib, 2003).

Similar effects as those described above have been demonstrated through crosslinking. For instance, Coma et al. (2003) reported an improvement in barrier performance of hypromellose following crosslinking with citric acid. This is because

crosslinking decreases polymer chain mobility, which should improve resistance to vapour and gas transport. Other workers (e.g., Maeda and Paul, 1987; Rezac and Schöberl, 1999; Coma et al., 2003), however, reported mixed results which somewhat brings into disrepute the exact usefulness of this approach with regard to low molecular penetrants. On the other hand, the effect of introduction of double bonds on permeability is demonstrated by the high permeability of polybutadiene to water vapour compared to that of polyethylene. The introduction of unsaturation into the polymer backbone lends greater ease of rotation to the chains resulting into higher diffusivity (Pascat, 1986).

As discussed by Pascat (1968), comparison of diffusion coefficients and permeability for two polymers with the same symmetry but different polarity shows that the polymer with higher polarity exhibits higher cohesion due to greater degrees of intermolecular attractive forces. This would then affect the degrees of freedom of groups in the polymer. Highly polar polymers, such as polysaccharides, exhibit large degrees of hydrogen bonding and may have low gas permeability at low activities. However, the chemical nature that yields good gas barrier properties often results in poor moisture barrier properties. Conversely, non-polar hydrocarbon-based polymers, which are excellent moisture barriers, are often reported to be less effective barriers to gases (Morgan, 1980; Pascat, 1986).

1.7.2.2 Membrane Composition

The addition of plasticizers, lipids, and other solid inclusions to a polymer may facilitate the increase in chain mobility. This manifests as an increase in penetrant transport. As is often the case with pharmaceutical coatings, plasticizers are added to modify generic properties of the polymers. This renders the polymer more suited to its role as a film former. Plasticizers with high solvent power for the polymer cause greater chain expansion than those with low solvent power. Detailed accounts of the effect of plasticizers on permeation have been given by Stannett et al. (1970) and also by Barrer (1968). A more recent case-study is that of Okhamafe and York (1983) who reported an increase in the diffusion coefficient of moisture in hypromellose on addition of polyethylene glycol (PEG). However, the addition of poly(vinyl alcohol) decreased permeability. These changes were ascribed to differences in the way PEG and poly(vinyl alcohol) interacted with the hypromellose polymer groups in the coating.

The effect of lipid components on moisture permeability is extensively discussed by Morillon et al., (2002). This is of special significance because lipids are routinely added

to moisture barriers as a way to repel moisture. The authors above reported that beeswax and stearic acid were more effective at reducing moisture permeability due to their high hydrophobicity. This was attributed to the high content of long chain fatty alcohols and alkanes. McHugh and Krochta (1994) established that the efficiency of fatty alcohols and fatty acids increased with the carbon number (from 14-18) because of the corresponding increase in the apolar part of the molecule. Other authors also showed that among carboxylic acids, inclusion of stearic and palmitic acids resulted in the lowest water vapour permeability (Hagenmaier and Shaw, 1991, Morillon et al., 2002).

Kemper and Fennema (1984) reported that the physical state and the concentration of the lipid components significantly influenced moisture permeability of the membrane. As water is less soluble in solid lipids than in their liquid counterparts, an increase in solid lipid content of the film decreased moisture permeability but only up to a certain level. This was later substantiated by the work of Hagenmaier and Shaw (1990), who showed that lower moisture permeability of hypromellose films was achieved with stearic acid concentrations between 40 and 50%.

Also, it has been demonstrated that the effect of solid additives on permeability of polymers depends upon the nature of the additive, its compatibility with the polymer matrix and effect on film adhesion, thermal stability and porosity. Generally, additives increase permeability since they create discontinuities in the film and thus reduce the homogeneity of the film. If the inert filler is compatible with the polymer matrix, the filler can take up some of the free volume in the polymer matrix and create a tortuous path for the permeation (Crank and Park, 1968). The degree of tortuosity is dependent on the volume fraction of the filler and the shape and orientation of the particles. On the other hand, when the filler is incompatible with the polymer, voids tend to occur at the interface.

The effect of hydrophilic fillers on moisture permeability of polymers is intriguing. The general effect of these substances is enhanced moisture uptake of the membrane due to their hygroscopicity (Wu and McGinity, 2000). However, whether this moisture is available for diffusion might depend on the extent to which this moisture is sequestered within the film, as well as the vapour pressure differential across the membrane. Also, such materials improve film adhesion and thermal stability, which are important qualities in their own right (Barranco et al., 2004).

1.7.2.3 Physical State of the Polymer

Polymers in the glassy state are brittle, these properties being closely related to the restricted chain mobility. The result is that polymers in this state are very dense structures, with little void space (estimated between 2-10%) (Vieth, 1991). Consequently, permeation is low. In contrast, polymers in the rubbery state are flexible. The segments are mobile and void space is much larger. In both glassy and rubbery states, these properties can be further modified by the presence of a crystalline phase. The crystalline microphase of a polymer is usually less permeable owing to its restricted or tightly packed configuration.

1.7.2.4 Membrane Thickness

Generally, the thicker the film, the longer the diffusion path. As maybe seen from Equation 1.1, this should translate into lower permeability of a thicker membrane. In some instances, however, anomalous behaviour has been observed. For instance, Martin-Paulo et al (1992) noted that the moisture transfer rate of cellophane films coated with paraffin wax increased with increase in thickness from 30-60 μm . Similar observations were made by Debeaufort et al. (1993; 1994) and Biquet and Labuza (1988) who explained that increase in permeability with film thickness was due to increase in water affinity due to more hydrophilic components and or discontinuities in the film. This may be relevant to the coating of solid dosage forms where it is always assumed that thicker coats promote barrier performance.

1.7.3 Nature and State of the Penetrant

The properties of the permeant such as molecular size, shape, polarity, concentration, and physical state not only affect the interactions with the membrane but also the rate of movement in the membrane. These factors do not necessarily apply to the water as a permeant but are nevertheless discussed for illustrative purposes. Thus, the size and shape of penetrant molecule is known to influence the rate at which it is transported within the polymer matrix. A decrease in diffusivity with an increase in the size of the penetrant has been reported by many investigators (e.g., Prager et al., 1953; Fujita et al., 1967; Soney and Sabu, 2001). Kim et al. (1993) reported a decrease in uptake with increasing penetrant chain length for the transport of alkanes from heptane to dodecane through crosslinked polystyrene.

Another aspect of permeants which has a noticeable effect on permeability is the shape. Flattened or elongated molecules have higher diffusion coefficients than

spherical molecules of equal molecular volume (Yi-Yen et al., 1980; Berens and Hopfenberg, 1982). Generally, these effects (permeant size and shape) are much more marked in glassy polymers than in rubbery polymers due to the differences in the permeant-polymer interactions.

In rubbery polymers, energy is required to generate sites for the permeant molecules to occupy, but since increasing permeant size tends to increase the heat of sorption, it follows that larger permeant molecules will be readily sorbed leading to enhanced plasticization of the polymer chains. Consequently, while smaller permeants exhibit greater diffusion coefficients, the polymer will be less plasticized, whereas the lower diffusion coefficient of the larger permeants will be compensated for by the higher degree of sorption. This compensates for the influence of size such that the overall effect is a minimal difference in the permeation coefficients for large and small permeants.

1.7.4 Environmental Conditions

Environmental conditions which are known to affect permeability are temperature, pressure and presence of water in membrane.

1.7.4.1 Temperature

The variation of diffusion, sorption and permeability coefficients with temperature has been shown to be temperature dependent (Barrer, 1939). Thus, since energy E_D is required for diffusion but energy released during sorption for vapours like water (implying that sorption decreases with temperature), from the definitions of permeability, the relationship between the energies is described as follows:

$$E_p = E_D + \Delta H_s \quad \text{Equation 1-19}$$

where ΔH_s is the heat of sorption, E_p is energy of permeation. E_D is positive, hence diffusivity increases with temperature. Consequently, permeability increases or decreases with temperature depending on whether the process is kinetically or thermodynamically driven. Barrer (1939) and Barrer et al. (1958) point out that the least permeable membranes are also the most sensitive to temperature changes. There are other reports describing deviations from the above relation, especially in the region of the T_g of the polymer concerned. A typical example of this pattern are the data of Mears (1954) for the permeation of oxygen in poly(vinyl acetate).

1.7.4.2 Pressure

The effect of pressure is demonstrated in Equation 1-1. It can be seen from this relationship that a direct proportionality exists between the transfer coefficient ($Q/A.t$) and the pressure differential Δp . Theoretically, permeability is independent of Δp . This is because the permeability should reflect a property of a material independent of the outside influences. For permanent gases, this relationship holds provided there are no interactions with the polymer. For other permeants, the relationship between ($Q/A.t$) and Δp is only valid when no such interactions are recorded, otherwise permeability increases with Δp (Koros, 1990; Piringer, 2000; Lin and Freeman, 2003).

1.7.4.3 Presence of Water in the Membrane

Depending on the permeant and polymer under consideration, the presence of water in the polymer may accelerate permeation (Barrie, 1968). This aspect of polymer performance is a key conundrum for the present study. It is found that for permeants where the solubility of water in the polymer is little, the effect of water is negligible. For intermediate cases, the effects appear mixed, with a reduction in gas permeation in some polymers and an increase in some others. Polymers which swell in the presence of water show increasing diffusivity with increasing relative humidity. Highly hygroscopic membranes, such as poly(vinyl alcohol) and cellophane, become plasticized by sorbed water leading to increased diffusivity, and undoubtedly, increased permeability (Lagaron et al, 2001).

The effect of plasticization on membrane permeation has been recently discussed in a review article by Ismael and Lorna (2002). It was reported that, generally, the permeability of a plasticized polymer does not remain constant but increases with as the partial pressure is increased. The authors also state that most glassy polymers, which exhibit Type II or Type III isotherms, show a typical trend of an initially decreasing permeability with increasing partial pressure of the permeant, which then increases after a certain pressure to reach a maximum.

A number of authors on this subject have claimed that that plasticization (by sorbed water, for instance) mainly depends on the number of penetrant molecules rather than polarity of the penetrant. Thus, unlike clustering (which is limited to water molecules), plasticization is observed with a wider variety of polymer-penetrant systems (Ismael and Lorna, 2002; Modesti et al., 2004).

1.7.5 Summary

From the above review of the literature on permeation, it is apparent that sorption and permeation, especially of moisture, into polymeric materials is very complex. Permeation through polymers is dependent on the chemical nature of the polymer as well as its physical state. Moreover, environmental factors, mainly relative humidity and temperature, influence both the extent of sorption as well as the rate of diffusion of a penetrant through the membrane. What is even more significant is the role played by residual moisture, which significantly influences the permeation characteristics of the membrane. In the next section, the philosophy of this thesis is presented. This section aims to present the thesis's problem statement and justification for undertaking research in this area. The research questions are enumerated as well as the objectives, aims and goals of the work.

1.8 THESIS PHILOSOPHY

1.8.1 Problem Statement and Justification of this Study

The problem is that the majority of polymers are sensitive to water. Water affects several physicochemical properties of polymer films, including the mechanical and adhesive strength, and in extreme cases, may lead to the production of cracks or leaching of soluble components in the polymer (Aulton and Abdul-Razzak, 1981; Felton and McGinity, 1997; Marais et al., 2000).

The detrimental effects of water in polymers are thought to arise from the strong plasticizing properties of the water molecules. Sorbed water molecules disrupt polymer inter- and intra-molecular hydrogen bonds, which has the effect of increasing the free volume of the polymer. This can potentially increase the permeability of the polymer to a given penetrant.

In addition, film coatings almost always require the addition of a plasticizer. The plasticizer renders the coating more workable (e.g., facilitates coating). However, plasticizers also lower the glass transition temperature (T_g) of polymers. Moreover, inclusion of a plasticizer, in itself, can modify the moisture sorption properties of a polymer membrane, as demonstrated by the countless studies, e.g., Sala and Tomka (1992), Slade and Levine (1993), Lourdin et al. (1997), Forssell et al. (1998), Lin et al. (2001), Stading et al. (2001), etc., whereby the water sorption isotherms of various polymer films were different depending on whether T_g of the film was above or below the temperature at which the sorption isotherm was recorded. In glassy polymers, the water content was a decreasing function of the surrounding relative humidity (RH) while

the opposite was found for rubbery polymers. Increase in RH was reported to increase mobility of the polymer, thus allowing swelling and sharp increase in permeability.

Moisture barrier coatings are applied onto solid dosage forms to stop the entry of moisture into the product. Being at the front-line, they inevitably become exposed to moisture stress. In functioning as barriers to moisture, therefore, there is a likelihood that their barrier functionality can be compromised. This is a Catch-22 situation. How then can moisture barrier polymer coatings act as a barrier to water when the same water destroys their barrier properties? It can be expected that exposure of a moisture barrier coating to a humid environment can lead to the moisture barrier coating taking up some of the moisture, and given that the deleterious effects of sorbed moisture on the polymer, this would, in turn, compromise the performance of the barrier coating. Clearly, one would like to control or inhibit moisture absorption to prevent these undesirable events. However, in order to control the moisture sorption, the transport mechanisms of the moisture through the barrier coating must be understood. It is a little wonder that moisture sorption by moisture barrier coatings is a topic that commands much technical relevance in applications utilizing coatings.

There is no denying that the topic of moisture sorption and permeation in polymers has been studied for several decades, from the days of Thomas Graham in the late 1800, through the 1960s and even during modern times. This interest has resulted in significant advances in our understanding of moisture-related effects in polymer membranes. One of the most notable factors identified is polymer polarity. Polymer polarity has often been marked out as an important parameter that influences the transport properties of polymers. This aspect has been discussed by a number of authors (e.g., van Krevelen, 1976; Jones, 1994; Prinderre, et al., 1997; Soles et al., 2000). Also, as discussed in section 1-7 above, various other factors which are known to affect permeation are now well documented.

It was stated (in section 1-2 of this thesis) that pharmaceutical moisture barrier coatings are somewhat conceptually different: the requirement for hydrophilicity to effect disintegration must be balanced by the requirement for barrier performance to water vapour. This requirement is not applicable in other moisture barrier coating systems utilised in parallel fields. For instance, there is no requirement for entero-solubility for moisture barrier coatings utilized in electrical circuits in a personal computer. Consequently, the formulation of pharmaceutical moisture barrier coatings imposes constraints. This fact also means that data generated from the functionality of a barrier

coating used for a parallel application may not necessarily be applicable to a moisture barrier coating used in the pharmaceutical sector.

To the present author's knowledge, no work has been previously undertaken to investigate the functionality of pharmaceutical moisture barrier coatings in relation to environmental conditions like relative humidity and temperature. Crucially, no work has been undertaken to determine the functionality of barrier coatings following application to tablet cores of dissimilar hygroscopicity. Given the growing interest in the use of environmentally sustainable technologies, understanding the mechanism of mass uptake and an appreciation of the factors that affect the barrier functionality of pharmaceutical moisture barrier coatings could be vital ingredients in the quest for better barrier coatings. However, the continued unavailability of data on the utility of moisture barrier coatings constitutes a significant obstacle to their successful exploitation.

1.8.2 Research Questions

The main questions that this thesis sought to address are enumerated below:

- (i). What is the effect of environmental conditions, especially relative humidity and temperature, on moisture sorption, desorption and permeation through moisture barrier coatings?
- (ii). Is there a relationship between the total moisture uptake and the amount transmitted by a barrier coating?
- (iii). In what states does sorbed moisture exist in coatings? What is the significance of these states to barrier performance?
- (iv). Many moisture barrier coatings incorporate hydrophobic additive(s) to repel moisture and/or a hygroscopic additive(s) to provide a desiccant function to the coating system. Which approach is more effective?
- (v). What is the role of the nature of the tablet core upon the distribution of sorbed moisture between the film and the core? Is the hygroscopicity of the tablet core significant?
- (vi). It was also intriguing to examine the viability of coating moisture sensitive cores with moisture barrier polymer coatings under drastic conditions typically employed with aqueous-based systems.

1.8.3 Aims and Objectives

This work therefore aimed to study the moisture sorption, desorption and permeation characteristics of four commercially available moisture barrier film coatings. The coatings investigated were ethyl methacrylate copolymer (Eudragit L30 D-55®), amino butyl methacrylate copolymer (Eudragit EPO®), poly(vinyl alcohol) based coating system (Opadry AMB®) and a hypromellose based coating system (Sepifilm LP 10®). Comparisons with two enteric coatings, namely, hypromellose acetate succinate (Aqoat® Type M) and poly(vinyl acetate phthalate) (Sureteric®) were also undertaken. All systems studied were aqueous based coatings, in line with the current industry trend of using environmentally benign aqueous-based dispersions. The coating systems were studied as supplied and used within the suppliers' recommended use levels in order to generate data that were directly relevant to practical situations. In line with the research questions, the goal of this work was to understand the functionality of moisture barrier coatings in relation to the type of the film coating formulation, the relative humidity, temperature and the hygroscopicity of tablet cores on the sorption, desorption and distribution of water in free films and tablet cores.

CHAPTER TWO

Chapter Two

2.0 MOISTURE SORPTION/DESORPTION BY CAST POLYMER FILMS

Outline of Chapter Two

2.1.	Introduction
2.2	Objectives
2.3	Methodology
2.4	Results
2.5	Discussion
2.6	Conclusions

2.1 INTRODUCTION

The moisture sorption-desorption characteristics of polymers are of interest to those involved in fields of technology where polymeric materials come in contact with water as part of their functional roles. Investigations in this area necessitate knowing the amount of moisture taken up by the material under certain conditions of relative humidity and temperature. In addition, details of molecular level interactions between the polymer and the sorbed water molecules are often sought.

There are available several techniques by which sorption in polymers can be studied, including gravimetry, chromatography, thermal-analysis, spectrophotometry, or wet-chemistry. These techniques are reviewed briefly below.

Gravimetry is probably the most common gravimetric technique used to study sorption-desorption phenomena. There are several adaptations of this technique, including the use of desiccators (with saturated salt slurries), climatic test chambers, vacuum systems, and more recently, controlled environment systems, e.g., the dynamic vapour sorption (DVS) (Callahan et al., 1982; Bergren, 1994; Buckton and Darcy, 1995). Desiccators are the most common method for studying sorption, possibly because they are inexpensive. Their main disadvantages relate to the fact the technique is laborious, and that equilibration takes a long time. Further more, temperature and relative humidity measurement can be particularly imprecise. Yet for small changes in mass, the gravimetric method used should have temperature and humidity stability and facilitate accurate measurement of the changes in mass at relatively short intervals. The dynamic vapour sorption technique has the advantage of fast equilibration times while also permitting precise mass measurements. This makes it ideal to monitor small differences materials, which may otherwise not be noticed with conventional methods.

Chromatographic techniques for measuring sorption are typified by inverse gas chromatography (IGC) (Demertzis and Kontominas, 1988; Surana et al., 1997). The principle of IGC is very simple, being the reverse of a conventional gas chromatography (GC) (Thielmann, 2004). A cylindrical column is uniformly packed with the solid material, typically as a powder, fibre or film. A constant concentration of gas, having a known amount of vapour, is then injected down the column at a fixed carrier gas flow rate, and the time taken for the concentration front to elute down the column is measured by a detector. Due to the mass transfer resistance in the solid phase, the vapour in the mobile phase is swept forward while that in the stationary phase lags behind. From the output of the elution peak of the chromatogram, the partition coefficient for the material-water vapour system is determined. The main drawbacks of the technique, perhaps relate to the fact that IGC equipment is expensive, and that even minor variation in surface characteristics of the materials under study can yield significant differences in measured parameters (Ticehurst et al., 1996).

Thermal analysis is a series of techniques in which a physical property is measured as a function of temperature while the substance is subjected to a controlled temperature programme. The two frequently used thermal analysis techniques are differential scanning calorimetry (DSC) and thermogravimetric analysis (TGA). DSC measures heat flow associated with transitions as a function of temperature (Ford and Timmins, 1989) while TGA measures changes in weight of a sample as a function of temperature (Giron, 1997; Heal, 2002). Both techniques have been used, among others, to measure moisture content (Bhaskar et al, 1998) and to discriminate between bound and unbound water fractions in polymer systems (Hatakeyama and Hatakeyama, 1998; Alvarez-Lorenzo et al, 2000).

Spectrophotometric methods include nuclear magnetic resonance spectroscopy (Tishmack et al, 2003), X-ray diffraction (Krogars et al., 2003), dielectric relaxation spectroscopy (Wanchai et al., 1996), infrared spectroscopy, raman spectroscopy, near infrared (NIR) spectroscopy (Ciurczak and Drennen, 2001; Stuart, 2004;), and positron annihilation lifetime spectroscopy (Sastri et al., 1998). These techniques have been used, among others, to identify different water fractions sorbed in polymers.

Wet chemistry methods for determination of water content of materials are typified by the Karl Fischer method. The principle behind this technique is the reaction between iodine and sulphur dioxide in a methanolic hydroxide solution, i.e., the Bunsen Reaction. In principle, the following chemical reaction takes place:



The alcohol reacts with sulphur dioxide and a base to form an intermediate alkyl sulphite salt, which is then oxidized by iodine to an alkyl sulphate. This oxidation reaction consumes water. The water and iodine are consumed in a 1:1 ratio, the excess quantity of iodine can be determined voltametrically, enabling the amount of water in the sample to be calculated. This method is widely used for determining water content in a variety of materials. In many cases, it is selected as a reference method. The main disadvantages are that the working method must be adapted to the specific sample, and that some moisture loss may occur during sample preparation.

2.2 SPECIFIC OBJECTIVES

The main aim of the work presented in this chapter was to compare and contrast moisture sorption, desorption and transmission characteristics of free films of moisture barrier coatings and enteric polymers under fixed-time study regimes. The goal was to understand the influence of the chemical nature of films and the role of environmental conditions on moisture uptake, loss and transmission through the films. An understanding of the sorbed water-polymer interactions was also sought.

2.2 MATERIALS AND METHODS

2.2.1 Materials

Materials used for this work comprised of polymers, plasticizers, surfactants, anti-tack agents, fillers and other formulation additives. They were used in the fabrication of the cast polymer free films. The descriptions, which are presented in the following paragraphs below, were mainly obtained from the Handbook of Pharmaceutical Excipients, 3rd Edition, 2000, unless otherwise specified, in which case, specific references applicable are indicated.

2.2.1.1 Polymers for Preparing Coating Dispersions

Coating dispersions from which free films were obtained (and subsequently for the coating of tablet cores as discussed in Chapter Four) were prepared from the following materials: Eudragit L30 D-55, having ethyl methacrylate copolymer as the main polymer; Eudragit EPO, which was composed of amino butyl methacrylate copolymer; Sepifilm LP 10, constituted from hypromellose; Shin-Etsu Aqoat, having Shin-Etsu Aqoat; Opadry AMB, containing poly(vinyl alcohol); and Sureteric, having poly(vinyl acetate phthalate). Further details on these polymers are provided below:

2.2.1.1.1 Eudragit L30 D-55

Eudragit L30 D-55 is a coating prepared with ethyl methacrylate copolymer as the main polymer. Ethyl methacrylate is a 1:1 copolymer of methacrylic acid-ethyl acrylate (molecular weight (M.W) 250000). It is usually supplied as a 30% aqueous dispersion under the trade name Eudragit L30 D-55® for formulation of enteric coatings (Lehmann, 1997). The obtained coatings dissolve above pH 5.5 (Bauer et al, 1998). However, the manufacturer recommends that a polymer weight loading of 1 mg/cm² corresponds to a film thickness of approximately 8 µm and can be used as a moisture barrier coating. The material for this work (Lot No. 1211214316) was a free of charge (FOC) sample from Rohm Pharma, Darmstadt, Germany.

2.2.1.1.2 Eudragit EPO

Eudragit EPO is amino butyl methacrylate copolymer, a cationic copolymer of butylmethacrylate-(2-dimethylaminoethyl) methacrylate–methylacrylate in the ratio of 1:2:1 (M.W ~150000) (Lehmann, 1997). It is a fine white powder with a slight amine odour. Coatings are formulated as aqueous emulsions of the polymer, with or without hydrophobic plasticizers, fatty acids and ionic surfactants, and exhibit pH dependent solubility (soluble in gastric fluids up to pH 5.0 but are swellable and permeable above this pH). The recommended application level is a polymer loading of 4 mg/cm². The material used was Eudragit EPO® (Lot No. 041 0231047) and was obtained from Rohm Pharma GmbH as an FOC sample.

2.2.1.1.3 Shin-Etsu Aqoat

Aqoat is essentially hypromellose acetate succinate, which is a relatively new polymer, developed by Shin-Etsu Chemical Company, Tokyo, Japan. It is marketed under a trade name of *Aqoat*®. It is available in three grades, all of which solubilize in buffer solutions above pH 5.5. Like other enteric polymer coatings, hypromellose acetate succinate possesses carboxyl functions that form salts in solution of high pH rendering the coating soluble. The recommended coating level is 8-10 % weight gain (Nagai et al., 1996) for enteric applications. *Aqoat*® (Type M) was a FOC sample from Shin-Etsu.

2.2.1.1.4 Opadry AMB Coating System

Opadry AMB is a proprietary coating system containing poly(vinyl alcohol) as the main polymeric film former. Poly(vinyl alcohol), is a synthetic water soluble polymer represented by the formula (C₂H₄O)_n where n lies between 500-5000 (M.W range of 30000 - 200000) (Bauer et al, 1998b). In addition to the polymer, titanium dioxide, talc,

lecithin soya and xanthan gum are included in the formulation. Coatings from this system have pH-independent solubility. They are prepared for use as a 20 % w/w aqueous suspension. The recommended coating levels are a minimum of 4.0% weight gain. The material used in this work was Opadry AMB (Batch No. DY S20061) which was obtained from Colorcon Limited, Dartford, UK as a FOC sample.

2.2.1.1.5 Sepifilm LP Coating System

Sepifilm LP is a proprietary ready-to-use formulation of hypromellose, stearic acid, microcrystalline cellulose and titanium dioxide. Hypromellose, which is partly-0-methylated and 0-(2-hydroxylatedpropylated) cellulose, is the film former. It has a molecular weight of 100000-1500000. Coatings are prepared as 12.5% w/w aqueous dispersions. A minimum application level of 3.0 % weight gain is the recommended level for moisture protective coatings (Sepifilm LP Technical Data Sheet, Seppic). The material used for this work was a FOC sample (Sepifilm LP 014® Lot No. 34371) from Seppic S.A, Paris, France.

2.2.1.1.6 Sureteric Coating System

Sureteric is also a ready-to-use coating system containing poly(vinyl acetate phthalate) as the film former. Poly(vinyl acetate phthalate) contains dicarboxylic phthalic acid in a partially esterified form, making it suitable for use as an enteric polymer. Sureteric is supplied as a white to yellowish powder ready-to-use system for sealing cores in sugar coating or as an enteric coating. Other constituents present are plasticizer (PEG 400) (11.8%), pigments, mainly titanium dioxide (11.8%) and 2.5% other materials. Enteric coatings are applied at a level of 8-10% weight gain and are soluble above pH 4.5 (Bauer, 1999b). Sureteric was also obtained as a FOC sample from Colorcon Limited.

2.2.1.2 Other coating formulation additives

Preparation of the different coating dispersions required several other additives, in addition to the constituent polymers. These were plasticizers, surfactants, antitacking agents, hydrophobic agents, fillers, etc. Further details are provided below:

2.2.1.2.1 Triethyl citrate

Triethyl citrate (2-hydroxy-1,2,3-propanetricarboxylic triethyl ester, formula $C_{12}H_{20}O_7$, M.W 276.29) is a water soluble colourless oily liquid. It is used as a plasticizer in film coatings (Gutierrez-Roca and McGinity, 1994). Triethyl citrate (Lot No. S35325 208) was purchased from Merck, Schuchard, Hohenbrunn, Germany.

2.2.1.2.2 Carboxymethylcellulose sodium

Carboxymethyl cellulose sodium (also known as carmellose sodium) is the sodium salt of a polycarboxymethyl ether of cellulose (M.W 90000 – 700000). It normally occurs as a white, odourless powder. It is sometimes used in film coatings as a film former, but also occasionally as glossant, pigment binder and as a stabilizing agent. Carboxymethylcellulose sodium (Batch No. 0244829) was purchased from Fisher Scientific, Loughborough, UK.

2.2.1.2.3 Polyethylene glycol

Polyethylene glycol (PEG) ($\text{HOCH}_2(\text{CH}_2\text{OCH}_2)_m\text{CH}_2\text{OH}$, where m is the number of oxyethylene groups, M.W 200-10000) is a series of addition polymers of ethylene oxide and water. It is used in a wide variety of dosage forms (Kellaway and Marriott, 1975; Ford and Rubinstein, 1980). In tablets, for instance, PEGs are used to improve the effectiveness of tablet binders and to impart plasticity to the granules. In film coatings, PEGs are used as pigment binders or as glossing agents. The material used in this study was PEG 6000 (Lot No. 440454/1) and was purchased from Sigma Aldrich Co. Ltd, Gillingham, Dorset, UK.

2.2.1.2.4 Talc

Talc [$\text{Mg}_6(\text{Si}_2\text{O}_5)_4(\text{OH})_4$] is a fine, white or whitish mineral powder. It is hydrophobic and insoluble in water. Talc is regularly used as a lubricant in tablets and capsules (Dawoodbhai and Rhodes, 1990) and also as a dissolution retardant (Fassihi, et al., 1994). In film coatings, talc is very commonly used as an opacifier and as an anti-tacking agent. Talc, extra pure grade (Lot No. K27404368) used in this study was purchased from BDH Laboratory Supplies, Poole, UK.

2.2.1.2.5 Magnesium stearate

Magnesium stearate (empirical formula $\text{C}_{36}\text{H}_{70}\text{MgO}_4$, M.W 591.34) is a fine, white impalpable powder with a faint odour of stearic acid. It is a very hydrophobic material and has been long known to retard dissolution of drugs in tablet and capsule formulations (Hussain et al., 1992). Magnesium stearate is also frequently added to coatings, where it is utilised as a moisture regulator (for instance, in moisture barrier coatings). Alternatively, magnesium stearate can be used in film coatings as an anti-tack agent, whereby it is used to minimise sticking during coatings. In tablet formulations, magnesium stearate is the lubricant of choice. Magnesium stearate used in this work was lot No. 03190 and was purchased from Sigma-Aldrich.

2.2.1.2.6 Stearic acid

Stearic acid is described in the USP as a mixture of stearic acid ($C_{18}H_{36}O_2$) and palmitic acid ($C_{16}H_{32}O_2$, M.W is 284.47). It is a white crystalline solid or powder obtained from fat or dehydrogenation of cotton seed oil. In solid dosage forms, stearic acid is used as a lubricant. In other cases, it is used as an emulsifying and solubilizing agent. It is included in moisture barrier coating formulations as a moisture repellent. The material used in this work was stearic acid, extra pure (Lot No. U05424) and was purchased from Sigma Aldrich.

2.2.1.2.7 Sodium lauryl sulphate

Sodium lauryl sulphate (otherwise known as dodecyl sodium sulphate) (empirical formula $C_{12}H_{25}NaO_4S$, M.W 288.88) is a whitish or sometimes yellowish powder, crystalline solid or flaky material. It is obtained by sulfation of lauryl alcohol. Sodium lauryl sulphate is used as an anionic surfactant, as a lubricant in solid dosage forms and as a wetting agent in film coating formulations. It is a non-hygroscopic material and is freely soluble in water and alcohols. Sodium lauryl sulphate used in this study (Lot No. 31K0089) was purchased from Sigma Aldrich.

2.2.1.2.8 Titanium dioxide

Titanium dioxide (TiO_2 , M.W 79.9) is a white, very fine powder (with an average particle size of 1.0 μm). Normally, however, it exists as agglomerated lumps with an approx. diameter of 100 μm . Owing to its unique light scattering properties, titanium dioxide is used as an opacifier and pigment in film coating formulations. With regard to its physical properties, it is practically insoluble in water and is also non-hygroscopic. Titanium dioxide (Lot No. 11780) was purchased from Sigma Aldrich.

2.2.1.2.9 Xanthan gum

In the USP, xanthan gum is described as a high molecular weight polysaccharide gum. It contains glucose and mannose as the dominant hexose units, but also D-glucuronic acid. The molecular weight is approx. 2×10^6 . Each xanthan gum monomer contains five sugar residues, i.e., two glucose units, two mannose units, and one glucuronic acid unit. The polymer backbone consists of four β -D-glucose units linked at the 1 and 4 positions, and is thus, identical in structure to cellulose. However, it is distinguishable from cellulose in having trisaccharide side chains on alternating anhydro-glucose units. It is widely used in tablet formulations as a stabilizing agent. The material used in this study (Lot 90K0157) was purchased from Sigma Aldrich.

2.2.2 Methods

2.2.2.1 Preparation of Coating Dispersions

2.2.2.1.1 Eudragit L 30 D-55

The formula for preparing an aqueous dispersion of Eudragit L30 D-55 is shown in *Table 2-1* below. This was a standard formula supplied by the manufacturer. The quantities shown in the table were computed on the basis of a 15% w/w aqueous polymer dispersion required to coat a charge of 500 g of tablet cores (7.0 mm diameter, 4.0 mm height, 200 mg in weight (W), surface area (A) = 183 mm²) at a polymer loading level $\lambda=1.0$ mg/ cm². The relationship below was used to establish the amount of polymer (per cent basis) for this batch:

$$\text{Polymer quantity (\%)} = \varphi = \frac{(A).\lambda}{W} = \frac{183 \times 1.0}{200} = 0.925 \quad \text{Equation 2-1}$$

Ingredient	Weight (g)
<u>Polymer solution</u>	
Eudragit L30 D-55 (30 % w/w dispersion)	4.625
Triethyl citrate (3.0 % of polymer)	1.250
Water (distilled/deionised–In-house)	5.000
<u>Pigment suspension</u>	
Talc (50.5 % by weight of polymer)	2.080
Titanium dioxide 30.0 % of polymer)	1.250
PEG 6000 (5.0% of polymer)	0.210
Carboxymethylcellulose sodium (1.5 % of polymer)	0.062
Water (distilled/deionised – In-house)	10.000

Table 2-1. Formula Used to Prepare Eudragit L30 D-55 Aqueous Dispersion

The procedure for preparing the Eudragit L30 D-55 polymer dispersion was as follows:

- (i). The specified quantity of Eudragit L30 D-55 and triethyl citrate were dispersed in water in a beaker with the aid a propeller stirrer. Mixing was undertaken for about 5 min at moderate stirrer speeds.
- (ii). In a separate beaker, the PEG 6000 was dissolved in the required quantity of water. Talc, titanium dioxide and carboxymethylcellulose sodium were then added and the mixture homogenised with the aid of a high shear stirrer (IKA-Werke GmbH & Co. KG, Staufen, Germany) for about 10 min.

- (iii). The pigment suspension was subsequently stirred into the polymer dispersion. The resulting mixture was passed through a 250 μm screen.
- (iv). Regular, gentle stirring of the prepared dispersions was undertaken throughout use to keep the dispersion particles in suspension.
- (v). Any excess amount of dispersion remaining was kept under refrigeration and used within 2 weeks of preparation.

2.2.2.1.2 Eudragit EPO

The formula for preparing an aqueous dispersion of Eudragit EPO is shown in *Table 2-2* below (This was also a standard formula supplied by the manufacturer). The quantities were computed on the basis of a 15 % w/w dispersion calculated for a charge of 500 g of tablet cores (7.5 mm diameter, 4.0 mm height, 200 mg in weight (W), surface area (A= 183 mm²) with a polymer requirement of $\lambda=4.0$ mg/ cm² using the relationship below:

$$\text{Polymer quantity (\%)} = \varphi = \frac{(A).\lambda}{W} = \frac{183 \times 4.0}{200} = 3.70 \quad \text{Equation 2-1}$$

Ingredient	Weight (g)
Eudragit EPO as a powder	18.500
Sodium lauryl sulphate (10.0 % of polymer)	1.850
Stearic acid (15.0 % of polymer)	2.800
Magnesium stearate (35.0 % of polymer)	6.5000
Water (distilled/deionised – In-house)	150.000

Table 2-2. Formula Used to Prepare Amino butyl methacrylate Dispersion

The Eudragit EPO polymer coating dispersion was prepared as follows:

- (i). First, the sodium lauryl sulphate (SLS) was dissolved in part of the water with the aid of a propeller stirrer. After about 2 min, when the SLS had dissolved, the polymer was added carefully to avoid the formation of lumps. The mixture was then stirred for about 10 min to obtain a consistent dispersion.
- (ii). The stearic acid was subsequently added to the polymer dispersion and stirred for a further 5 hours. It was found necessary to raise the temperature of the dispersion to about 45 °C to facilitate dispersion of the stearic acid.

(iii). In a separate container, a homogenate of magnesium stearate and the remaining water was prepared using a high shear stirrer for 10 min.

(iv). The obtained suspension was then gently stirred into the polymer dispersion. It was necessary to pass the resultant dispersion through a 250 μm screen to remove froth and trapped air bubbles.

2.2.2.1.3 Shin-Etsu Aqoat (Hypromellose acetate succinate)

The manufacturer's recommended formula for preparation of Aqoat aqueous dispersion is shown in *Table 2.3* below (Nagai et al., 1996). The manufacturer also recommends a standard procedure by which an aqueous dispersion of this polymer must be prepared. This is as follows: First, the water must first be cooled to ≤ 15 $^{\circ}\text{C}$ (this low temperature is required to prevent the coagulation of the plasticizer during coating when the temperature is raised). After which, the plasticizer is added, which in this case, is triethyl citrate. The mixture is then stirred for 2-3 min. Sodium lauryl sulphate is then added to this mixture and stirring continued until the mixture has adequately dispersed/dissolved. The required amount of hypromellose acetate succinate and the talc are then added and the dispersion stirred for a further 30 minutes to produce a consistent dispersion. The dispersion is subsequently passed through a 250 μm screen to remove any extraneous materials. This procedure was what was used to prepare an aqueous dispersion of this polymer.

Ingredient	%
Hypromellose acetate succinate	10.0
Triethyl citrate	3.0
Talc	1.0
Sodium lauryl sulphate	1.0
Water	85

Table 2-3. Formula Used to Prepare Shin Etsu Aqoat Dispersion

2.2.2.1.4 Opadry AMB, Sepifilm LP and Sureteric

Opadry AMB, Sepifilm LP and Sureteric are ready-to-use powders that, unlike the polymers above, required very little input, in terms of preparation of the dispersions. Table 2-4 below gives a summary of the main constituents in the respective polymer film systems (The quantitative formulas were not supplied by the manufacturers since these are proprietary products):

Opadry AMB®	Sepifilm LP®	Sureteric®
Poly(vinyl alcohol)	Hypromellose	Poly(vinyl acetate phthalate)
Xanthan gum	Microcrystalline cellulose	PEG 4000
Lecithin soya	Talc	Stearic acid
Talc	Stearic acid	Sodium alginate
Titanium dioxide	Titanium dioxide	Titanium dioxide

Table 2-4. Qualitative Formulas for Opadry AMB, Sepifilm LP and Sureteric Coating Systems

The procedure for preparing the coating dispersions in all the cases above was very straightforward. In the first place, the appropriate amounts of the powders were reconstituted with water in order to obtain, respectively, 20 % w/w, 15 % w/w and 12 % w/w aqueous dispersions. Powders were dispersed with the aid of a propeller mixer and were stirred at medium speed for a minimum of 45 min. The obtained dispersions were subsequently filtered through a 250 µm sieve.

2.2.2.2 Preparation of Free Films

Free films were prepared by the casting technique from dispersions of the polymers prepared as described above. The procedure is outlined below:

- (i). A quantity of the dispersion, left standing overnight to expel trapped air, was poured onto a clean Teflon coated glass plate mounted on a level surface. The dispersion was spread over the surface with the aid of a draw down bar.
- (ii). The casts were left to air dry for 3 hours and then transferred into an oven and where they were dried at 40 °C under vacuum (1000 mbar) for 8-12 hours.
- (iii). Thereafter, moulds were removed from the oven and allowed to cool to room temperature. Subsequently, the casts were transferred into a desiccator containing a saturated solution of potassium carbonate at room temperature (to provide 45 % RH) where they were left for 6 hr.
- (iv). The obtained films were then peeled from the moulds and examined under a microscope for any defects and cracks.
- (v). Film thickness was measured to the nearest 0.001 mm with a digital micrometer (Mitutoyo Corporation, Japan). Measurements were made in at least three separate areas of the film from which an average thickness was obtained.

(vi). The films were subsequently placed in resealable plastic bags and stored in amber coloured glass bottles pending further use.

2.2.2.3 Scanning Electron Microscopy Studies

Scanning electron microscopy (SEM) studies were performed using a Philips XL 20 scanning electron microscope (Philips, Cambridge, UK) on representative samples from each set. The specimens were coated with a gold palladium mixture and mounted on a sample holder whereupon they were examined at an accelerating voltage of 5–15 kV depending on the magnification required.

2.2.2.4 Gravimetric Moisture Sorption and Desorption Studies

2.2.2.4.1 Description of technique

Moisture sorption-desorption studies were undertaken by the gravimetric sorption technique. This technique employs an integrated microbalance system to automatically measure changes in the mass of a material in response to sorption or desorption of a gas or vapour. There are two main variations of gravimetric vapour sorption systems, namely, systems which employ a vacuum and rely on the system pressure to measure the relative humidity; and controlled atmosphere systems which use an inert gas (e.g., N₂) to transport vapour to the sample. Unlike vacuum systems, pressurisation is not required in controlled atmosphere systems. These systems can be operated at room temperature, even at high relative humidity, since gas flow is able to restrict a high dew point gas to the sample.

The dynamic vapour sorption (DVS) apparatus (manufactured by Surface Measurement Systems, London, UK) is an example of controlled atmosphere gravimetric vapour sorption system and was the one used in this work to study moisture sorption and desorption. This apparatus consists of three sub-components, namely, a balance system, flow controller and saturator, and a relative humidity measuring system. The three sub-components are interfaced by a computer which serves as the data management system. A schematic illustration of the DVS equipment is shown in Figure 2-1 below.

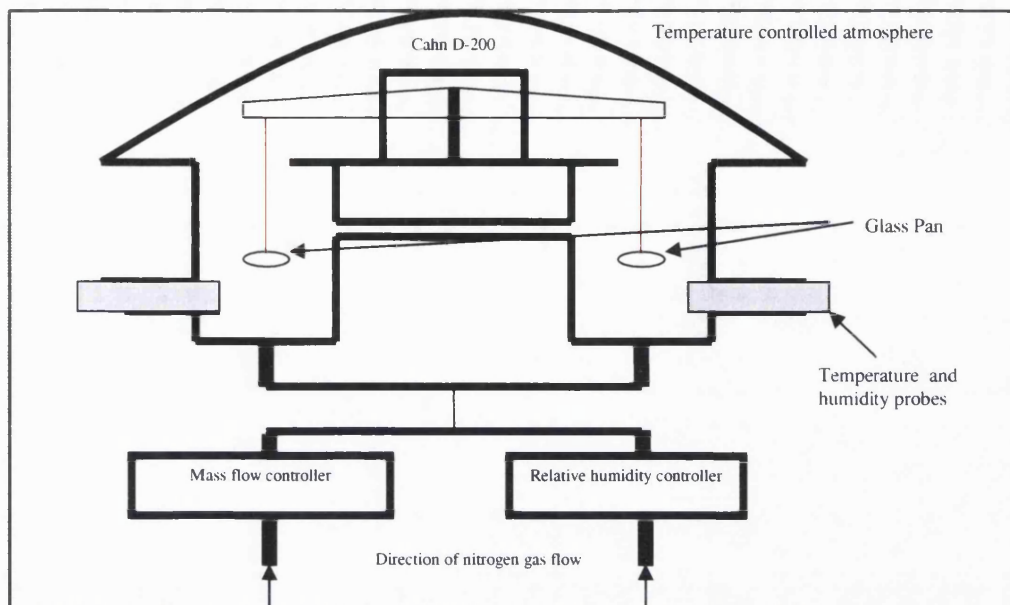


Figure 2-1. Schematic Illustration of a Dynamic Vapour Sorption (DVS) Apparatus

The balance system, which is a key component of the DVS, is a taut band suspension electromagnetic compensation type-balance. The DVS uses a CAHN D200 balance, mounted inside a glass vacuum bottle and completely sealed from the sample environment. Two glass pans, one for the sample and the other as the reference, are suspended from inside the glass vacuum bottle.

Humidity is generated by bubbling dry N_2 through water while flow controllers, via a set of valves, regulate the ratio of the dry N_2 to the humidified gas, hence the RH. The RH is measured downstream of the sample by sensors. The DVS uses polymer capacitance sensors and digital RH indicators with a response time of 5 s, and an output signal readable to ≥ 0.05 %RH. The accuracy of the polymer sensor is specified as $\pm 2\%$ over a 0-90 % RH range. The computer, with specialised software (DVS WIN, Surface Measurement Systems) allows pre-programming of the sorption-desorption regimes for a given experiment.

Typically, an experiment consists of several step changes in RH. These initiate changes in the flows, hence the RH of the gas. The sample responds to the new RH with a change in weight. The step change is deemed complete when the sample attains a new equilibrium weight, which is confirmed by the software when successive points lie in a pre-defined interval. At each time point, the time, sample weight, temperature and % RH. Uptake (or loss) M (% dry basis, db) is calculated from the

weight, M_t recorded by the balance at time t and the weight, M_d of the dry sample at time $t=0$ (Equation 2-3).

$$M = \frac{M_t - M_d}{M_d} \times 100 \quad \text{Equation 2-3}$$

Calibration and validation for weight and RH are performed on monthly basis under regular use. Weight calibration is done using a 100 mg tare weight while % Rh calibration is by the use of saturated salt solutions of LiCl and NaCl. Accuracy of the technique may be assessed by the weight variation of an empty pan.

2.2.2.4.2 Experimental procedure

Rectangular film samples, weighing between 85-100 mg, were used for moisture sorption-desorption studies in the DVS. All experiments were repeated at least three times. Moisture-sorption desorption profiles were obtained by using three test protocols, i.e.: 0-50-0-50-0, 0-75-0-75-0 and 0-90-0-90-0 with each step change lasting 300 min. Experiments were done at 25 and 40 °C, unless indicated otherwise.

2.2.2.5 Measurement of Moisture Vapour Transmission Rate

2.2.2.5.1 Description of the technique

The moisture vapour transmission rate (MVTR) is the amount of water vapour that flows through a unit surface area of film under steady-state conditions at constant pressure. It is commonly measured by the cup method (ASTM E96-93). In this method, a polymeric film under test seals a container with water or a suitable desiccant. The container is then placed in a humidity-controlled environment. The water vapour permeating through the film is determined by the rate of weight decrease of the container.

Several semi-automated or fully automated techniques are commercially available for measuring MVTR. These techniques are described by the ASTM F-1249-90 standard. An example of such systems is the WPA-100 Permeability Analyzer from VTI Corp, Florida, USA. This system, a simplified flow plan of which is shown in Figure 2-2 below, is made up of the five components, namely, a gas supply system, which is usually dry N_2 gas, a permeation cell; mass flow controllers, a humidity generator, and a data acquisition system. (Humidity generators and Mass flow meters are very similar to those described for the DVS).

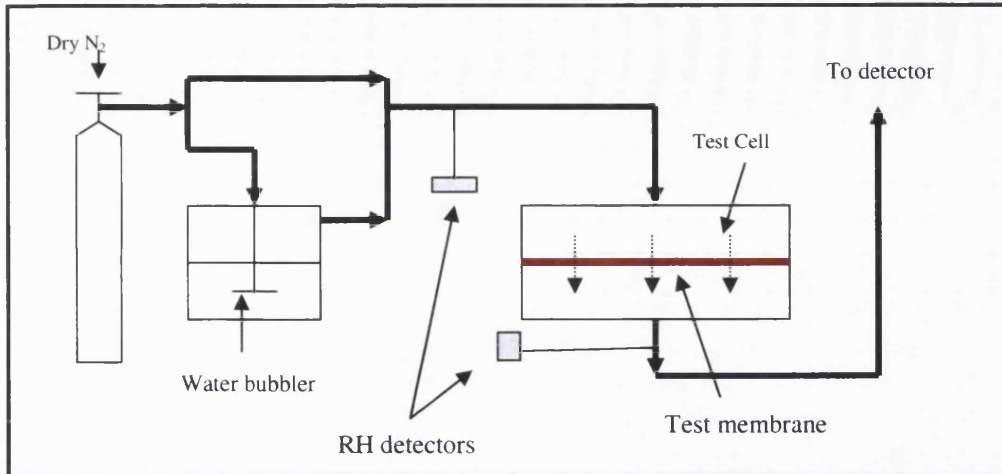


Figure 2-2. Schematic Flow Diagram of a WPA-100 Permeability Analyser

The film, of known thickness and surface area, is placed in the permeation cell. The cell is sealed with the help of cork screws. Water vapour, generated by the system, then crosses the membrane to reach an opened volume swept away by a gas stream. The stream of gas (N_2) flowing at a known rate (f) at normal pressure, carries the vapour with a partial pressure p_1 . This gas pulls the penetrant towards the RH detector. At steady state permeation, the value of partial pressure in the second chamber p_2 is reached. The moisture transmission rate can then be obtained with the aid of Equation 2-3, where c_2 is the concentration of the test gas in the second chamber expressed as a dimensionless ratio of p_2 to the total chamber pressure p (Piringer, 2000; Hu et al., 2001; Flaconnéche et al., 2001):

$$MVTR = \frac{p_2 \cdot l}{p \cdot A} = \frac{f \cdot c_2}{A} \quad \text{Equation 2.3}$$

Routine calibration of the humidity detectors is done with a chilled-mirror dew point meter (accuracy of 0.1 °C) and saturated NaCl solutions. The flow meters are calibrated with a floating ball flow meter (10 ml/min).

Since the WPA-100 is an automated system, minimal operator effort is required after this other than loading the sample and recalling the experimental protocol from an archived template. Temperature ranges within which the machine operates are 23° C to 50° C, while the humidity ranges from 2% to 98% RH. The data is generated on-line and is accomplished using a simple MS Excel macro that also provides tabular and graphical representation of the generated data.

2.2.2.5.2 Experimental procedure

In this experiment, films were carefully cut into thin sheets (measuring at least about 50 cm² in area). The thickness was measured with a micrometer gauge. The films were then placed in the permeation cell and the upper cork screws fastened. Once the system had attained steady-state (judged by a stable baseline), measurement of the WVTR was then commenced. Experiments were done in triplicate at 0-50, 0-75 and 0-90 % RH (25 °C) gradients.

2.2.2.6 Thermogravimetric Analysis

2.2.2.6.1 Description of technique

Thermogravimetric analysis (TGA) was undertaken using a Hi-Res TGA, Model 2950 (Thermal Analysis Instruments, Delaware, USA). This was to determine mass loss and hence moisture content, and the state of moisture in the polymer films.

TGA uses a precise thermobalance to measure the change in mass of a sample as a function of temperature or time. The sample, placed on a pan suspended from a microbalance, is heated in a furnace under a purge of N₂ gas according to a defined time-temperature programme. Figure 2-3 is a schematic illustration of a typical TGA instrument. The instrument is linked to the computer via a thermal analysis controller (TAC 7/DX for TA Instruments TGA) which converts the analogue signal from the TGA into digital format for the computer. The computer is equipped with software that enables the operator to programme the analysis.

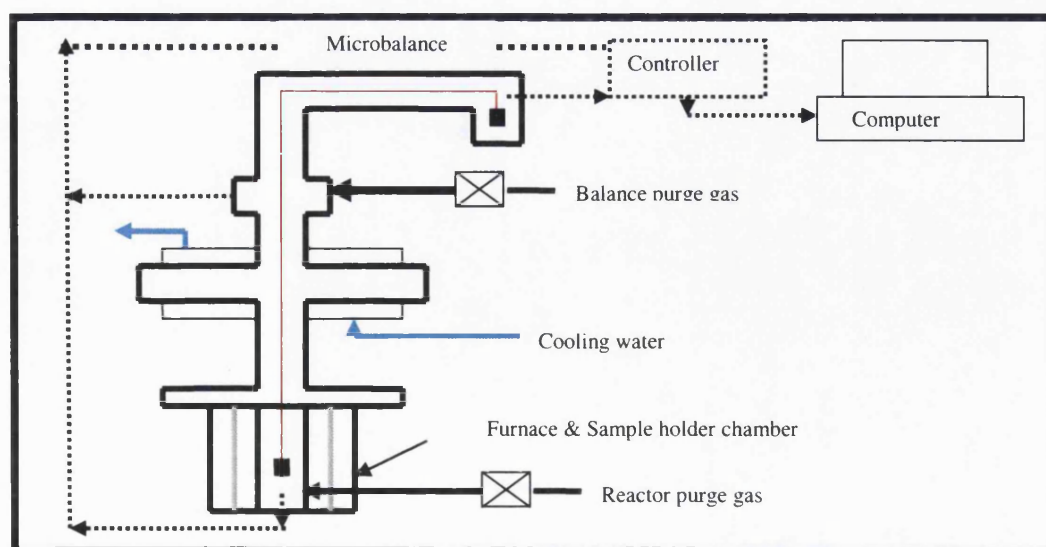


Figure 2-3. Schematic Illustration of a Thermogravimetric Analysis (TGA) System

2.2.2.6.2 Experimental procedure

To carry out an analysis, the sample (usually 5-15 mg) is placed into a sample pan. The balance is zeroed, and the sample heated according to a predetermined thermal cycle. The weight signal is sent to the computer for processing, along with the sample temperature and the elapsed time.

In the present study, thermogravimetric analysis was performed on sample moisture barrier films (pre and post-exposure to 50, 75 and 90 % RH) using a Thermal Analysis Instruments TGA (Model Hi-Res TGA 2950, Thermal Instruments, Delaware, USA). Mass and temperature calibrations were performed on the instrument before use. The sample pans used were aluminium open-type pans (non-hermetic/without a lid). The weight of film samples varied between 5 and 10 mg. The heating cycle consisted of an isothermal scan at 25 °C for 30 min. This was immediately followed by a temperature scan from 25 to 400 °C or until the sample decomposed.

2.2.2.7 Near Infrared Spectroscopy

2.2.2.7.1 Description of technique

NIR spectra of the moisture barrier films were collected with the aid of a specially adapted optical reflectance NIR probe (Foss NIRSystems, Maryland, USA). The probe was placed approx. 4 mm below the DVS quartz glass sample pan (refer to Figure 3.1) enabling collection of spectra simultaneously as moisture sorption-desorption studies were being undertaken. A description and applicability of this technique has already been provided by Lane and Buckton (2000).

In NIR spectroscopy, four absorption bands at 760, 970 nm, 1190 nm, 1450 nm and 1940 nm are attributed to the second overtone of the O-H stretching band ($3\nu_{1,3}$), the combination of the first overtone of the O-H stretching and the O-H bending band ($2\nu_{1,3}+\nu_2$), first overtone of the O-H stretching band ($2\nu_{1,3}$) and the combination of the O-H stretching band and the O-H bending band ($2\nu_{1,3}+\nu_2$). The presence of shifts in wavelength is the result of altered bond strengths due to molecular conformational changes arising from bending of the bonds, or by forming, bending or breakage of other bonds in the vicinity of the O-H bond, while changes in intensity are due to changes in the number of bonds vibrating with a specific frequency (Luck, 1974; Ciurczak, 2001). This is the reason why NIR technique can be used to measure moisture uptake as well as the state of sorbed water in polymeric films since these changes instigate shifts in intensity/wavelength of the NIR spectra.

2.2.2.7.2 Experimental Procedure

The first step in using NIRS is to perform a calibration. This requires collection of reference spectra containing all the chemical or physical attributes likely to be present in the samples to be analysed. Where quantitative measurement is to be done, this allows the user to establish a multiple linear regression between the NIR spectra data and the chemical parameters of the analysed samples.

In this study, data collection was set at $t=0$ and every 30 min from commencement of the sorption-desorption experiment. The NIRS instrument recorded the mean spectra of 32 scans over the wavelength region of 1100 to 2500 nm. Data were processed and analysed with the aid of Vision® software (Version 2.21) (Foss NIRSystems). Calibration of the instrument was undertaken with a supplied ceramic crystal, which provided a background spectrum against which experimental data were recorded. Calibration was undertaken before each experiment was done.

2.4. RESULTS

2.4.1 Film Appearance and Characteristics

In order to minimize unacceptable variations in the results arising from the possible use of sub-standard film samples or films with variable characteristics, it was necessary to examine the manufactured films to establish whether they were suitable for use in the subsequent investigations. This undertaking also served as a way of verifying the film manufacturing technique. This task was undertaken, first by examining the films with the aid of a scanning electron microscope, and secondly by determining their dimensions. There was no opportunity to measure mechanical properties, like tensile strength and elasticity, due to lack of equipment.

In general, the manufacturing technique used yielded films that were satisfactory. The typical average thickness of the films, measured in at least three places across the film, was as follows: Eudragit L30 D-55, 193.3 (13.1) μm , Eudragit EPO, 249.7 (16.6) μm , Opadry AMB, 228.1 (15.8) μm , Sepifilm LP (208.3 (30.7) μm , Aqoat, (187.0 (22.1) μm and Sureteric 202.1 (10.5) μm . These films were much thicker than what would be applied on a typical tablet core. This was borne out of the need to obtain films that would yield a weight of >80 mg for an area of $\approx 1.5 \text{ cm}^2$ so that the full area of the sample pan in the dynamic vapour sorption equipment was covered by the film. One way of achieving this was to make the films thicker.

Scanning electron microscopy was used to assess the adequacy of the method to produce films without cracks and defects. An example of a typical film sample is shown in Figure 2.4 below. It can be seen from this micrograph that the film was of a consistent texture and no cracks are visible even at this high magnification.

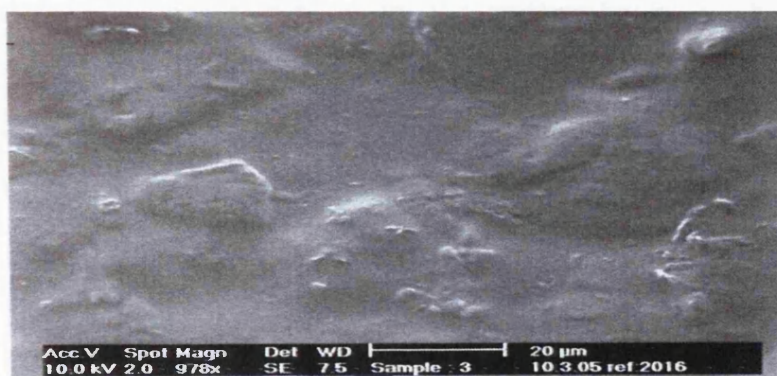


Figure 2-4. Scanning Electron Micrograph (SEM) of a Typical Sepifilm LP Cast Film (Magnification x 978)

The mechanism by which polymer films are formed from aqueous dispersions is not well understood. It is, however, accepted that film formation process involves several successive steps, i.e., concentrations of the dispersion resulting from evaporative loss of water, particle contacting, penetration and deformation, and polymer chain interdiffusion (Bradford and Vanderhoff, 1973; Guo et al., 1993). It is thought that the evaporative loss of water drives the polymer particles close together which causes the film of water surrounding the particles to shrink. This generates forces which drive the particles even closer. The film is then formed as a result of particles coalescing. Coalescence is facilitated by appropriate plasticization and/or drying at the so-called minimum film forming temperature.

It can be judged from the paragraph above that in order to obtain a polymer film, some form of phase inversion is required. Therefore, most film manufacturing techniques involve rendering an initially homogeneous polymer solution or dispersion thermodynamically unstable. This causes the phases to separate into polymer-lean and polymer-rich phases. The polymer-rich phase forms the matrix of the membrane, while the polymer-lean phase, rich in solvents and nonsolvents, fills the pores. Depending on factors like the evaporation conditions, initial thickness and composition of the polymer solution, membranes ranging in characteristics, e.g., dense to highly asymmetric, can be obtained (Altinkaya et al., 2005).

The range of techniques that can be used to manufacture films is wide. These techniques include casting, coacervation, solidification (of molten film forming material by cooling), dipping/immersion followed with drying, and, spray application. Casting, however, is the most widely used because it yields films of fairly uniform thickness, and provided the casting surface is smooth and flat, the thickness of the film can be controlled by using a spreader (Spitael and Kinget, 1977; Donhowe and Fennema, 1994). Some workers have questioned the reliability of data generated from cast free films. This is because casting, owing to its static character, will usually generate films with a more tightly packed structure than the alternative methods for obtaining free films. For purposes of simulating coatings on solid dosage forms, for instance, it has been suggested that spray application would be more appropriate. Aulton (1995) explained that although sprayed films were more realistic, they were less easy to control during manufacture. Cast films, on the other hand, were more consistent and well suited to studying fundamental material properties. For this reason, casting was adopted as the method of choice for manufacturing free films for this work.

2.4.2 Moisture Sorption-Desorption Profiles

The main objective of undertaking moisture sorption-desorption experiments was to determine qualitative and quantitative differences in the moisture uptake and loss from free films following exposure to repeat cycles of dry and humid conditions for a fixed time period. These experiments were conducted in a dynamic vapour sorption apparatus (DVS) as described in section 2.2.2.3.

The results obtained from these studies for the four moisture barrier films, i.e., Eudragit L30 D-55, Eudragit EPO, Opadry AMB and Sepifilm LP, are graphically presented in Figures 2-5, 2-6, 2-7, and 2-8. All the charts shown below were generated using the DVS Win software macro in MS Excel. They depict the percentage dry basis (db) mass change of the films (% g of moisture/g of film) on the primary y-axis versus time (in minutes) on the x-axis as the RH was alternated between dry (0 % RH) and wet phases (either 50, 75 or 90 % RH) (on the secondary y-axis). It is also worthwhile to mention that the figures shown are representative of trends observed in at least three experimental runs.

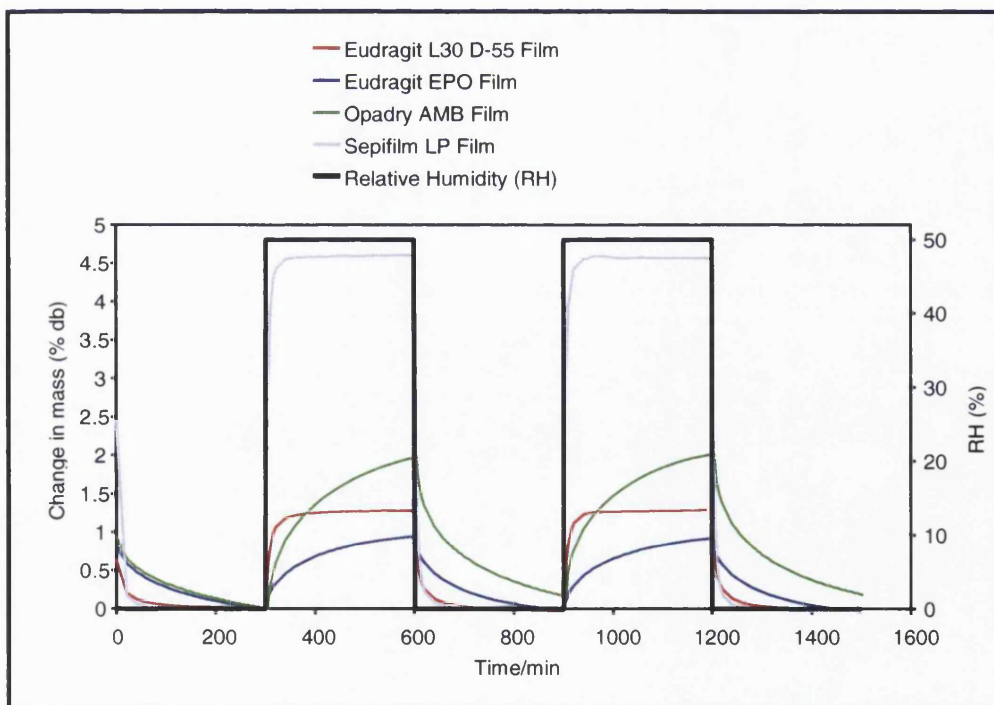


Figure 2-5. Fixed-Time Moisture Sorption-Desorption Profiles of Moisture Barrier Films Exposed to 0-50-0-50-0 % RH Cycle DVS (25 °C)

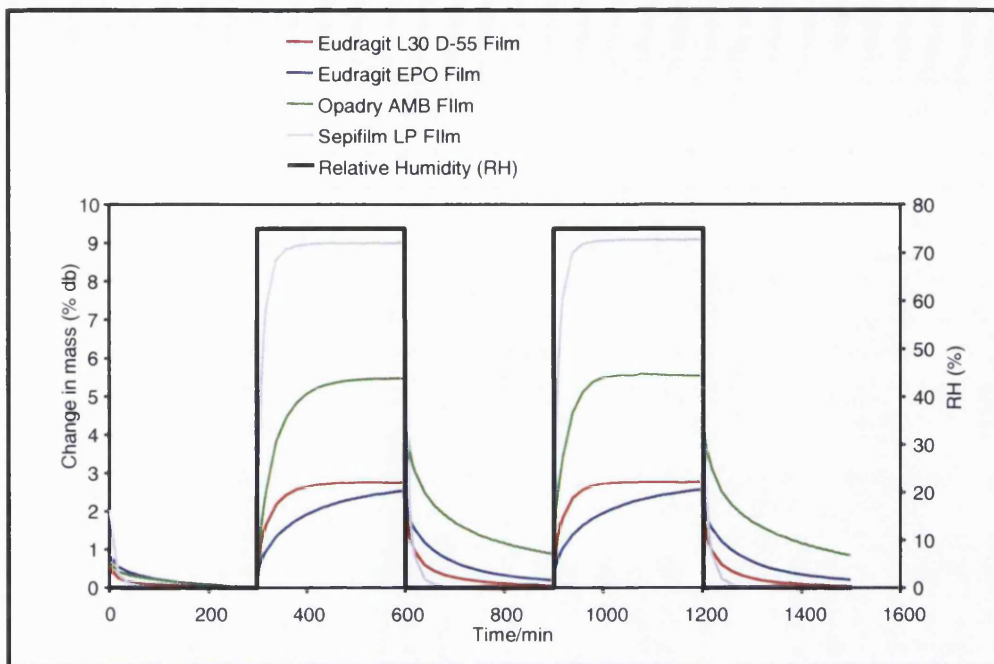


Figure 2-6. Fixed-time Moisture Sorption-Desorption Profiles of Moisture Barrier Films Exposed to 0-75-0-75-0 % RH Cycle (25 °C)

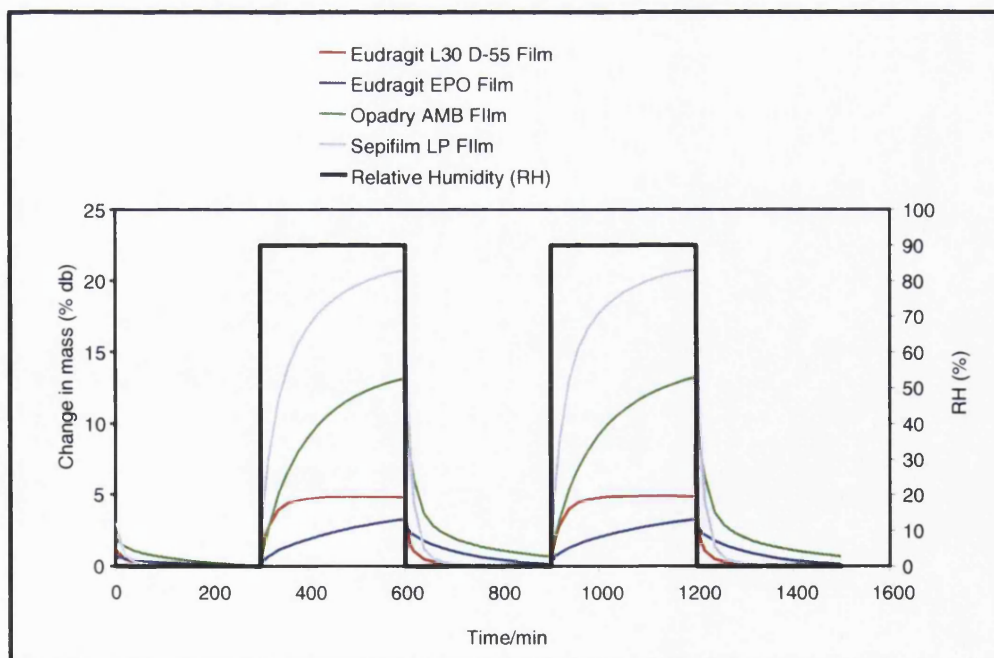


Figure 2-7. Fixed-Time Moisture Sorption-Desorption Profiles of Moisture Barrier Films Exposed to 0-90-0-90-0 % RH Cycle (25 °C)

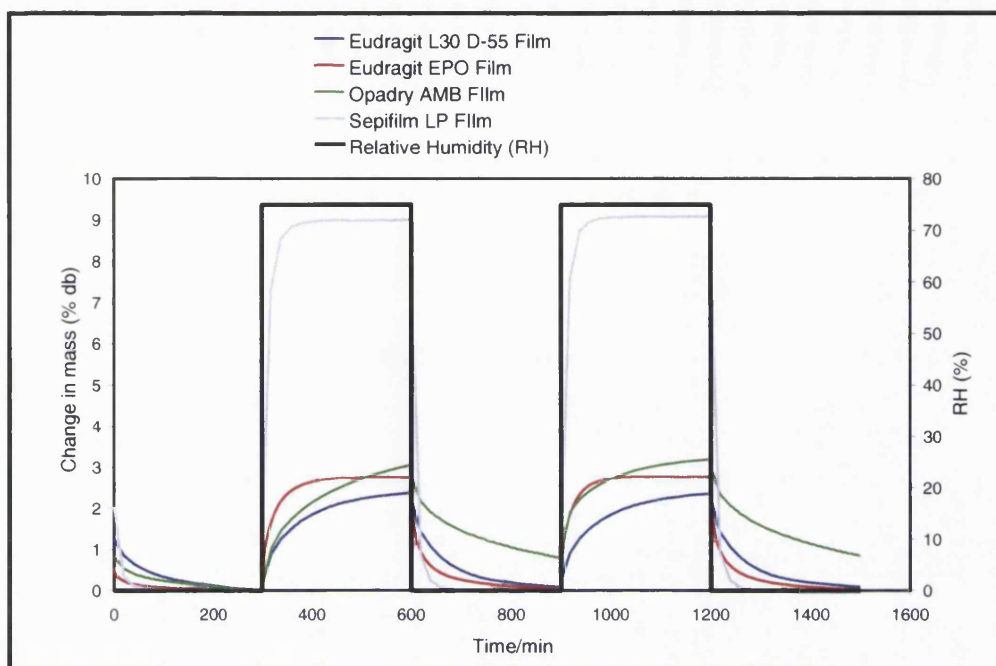


Figure 2-8. Fixed-time Moisture Sorption-Desorption Profiles of Moisture Barrier Films Exposed to 0-75-0-75-0 % RH Cycle (40 °C)

In addition to studying the sorption-desorption characteristics of the four moisture barrier films above, two enteric polymer films were also investigated in a similar fashion. The aim of this undertaking was to understand the relationship between moisture uptake and/or loss, and pH-dependent solubility. As demonstrated by the relatively low hygroscopicity of the Eudragit L30 D-55 film, enteric polymers are generally perceived to be good barriers to water. Perhaps, this is the reason why poly(vinyl acetate phthalate) has been used to seal cores against moisture in sugar coating applications. It was therefore of great interest to pursue this line of investigation in order to gain more insight into the role of pH-dependent solubility with regard to moisture sorption-desorption characteristics of polymers.

The two polymers studied, i.e., Sureteric, constituted from poly(vinyl acetate phthalate), and Aqoat, which contained hypromellose acetate succinate as the main film former, were selected due to their chemical similarity to poly(vinyl alcohol) and hypromellose. However, due to time constraints investigations were limited to the 0-90-0-90-0 % RH study protocol at 25 °C. The typical sorption-desorption profiles obtained for these samples are shown in Figure 2-9 below. The Eudragit L30 D-55 data are also included in Figure 2-9 for the convenience of comparison with the data for moisture barrier films described in the previous pages. It is worthwhile mentioning that the profiles shown here were typical of trends observed in at least three experimental runs.

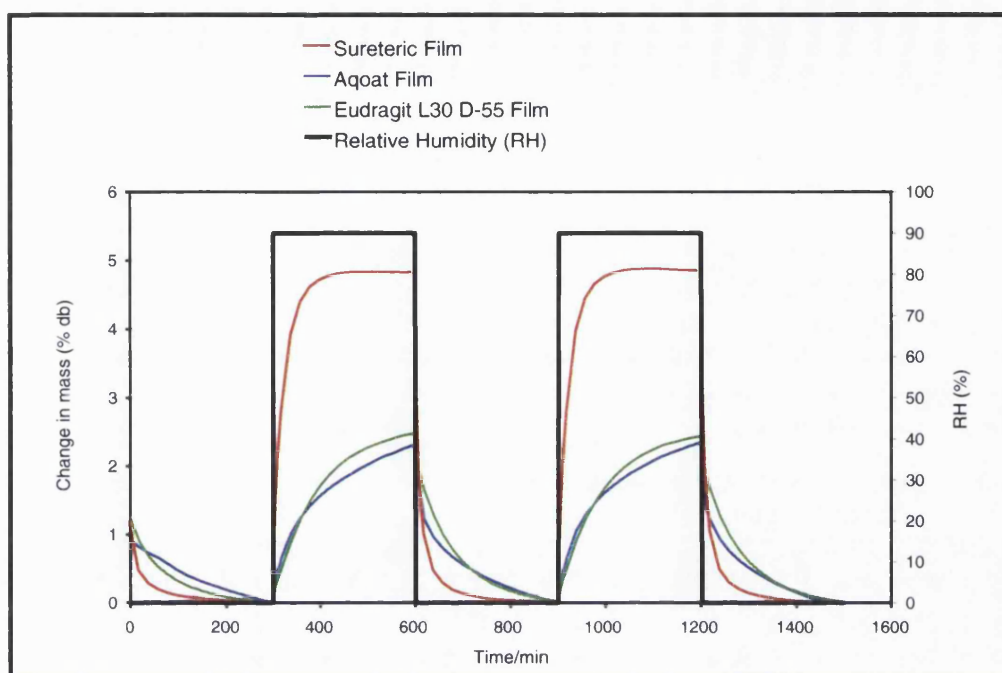


Figure 2-9. Fixed-time Moisture Sorption-Desorption Profiles of Enteric Polymer Films Exposed to 0-90-0-90-0 % RH Cycle (25 °C)

The data shown above demonstrated key differences in the behaviour of the different film samples in response to changes in relative humidity (RH) and or temperature. Both the RH and temperature were seen to influence not only the amount of water taken up and lost, but also the (apparent) sorption-desorption rates. These aspects of the results are further expounded in the following paragraphs:

With respect to the four moisture barrier film samples, it can be seen that the RH was a key factor in the extent of sorption exhibited by the films. For instance, at the 0-50-0-50-0 % RH cycle, the dry basis (db) amount of moisture sorbed by the Eudragit EPO film was 0.758 % (0.013). In comparison, the Eudragit L30 D-55, Opadry AMB and Sepifilm LP films were observed to have sorbed, respectively 1.247 (0.002), 1.967 (0.006) and 4.573 (0.021) % db moisture.

Increasing the RH to 75 % RH led to an increase in the amount of water sorbed i.e., Eudragit EPO film 2.251 (0.108) % db moisture, Eudragit EPO sorbed (2.738 (0.004) while the Opadry AMB and Sepifilm LP films respectively sorbed 5.465 (0.010) and 9.166 (0.007) moisture. A similar pattern was obtained at the 0-90-0-90-0 % RH cycle.

The mass changes of the films during the desorption cycles, with the exception of the Opadry AMB sample, were equal to the mass changes during sorption. Even when exposed to the second sorption-desorption cycle, the two cycles were seen to be super-imposable. The behaviour of this film sample, thus, suggested that the desorption cycle was perhaps a two-step process, i.e., a rapid event which was followed by a slower event, culminating in the incomplete loss of moisture from this sample. In general, it can be said that all the moisture barrier film samples were very responsive to changes in the RH in the DVS.

Another aspect of the results relates to the differences in the profiles of the curves. In this case, key differences can also be seen. For instance, the profiles for the Eudragit L30 D-55 and Sepifilm LP films exhibited comparatively fast sorption and equilibration rates. Both samples showed very rapid desorption as well, and fully equilibrated to the dry state by the time the experiment was terminated. The Eudragit EPO and Opadry AMB film samples, on the other hand, had nearly identical sorption profiles (which were slower) and neither film achieved equilibration in the experimental time. For these two samples, the desorption rates were seen to be relatively slow compared to those of Eudragit L30 D-55 and Sepifilm LP films, although only the Opadry AMB film sample retained moisture in its film by the time the experiment was terminated.

It is also of interest to note that the apparent sorption-desorption rates obtained at subsequent conditions, i.e., 0-75-0-75-0, 0-90-0-90-0 % RH (at 25 °C) and 0-75-0-75-0 % RH (40 °C) did not seem to be affected by changes in study conditions across the film samples, i.e., although changes were observed in the extent of sorption as the RH and or temperature was changed, the sorption-desorption profiles for a given film sample were not altered greatly. Thus, the behaviours exhibited were fairly constant at each of the four conditions studied.

The role of temperature on the extent of sorption can be seen when Figures 2.6 and 2-8, which, respectively, show sorption profiles of the films following exposure at 0-75-0-75-0 % RH at 25 °C and the same cycle at 40 °C, are compared. It can be seen that the Sepifilm LP sample was still the most hygroscopic film. However, the amount of moisture sorbed marginally decreased, i.e., 8.896 (0.353) % db compared to that taken at 25 °C. Crucially, the least hygroscopic film this time round was the Eudragit L30 D-55 film, which sorbed 1.483 (0.087) % db moisture. The Eudragit EPO film sorbed 2.374 (0.012) % db moisture, which was nearly double that sorbed at 25 °C. Both the Opadry AMB and the Eudragit L30 D-55 film samples exhibited a decrease in the amount of moisture sorbed at 40 °C over that sorbed at the lower temperature.

With respect to enteric polymer films (see Figure 2-9), the data demonstrates that both samples (i.e., Sureteric and Aqoat film samples) sorbed less moisture compared to the moisture barrier film samples described above. The mean dry basis amount of moisture taken up by the Sureteric film at the 0-90 % RH step change was 2.542 (0.112) %. At this condition, the Aqoat film sample exhibited nearly identical hygroscopicity. For reasons explained previously, these samples were not studied at the 0-50-50-0 % RH and the 0-75-0-75-0 % RH cycles. However, it is reasonable to suppose that similar sorption-desorption tendencies could have been obtained if the work had been undertaken at the lower RH cycles and/or the higher temperature as was the case for the four different moisture barrier films.

On the basis of the available data, it can thus be assumed that the two enteric polymer film samples exhibited very minimal attraction for water, and judging from the profiles of the sorption-desorption curves, the apparent rates of sorption for both films were comparatively slower, such that neither enteric polymer film achieved equilibration within the time frame of the experiments. During the drying stage, none of the enteric films retained moisture by the end of the experiment.

In summary, the findings of moisture sorption-desorption studies were:

- (i). The effect of the relative humidity (RH) on the extent of sorption (and desorption) was such that all the moisture barrier film samples studied were very responsive to changes in the RH of the system. Increase in RH resulted in a corresponding increase in the extent of moisture sorbed by the sample.
- (ii). It was shown that an increase in temperature resulted in a marginal decrease in the amount of water taken up by some of the film samples (i.e., Eudragit L30 D-55, Opadry AMB and Sepifilm LP) while in some films (i.e., Eudragit EPO film sample), an increase in temperature appeared to lead to an increase in sorption.
- (iii). The data from the sorption-desorption profiles of the four moisture barrier film samples demonstrated that although the amount of water taken up by the samples was altered by RH or temperature, in general, the profiles of the curves were not significantly altered by increase in RH and/or temperature.

The data on moisture sorption and desorption which is presented above for the Eudragit L30 D-55, Opadry AMB and Sepifilm LP films are also simultaneously published and cited in Mwesigwa et al., (2005), a copy of which is included in Appendix 5 of this thesis.

2.4.3 Measurement of Moisture Vapour Transmission Rates

The purpose of measuring the moisture vapour transmission rates (MVTR) of the polymer films was to generate data that would show the amounts of moisture that the samples were capable of transmitting as opposed to the amounts taken up. This work was undertaken only on moisture barrier coatings, i.e., Eudragit L30 D-55, Eudragit EPO, Opadry AMB and Sepifilm LP films. The procedures for MVTR determination was described in section 2.3.4. All film samples were, generally, of similar nature to those used in moisture sorption-desorption studies (*q.v* section 2.4.1). Studies were done at three relative humidity (RH) gradients, i.e., 0-50 % RH, 0-75 % RH and 0-90 % RH.

The results obtained from this undertaking are presented in two formats: Figure 2-10 through to Figure 2-13 show the typical plots obtained at the 0-50 % RH gradient. The shown charts depict the variation of the wet side and dry side RH with time and the corresponding MVTR of the film under study. Table 2-5 gives a summary of the data covering the 0-75 and 0-90 % RH gradients. It was necessary to include the data at the 0-50 % RH gradient in this table as well just for the convenience of comparison. All the data shown were based on measurements from at least three experimental runs performed on the same film sample.

It is necessary to clarify that the software for the pc linked to the VTI equipment by which the MVTR data was handled, was, by default, programmed by the equipment manufacturer to calculate the MVTR data in imperial units, i.e., g H₂O/ day/100 inch²). This is the reason why the units of inch appear in the data presented in Table 2-5 and are also used in the Figures 2-10, 2-11, 2-12 and 2-13.

Also, it is essential to clarify how the MVTR data, as shown in Table 2-5 figures, were arrived at. This is necessary because the shown MVTRs curves present a very mixed picture. For instance, the MVTR curves can be seen to exhibit values that were initially high and, in some respects, erratic (e.g., within the 0-10 min window). These values then appeared to tail off with time. This aspect is explained as follows: Initially when the equipment was switched on with a film sample in the permeation cell, it was necessary to outgas the dry side of the permeation cell before measurements started. This is a routine procedure. The out-gassed air exits in the same way as the transmitted moisture would and was, obviously, detected by the equipment, thus appearing as "MVTR values" in the initial period. However, when the system nears 0% RH, these "MVTR values" can be seen to have stabilized to zero. After a baseline is established (typically $\geq 0.01\%$ change between data points), the program RH is then recalled. A rise in the wet side RH is effected whereupon measurement of the actual MVTR commences. This is shown by a more stable measurement.

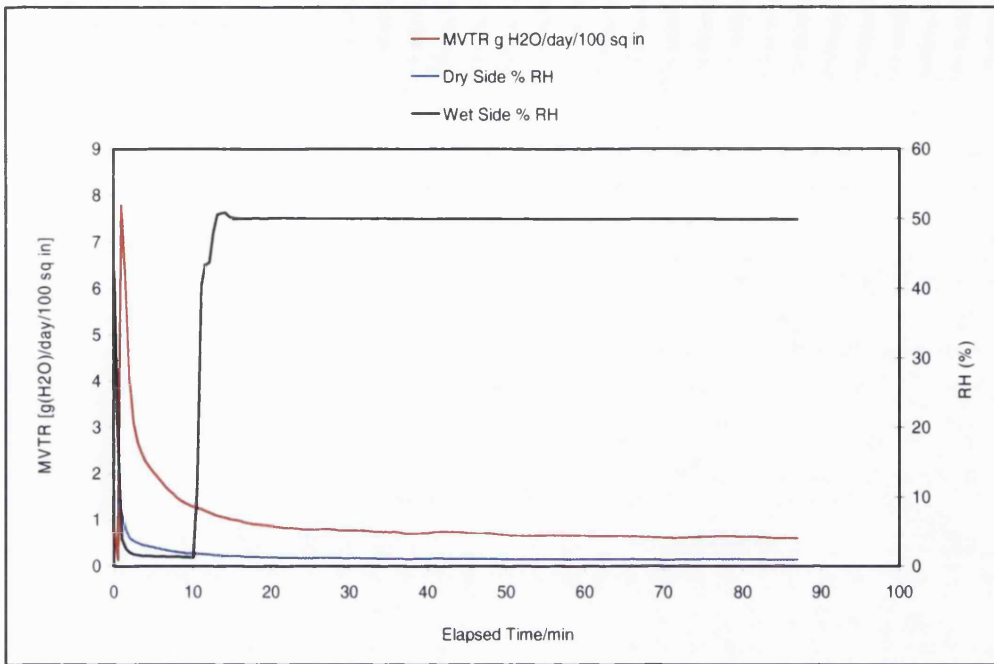


Figure 2-10. Moisture Vapour Transmission Rates [g (H₂O)/day/100 sq. inch], Wet-Side and Dry-Side RH Versus Elapsed Time (min) Plot for Eudragit L30 D-55 Film at the 0-50 % RH Gradient (25 °C)

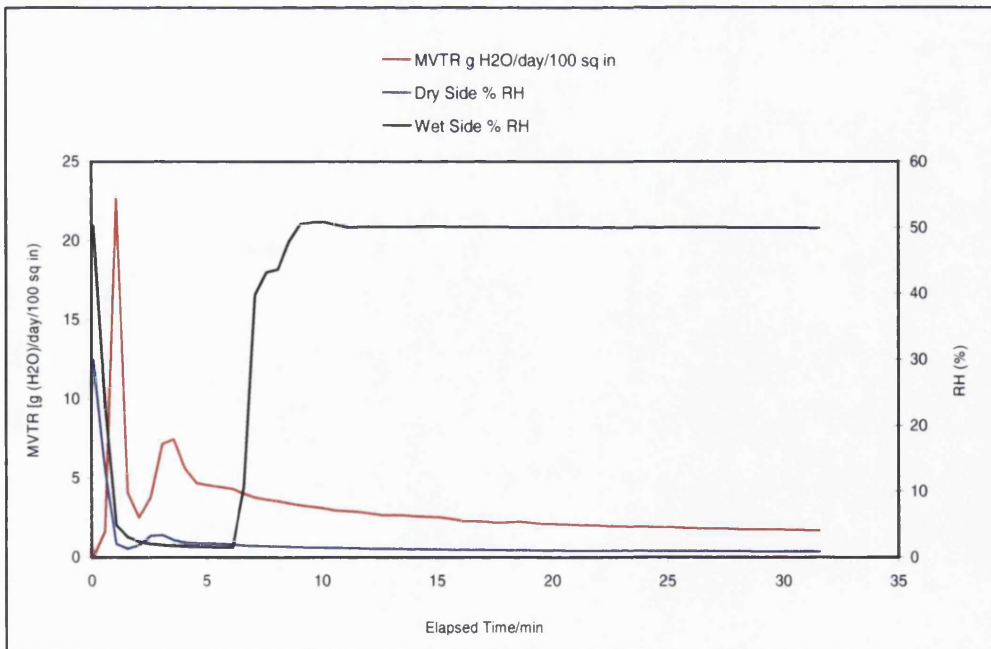


Figure 2-11. Moisture Vapour Transmission Rates [g (H₂O)/day/100 sq. inch], Wet-Side and Dry-Side RH Versus Elapsed Time (min) Plot for Eudragit EPO Film at 0-50 % RH Gradient (25 °C)

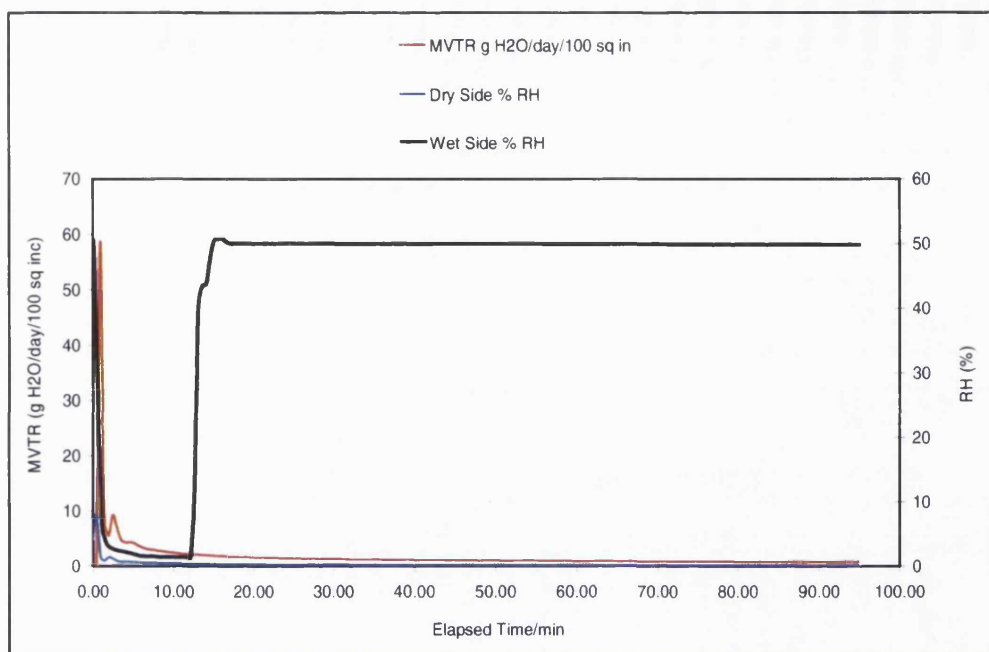


Figure 2-12. Moisture Vapour Transmission Rates [g (H₂O)/day/100 sq. inch], Wet-Side and Dry-Side RH Versus Elapsed Time (min) Plot for Opadry AMB Film at 0-50 % RH Gradient (25 °C)

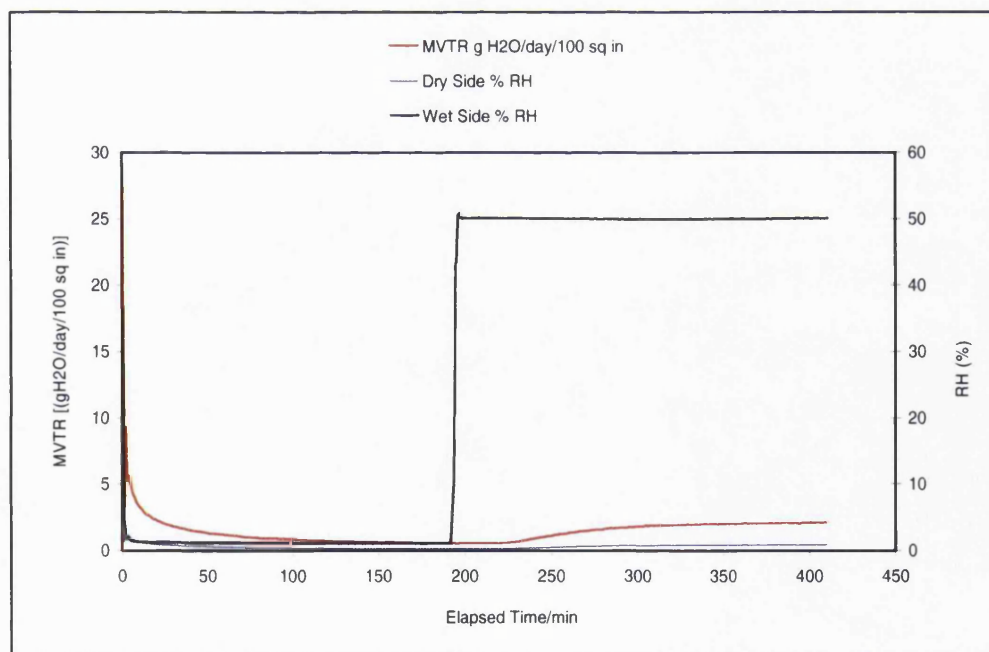


Figure 2-13. Moisture Vapour Transmission Rates [g (H₂O)/day/100 sq. inch], Wet-Side and Dry-Side RH versus Elapsed Time (min) Plot for Sepifilm LP Film at 0-50 % RH Gradient (25 °C)

The data in Table 2-6 below, reference of which was made to earlier, are the mean values of MVTR (g (H₂O)/day/100 sq.inch) obtained from the test after steady state had been attained (hypothetically taken as time point when the difference between two consecutive MVTR values was $\leq 1\%$). Although the unit of choice for MVTR in the American Society for Testing and Materials (ASTM) standard (e.g., ASTM– E96) is g/day/m², in this study, it was preferable to use g/min/cm² because the measurements were done in the time-scales of minutes rather than days whereas the unit of centimeters is more appropriate to dosage forms than meters. Also, because the thicknesses of the four film samples were not exactly similar, the MVTR values obtained required to be normalized to film thickness to obtain a specific MVTR, thus allowing for a fair comparison between the four film samples studied. The values of the normalized or specific MVTR [g(H₂O).cm/min/cm²] are shown in Table 2-6 below.

Film sample	RH Gradient		
	0-50 %	0-75 %	0-90 %
Eudragit L30 D-55	2.135 (0.064)	3.100 (0.079)	5.852 (0.230)
Eudragit EPO	1.910 (0.149)	2.391 (0.201)	3.765 (0.249)
Opadry AMB	1.288 (0.060)	1.814 (0.105)	8.447(0.700)
Sepifilm LP	2.398 (0.015)	5.703 (0.015)	11.493 (0.514)

Table 2-5. Summary of Moisture Vapour Transmission Rates (MVTR) [g (H₂O)/day/100 sq. inch) (\pm Std.Dev, n=3). Data for Barrier Films measured with the WPA-100 Equipment at 0-50, 0-75 and 0-90 RH gradients (25 °C) (Using the analysis of variance (ANOVA), differences between values were significant (P value >0.05).

Film sample	RH Gradient		
	0-50 %	0-75 %	0-90 %
Eudragit L30 D-55	2.076 (0.062)	3.028 (0.077)	5.715 (0.225)
Eudragit EPO	2.215 (0.193)	2.775 (0.260)	4.368 (0.322)
Opadry AMB	1.465 (0.068)	2.064 (0.119)	9.612 (0.253)
Sepifilm LP	2.471 (0.016)	5.876 (0.113)	11.842 (0.117)

Table 2-6. Mean Specific Moisture Vapour Transmission Rates (MVTR) [g (H₂O) cm /min. cm²] (\pm Std.Dev, n=3). Values Shown are $\times 10^{-6}$. Using the analysis of variance (ANOVA), differences between values were significant (P value >0.05)

It is highly desirable to be able to reliably and quickly determine the barrier properties of film coatings, for instance, during the design and optimization of the moisture barrier coating performance. The MVTR permits the characterization of water vapour permeability by measuring the amount of vapour that a film transmits.

For a long time, the only technique available for determining the MVTR of a film sample was the cup method. This technique is still widely in use, and, as explained earlier, it involves introducing a desiccant (e.g., anhydrous CaCl_2 to provide 0 % RH) into a cup which is then sealed with the film under study. The cup is then placed in a desiccator of a known RH. This arrangement is known as the dry cup method. An alternative approach is the wet cup method. Here, distilled water is placed in the cup to maintain the humidity at 100 % RH. The MVTR is then calculated from the change in weight of the cup with time. Shortcomings of the cup method mainly arise from the static nature of the test. They include the potential for resistance to the permeation of the moisture from still air in the cup and potential for leakages due to inappropriate sealing of the film on the cup. Also, the test requires several days to undertake, sometimes subjecting films to microbial attack or deterioration.

Nowadays, there are available several commercial equipments by which the MVTR may be determined. The “heart” of these machines is the permeation cell. This is the sample holder for the film of known thickness and cross-sectional area. The permeant current is allowed to flow through one side of the cell where it accumulates in the other side of the cell, the amount of which is detected by some analytical technique. A carrier gas (e.g., N_2) may be used to carry the permeant to a sensor. Figure 2-14 below shows, in detail, the gaseous flow in the permeation cell.

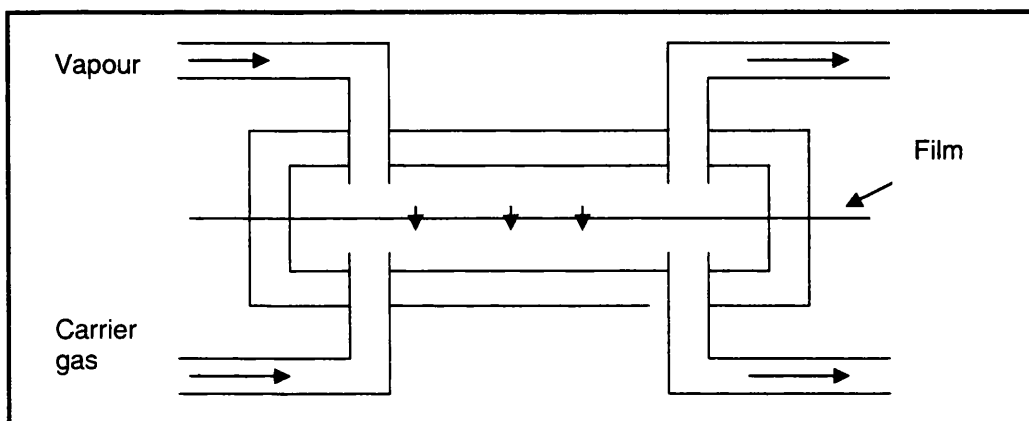


Figure 2-14. Schematic Diagram of an MVTR Testing Cell

In this work, the VTI permeability equipment enabled MVTR data to be rapidly obtained. As shown in Figures 2-10 to Figure 2-13 as well as Tables 2-4 and 2-5, the different moisture barrier film samples exhibited different MVTR values at the RH gradients studied. At 0-50 % RH gradient, the MVTR values were low indicating that the films transmitted relatively less moisture. The most effective barrier at this condition was the Opadry AMB sample (specific MVTR $1.466 (0.068) \times 10^{-6}$ [g (H₂O). cm /cm².min]). This was followed by the two methacrylate film samples, both of which exhibited intermediate values (i.e., specific MVTR for Eudragit L30 D-55 was $2.076 (0.062) \times 10^{-6}$ and $2.215 (0.193) \times 10^{-6}$ for Eudragit EPO). The Sepifilm LP sample exhibited higher permeability, i.e., specific MVTR of $2.471 (0.016) \times 10^{-6}$ g/cm².min). This was higher relative to the Opadry AMB film sample.

When the RH was increased, the amount transmitted was also seen to increase. For instance, at the 0-75 % RH gradient, there was a proportionate increase in the MVTR over that obtained at the 0-50 % RH gradient. At the 0-90 % RH gradient, the MVTR values were even higher, similar to pattern seen with the sorption-desorption data. In relative terms, however, this behaviour was more extreme in the Opadry AMB sample at this condition. In fact, the values obtained for this sample were very close to those obtained for the Sepifilm LP sample. This indicates that the moisture transmission properties of the Opadry AMB sample changed, in such way that this sample shifted from being the least permeable to being one of the most permeable. Although similar changes were seen in the methacrylate samples, they were not to the scale seen in the Opadry AMB film sample.

To summarise, the findings of the MVTR studies were as follows:

(i). At low RH gradients, the Opadry AMB film sample exhibited the lowest moisture transmission properties. This was closely followed by the two methacrylate film samples (i.e., Eudragit L30 D-55 and Eudragit EPO). The Sepifilm LP film exhibited the highest moisture transmission rates.

(ii). Increasing the RH also resulted in an increase in the moisture transmission properties of the film samples. However, while the two methacrylate samples still maintained low MVTR values, the Opadry AMB film sample appeared to be transformed from being a low permeability membrane into one that transmitted moisture to the same scale as the hypromellose film sample.

(iii). On the whole, there was no clear correlation between MVTR data with the sorption data presented in section 2.4.2, especially at low RH gradients.

2.4.4 Thermogravimetric Analysis of Moisture in Films

Thermogravimetric analysis (TGA) was undertaken on films post exposure at 0, 50, 75 and 90 % RH. The purpose of this work was to determine the nature of polymer-sorbed water interactions and the state of the sorbed water within the films. The Eudragit EPO, Sureteric and Aqoat film samples were not studied because the equipment become unserviceable and was subsequently decommissioned before these studies on these particular film samples could be undertaken.

The data obtained post exposure at the 0-75-0-75-0 % RH cycle are summarised in Figures 2-15, 2-16, and 2-17, respectively for the Eudragit L30 D-55 film, the Opadry AMB and Sepifilm LP film sample. The profiles shown below are, in fact, representative of trends seen in at least two experimental runs on films similarly exposed to the 0-75-0-75-0 % RH cycle. (However, the selection of this cycle was arbitrary). The TGA charts show two curves, i.e., weight loss versus temperature ($^{\circ}\text{C}$) curve, (*the TG curve*, plotted in red), and per cent weight loss/time versus time (min) (*the TG derivatogram*, plotted in black). To determine if these were not experimental artefacts, samples maintained at 0 % Rh were similarly analysed (data not shown). The thermograms obtained showed no real weight loss between 0 and 75-100 $^{\circ}\text{C}$. However, there was a moderate weight loss at the higher temperatures (e.g., 350 $^{\circ}\text{C}$) in the same way as hydrated film samples.

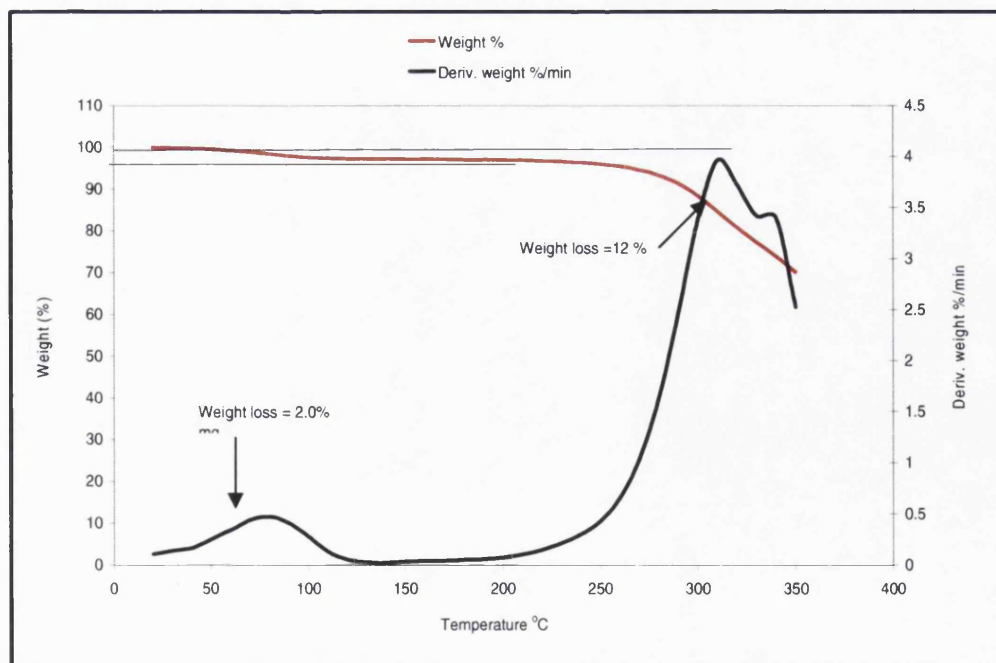


Figure 2-15. Thermogravimetric Curve and Derivatogram of Water Sorbed in Eudragit L 30 D-55 Film Post Exposure to 0-75% RH (25 0C)

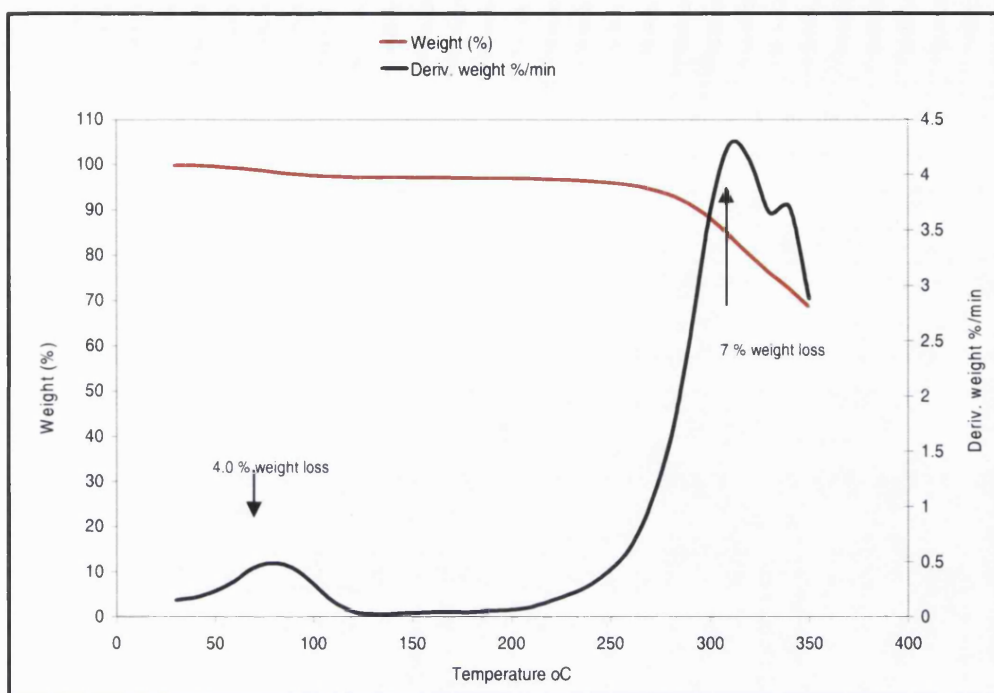


Figure 2-16. Thermogravimetric Curve and Derivatogram of Water Sorbed in Opadry AMB Film Post Exposure to 75% RH (25 °C)

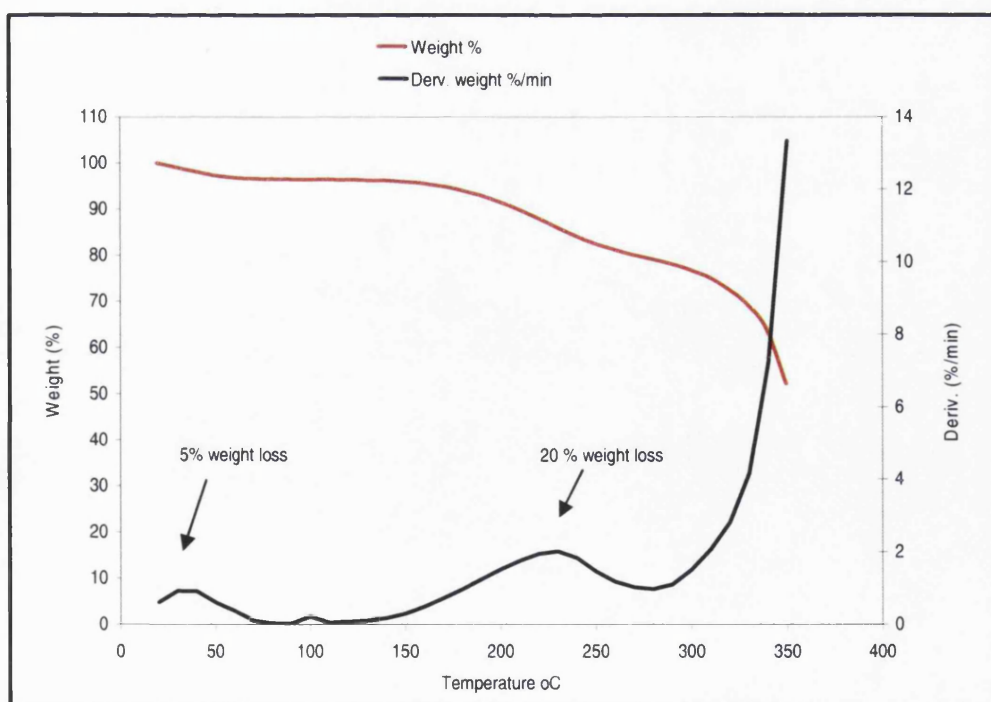


Figure 2-17. Thermogravimetric Curve and Derivatogram of Water Sorbed in Sepilm LP Film Post Exposure to 75% RH (25 °C)

Understanding the water-polymer interactions is essential if a correct picture of barrier functionality of moisture barrier coatings is to be obtained. In the previous sections (q.v, sections 2.4.2 and 2.4.3), it was shown that some of the sorption-desorption behaviour and MVTR data obtained (e.g., data for the Opadry AMB film) were somewhat idiosyncratic. Although not mentioned at that stage, unique water-polymer film interactions in that sample were speculated as being behind the sorption and moisture transport properties of the films studied.

Thermal analysis (TA) was, therefore, adopted as a means for gaining insight into water polymer interactions. TA is, essentially, a group of techniques by which some property of a material is studied as a function of temperature. Examples of TA techniques include thermomechanical analysis, dynamic mechanical analysis, differential scanning calorimetry (DSC), thermogravimetric analysis, etc. The use of thermal analysis to study water-polymer interactions was reviewed by Hatakeyama and Hatakeyama (1998) and Ford (1999), among others.

DSC is the most commonly used TA technique for the purpose of studying water-polymer interactions. It has been successfully employed by several workers interested in this field (e.g., Ford and Timmins, 1989; Kyritsis et al., 1995; Hodge et al., 1996; McCrystal et al., 1997; Alvarez-Lorenzo et al., 2000, etc). However, DSC requires deliberate addition of a known quantity of water to the film sample. The film must then be allowed equilibrate with the water. Also, the film sample must be sealed in hermetically closed sample pans. Using a cooling and or a heating cycle, the melting or crystallization endotherms are then determined and used to identify the quantities of the different types of water in the film. It is reported (e.g., Ford, 1999) that the water content in the film must be > 40 % for the water molecules to be able to collect and exhibit visible melting/crystallization peaks.

In this study, DSC was initially used to identify the water-polymer interactions in the films. Film samples were subjected to a cooling and a heating cycle in a PerkinElmer DSC 7 instrument post exposure in the DVS at 0-75 % RH. Unfortunately, the results were negative as no peaks were evident. This was possibly due to the very low water levels in the films such that the water molecules were not capable of crystallizing to yield the expected peaks. An attempt was subsequently made to study films to which a known amount of water had been deliberately added. However, in the process of adding water to the films, the samples dissolved in the added water. Due to these complications, the technique was abandoned. Thermogravimetry was, hence, adopted as the alternative to DSC.

Modern TGAs are very sophisticated equipment and will usually be linked with another analyzer, e.g., an infrared spectrometer, a mass spectrometer, FT-IR spectrometer, etc. Thus, they are capable of yielding even more specific and often very useful information on a sample. In the basic form, however, the main type of data acquisition involves the heating a sample in a N₂ atmosphere. This enables information relating to the volatile matter in the sample, e.g., mass of water, for the case of water in polymers, to be readily obtained from TGA plots.

The TGA plot of a polymer sample undergoing dehydration is the form of mass versus temperature trace. It describes how much and how fast the water is released when the sample is heated at a constant rate. When the mass loss is due to a single process, (for instance, the dehydration of a salt) the TG trace shows a sigmoid descending trend with a flexus at some temperature where the water loss rate is maximum (Ford, 1999). The trace of the time derivative, i.e., derivative of thermo gravimetry, shows a well defined peak, the maximum of which corresponds to the flexus point in the TG trace.

In some modern instruments, a combined output, e.g., TG and DSC, may be given: the latter signal allowing determination of the enthalpy drop relevant to the process that produces the mass loss. In the case of water vaporization, on verification, this will be close to 2.3 kJ g⁻¹, the vaporization enthalpy of pure water. Otherwise, when the system contains water in different fractions, the derivatogram plot shows several peaks or shouldered peaks which can be easily singled out. For each of these peaks, the corresponding enthalpy drop can be analysed to ensure that the underlying process still deals with water vaporization.

With respect to the results obtained from the present studies, it is apparent that the TG curves of the samples exhibited two phases: the first phase mass loss commenced almost instantaneously and carried on up to about 100 °C. The second mass loss and commenced at 250±50 °C (depending on the sample) and carried on until the samples eventually decomposed. For each TG curve, there was a corresponding TG derivatogram showing peaks at around 75 °C for the Eudragit L 30 D-55 and the Opadry AMB film samples, and 50 °C for the Sepifilm LP film sample. In addition, more TG derivatogram peaks appeared at 350 °C for the Eudragit L30 D-55 and the Opadry AMB film samples and at about 240 °C for the Sepifilm LP film sample. It is logical to suppose that these patterns of moisture loss, as shown from the TG data, perhaps, reflect the binding characteristics of the sorbed moisture within the different film samples studied in this work.

In conclusion, the different aspects of the results of thermogravimetric analysis of the moisture barrier films can be summarized as follows:

(i). The DSC technique failed to yield any results which were ascribable to the different fractions of water sorbed in the film samples. This was attributed to the very low water levels within the film samples. It was speculated that as a result the water molecules were not capable of crystallizing to yield a peak.

(ii). Using TGA, peaks that showed that the mass loss from the different film samples occurred in two phases were seen. The first phase occurred at temperatures that were typically below 100 °C. These peaks were generally smaller but corresponded well with the extent of sorption expected from the film samples. There was observed a second phase of mass loss which occurred at temperatures typically above 250 °C. These peaks were much larger.

2.4.5. Near infrared spectroscopy studies

The aim of near infrared (NIR) spectroscopy studies was to further understand the nature of polymer film-water interactions but through the use of a different technique. The NIR technique has rapidly emerged as a highly reliable way of investigating structural differences in pharmaceutical systems. Lane and Buckton (2000) recently described a combined NIR spectroscopy-gravimetric sorption (DVS) technique, which allowed the study of the crystallization of lactose simultaneously by the two independent techniques (i.e., gravimetry and NIR). Since the two techniques were linked, the sample was studied in a way that enabled comparable information to be gathered without the need for separate measurements. In this study, a similar set-up was adopted to study moisture sorption-desorption phenomenon in the film samples. This was described earlier in section 2.2.2.3 and 2.2.2.6.

The results of NIR spectroscopy studies are shown in Figure 2-18 (a, b, c, d) below. The shown charts demonstrate the variation of the absorbance [$\log (1/\text{Absorbance (T)})$] versus wavelength (nm) obtained while the samples were subjected to the 0-75-0-75-0 % RH cycle in the DVS. This is a standard format by which NIR spectra are usually plotted. In this work, only a few time points, corresponding to 0, 300, 600, 900, 1200 and 1500 min) are used for illustration so that the plots are more neat and legible. Otherwise, the NIR spectra were collected every 30 minutes during the time the film samples were under study in the DVS chamber.

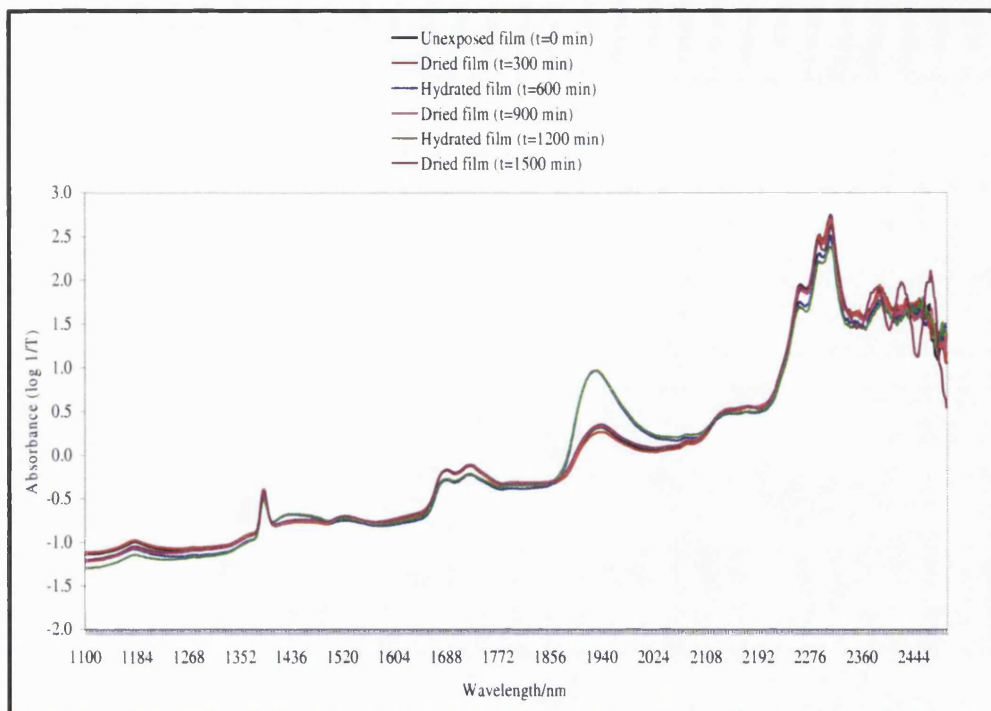


Figure 2-18a. NIR Spectra [Absorbance Versus wavelength (nm)] for Eudragit L30 D-55 Film During Exposure to the 0-75-0-75-0 % RH Cycle (25 °C)

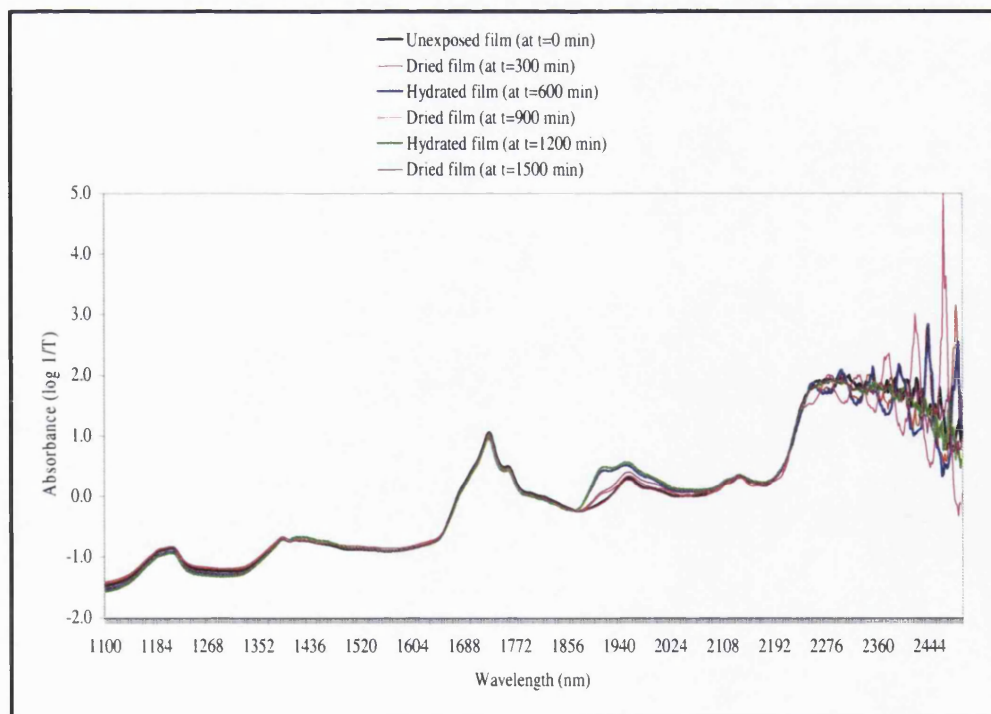


Figure 2-18b. NIR Spectra [Absorbance Versus wavelength (nm)] for Eudragit EPO Film During Exposure to the 0-75-0-75-0 % RH Cycle (25 °C)

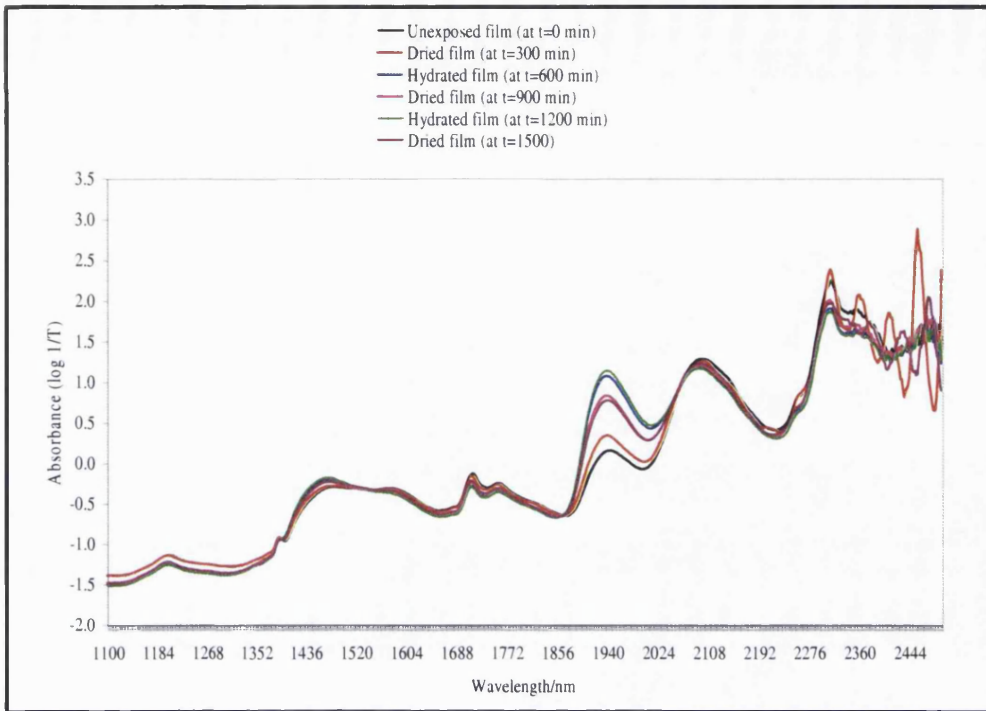


Figure 2-18c. NIR Spectra [Absorbance Versus Wavelength (nm)] for Opadry AMB Film During Exposure to the 0-75-0-75-0 % RH Cycle (25 °C)

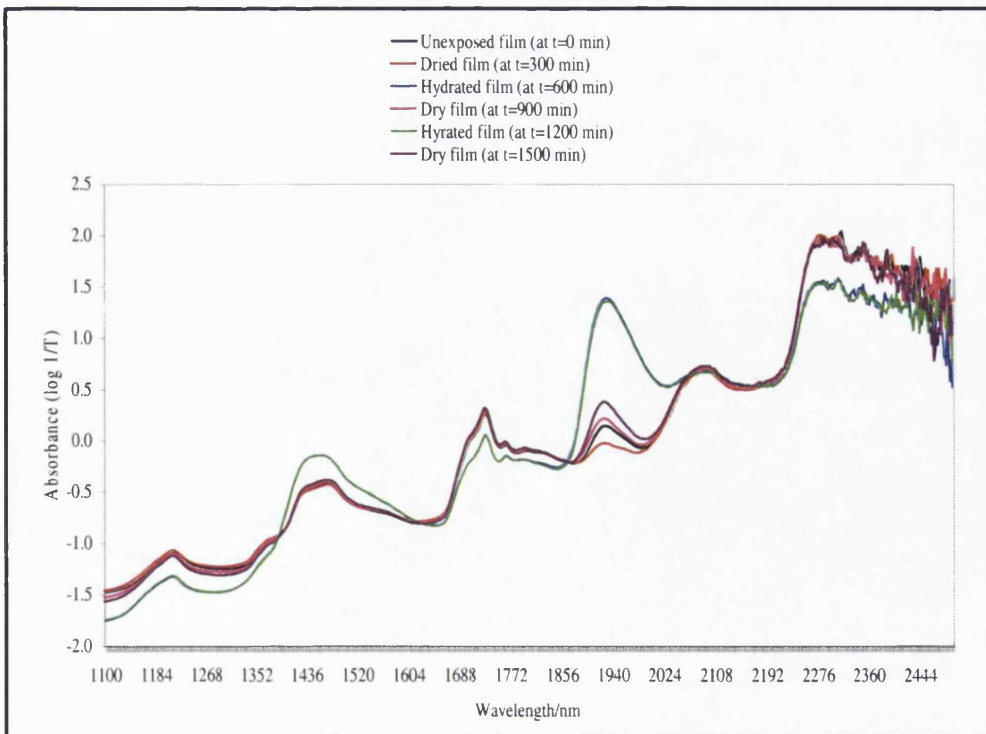


Figure 2-18d. NIR Spectra [Absorbance Versus Wavelength (nm)] for Sepifilm LP Film During Exposure to 0-75-0-75-0 % RH Cycle (25 °C)

In the charts presented above, several absorption maxima and minima in the NIR region at selected wavelengths can be seen. Some differences between dried and hydrated films, demonstrating the effect of hydration in the DVS can also be seen. However, to facilitate detailed examination, the spectra were further subdivided into two broad regions, i.e., 2500-2200 nm, and 2200-1100 nm. It can be seen that the 2500-2200 nm region was dominated by peaks at 2100, 2280 nm and 2256 nm bands although other peaks at 2360 ± 20 nm, up to 2500 nm were seen. These peaks were mainly ascribed to $-\text{CH}$, $-\text{CH}_2$ and $-\text{CH}_3$ stretching and bending modes. The 2200-1100 nm region was dominated by four bands, i.e., 1940 ± 60 nm (combination of $-\text{OH}$ stretching and bending), 1700 ± 40 nm (due to 1st overtones of $-\text{CH}$ stretches), 1400 ± 10 nm ($-\text{OH}$ stretching). There was also a somewhat weak peak in 1180-1190 nm region (ascribed to $-\text{OH}$ stretching). The NIR data in the 2200-1100 nm region was subsequently converted into second derivative of absorbance by multivariate analysis. The resulting plots are shown in Figure 2-19. Second derivative absorption spectra are essentially the original absorption spectra that have been mathematically manipulated to resolve peaks of interest. This enhances differences in intensity and wavelength (Lane and Buckton, 2000) in those peaks of interest since the resolution of overlapping bands is improved while baseline offsets are reduced. It can be seen that the plots of the second derivative of absorbance versus wavelength reveals the same effects as the "raw" plots shown in Figures 2-18 above but the peaks are sharper.

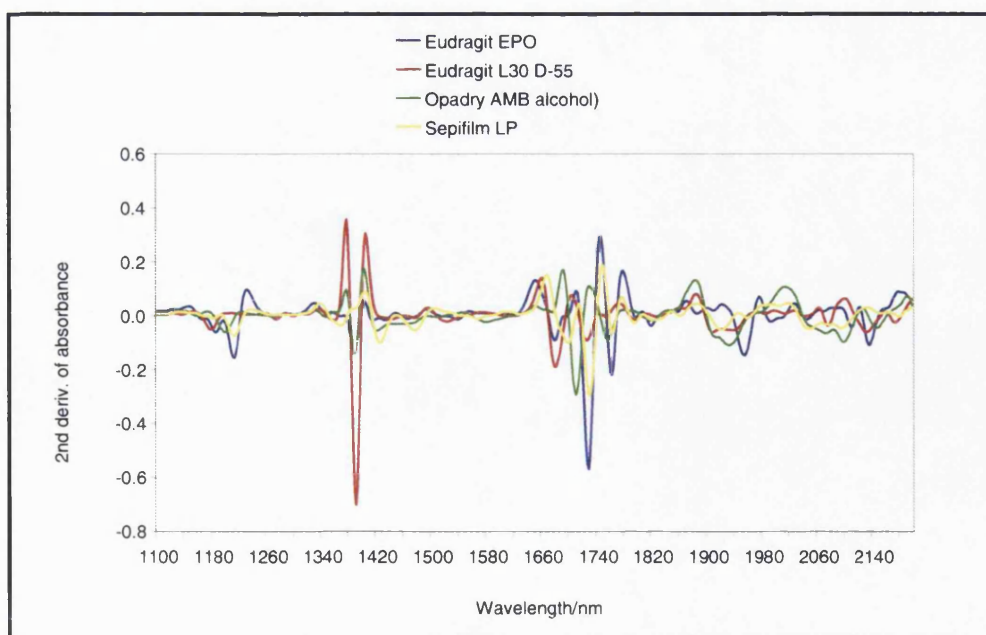


Figure 2-19. SNV-2nd Derivative Spectra of Films over the 2200-1100nm Wavelength Band. The Spectra Shown Were Collected at $t=300$ min after Films Were Exposed in the DVS to 0-75-0-75-0 % RH (25 °C) Cycle

The region corresponding to the main water absorption band between 2000 -1800 nm, covering the band corresponding to the combination of -OH stretching and bending modes of the -OH bond was selected for detailed analysis. This region represents the changes in the water structure induced by sorption of water (Luck, 1974). The spectra obtained were overlaid in such a way that nine spectra collected as a function of the hydration status of the film could be seen. The resulting plots are shown in the Figures 2-20 (a, b, c, d), which follow below, corresponding to Eudragit L30 D-55, Eudragit EPO, Opadry AMB and Sepifilm LP film samples (The enteric film samples were not investigated using this technique). From the displayed charts, it can be seen that the bands were displaced with respect to the intensity and wavelength on sorption of moisture. Also, the displacement increased with increase in sorption. This demonstrates the existence of intermediate states of water coexisting simultaneously, each with slightly different IR absorption energies.

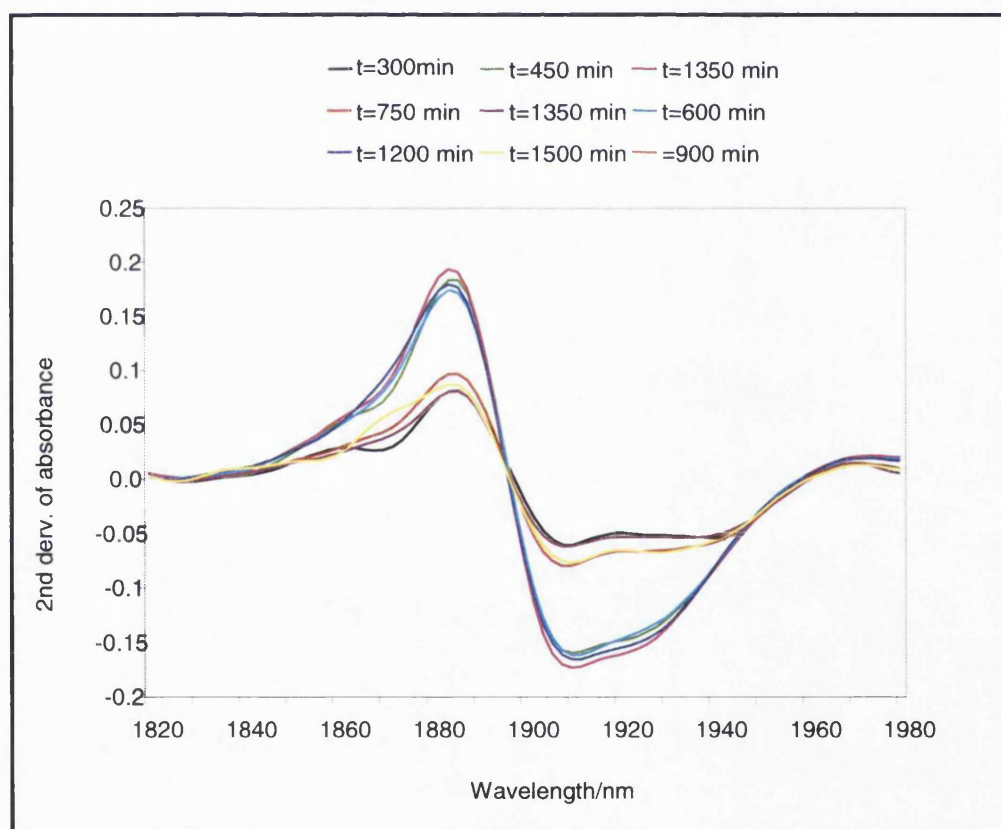


Figure 2-20a. SNV-2nd Derivative Spectra (1960-1820nm) for the Eudragit L30 D-55 Film

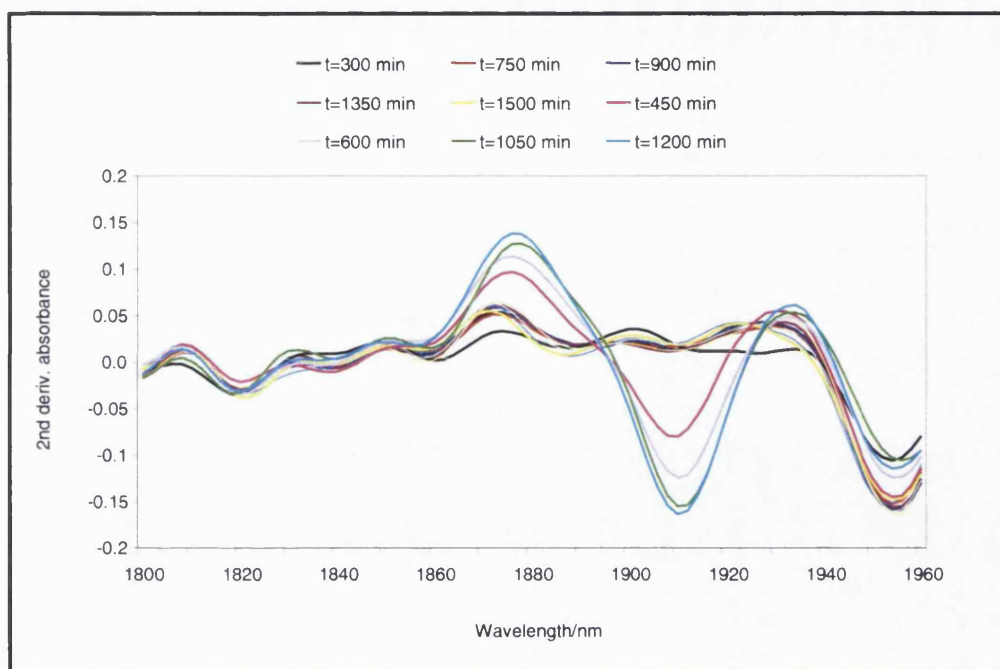


Figure 2-20b. SNV-2nd Derivative Spectra (1960-1800nm) for the Eudragit EPO Film

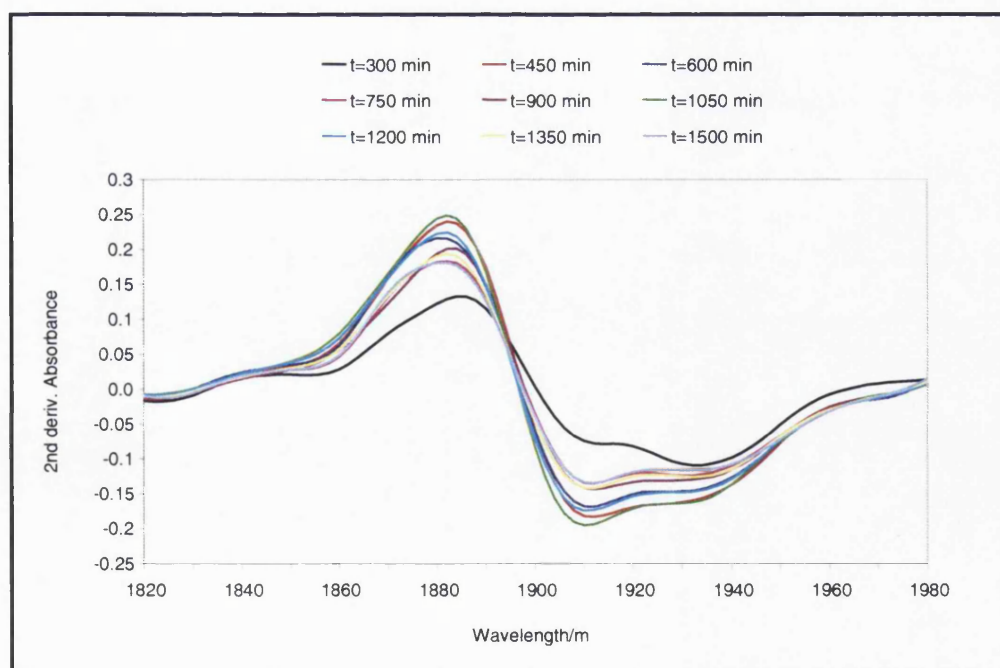


Figure 2-20c. SNV-2nd Derivative Spectra (1980-1820nm) for Opadry AMB Film

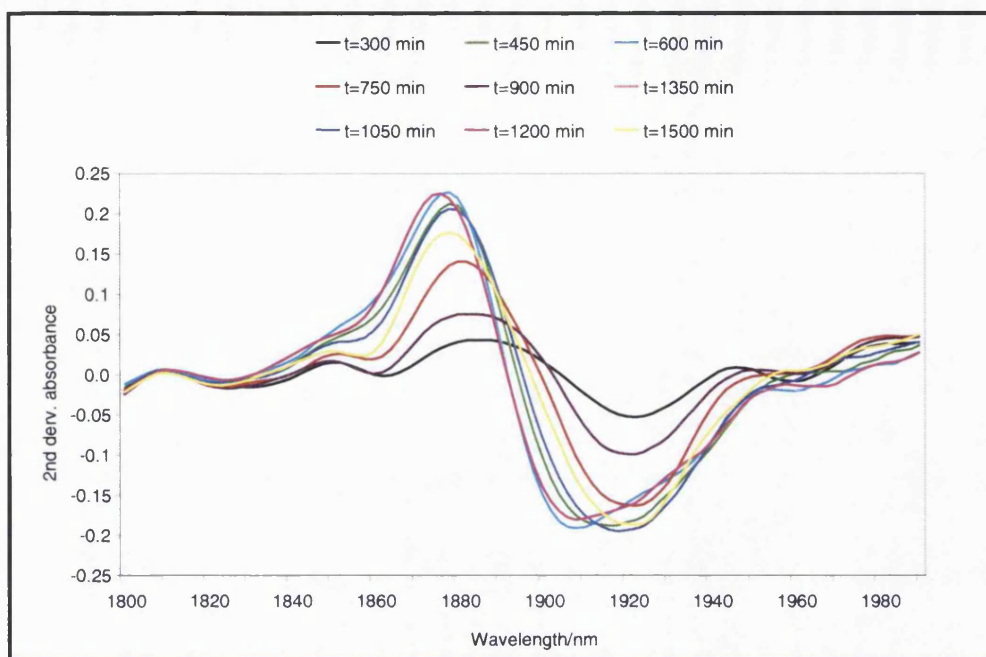


Figure 2-20d. SNV-2nd Derivative Spectra (1990-1800nm) for Sepifilm LP Film

NIR light is in the wavelength region from 750 to 2500 nm, lying between the visible light and the infrared light. Because the water molecule is a strong absorber in the infrared (IR) region, including the near IR (NIR), NIR spectroscopy has been used to study water related effects in many different materials, including polymers. As mentioned previously, NIR spectra are characterized by overtone and combination bands which are ascribed to vibrations of similar wavelength as the mid infrared.

As an analytical technique, NIR spectroscopy offers several advantages over traditional chemical methods (Ciurczak, 2001): These are (i) it is purely physical, non-destructive, and requires minimal or no sample preparation. (ii) the NIR spectrometer has a high signal to noise ratio, typically 10000:1. (iii) also, it offers the possibility to measure both physical and chemical properties. The main disadvantage is the need for calibration, which can be extremely time-consuming, and the complexity of the spectra obtained.

In this study, NIR spectroscopy provided an opportunity to supplement the TGA data, thus enabling a more complete picture to be obtained on the nature of sorbed water-polymer interactions in the films. The spectra were collected in real time as the moisture sorption-desorption experiments in the DVS. Thus, the spectra between the time periods of 300 to 600 or 900 to 1200 min corresponded to stages when the films were exposed to moisture stress (75 % RH) while the times between 600 to 900 or

1200 to 1500 were the stages when the films were being dried (0 % RH). The collected spectra demonstrated that changes were occurring as a result of hydration of the films.

By focussing on a narrow spectral zone, it was possible to view the spectra at even greater detail. In this case, the spectral region between 2000 and 1800 nm was selected because of the water combination band occurring around 1928 nm wavelength. It can be seen from Figures 2-17 (a to d) that this water band became more symmetric and there was a shift to longer wavelengths as the water content in the films increased. To determine if the bands were due to changes in the water sorption characteristics of the samples rather than experimental artefacts, the films were similarly studied in a Nicolet 700 FT-IR spectrometer (Thermo Electron Corporation, MA, USA). Similar shifts in intensity of the IR spectrum were seen in the 3400-3000 cm^{-1} region for this experimental set-up (data not presented).

The significance of the NIR spectra collected in relation to the objective of the work stems from the fact that the frequencies and intensities ascribed to the -OH bond change in response to changes in the strength of a hydrogen bond with the -OH and/or the state of hydration around this bond. Two remarkable behaviours that can be seen with the samples studied relate to the spectra for the amino butyl methacrylate sample and the hypromellose sample. In the former sample, a typically sharp peak between 1920 and 1910 nm, which shifted in intensity and wavelength as the content of water increased, can be seen. The same effect can be seen in the hypromellose sample but this time, the shift in this band is more prominent. In other samples, this effect can also be seen, although it is not as pronounced as was the case for the hypromellose film, perhaps reflecting the fact that relative extents of sorption in these samples were less than in the hypromellose sample.

No effort was put into measuring the extents of sorption with this technique as this would have required a separate (and laborious) calibration exercise. Therefore, the focus of NIR studies was to understand the water interactions in the polymer films rather than quantify the amounts of the sorbed water (which had already been undertaken by the dynamic vapour sorption technique).

In conclusion, NIR data showed that changes occurred in the film samples in response to the state of hydration. The water combination band occurring around 1928 nm wavelength was seen to become more symmetric and there was a shift to longer wavelengths as the water content in the films increased.

2.5. DISCUSSION

2.5.1 Introduction

The dynamic vapour sorption (DVS) technique offers many advantages over static methods, such as desiccators, which include fast equilibration times, which are in the scale of hours as opposed to days or weeks which are typically seen with static methods. When the DVS technique is combined with thermal analytical and spectroscopic techniques, moisture sorption studies can yield valuable information on the behaviour of water in polymers.

The discussion of the results which is presented below under three main sub-headings, i.e., moisture sorption-desorption characteristics, moisture vapour transmission rates data, and sorbed water-polymer interactions as adjudged from thermogravimetric studies and near infrared spectroscopy, aims to give an account and the significance of the results presented in section 2.4.

2.5.2 Moisture Sorption-Desorption Characteristics

It is necessary to explain what constitutes a polymer film, and what determines the properties of the specimen. In doing so, two aspects of the film are considered, i.e., the macro structure on one hand, and the micro structure, on the other. At a macro-structural level, a polymer film can be envisaged as a three-dimensional network of the particles of the constituent polymer plus other additives in the film formulation which have been fused together to yield a membrane. At a molecular level, the polymer, being the backbone for the film, consists of a large number of monomer units which are chemically linked to form a long chain. The polymer chain may be linear or branched with or without side groups. Many properties of the polymer are a function of the properties of the polymer chains. For instance, the shape, arrangement, and the number of monomers on the chain determine the morphology of the polymer. Figure 2-21 below is a schematic representation of two commonly encountered morphologies, i.e., crystalline and amorphous (Doi, 1995).

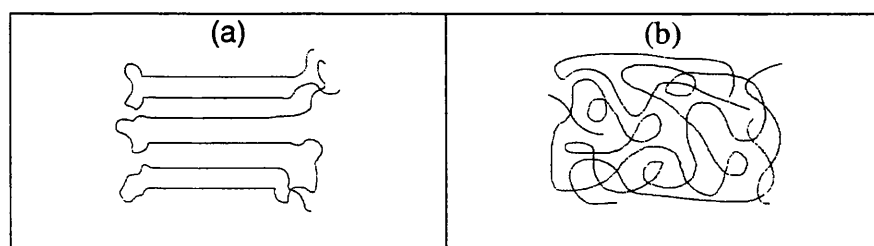


Figure 2-21. Schematic Diagram Illustrating How Polymer Chains of a Hypothetical Polymer Result into (a) Crystalline (b) Amorphous Morphology (from Doi, 1995)

In the DVS equipment, water vapour is generated by bubbling dry nitrogen gas through a flask of distilled water. Through the use of mass flow controllers and valves, the DVS is able to provide a micro environment of a given relative humidity (RH). The RH, in this case, represents the concentration of water vapour in that environment (of the DVS) in relation to the total amount of water vapour that that environment is capable of carrying if it were to be totally saturated. This amount is usually represented as a per cent or in some cases as a fraction.

When the polymer films were exposed to the study RH conditions in the DVS, the water molecules, existing as a vapour, came into contact with the polymer films. The sorption of the water molecules that was observed among the different film samples occurred because some form of interaction between the incident water and the films was possible. It is worthy remembering that sorption is a "storing" process. Thus, for the water molecules to be sorbed, there must be available "centres" where the water molecules can be stored. These can be in the form of voids, micro pores, cracks, or crevices present in the film, or specific polar groups or ions on the polymer chains of the polymer. The availability of these active centres depends on the physical and chemical nature of the polymer.

In Chapter 1 (section 1-6), a review of some of the factors known to affect permeation of moisture through polymers was undertaken. These factors were classified as (i) nature of the membrane (i.e., chemical and physical factors), (ii) nature of the penetrant, and (iii) environmental factors. With respect to chemical nature, a number of factors, i.e., molecular weight, nature of polymer chains (i.e., degree of polymerization, presence of side groups, degree of cross-linking, presence/absence of unsaturation), type of polymer chain (linear or branched) were reviewed. Also, the role of composition, viz, inclusion of plasticizers, and other solid inclusions such as lipids, fillers, etc., was mentioned. Some of the physical factors which were discussed included the state of the polymer membrane, i.e., glassy state, rubbery state, crystalline or amorphous, all of which are known to affect the packing of the chains, and hence the accessibility of the water to the sorption centres.

It will be reiterated that each of the above-mentioned factors (with regard to the chemical and physical nature), were expected to affect sorption to the same extent as they affect permeation, especially given the consideration that sorption is a sub-component of the permeation process. It is also logical to suppose that the differences in the extents of sorption seen among the different films studied reflected differences in both the chemical and physical properties of the samples. However, as no specific

The polar groups in the respective polymers not only provide the required sites with which sorbed water molecules interact, they also provide the necessary hydrophilicity required for retaining the water within the polymer matrix. Thus, it can be confidently said that the lower hygroscopicity exhibited by the Eudragit EPO and the Eudragit L30 D-55 film samples were, respectively, attributed to the fewer polar groups compared with hypromellose (notwithstanding the effect of the presence of the hydrophobic additives like stearic acid, magnesium stearate, and talc). The relatively fast sorption and equilibration rates seen in the Eudragit L30 D-55 film could have been due to proportionately fewer polar groups in this sample, which caused relatively quicker saturation (filling-up) of this film with moisture. For the Eudragit EPO sample, the high levels of magnesium stearate (35 % w/w) were possibly the main reason for the slow sorption-desorption rates seen because of this material's ability to repel water since the constituent polymer in this sample can be expected to exhibit higher polarity due to the presence of –NR– groups, compared to the ethyl methacrylate in Eudragit L30 D-55. On the basis of these assumptions, however, the lower hygroscopicity and the unique desorption profiles exhibited by the Opadry AMB film sample would seem to be a contradiction, especially given the understanding that both poly(vinyl alcohol) and xanthan gum (the other component in this film), are highly hygroscopic substances, being also well endowed with OH groups. This aspect of the present work was of great interest and is discussed in a subsequent paragraph.

With respect to the contribution to sorption by environmental factors, namely temperature and relative humidity (RH), again, these two factors were reviewed in relation to permeation in section 1-6 of Chapter 1. It is not the intention to go over this again. However, it is worthy to remember that the RH, as mentioned at the beginning to this discussion, can be taken as a measure of the concentration of water molecules in a given environment. Thus, as far as the results are concerned, the contribution of RH to the extent of sorption as seen with the different film samples was generally not unexpected. The disproportionately high sorption at 90 % RH was possibly due to changes in the structure of the polymer films. The sorbed water in the polymer, acting as plasticizer could have lowered the glass transition temperature (T_g) of the films, potentially transforming the polymers from a glassy state into a rubbery state. In the rubbery state, the films could have exhibited increased chain mobility, less tortuosity and an increase in diffusivity (Bair, 1981; Hancock and Zografis, 1994; Coyle, 1996), favouring access to sorption centres within the polymer matrix or aggregation to form water clusters. Some of these aspects of sorption were highlighted in section 1-5 (Chapter 1) and are further explored in Chapter 3.

The contribution of temperature, as the results demonstrated, on the extent of sorption was mixed. In some cases, there was observed a marginal increase in the extent of sorption with an increase in temperature (e.g., Eudragit EPO), while in other film samples (i.e., Eudragit L30 D-55, Opadry AMB and Sepifilm LP), the amount of moisture sorbed by the films appeared to decrease. Since the sorption process is essentially exothermic in nature, the observed decrease in sorption would rightly be attributed to the inhibition of forward reaction. The apparent increase in the extent of sorption in the Eudragit EPO film would suggest that a parallel process occurred at the higher temperature which favoured sorption, e.g., conversion of this film into rubbery state, which as explained above, could also have favoured higher sorption.

A point of interest relates to how the results obtained in the present study compare with the results reported in the literature. It would appear that the studied moisture barrier films sorbed comparatively less moisture than respective film samples fabricated from pure polymers. For instance, Petereit and Weisbrod (1999) reported values of between 6 and 12 % db for a film sample of ethyl methacrylate, while Srinivasa et al., 2003 reported values of 25-35% db (between 50 and 90 % RH) for poly(vinyl alcohol) films. It is clear, therefore, that the moisture barrier film systems studied in this work, generally, achieved lower levels of sorption compared to the corresponding pure polymer film samples. It is speculated that the inclusion of hydrophobic materials, like stearic acid, talc, or magnesium stearate, in some of the films contributed to lowering the sorptive capacity of the pure polymer film samples. The effect of hydrophobic ingredients has already been reported by several other workers (e.g., Debeuafort et al., 1994; Donhowe and Fenema, 1994; Morrilon et al., 2002).

While the lower hygroscopicity evident in the Opadry AMB film sample studied in this work (compared with the expected sorption as a result of the two hygroscopic materials in this film) could not have resulted from the inclusion of the talc (which is also hydrophobic and hence repels water). The fact that the unusual sorption-desorption pattern obtained with this film was, generally, not replicated in other film samples to which talc, stearic acid, etc., were present, suggests that this result was perhaps related to different phenomenon. That is to say, it is possible that the xanthan gum, though a hygroscopic material, could have achieved the effect of reducing sorption, just as well as any of the hydrophobic additives, albeit by a different mechanism. This conclusion is arrived at on the evidence of work reported by several investigators. For instance, Achanta et al (2001ab) reported unusual sorption behaviour of an Opadry AMB film similar to the one investigated in this study. In another study, Srinivasa et al

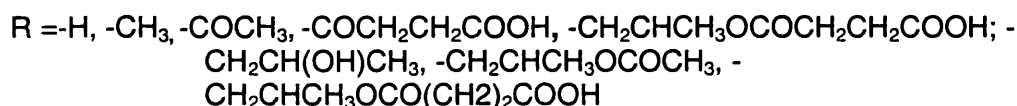
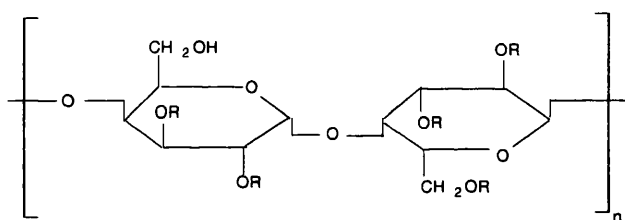
(2003) reported "unusual" behaviour for a poly(vinyl alcohol)-chitosan film, while Hartley et al (1995) reported what they termed non-ideal sorption for a starch-xanthan gum polymer film. Achanta and co workers suggested "irreversible hydrogen bonding" as the likely reason for the sorption-desorption characteristics of their Opadry AMB sample. However, given the fact hydrogen bond energies are quite low, typically 1-5 kcal/mol (compared with 10-30 kcal/mol for covalent bonds), the general expectation is that hydrogen bonds are reversible. Hartley et al., (1995), suggested a more plausible explanation of interpolymer hydrogen bonding and/or polymer interpenetration for the sorption behaviour of this system. Other types of interactions between poly(vinyl alcohol) with other polymers (e.g., polyethylene glycol through complexation) have been demonstrated elsewhere (e.g., Okhamafe and York, 1986).

In this study, an attempt was made to investigate the sorption-desorption behaviour of pure xanthan gum in relation to the poly(vinyl alcohol). The obtained sorption-desorption behaviour of this material can be seen in Appendix 1. The result showed the amount of water sorbed by the gum was very high. However, the xanthan gum did retain moisture at the end of the two desorption cycles in a similar way to that of the Opadry AMB film. This behaviour was not seen in pure poly(vinyl alcohol) powder or materials like sorbitol, guar gum, or sodium carboxymethyl cellulose (data not shown) similarly studied. It is possible, therefore, to suppose that the poly(vinyl alcohol) and xanthan gum polymers interacted during the film formation process, perhaps by a process similar to interpolymer penetration or complexation, which could have resulted in a more taut or closely packed film membranes. Interpenetrating polymer membranes have been defined as a combination of two or more polymers with a physically interlocked network structure between the component polymers giving rise to an advanced system with new property profiles (Kim et al., 2003a,b). On the basis of these postulations, the complexation or interpolymer penetration concepts may well serve to explain the unusual sorption-desorption characteristics of the Opadry AMB film sample. The unexpectedly low hygroscopicity at low RH that was observed with this sample perhaps represented behaviour moderated via a physical barrier process as opposed to specific bonding or the presence of hydrophobic ingredients, *per se*. Otherwise, the possibility for the presence of crystalline regions in this membrane as suggested by Hodge et al. (1996), among others, to account for the low sorption in this sample, cannot also be ruled out. However, these claims are unsupported by experimentation and clearly more investigations would be required.

The behaviour exhibited by the two enteric films, i.e., Sureteric and Shin-Etsu Acoat, whereby far less moisture was sorbed compared to the moisture barrier films was not

an expected outcome. In fact, on the basis of water-polymer interactions concept, the less moisture sorbed by enteric films could not be rationalised, especially given the close similarity in chemical structures between, say the poly(vinyl alcohol) and poly(vinyl acetate phthalate) on one hand, or hypromellose and hypromellose acetate succinate, on the other. Also, since the enteric polymers possess extra polar groups [phthalate, and acetate for the poly(vinyl acetate phthalate film)], it would be expected that the two enteric based polymer film samples would have, at least, taken up the same amounts of water, or in the extreme case, taken up more water due to the introduction of more polarity in the molecules. Figure 2-23 below shows the structural formulas of the two enteric polymers. Comparison with the structural formulas of hypromellose or poly(vinyl alcohol) which are shown in Figure 2-22 above, clearly shows that the enteric samples have a higher content of polar groups in the monomer units than the moisture barrier polymers.

Hypromellose acetate succinate



Poly(vinyl acetate phthalate film)

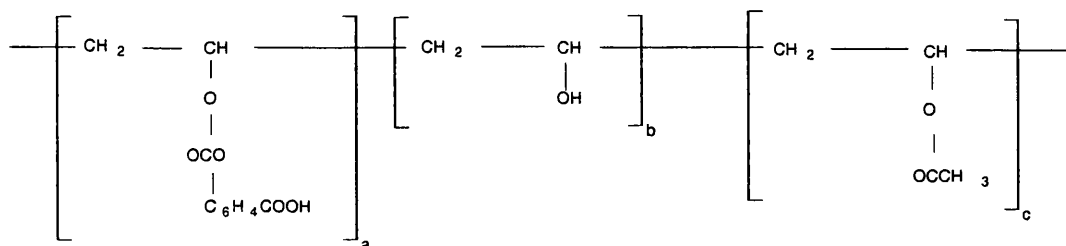


Figure 2-23. Structural Formulas of Hypromellose acetate succinate and Poly(vinyl acetate phthalate).

Thus, the lower hygroscopicity exhibited by the two enteric polymer samples could have been due to a more tightly packed film structure or by account of the polar groups being sterically unfavourable for moisture sorption.

2.5.3 Moisture Vapour Transmission Rates (MVTR)

In section 1-5 (Chapter 1), it was explained that the transport of a vapour through polymer membranes involves sorption, diffusion and desorption. This is demonstrated in Figure 2-24, this time as a flow sketch diagram:

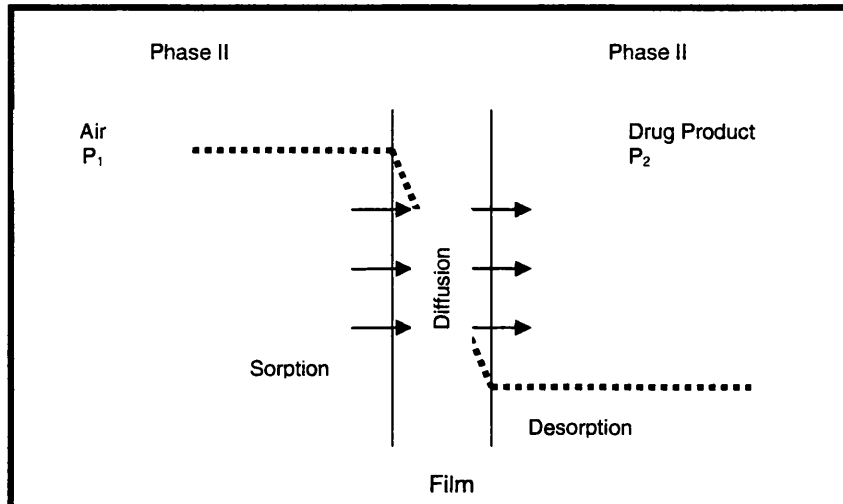


Figure 2-24. Sketch Diagram Illustrating the Transport of Vapour Through a Film

The sorption process involves the take-up of the vapour molecules into the film, but not through it. Thus, although sorption data, such as described in the previous sections, are important in describing barrier performance in certain respects, such data may not relate directly with barrier performance. In other words, it is perhaps possible for a film to have a high sorptive capacity while at the same time exhibit low moisture transmitting properties. This arises because of the fact that permeation is a kinetic process, contributed to by the diffusion of the water molecules in the polymer, as well. It may directly correlate with the sorption phenomenon or it may not. Therefore, and for this reason, it is often desirable to quantify the diffusive aspect of permeation as well. However, the measurement of this aspect of permeability can be difficult, requiring the measurement of pressure, which for a condensable gas like water vapour, may not be possible. Since the MVTR parameter, however, measures the quantity of the vapour rather than pressure, it makes it more possible to characterize the extent by which a given barrier membrane transmits a permeant.

In an attempt to understand these results, it is necessary to analyse the relationship between MVTR and permeability. The specific MVTR is related to the permeability coefficient, P , of the film by the following relationship (Piringer, 2000):

$$P = MVTR \left(\frac{l}{\Delta p} \right)$$

Equation 2-5

where l is the thickness of the film and Δp is the partial pressure difference across the film. To determine Δp , it is essential to know the dimensions of the permeation cell and the thickness and the permeability of the still air layer in the vicinity of the film. Unfortunately, it was not possible to obtain these parameters (data was not supplied by the equipment manufacturer). It was therefore not possible to calculate the permeability of the membranes using this approach. However, it should be apparent that both the permeability P and MVTR functions (from equation 2-5) are directly proportional. Therefore, if Δp is taken as a constant, then the specific MVTR ($MVTR_x$) and P should be somewhat equivalent, sample for sample.

Therefore, from consideration of the solution diffusion theory, it is not by coincidence that there was some form of correlation between MVTR data and the sorption-desorption data since, for a sample to transmit moisture, the water molecules must first be sorbed by the film. In other words, the film cannot transmit what it does not have. It would therefore be expected that highly sorbing films present more water molecules for transmission across their films than those which sorbed lesser quantities of water. The fact that the data for the Opadry AMB sample did not adhere to this generalisation requires that the second aspect of the solution-diffusion theory, i.e., the kinetics or diffusion of the sorbed water molecules, is considered. This diffusion process essentially defines the speed with which the sorbed water molecules can traverse the membrane. The higher the speed, the greater will be the amount reaching the second chamber, and hence the MVTR value obtained. With this picture, it is logical to suppose that diffusion process can be checked by the presence of "obstacles", which for a polymer membrane, could be in form of interactions with the polymer segments, or perhaps the presence of crystalline regions in the film (which are resistant to water) or perhaps due to hydrophobic additives which can repel the advancing water front.

There was no opportunity to measure the extent of diffusion of the water molecules with the present experimental set-up except perhaps, by visually examining the apparent rates of equilibration as presented in the sorption-desorption profiles. It is interesting to note that there appears to be a relationship between these apparent sorption-desorption rates and the patterns seen with the MVTR data. For instance, films which exhibited fast sorption-desorption rates and equilibrated fairly quickly (namely Sepifilm LP and Eudragit L30 D-55), on the whole, exhibited high MVTR rates. The converse was also true, i.e., samples that exhibited apparently slower sorption-

desorption rates were observed to yield lower MVTR values. Therefore, rather than the amount of moisture sorbed *per se*, it appears that it is the speed of movement, was the determinant of the MVTR values. This aspect is re-examined in Chapter 3.

While the moisture vapour transmission rate is a useful tool to measure mass flux through a membrane it does not provide any real insight into the underlying mechanism controlling the permeation process. For purposes of design and optimization, this is a significant setback since one has no idea about what aspect of the film performance needs to be tweaked. The other limitation relates to measurements on very permeable materials. In this case, the pressure P_2 , (see Figure 2-20) can be significantly reduced if the flux through the film is very high as a result of high permeability. In this case, the measured MVTR values may be lower than if $P_2=P_1$. If the same test was applied to a film of larger area, the flux would be much more increased, further magnifying the effect. By requiring the largest film area to be used in this test, the ASTM methodology may lead to the MVTR test yielding false (higher) results or results that depend on the dimensions of the sample tested. To overcome these limitations, the further analysis of the sorption-desorption data will be undertaken in Chapter 3.

2.5.4 Water-Polymer Interactions

For the sorption process to occur, the polymer film should have sorptive centres to which the sorbed water may bind. This was introduced in section 2.5.2 above. In general, there are three possible ways by which water interacts with a sorption site, i.e., dipole-dipole or dispersive interactions, hydrogen-bonding, and ion-dipole interactions (e.g., with a quaternized ammonium ion). Of these three, hydrogen bonding is the most dominant interaction (Semanova, et al., 1997). Hydrogen bonding of water to an active sorption site is made possible if the polymer possesses groups like hydroxyl, imide, ether, etc., in the polymer chain or as side groups. The presence of these groups also renders the polymer more hydrophilic.

Water associated with a polymer can display various types of thermodynamic behaviours. As highlighted in Chapter 1, there are at least three different types of thermodynamic water which are recognised. The first type of water corresponds to bulk/liquid or free water. This fraction is the one which does not interact with the polymer groups. It behaves as normal water in terms of its melting and freezing properties. Some authors describe it as freezing water (Hatakeyama and Hatakeyama, 1998). The second type of water corresponds to water that is loosely bound to the polymer. This fraction shows considerable supercooling and therefore freezes at a

temperature lower than that of bulk water. This type of water may display a significantly smaller enthalpy than that of bulk water and is sometimes termed freezing bound water. The third water type is water tightly bound to the polymer and is incapable of freezing. This water fraction will generally show no phase transitions. The sum of types two and three water are what is collectively defined as the bound water content.

It was necessary therefore to understand the nature of these interactions in order to build a correct picture about the binding of the sorbed water molecules to polymers in the different barrier films. This opportunity was provided by thermogravimetric analysis and near infrared spectroscopy. Thus, as discussed by Hatakeyama and Hatakeyama (1998), when water molecules exist in polymers without intermolecular interactions, both the TG and TG derivatogram curves terminate at temperatures less than 100 °C. Accordingly, such water fractions represent the “free” water in the material. Samples with bound water will show weight losses at temperatures ≥ 100 °C because such water fractions are more tightly bound in the polymer.

With respect to the present study, it can therefore be stated that the sorbed water molecules existed in more than one state within the films. The first fraction, characterised by rapid TGA loss data at temperatures below 75 °C, must have represented water molecules present as unattached water molecules or perhaps those less tightly bound to the film components. The second water fraction, exhibiting a transition at a high temperature, typically ≥ 250 °C, was that corresponding to water molecules bound to polar groups in the different film components, perhaps through hydrogen bonding. However, at this temperature, the possibility for loss of other volatile constituents in the films cannot be ruled out.

Part of the problem with this set-up is the potential moisture loss resulting from sample transfer from the DVS to the TGA. Also, the possibility that the mass of the samples increased or decreased depending on whether the samples were dry relative to the ambient RH cannot be ignored. This rendered it difficult to accurately relate the TG weight loss data to DVS moisture sorption data or the even to quantify the relative proportions of the different water fractions. Therefore, the purpose of this work mainly centred on studying the qualitative aspects of the moisture loss from the samples. The NIR data allowed verification of the data obtained from TGA. Thus, the apparent shifts in wavelength in the NIR region were due to the altered bond strengths caused by molecular conformational changes due to bending of the bonds, formation of bonds or breaking of bonds in the vicinity of the OH bond. The changes in intensity, on the other hand, reflected changes in the number of OH bonds vibrating with a specific frequency.

Both phenomena were caused by the addition of water to the samples. Thus, the sorbed water disrupted the free water clusters, breaking some hydrogen bonds and generating some new bonds, both in the bound (non-solvent) water and in the water involved as the solvent (free water). The fact that there were more water hydrogen bonds compared to those in pure water gave rise to new bands manifesting as wavelength/intensity shifts. The greater the disruption, the higher were the shifts observed. Thus, on the basis of the two sets of data, it can be assumed that the displacements in the bands in response to an increase in water content were due to intermediate states of water coexisting simultaneously, each with slightly different IR absorption energies. These intermediate water states correspond to water molecules hydrogen bonded to the polymer or to other water molecules sorbed in the polymer matrix. This means that hydrogen bonding was an important mechanism by which the sorbed water was bound within the films. In samples with a greater extent of polar groups, the extent of hydrogen bonding was higher while in samples with fewer polar groups, there was less hydrogen bonding of the sorbed water.

2.6 CONCLUSIONS

2.6.1 Introduction

Experimental investigation of moisture sorption and desorption characteristics of four moisture barrier films, i.e., Eudragit L30 D-55, Eudragit EPO, Opadry AMB and Sepifilm LP, as well as two enteric polymer films, i.e., Sureteric (Poly(vinyl acetate phthalate) and Shin-Etsu Aqoat (hypromellose acetate succinate), was undertaken by dynamic vapour sorption (DVS), moisture transmission rate (MVTR) measurements, thermogravimetric analysis (TGA) and near infra-red (NIR) spectroscopy. Important differences in the amount of moisture sorbed or desorbed, the rate of sorption, and whether equilibration was attained, were observed. The manner by which the sorbed moisture interacted with the different polymers in the films was also speculated. These findings are summarized below:

2.6.2 Effect of Film Type

Moisture barrier films exhibited wide differences in the extents of moisture sorption and desorption. The sorption behaviours of the two enteric polymer samples were very similar. However, these samples sorbed very little moisture. Moisture barrier samples, on the other hand, sorbed more moisture. The differences in hygroscopicity exhibited by barrier films were attributed to the differences in chemical properties of the constituent polymers in the different film samples. Thus, the more hygroscopic samples were presumed to have a higher moisture sorption due to the availability of more polar groups in the respective polymers or other ingredients to which water molecules were capable of binding. Inclusion of hydrophobic materials, like stearic acid, talc, or magnesium stearate had the effect of lowering the sorption of moisture in the film samples. It was suggested that the enteric polymer samples had very minimal attraction for water due to steric hindrance of polar groups or more taut membranes. The unusual behaviour of the Opadry AMB samples was attributed to physically moderated barrier action which restricted moisture sorption and desorption.

2.6.3 Effect of RH and Temperature on Moisture Sorption

An increase in RH resulted in an increase in the extent of sorption. At high RH, all samples exhibited a disproportionately high extent of sorption. This was attributed to plasticization of the polymer by the sorbed water which rendered the films more fluid and open with the result that the water molecules were able to gain access to the matrix. Increase in temperature resulted in a decrease in sorption in Eudragit L30 D-55, Opadry AMB and Sepifilm LP film samples. It was speculated that the increase in

sorption in Eudragit EPO sample was due to plasticization, which rendered the membrane more fluid, and thus, more accessible to water molecules.

2.6.5 Moisture Vapour Transmission Rates

In general, there was established a correlation between MVTR data and the sorption data. The less hygroscopic films were observed to transmit less moisture compared with the more hygroscopic samples. The data for Opadry AMB samples did not correspond to this generalization. Also, films which exhibited fast sorption-desorption rates and equilibrated exhibited high MVTR rates compared with those that had apparently slower sorption-desorption rates. It was concluded that the rate of equilibration rather than the amount of moisture sorbed *per se*, determined the MVTR values. The high values obtained at the 0-90 % RH gradient were attributed to possible plasticization of the polymer matrix.

2.6.4 Nature of Water-Polymer Interactions

Thermogravimetric analysis and NIR spectroscopy of hydrated films demonstrated that the major sorbed water-polymer film interactions were via hydrogen bonding. It was concluded that a proportion of the sorbed water was bound to the polymer segments by hydrogen bonding while another proportion existed as free unbound water. The higher the propensity for hydrogen bonding, the greater was the extent of sorption observed.

CHAPTER 3

Chapter 3

3.0 MOISTURE PERMEATION IN CAST POLYMER FILMS

Outline

- 3.1. Introduction
 - 3.2 Aims and Objectives
 - 3.3 Materials and Methods
 - 3.4 Results
 - 3.5 Discussion
 - 3.5 Conclusions
-

3.1 INTRODUCTION

In a permeative process, matter, for instance, water vapour is exchanged in systems formed by two or more contacting phases. This process usually proceeds until a state of thermodynamic equilibrium is attained. For a polymer coating applied onto a tablet core, the resulting specimen can be envisaged as a system of contacting phases, i.e., the external environment having a certain concentration of water molecules, characterized by a certain relative humidity (RH), and the core of the tablet, consisting, perhaps of a lower RH. The two phases are separated by a polymer coating across which the water vapour may be transmitted.

Investigations in permeative processes involving the transport of water vapour through polymer membranes can be described in terms of the solution-diffusion mechanism, comprising sorption of the vapour at the polymer coating surface, diffusive transport of the permeant through the coating and desorption of the penetrant from the membrane at the polymer coating-tablet core boundary. The theoretical basis for the solution-diffusion mechanism, including its quantitative solution (i.e., $P=[S][D]$), was extensively reviewed in Chapter 1 of this thesis. With regards to the solution diffusion mechanism, sorption of water vapour comprises the uptake by and interaction with the polymeric material. This process is thermodynamic in nature and can be further analysed in terms of a thermodynamic equilibrium. Many aspects of equilibrium sorption can be expounded with the aid of the sorption isotherm. Diffusion, on the other hand, is the process by which the sorbed water molecules are transported through the membrane. The diffusion coefficient describes the speed of this transport, and hence, the overall kinetics of the permeation process. The concepts of the sorption isotherm and diffusion were also reviewed in Chapter 1, and will not be repeated here.

3.1.1 Measurement of Sorption Isotherms

When the sorption process is slow relative to the time the water vapour and the polymeric material are in contact, non-equilibrium sorption may be seen. This was observed in Chapter 2, whereby some of the film samples studied under fixed-time regimes were not able to achieve equilibration. If sufficient time for sorption were to be allowed, a point may be reached when a state of dynamic balance is achieved. Therefore, like any other equilibrium driven process, the system will have molecules of water vapour interchanging continuously across the phases but the rates of interchange will be equal and no net mass change is observed.

Equilibrium sorption is attained because the rate of sorption and desorption are equal. Under such conditions, the chemical potential of the water (μ_v) in the vapour above the polymer and the chemical potential of the sorbed water in the polymer (μ_p) will be equal, i.e. $\mu_v = \mu_p$. This relationship describes a very important dictum and is the basis for describing the thermodynamics of the sorption process. By chemical potential is meant the change in a characteristic thermodynamical state function, such as the free energy (ΔG), enthalpy (ΔH), etc., per change in the number of molecules of a system (Smith, 1973). The chemical potential cannot be determined directly, however, for gaseous substances, and vapours like water vapour, it can be expressed in terms of the sorbate activity, which is related to partial pressure. For water-polymers systems, the water activity (a_w) is equivalent to the equilibrium vapour pressure (p) divided by the saturated vapour pressure (p^0). Water activity is very roughly equivalent to relative humidity (Zografis, 1988; Martin, 1993).

The sorption isotherm is the relationship between the amount of water vapour sorbed and the equilibrium vapour pressure (or the water activity, for that matter) for a given amount of water vapour sorbed on a given solid (polymer) at a fixed temperature. The isotherm is a fundamental concept in sorption science, and is frequently utilised to derive valuable information pertinent to the sorbent-sorbate interactions (Cerofolini and Rudzinski, 1997). Further, the interpretation of sorption isotherms is facilitated by the use of several mathematical models that offer a physical description for the isotherm. Several of these sorption isotherm models, e.g., Langmuir model, BET model, Flory-Huggins theory, etc., were reviewed in Chapter 1. Generally, the interpretation of sorption in terms of the above-mentioned isotherm models is one of the main tasks of sorption theory, and aims to generate quantitative parameters which have real physical meaning to the behaviour of the sorbent-sorbate system.

Although the amount sorbed at equilibrium is, on its own, an important parameter as far as the performance of polymers is concerned, in the respect of permeation, a more useful parameter is the sorption or solubility coefficient, S . The solubility coefficient, which is a key term in the solution-diffusion mechanisms, measures the amount of water vapour that partitions in a given polymer. It may be obtained from the slope of the linear portion of the isotherm at low water activities where it is assumed that Henry's Law applies (Debeaufort, 1993), or it can be calculated from the equilibrium sorbed amount using *Equation 3-1* below:

$$S = \frac{c}{p} \quad \text{Equation 3-1}$$

This relationship defines the solubility coefficient in terms of the vapour pressure (p) exerted by the water above a solid, and can easily be derived from *Equation 1-6* (see section 1-5, Chapter 1).

The term c in *Equation 3-1* above, is the equilibrium concentration. It can also be readily computed with the aid of *Equation 3-2* below, from the knowledge the initial and final mass of the polymeric material following a known amount of water uptake, the volume of the polymer and the molecular weight of the water.

$$c = \frac{M_{\infty} - M_0}{V_p M.W} 22414 \quad \text{Equation 3-2}$$

Thus, c is the equilibrium concentration of the water in the membrane [mass per volume units (g/cm^3)]; M_{∞} and M_0 are the final and initial mass of the film at a given RH. The units of S are [cm^3 (STP)/ cm^3] for water vapour with partial pressure p (cmHg) having a molecular weight (g mol^{-1}) of 18.01. The constant 22414 is the value for molar volume (cm^3) of an ideal gas at STP. The volume V_p of the polymer can be obtained from knowledge of the film density (ρ , g/cm^3) and it's mass.

3.1.2 Methods for Measurement of Diffusion Coefficients

There are several methods for measuring diffusion coefficients of gases and/or vapours in polymer membranes which are described in the literature. For practical purposes, most of the techniques involve at least one of the following approaches: (i) permeation through a membrane into a closed chamber (constant volume); (ii) permeation through a membrane into a flowing stream (constant pressure), and (iii) sorption-desorption studies. The three proceeding techniques, as mentioned in this paragraph above, are briefly reviewed in the paragraphs that follow below:

3.1.2.1 Permeation through a Membrane (Constant Volume)

This method is sometimes known as the time lag technique. It combines evaluation of the steady state permeation with the analysis of the earlier transient enabling the determination of both the permeability coefficient, P , and the diffusion coefficient, D , from one experiment. The theoretical basis for this technique is as follows:

If the diffusion coefficient is assumed constant, for a membrane that is initially free of permeant, from the instant the diffusant is admitted to one side of the membrane prior to the establishment of steady state, both the rate of flow and concentration at any given point in the membrane vary with time. Under these conditions, Barrer (1939), using a constant value of the diffusion coefficient, D , proposed a unique solution for Fick's Second Law (Equation 1-17, section 1-5, Chapter 1) for steady state permeation through the polymer membrane, i.e.:

$$Q_t = \frac{DC_1}{l} \left(t - \frac{l^2}{6D} \right) \quad \text{Equation 3.3}$$

where Q_t is the amount of permeant passing through a film of thickness l in time t , C_1 is the concentration at the upstream side of the membrane. The necessary boundary conditions are an initially large gas-free film, attainment of equilibrium at the inlet gas-polymer face, and zero concentration of gas at the outflow face. Under these conditions, a plot of Q_t versus t yields a straight line whose intercept θ on the t -axis is equal to $l^2/6D$.

The permeability coefficient may be obtained with the help of Equation 1.3 using the slope of the asymptote in Figure 3.1 below when steady state permeation has been reached, i.e.:

$$P = \frac{\Delta Q l}{\Delta t \cdot A \cdot p_1} \quad \text{Equation 3-4}$$

The experimental set-up for this technique involves determination, as a function of time, the amount of vapour that crosses a polymer membrane to accumulate in a closed receiving chamber. The upper pressure is maintained constant and is much higher than the downstream pressure. This results in a pressure difference across the membrane that is almost constant. The amount of gas Q_t found in the container's chamber as a result of permeation through the membrane is then plotted as a function of time t . A typical plot is shown in Figure 3.1 below.

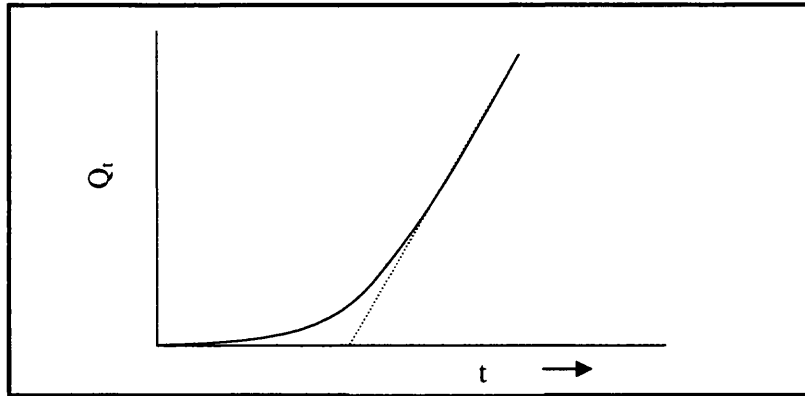


Figure 3.1. Time dependence of Permeation (Piringer, 2000)

The permeation curve approaches asymptotically a straight line, and the coefficients can be then determined by the time lag method. The amount of permeant that crosses the polymer membrane to accumulate in the cell may be measured by a variety of methods, including gravimetry, volumetric methods, and manometric methods.

3.1.2.2 Permeation through a Membrane (Constant Pressure)

In this method, the diffusing species cross the polymer membrane to reach an opened volume swept away by a gas stream. The stream of gas, e.g., nitrogen, helium, etc., flowing at a known flow rate f at normal pressure, carries the gas or vapour being studied (e.g., oxygen, carbon dioxide or water vapour) with a partial pressure p_1 . This gas serves to pull the penetrant towards an appropriate detector measuring the present proportion. After reaching steady state permeation, the value of partial pressure in the second chamber, p_2 , is then reached. The permeability P of the polymer membrane can be obtained with *Equation 3.5* below:

$$P = f \frac{p_2 l}{p \cdot A \cdot (p_1 - p_2)} = \frac{f \cdot c_2 \cdot l}{A(p_1 - p_2)} \quad \text{Equation 3.5}$$

where c_2 is the concentration of the test gas in the second chamber expressed as a dimensionless ratio of p_2 to the total pressure p in this chamber. The gas can be detected by UV/Vis spectroscopy or mass spectrometry, among others. This kind of measurement is advantageous as it can be applied to membranes susceptible to tear under high pressures. An extension of this technique has been used in the study of mixed gas permeability. This is relevant to industrial applications that demand materials able to support not just a single pure gas but, rather, mixtures of gases with different properties (Stern et al, 1983; Flaconnéche et al, 2001).

3.1.2.3 Gravimetric Sorption-Desorption Techniques

The diffusivity of a vapour can be readily obtained from equilibrium sorption-desorption data. For this purpose, there are several expressions available by which the diffusion coefficient, maybe defined and hence, determined. The two most commonly used expressions include the exponential dependence of the diffusion coefficient on concentration (Prager and Long, 1951; Mears, 1993) and the classical Fickian model approach (Crank, 1975). For the exponential diffusion approach, the experimental determination of the accompanying parameters is not easy.

The theoretical basis for the Crank model above is as follows: In a gravimetric sorption experiment, it has been shown that Equation 3-6 can be derived from Equation 1.10:

$$\frac{M_t}{M_\infty} = 1 - \frac{8}{\pi^2} \sum_{n=0}^{\infty} \frac{(1)}{(2n+1)^2} \exp\left(\frac{-D(2n+1)^2 \pi^2 t}{4l^2}\right) \quad \text{Equation 3.6}$$

where M_t is the total amount of penetrant sorbed into the polymer at a time t and M_∞ is the corresponding amount at equilibrium. The obtained diffusion coefficient, D , in Equation 3-6 above corresponds to either a constant or a mean of concentration dependent diffusion coefficients.

It can be seen that Equation 3-6 that the diffusion process can be described in terms of the equilibrium sorption-desorption data. When equilibration times are relatively short, e.g., $0.1 \geq M_t/M_\infty \geq 0.5$, Equation 3-6 reduces to Equation 3-7 below. This enables the diffusion coefficient D to be graphically extrapolated from the initial gradient of the plot M_t/M_∞ (fractional mass uptake or loss) versus $(\sqrt{t/l^2})$.

$$\frac{M_t}{M_\infty} = 4 \sqrt{\left(\frac{Dt}{\pi l^2}\right)} \quad \text{Equation 3-7}$$

On the basis of the obtained results, the diffusion process through the polymer may be described as Fickian or non-Fickian. It is reported that the diffusion mechanism is influenced by the relative magnitude of the rate of polymer chain relaxation and the rate of diffusion of the water molecules (Franson and Peppas, 1983). It is reported that for most hydrophilic polymers, non-Fickian kinetics are observed. This is attributed to the fact that the diffusion process is limited by the relaxation of the chains of the polymer in order to accommodate the advancing water molecules (Alfrey, 1966; Franson and Peppas, 1983; Sun and Lee, 1996).

The determination of the diffusion coefficient with this approach involves measuring the weight variation of a polymer sample submitted to the vapour, for instance, with a sensitive electronic balance. There are various evolutions of this technique, with some allowing measurements at high pressures and/or temperatures, and a resolution typically in micrograms. In the dynamic vapour sorption (DVS) equipment, electromagnetic coupling is used to transmit the sample weight to an external balance, which results in the system known as magnetic suspension balance. The technique was described in Chapter 2 of this thesis.

Alternatives to electronic microbalances include quartz crystal microbalances, where the weight is indirectly determined from resonance characteristics of a piezoelectric crystal, and; oscillating systems in which the mass change is linked to the oscillation frequency of a specific support. Some equipment couple the oscillation approach with a gravimetric technique to simultaneously obtain the weight variation and the swelling of the sample. There are also available other, somewhat less usual techniques, such as inverse gas chromatography or freeze-purge-desorption, which have been described in the literature. The main limitation of these techniques is the weak pressure that can be supported by the chromatography columns (Bergren, 1994, Piringer, 2000).

Generally, of the three techniques reviewed above for the determination of the diffusion coefficient, the sorption-desorption approach by gravimetry, is considered the most insightful. This is because of the ability to demonstrate how the three parameters of the solution-diffusion theory vary with the moisture content of a sample at the same time as the diffusion coefficient is determined. This is not possible with the constant volume or pressure approaches. This is the reason why this technique was selected for this work.

3.2. SPECIFIC OBJECTIVES

The main aim of the work presented in this chapter was to obtain equilibrium sorption-desorption characteristics of moisture barrier film coatings enabling the computation of the permeability coefficients. The goal of the work was to understand the influence of the constituent polymer and the role of environmental conditions, i.e., temperature and relative humidity (RH), on equilibrium moisture uptake and permeation from the films. The study required the determination of equilibrium moisture sorption-desorption profiles of films at several RH and temperature conditions from which isotherms and sorption-desorption kinetics were determined. The studies were limited to the four moisture barrier coatings, namely Eudragit L30 D-55, Eudragit EPO, Opadry AMB and Sepifilm LP. Enteric polymer coatings were not studied.

3.3. MATERIALS AND METHODS

3.3.1 Materials

All the materials, i.e., polymer films, used in the work undertaken in this chapter were similar to those described in Chapter 2. For more details on the descriptions of their characteristics, reference to section 2.3.1 is recommended.

3.3.2 Methods

3.3.2.1 Equilibrium Moisture Sorption-Desorption Studies

Equilibrium sorption-desorption studies were undertaken on moisture barrier film samples using the dynamic vapour sorption equipment as described in Chapter 2 (refer to Section 2.3.3). Enteric polymer films were not studied, the reasons being that these films were subsequently found to be poor barriers following application on to tablet cores (This aspect is separately discussed in Chapter 4).

The sorption-desorption protocols used for equilibrium conditions were different from those used for fixed-time studies. Samples were subjected to increasing RH conditions, i.e., 0-10-25-35-50-65-75-90 % RH, with step changes lasting between 300 and 600 min in the DVS equipment. These experiments were done at 25, 30 and 40 °C. The number of replicates was at least three, unless otherwise indicated. The weight of films used in these studies was maintained between 80 and 100 mg.

For the study of moisture sorption/desorption kinetics, the films, of known thickness, were subjected to 0-25-0-35-0-50-0-65-0-75-0-90-0 % RH test protocol, with step changes lasting between 300 and 600 min in the DVS equipment. Experiments were also done at 25, 30 and 40 °C. The minimum number of replicates was three.

3.3.2.2 Determination of Film Density

The density of films was determined on the basis of the Archimedes principle. Thus, a film of known weight was placed in vegetable oil of known volume. The displacement in volume of oil was taken as volume of the film enabling density to be determined.

3.3.2.2 Model Fitting

Modelling of the data to isotherm models was undertaken using linear and non-linear regression analysis. This was performed with the aid of Origin 7.5® software (OriginLab, Northampton, MA, USA). Statistical analysis, where undertaken, was with the aid of MINITAB® Statistical software (Minitab Inc, State College, PA, USA).

3.4. RESULTS

3.4.1 Introduction

The results in this chapter are presented under three main sections as follows: Sections 3.4.2 and 3.4.3 describe the results of the equilibrium moisture sorption-desorption studies; section 3.4.4 describes the results of the studies for moisture sorption-desorption kinetics, while section 3.4.5 describes the permeability coefficients of moisture in the films.

3.4.2 Equilibrium Moisture Sorption-Desorption Studies

The purpose of undertaking equilibrium moisture sorption-desorption experiments was to determine qualitative and quantitative differences in the moisture uptake and loss characteristics of the moisture barrier films following prolonged exposure to a range of relative humidity (RH) and temperature conditions. Experiments were conducted in a dynamic vapour sorption (DVS) equipment. Films were subjected to 0-10-25-35-50-65-75-90-75-65-50-35-25-10-0 % RH cycle at 25, 30 and 40 °C.

The results obtained from equilibrium moisture sorption-desorption studies are presented in five different formats as follows: (i) equilibrium sorption-desorption profiles, (ii) summarized equilibrium sorption-desorption data, (iii) equilibrium moisture sorption-desorption isotherms, (iv) solubility coefficients and (v) theoretical analysis of sorption-desorption isotherms. This multi-dimensional approach was necessary to allow derivation, analysis and interpretation of the different aspects of the moisture sorption-desorption data obtained from gravimetric sorption analysis.

3.4.2.1 Equilibrium Sorption-Desorption Profiles

Moisture sorption-desorption profiles are graphically presented as the dry basis (db) mass of the films following uptake or loss of moisture (% g of moisture/g of film) on primary y-axis versus time (in minutes) on the x-axis, as the RH was ramped between 0 and 90 and back to 0 %RH. These results can be seen in Figure 3-2 to 3-5 below, respectively for the Eudragit L30 D-55, Eudragit EPO, Opadry AMB and Sepifilm LP films at 25 °C. It was not possible to batch plot all the sorption-desorption profiles obtained at 30 and or 40 °C because of variations in equilibration times. The profiles obtained at 30 and 40 °C are presented in Appendix 2. It is worth mentioning that the figures presented generally reflect trends seen in at least three experimental runs performed on the film samples.

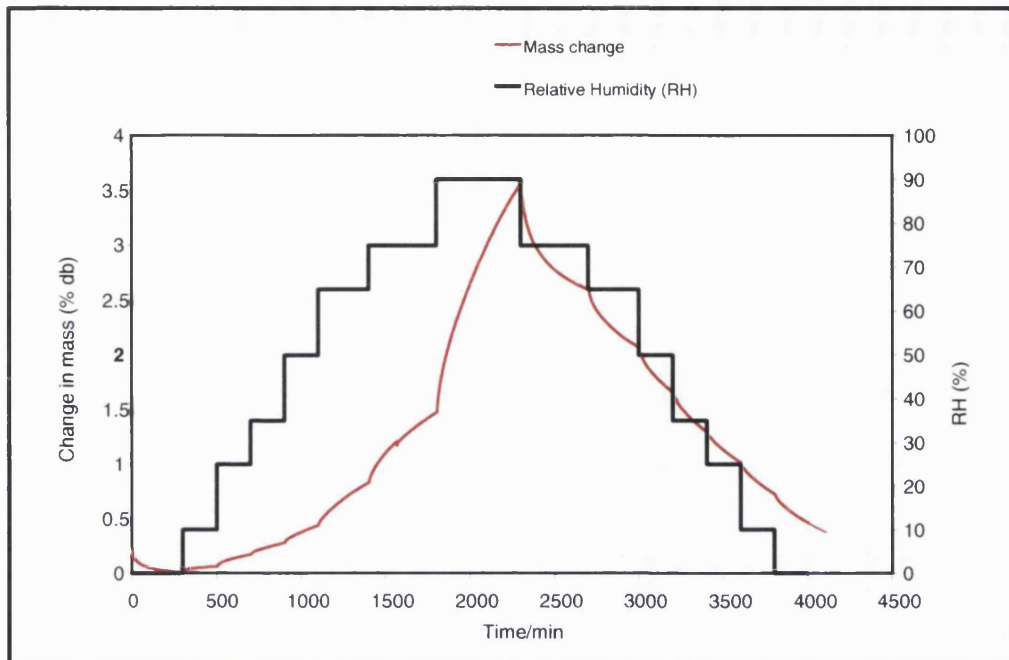


Figure 3-2. Equilibrium moisture Sorption-Desorption Profile of Eudragit L30 D55 Film Exposed to 0-10-25-35-50-65-75-90 % RH Cycle (25 °C)

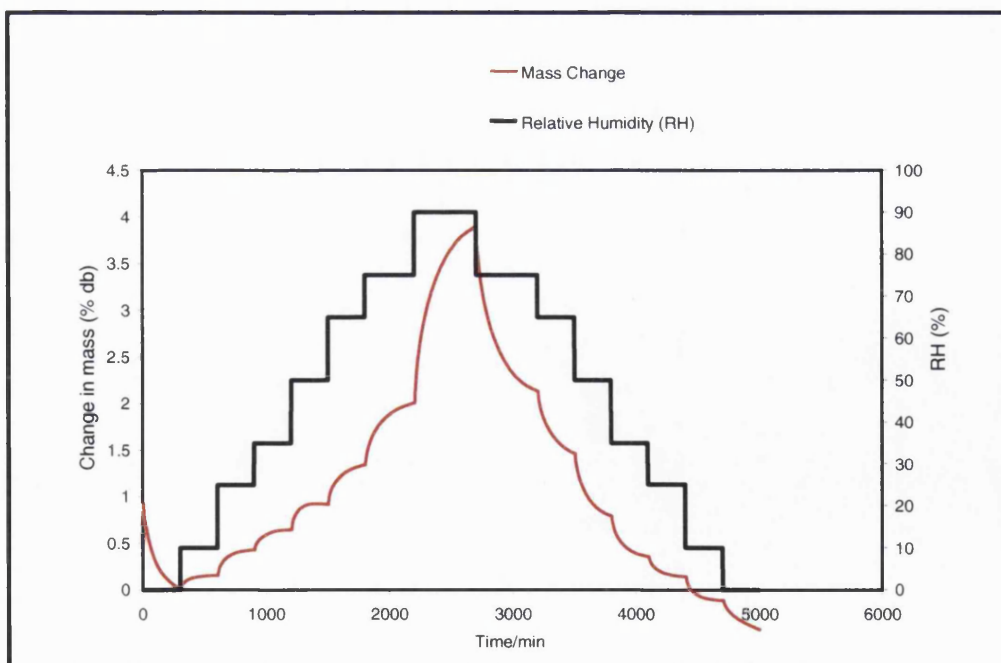


Figure 3-3. Equilibrium Moisture Sorption-Desorption Profile of Eudragit EPO Film Exposed to 0-10-25-35-50-65-75-90 % RH Cycle (25 °C)

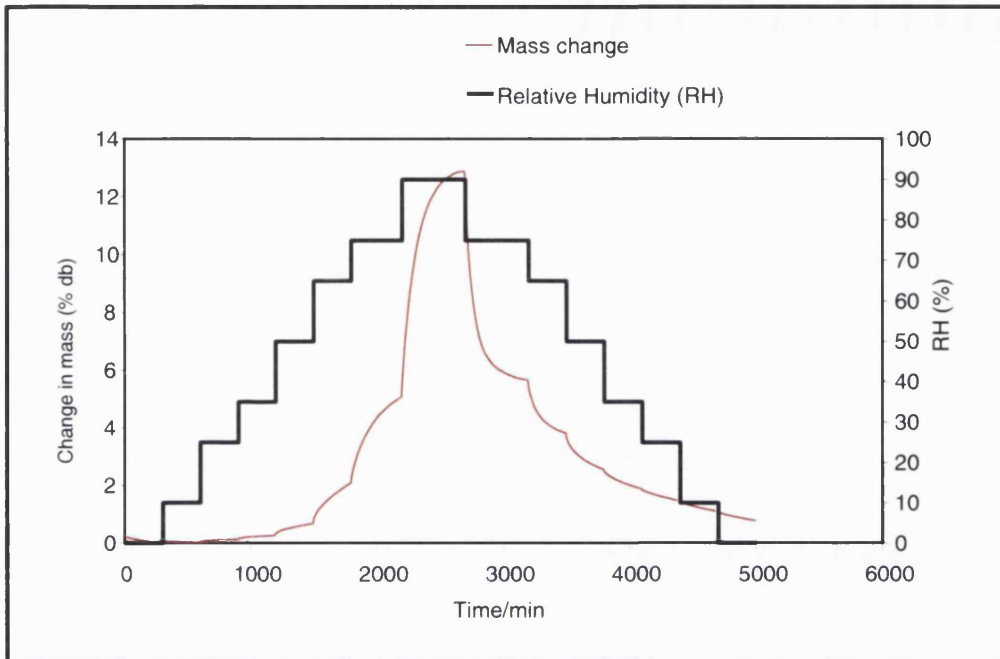


Figure 3-4. Equilibrium moisture Sorption-Desorption Profile of Opadry AMB Film Exposed to 0-10-25-35-50-65-75-90 % RH Cycle (25 °C)

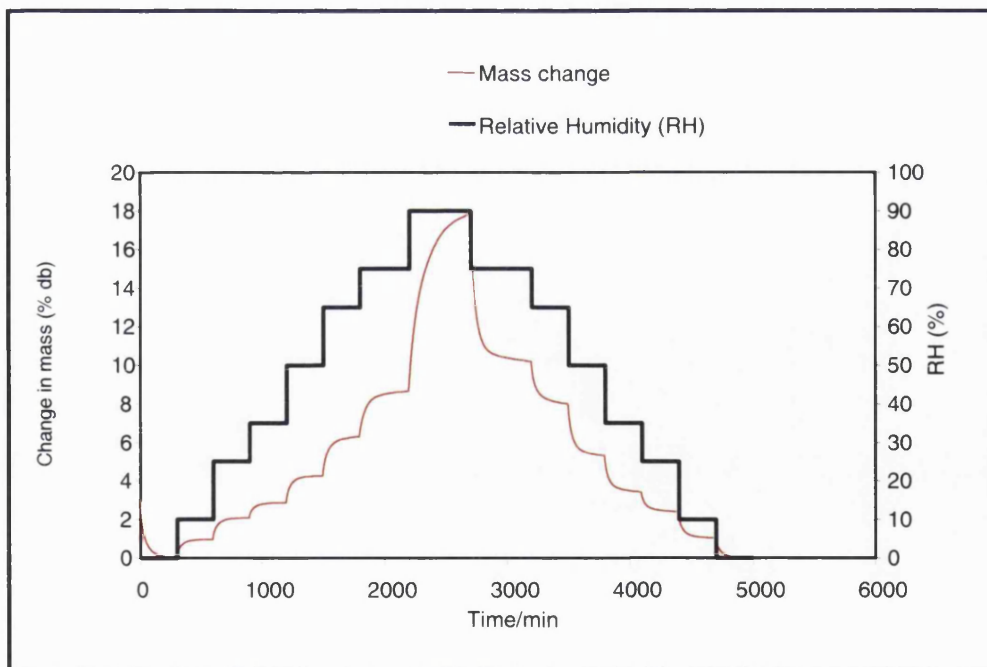


Figure 3-5. Equilibrium moisture Sorption-Desorption Profile of Sepifilm LP Film Exposed to 0-10-25-35-50-65-75-90 % RH Cycle (25 °C)

The equilibrium sorption-desorption profiles shown above demonstrate that, just like the investigations done under fixed-time regimes, the film samples studied were able to achieve equilibration with moisture fairly quickly even under this experimental set-up. "True" equilibrium was ascertained for each RH step change by programming the software to effect step changes in RH only when the difference between two successive data points was less than 0.1%. It can be seen from the sorption-desorption profiles that plateaus were obtained in most of the samples. This was an indication the sorption equilibrium was attained in those samples.

3.4.2.2 Equilibrium Sorption-Desorption Isotherms

The equilibrium moisture sorption-desorption profiles, examples of which are shown in Figures 3-2 through to 3-5 above, facilitated the computation of the equilibrium amount of moisture sorbed or desorbed for each of the seven RH conditions. The resulting equilibrium sorption-desorption data are summarised in Table 3-1 below. Subsequently, the equilibrium mass sorbed-desorbed data (here in referred to as the equilibrium moisture content, EMC) were plotted against the relative humidity (RH) to yield moisture sorption-desorption isotherms. These charts are shown in Figures 3-6 to 3-8, corresponding to data obtained at 25, 30 and 40 °C.

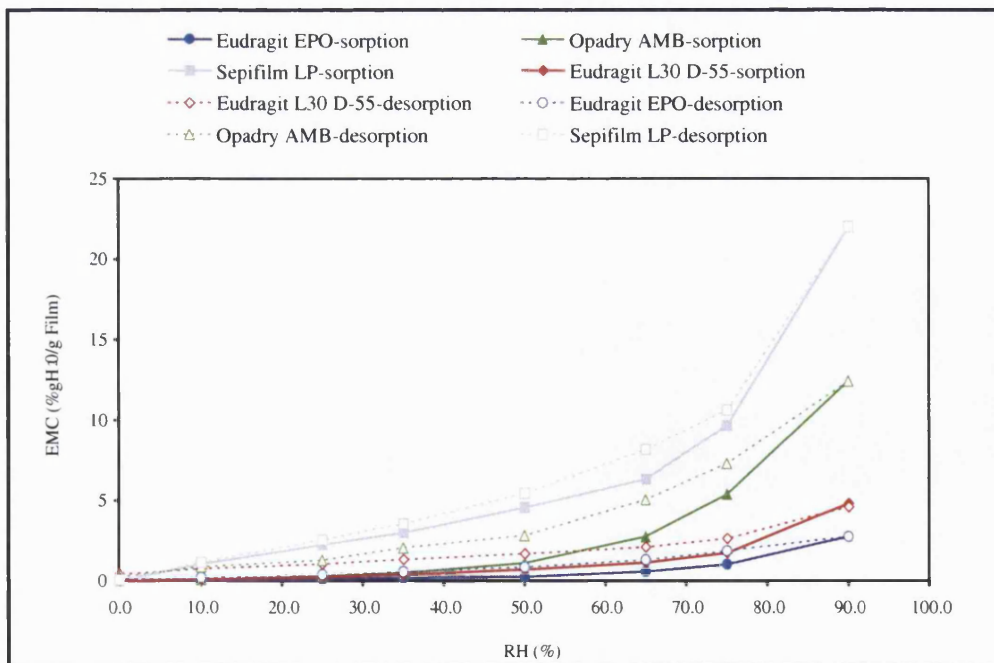


Figure 3-6. Moisture Sorption-Desorption Isotherms of Eudragit L30 D-55, Eudragit EPO, Opadry AMB and Hypromellose Films Measured at 25 °C

RH	Eudragit L30 D-55 Film			Eudragit EPO film		
	25.0 °C	30 °C	40.0 °C	25.0 °C	30 °C	40 °C
0.0	0.000 (0.000)	0.0000 (0.000)	0.0000 (0.000)	0.000 (0.000)	0.000 (0.000)	0.0000 (0.000)
10.0	0.061 (0.013)	0.0541 (0.001)	0.0859 (0.003)	0.009 (0.002)	0.153 (0.052)	0.241 (0.085)
25.0	0.171 (0.212)	0.1972 (0.193)	0.2168 (0.121)	0.060 (0.018)	0.425 (0.001)	0.536 (0.1006)
35.0	0.280 (0.001)	0.3571 (0.078)	0.4228 (0.021)	0.156 (0.049)	0.642 (0.007)	0.751 (0.301)
50.0	0.440 (0.062)	0.6590 (0.195)	0.8284 (0.154)	0.235 (0.003)	0.912 (0.144)	1.149 (0.015)
65.0	0.833 (0.284)	1.0889 (0.366)	1.2505 (0.474)	0.546 (0.117)	1.336 (0.008)	1.796 (0.418)
75.0	1.475 (0.144)	1.6990 (0.303)	1.9392 (0.268)	1.000 (0.547)	2.004 (0.502)	2.564 (0.842)
90.0	4.571 (1.357)	4.7863 (1.050)	4.9182 (1.285)	2.715 (0.410)	3.899 (1.755)	4.659 (0.995)
75.0	2.592 (0.995)	2.7073 (0.218)	2.5765 (0.019)	1.841 (0.553)	2.129 (0.193)	1.958 (0.259)
65.0	2.064 (0.618)	2.0331 (1.000)	1.8314 (0.363)	1.268 (0.104)	1.463 (0.403)	1.149 (0.104)
50.0	1.649 (0.015)	1.4218 (0.375)	1.1427 (0.870)	0.827 (0.282)	0.787 (0.269)	0.377 (0.189)
35.0	1.289 (0.075)	0.9570 (0.001)	0.6440 (0.223)	0.541 (0.148)	0.353 (0.100)	0.125 (0.087)
25.0	1.013 (0.320)	0.629 (0.0800)	0.323 (0.196)	0.3650 (0.135)	0.137 (0.095)	0.078 (0.001)
10.0	0.720 (0.096)	0.293 (0.0811)	0.11 (0.010)	0.182 (0.000)	0.117 (0.002)	0.056 (0.014)
0.0	0.374 (0.021)	0.008 (0.0019)	0.003 (0.000)	0.106 (0.059)	0.103 (0.061)	0.010 (0.001)

Table 3-1. Mean Equilibrium Sorption-Desorption Moisture Content of Eudragit L30 D-55, Eudragit EPO, Opadry AMB and Sepifilm LP Films Measured Between 0 and 90 %RH. Data Shown are (\pm Std Deviation) for n=3 Measurements Undertaken at 25, 30 and 40 °C

%Rh	Opadry AMB Film			Hypromellose Film		
	25.0 °C	30 °C	40.0 °C	25.0 °C	30 °C	40 °C
0.0	0.0000 (0.000)	0.000 (0.000)	0.000 (0.000)	0.000 (0.000)	0.000 (0.000)	0.000 (0.000)
10.0	0.1113 (0.000)	0.012 (0.005)	0.025 (0.010)	1.008 (0.499)	0.930 (0.000)	0.921 (0.260)
25.0	0.409 (0.097)	0.117 (0.041)	0.056 (0.002)	2.217 (0.811)	2.058 (1.025)	1.994 (1.200)
35.0	0.692 (0.179)	0.248 (0.008)	0.185 (0.052)	2.956 (0.044)	2.850 (1.195)	2.758 (1.972)
50.0	1.419 (0.008)	0.862 (0.032)	0.617 (0.660)	4.523 (1.353)	4.231 (1.300)	4.209 (0.018)
65.0	3.379 (0.964)	2.464 (0.129)	2.207 (0.355)	6.282 (1.898)	6.290 (1.344)	6.239 (1.850)
75.0	5.1883 (1.695)	5.057 (0.845)	4.777 (0.226)	9.637 (0.252)	8.635 (0.788)	8.148 (1.471)
90.0	13.527 (0.982)	12.872 (0.170)	11.23 (0.779)	21.989 (1.296)	17.864 (2.680)	16.004 (1.750)
75.0	7.6889 (1.245)	5.644 (1.069)	5.630 (0.514)	10.608 (0.639)	10.183 (1.475)	9.144 (0.904)
65.0	5.0034 (0.202)	3.811 (0.393)	3.904 (1.327)	8.122 (0.102)	7.992 (0.595)	6.996 (1.348)
50.0	3.3907 (1.199)	2.550 (0.168)	2.511 (0.684)	5.407 (1.149)	5.285 (1.559)	4.628 (1.180)
35.0	2.0219 (1.069)	1.872 (0.212)	1.696 (0.354)	3.519 (1.749)	3.413 0.324)	3.007 (0.922)
25.0	1.2287 (0.052)	1.458 (0.154)	1.197 (0.101)	2.514 (0.699)	2.388 (1.214)	2.101 (0.432)
10.0	0.8457 (0.151)	1.089 (0.135)	0.805 (0.243)	1.121 (0.426)	1.029 (0.012)	0.869 (0.234)
0.0	0.2350 (0.0129)	0.177 (0.062)	0.235 (0.052)	0.050 (0.018)	0.0703 (0.020)	0.167 (0.063)

Table 3-1 (Continuation). Mean Equilibrium Sorption-Desorption Moisture Content of Eudragit L30 D-55, Eudragit EPO, Opadry AMB and Sepifilm LP Films Measured Between 0 and 90 %RH. Data Shown are (\pm Std Deviation) for n=3 Measurements Undertaken at 25, 30 and 40 °C

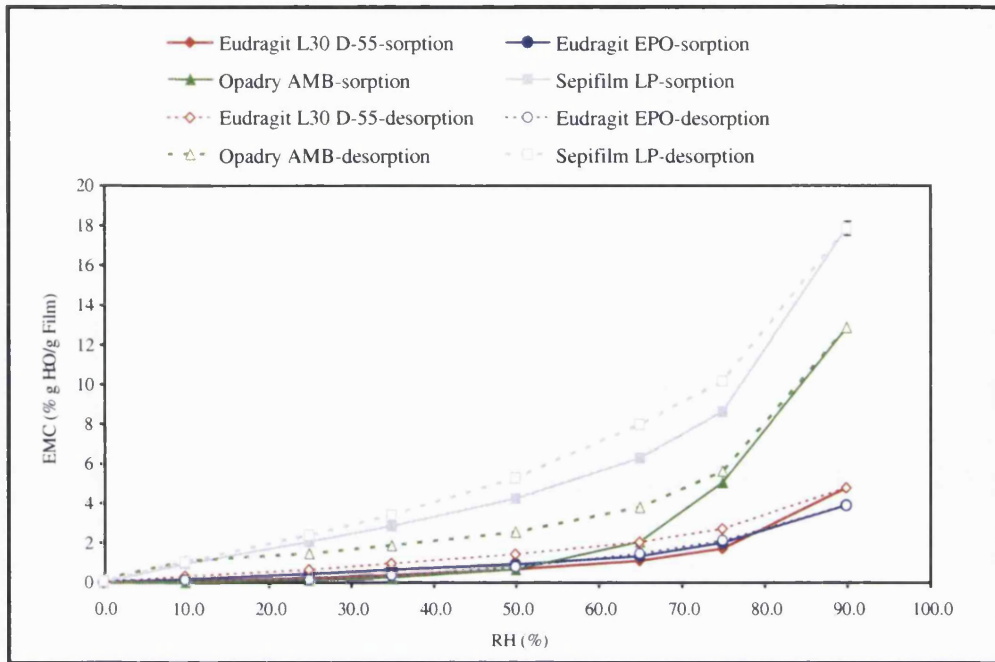


Figure 3-7. Moisture Sorption-Desorption Isotherms of Eudragit L30 D-55, Eudragit EPO, Opadry AMB and Hypromellose Films Measured at 30 °C

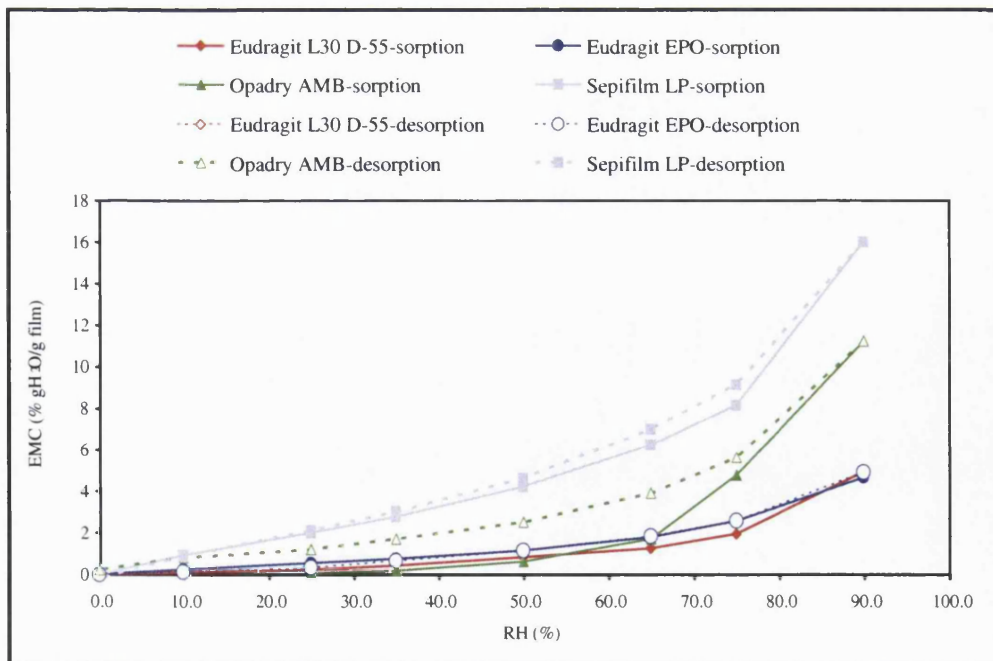


Figure 3-8. Moisture Sorption-Desorption Isotherms of Eudragit L30 D-55, Eudragit EPO, Opadry AMB and Hypromellose films measured at 40 °C

From the data presented above, the generalised effect of increasing the RH stepwise from 0 to 90 % was a corresponding increase in the equilibrium moisture content (EMC) of the samples. The specific trends are described as follows:

-At low RH (between 0 and up to 35-50 % RH), the EMC increased almost linearly. This is especially apparent from the data for the sorption cycles (indicated by solid lines in Figures 3-6 to 3-8). It can also be seen that a further increase in the RH from 50 to 90 % RH resulted in an exponential rise in the EMC of the samples, the highest sorption being achieved at the 90% RH condition.

-When the cycle was reversed, the EMC decreased accordingly in a stepwise fashion, but the sorption-desorption curves were not super imposable. This resulted in a hysteresis. Most hystereses in the literature display a closed loop, delimited by the sorption curve and desorption curve. The lowest value of the loop corresponds to the onset of the hysteresis phenomenon whilst the highest point at which the loop closes is the closure point, at which point both the sorption and the desorption curves coincide. In this work, however, the hystereses exhibited by the films were actually of the open type and did not reveal the onset RH. The shapes of the isotherms closely resemble Type III isotherms (according to the BET classification).

-It is of interest to observe that the trends in the equilibrium moisture content (EMC) values closely match data obtained under fixed-time regimes, more especially for the data obtained at ≥ 50 % RH. Thus, the hypromellose film still emerged as the most hygroscopic sample while the methacrylate films were among the least hygroscopic. As before, the Opadry AMB film was intermediate. However, it can be seen that at $\text{RH} \leq 50$ %, the Opadry AMB film was the least hygroscopic. This sample sorbed the least moisture (at 10, 25 and 35 %RH), an outcome not evident under fixed sorption test protocols (refer to Chapter 2). It would appear, therefore, that at a critical % RH (perhaps $35 \leq \text{RH} \leq 50$), there was a change in the affinity for moisture in this film sample whereby it ceased being the least hygroscopic sample and assumed the intermediate hygroscopicity that is so evident at higher RH.

The effect of temperature on the extent of sorption by the four samples can also be seen by examining the data presented above. Thus, increase in the study temperatures (i.e., from 25 °C to 40 °C) resulted in an increase in the extent of sorption in the Eudragit L30 D-55 and Eudragit EPO samples. However, the same factors were

observed to lead to a decrease in the extent of sorption for Opadry AMB and hypromellose films. This outcome somewhat differs from that obtained under fixed-time sorption-desorption regimes whereby only amino butyl methacrylate samples registered a net increase in sorption when the temperature was raised from 25 to 40 °C while the other samples exhibited a net decrease in the extent of sorption.

The above results, perhaps reflect the fact that under fixed-time regimes, equilibration was attained only in hypromellose samples. Thus, the trends evident under equilibrium regimes perhaps represent true behaviour. Similar results were reported by Achanta et al (2001ab) who observed a decrease in the extent of sorption in Opadry AMB films at 20, 30 and 40 °C. The effect of temperature on the behaviour of hypromellose and the methacrylate barrier coatings does not appear to have been reported previously in the main-line pharmaceutical literature.

3.4.2.3 Moisture Solubility Coefficients

The solubility coefficients, as defined previously, are summarised in Table 3-2 below. The data refer to the means of the respective coefficients obtained from the two cycles (i.e., sorption and desorption) for a given film sample. These values were determined with the aid of Equations 3-1 and 3-2.

Film Sample	RH	Temperature		
		25.0 °C	30 °C	40.0 °C
Eudragit L30 D-55 (density =1.347)	10	3.499	2.585	0.613
	25	4.374	2.861	2.086
	35	5.013	3.700	2.902
	50	15.986	11.072	3.981
	65	18.331	11.469	5.560
	75	19.139	13.816	7.657
	90	29.740	19.610	13.827
Eudragit EPO (density =1.028)	10	3.977	3.619	3.537
	25	9.093	4.709	4.880
	35	9.951	6.010	6.539
	50	10.568	5.589	5.353
	65	12.987	7.622	7.521
	75	15.386	8.327	8.111
	90	23.065	10.909	11.094
Opadry AMB (density = 1.115)	10	3.387	1.154	0.616
	25	5.026	1.722	0.786
	35	5.721	2.710	1.602
	50	24.926	9.763	3.975
	65	32.902	13.790	8.223
	75	44.444	23.535	15.988
	90	93.566	50.016	30.565
Sepifilm LP (density = 0.836)	10	72.401	35.525	23.308
	25	68.153	31.441	20.184
	35	65.820	31.0805	19.946
	50	67.140	32.304	21.303
	65	74.279	36.947	24.289
	75	86.403	43.969	27.479
	90	170.529	75.772	56.214

Table 3-2. Calculated Mean Moisture Solubility Coefficients [(cm³ (STP)/cm³ (polymer) cmHg) for Moisture Barrier Films in the 10-90 % RH Range

The data shown demonstrates the effect of RH and temperature on the extent of moisture sorption by the different films. It can be seen that increasing the RH resulted in an increase in the solubility coefficients. For a given film sample at a given RH, the effect of temperature was however, the opposite of RH in that the solubility coefficients can be seen to decrease.

The solubility coefficient (S), as explained earlier, is a thermodynamic parameter that can also be used as measure of the amount of water dissolved in a polymer film sample under equilibrium conditions in relation to the amount in the vapour phase above the polymer film. This is why this parameter was previously described as the equivalent of a partition coefficient of water between the film and the vapour phase. Thus, this parameter can add another dimension to the interpretation of the sorption-desorption data and assist in understanding key differences between materials.

From the data presented in Table 3-2 on solubility coefficients, the following trends in the values of the solubility coefficient emerge:

- The data for the Sepifilm LP sample, compared with the two Eudragit samples and in some cases Opadry AMB, show that Sepifilm LP sample had the highest solubility coefficients, demonstrating the preference of water vapour for this film.

- The values for the solubility coefficient were not constant for a given sample. This was in keeping with the non-ideal sorption characteristics of moisture in the polymers. The variation of the solubility coefficients with RH followed two general patterns. In the first case, represented by Eudragit L30 D-55, Eudragit EPO, and Opadry AMB, the solubility coefficients can be seen to increase progressively as the RH was increased. In the second case, typified by the Sepifilm LP film, there was an initial decrease in the values of the solubility coefficient which then appeared to increase with the RH.

- The effect of temperature is demonstrated by a general decrease in the values of the solubility coefficients for all the film samples studied. This data appears to contradict the "raw" data shown in Table 3-1, whereby temperature was shown to increase the extent of sorption in Eudragit L30 D-55 and Eudragit EPO samples but led to a decrease in sorption in Opadry AMB and Sepifilm LP films. In the case of the solubility coefficient, it is clear that the solubility coefficients for all the samples responded uniformly (i.e., increased) when the temperature was increased.

3.4.3 Modelling of Sorption-Desorption Isotherm Data

Sorption-desorption isotherms were further analysed by fitting the equilibrium moisture sorption-desorption data (Table 3-1) to the BET isotherm model and the Zimm and Lundberg Clustering Function equation. This was to facilitate the further understanding of the sorbed water-polymer interactions, to derive physically descriptive parameters that were able to quantify the binding of the sorbed water onto polymer segments, and to validate the experimental results obtained. Thus, this undertaking helped generate data to prove/disprove the hypothesis that the extent of moisture binding and barrier performance of a given sample film were related. In other words, films which bind water more tightly are more effective moisture barrier coatings. Data fitting to the different equations was undertaken with the aid of LabOrigin software. The results of this undertaking are presented separately to reflect the application of the data to the above-mentioned models as follows: section 3.4.3.1 presents the results for the BET while section 3.4.3.2 is for the Zimm and Lundberg clustering model.

3.4.3.1 BET model

The BET model provides parameters which measure the extent of moisture binding to the polymer. One of these parameters is the monolayer capacity, which, as will be explained, represents a physical entity. The other parameters are the energy constants, which are equally descriptive. Although the dual-mode sorption model (described in Chapter 1) also provides a similar parameter, its use is not very well established.

The BET plots were obtained by linear regression analysis (refer to section 1.5.2.3). The obtained plots are shown in Figures 3-9 to 3-12, respectively for the Eudragit L30 D-55, Eudragit EPO, Opadry AMB and Sepifilm LP film samples. The derived constants are summarised in Table 3-3. The data in Table 3-3 below show two key parameters, the monolayer value, M_0 , being the moisture content at which each polar group has a water molecular attached to it (Bell and Labuza, 1984), and the C_B , which is the energy constant. For each sample, the goodness of fit of the BET model to the experimental results is also presented.

As the results show below, the BET model was not able to give a global fit to all the isotherm data generated. For instance, in the case of Eudragit L30 D-55, only data at 25 °C were adequately linearized. Linearization was attained for Eudragit EPO and Sepifilm LP data sets corresponding to the three study temperatures. However, for

Opadry AMB, neither the sorption nor desorption data were linearized at any of the three study temperatures. The only sample where both sorption and desorption data at the three study temperatures were linearized was the Sepifilm LP sample. On the whole, typical goodness of fit measures (R^2) were >0.995 for this sample. Further attempts to linearise the data for the Opadry AMB using a smaller RH range (0-25 and 0-30 % RH) did not improve the fit obtained while uncertainties were much higher. It was clear that this model was not suitable for the analysis of the data for this sample.

		25.0 °C	30 °C	40.0 °C
Eudragit L30 D-55	M_{oB}	0.004	Data Not Available. Linearization was not possible with the BET model	
	C_B	2.590		
	R^2	0.925		
Eudragit EPO	M_{oB}	0.003	0.007	0.007
	C_B	6.231	2.539	3.810
	R^2	0.999	0.869	0.996
Opadry AMB	M_{oB}	Data Not Available. Linearization was not possible with the BET model		
	C_B			
	R^2			
Sepifilm LP	M_{oB}	0.028	0.026	0.025
	C_B	4.432	4.274	3.872
	R^2	0.998	0.999	0.979

Table 3-3. Calculated BET Model Constants M_{oB} (mg H₂O/mg Film) and C_B (Dimensionless) for the Film Samples (RH range of 0.0–0.5 %)

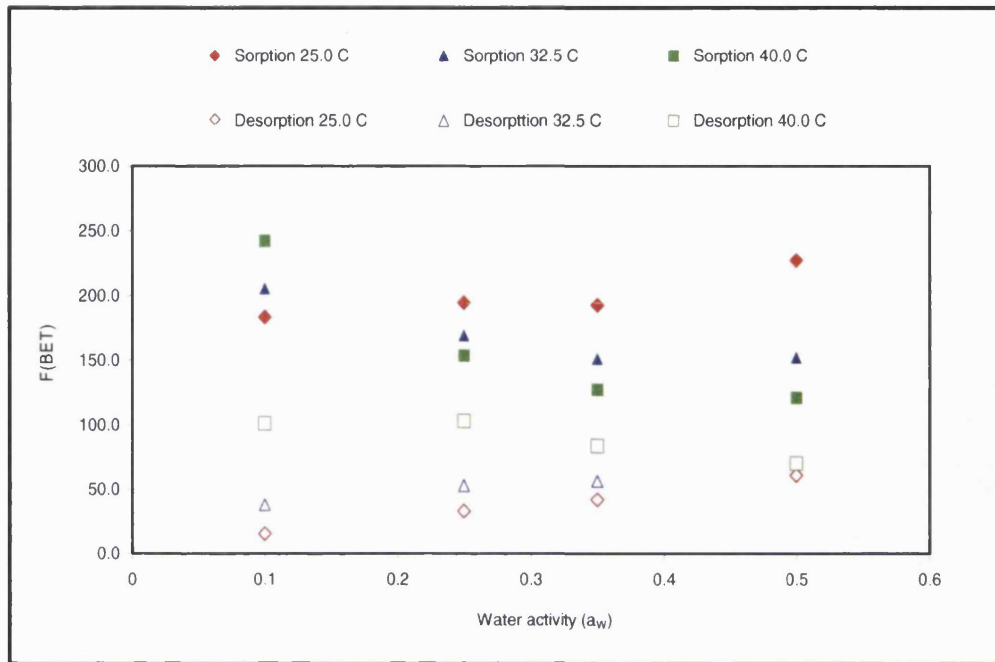


Figure 3-9. BET Isotherm Model Linearization Plot of the Equilibrium Moisture Sorption-Desorption Data for Eudragit L30 D-55 Film

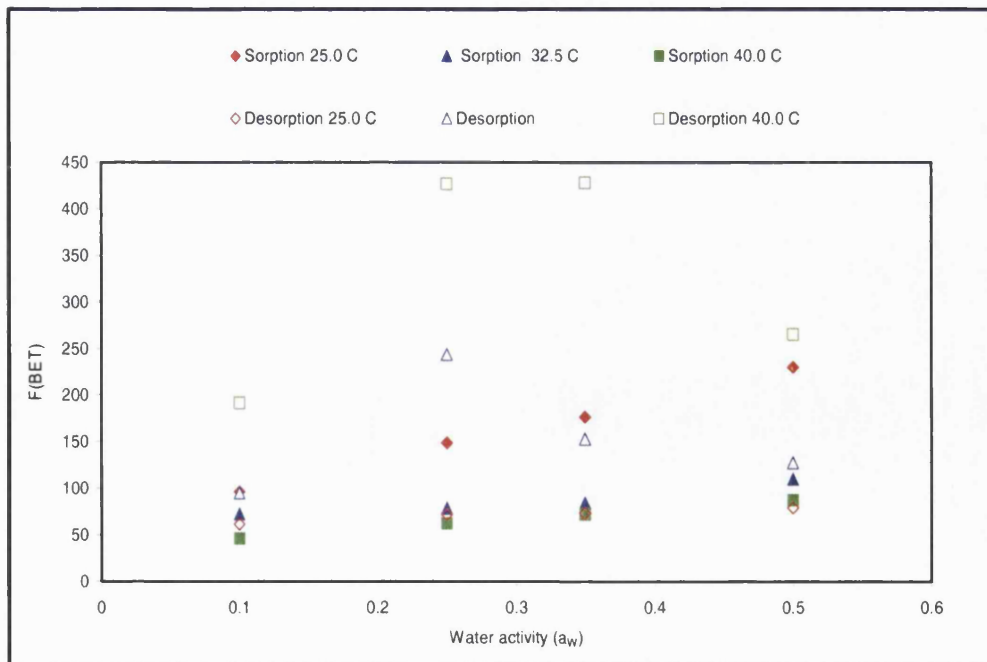


Figure 3-10. BET isotherm Model Linearization Plot of the Equilibrium Moisture Sorption-Desorption Data for Eudragit EPO Film

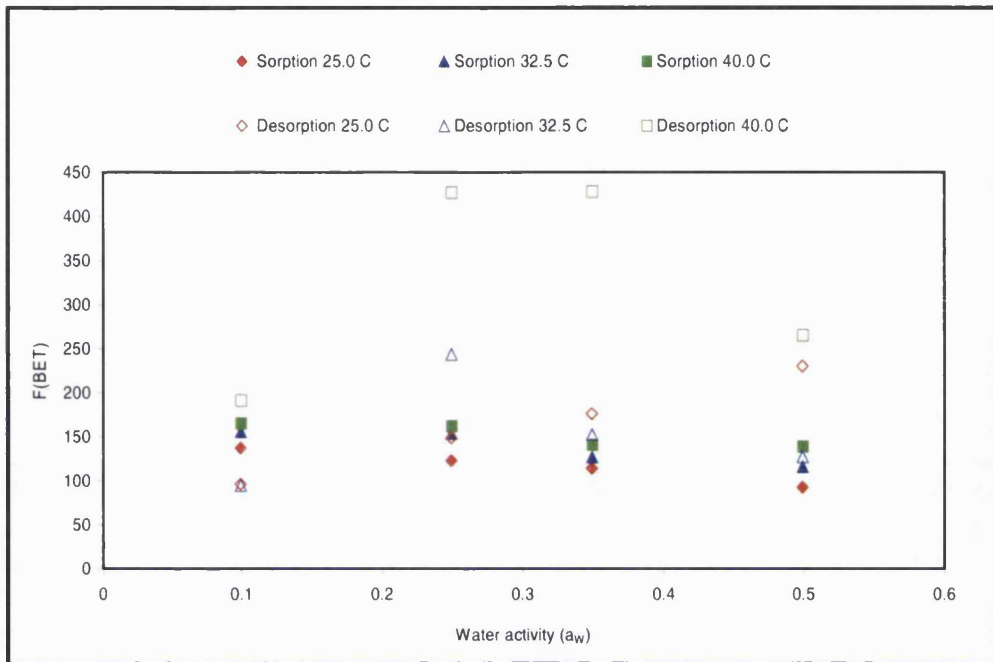


Figure 3-11. BET Isotherm Model Linearization Plot of the Equilibrium Moisture Sorption-Desorption Data for Opadry AMB Film

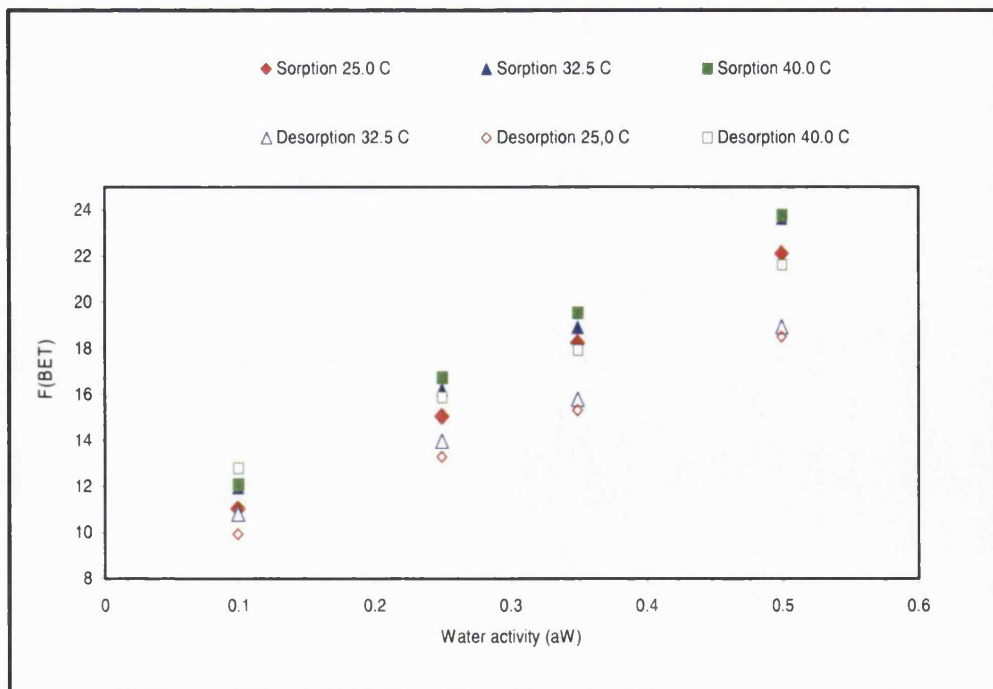


Figure 3-12. BET Isotherm Model Linearization Plot of the Equilibrium Moisture Sorption-Desorption Data for Sepifilm LP Film

Modelling experimental sorption data is an important aspect of measuring isotherms. It can greatly facilitate the interpretation of the isotherms in the context of a physical model. In fact, it can be seen in the literature on this subject that to the extent interrelation of sorption behaviour with polymer microstructure has been made, an understanding of the sorption process and its correlation with localised water structure has been regularly sought by these theoretical approaches. Isotherm modelling also adds another dimension to this field of inquiry. Not only does it provide a predictive element to the work, but it also helps unify or validate experimental results.

Taking the data at 25 °C, both Eudragit-based samples exhibited lower monolayer values. The Sepifilm LP sample exhibited a relatively much higher monolayer value. For validation purposes, the M_{oB} and C_B values for Sepifilm LP obtained in the present study compare well with those reported by Villaloboo et al., (2005) i.e., $M_{oB} = 0.019$ and $C_B = 4.2$ for a hypromellose-Tween 80 film system. The effect of temperature on monolayer values was demonstrated by the data for Eudragit EPO and Sepifilm LP samples, where the model provided a fit. Increase in temperature resulted in an increase in the M_o value for the Eudragit EPO, while the opposite effect was observed in the Sepifilm LP film. With respect to the energy constant (C_B), Eudragit L30 D-55 samples (at 25 °C) exhibited lower C_B values compared to the Sepifilm LP samples. Increase in temperature resulted in a decrease of C_B values in Sepifilm LP whilst an increase was observed for Eudragit EPO.

Furthermore, it is evident from Table 3-3 that there was a clear-cut correlation between the amount of water sorbed by the samples and their monolayer values. Sepifilm LP, the most hygroscopic sample, yielded an M_o value of 0.0276 (0.0003) g/g of water compared with a value of 0.0025 (0.0005) g/g of water for the Eudragit EPO sample. Initially, the high M_o value for the Sepifilm LP sample appeared odd, given the understanding that this sample had a fairly high water vapour transmission rate. However, on reflection, it emerged that this value correlated with the sorption of water molecules in the low activity ranges where the proportion of active sites is important. The sample with more polar groups would therefore have a higher M_o . It can also be seen that there is a correlation between the monolayer sorption data, on one hand, and TGA data, on the other, described in Chapter 2, where it was speculated that the Sepifilm LP film had a higher proportion of sorbed water bound to the polymer segments of the constituent polymer.

3.4.3.2 Zimm and Lundberg Clustering Function (G/v)

The cluster analysis of Zimm and Lundberg (Zimm and Lundberg, 1956; Lundberg, 1972) has been used to explain certain aspects of the moisture sorption in polymers. For instance, polymers with a strong interaction with water have negligible degrees of water clustering, while the more hydrophobic polymers exhibit a higher degree of clustering (Rodriguez et al, 2003). Clustering of water in a polymer membrane is important to the permeation process. This is briefly explained below as follows:

The degree of clustering has an important impact on the prediction of moisture sorption (and therefore permeation) from environments of high humidity and, possibly, on barrier performance of polymer coatings, as well. It was instinctive, therefore, to attempt to estimate the degree of water clustering in the respective samples. The Zimm and Lundberg clustering function (G/v) was adopted for this task. The definition of this function was provided in Chapter 1.

The clustering function was estimated from the data in Table 3-1. Only the data corresponding to experiments conducted at 25 °C were analysed. The procedure was as follows: The activity coefficient (a/ϕ) was first plotted against the water activity (a_w) to obtain a slope of the regression line. This was then fitted to equation 1-14 (Chapter 1) to calculate the clustering function, G/v. Typical plots of the activity coefficient versus the water activity are shown in Figure 3-13 below. The data for the calculated clustering functions are tabulated in Table 3-4 below.

RH	Clustering Function (G/v)			
	Eudragit L30 D-55	Eudragit EPO	Opadry AMB	Sepifilm LP
10	164.900	118.111	87.589	3.132
25	164.702	117.757	87.283	3.081
35	164.508	117.500	87.082	3.055
50	164.233	117.105	86.321	3.000
65	163.547	116.453	84.495	2.924
75	162.444	115.710	82.871	2.853
90	158.935	113.769	78.427	2.611

Table 3-4. Calculated Clustering Function (G/v) Values for Moisture Barrier Films. Data Shown only for Measurements Undertaken at 25 °C (Refer to Table 3-1)

The data, as shown in Table 3-4 above, demonstrate a number of important features. In the first case, there are distinct differences in the values of the clustering function for

the different film samples that can clearly be seen. The main feature of the results above is the sheer disparity of the values of the clustering function among the different samples. For instance, the differences between the data for Eudragit L30 D-55 and Sepifilm LP are of one order of magnitude. Secondly, a pattern of variation of this function with the RH is as follows: the function was highest at low water contents and appeared to decrease as the amount of water in the samples increased. However, the change in the function was not so big in relation to the change in the hydration of the samples. In some respects, the values actually appeared to remain constant to the extent that the temptation to interpret this parameter this way is irresistible.

It can also be seen that the clustering parameter was not discriminative enough to distinguish between the different hydration states of the samples, which is a disadvantage. However, it is also worthy mentioning that the theory of Zimm and Lundberg (1956), which is based on statistical mechanics of fluctuations, does not attempt to predict isotherms. Rather, it serves to interpret the isotherm in molecular terms in terms of the tendency for the water molecules to cluster. The advantage with this approach, compared, with the isotherm models discussed before, is that a direct means to measure non-random mixing is afforded without the need for ad hoc assumptions about the system.

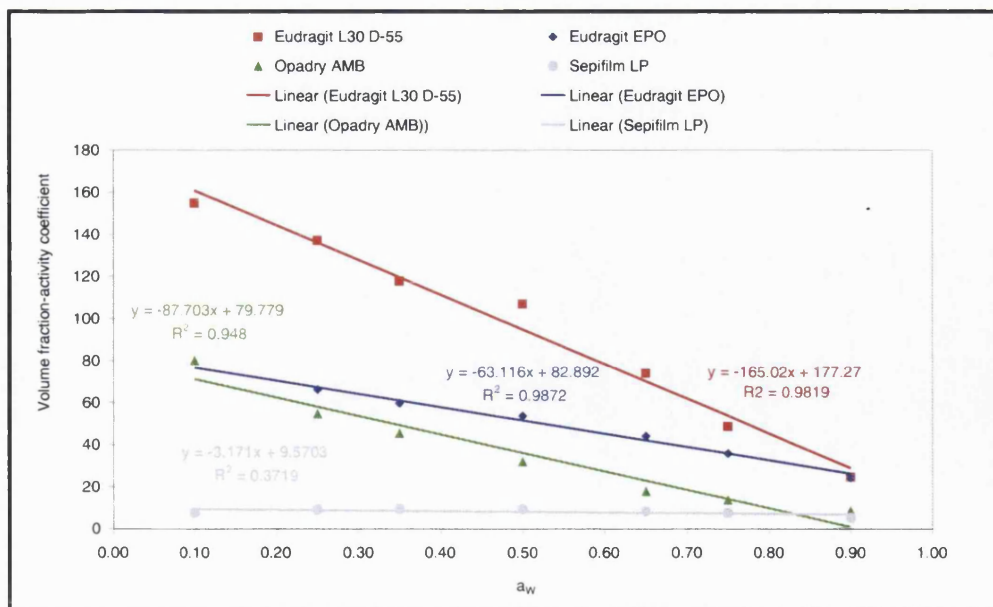


Figure 3-13. Regression Plots of Sorbed Water Volume-Fraction-Activity-Coefficient (γ) versus Water Activity (a_w) for the Equilibrium Sorption-Desorption Data for Moisture Barrier Films

According to Zimm and Lundberg (1956), for an ideal sorption process, the water activity, a_w , varies linearly with Φ , therefore $G_{11}/V_1 = -1$. This is reported to be the case for the sorption of permanent gases in polymer systems where the sorbate-polymer interactions are non-existent. In such a systems, the penetrant molecule excludes its own volume relative to other penetrant molecules and does not affect their distribution.

For non-ideal sorption processes, the clustering function decreases with increasing volume fraction of the sorbate such that $G_{11}/V_1 > -1$. This means that the concentrations of the sorbate molecules are higher than the average in the neighbourhood of a given sorbate molecule, which signifies a tendency to cluster. Thus, the quantity G/V can be used as a measure of the clustering tendency in such a way that when $G_{11}/V_1 > -1$ (isotherm convex towards the activity axis), there is an overall tendency for penetrant-penetrant pairs to be preferred (Lundberg, 1972).

The concepts reviewed above, when applied to the data, demonstrate that the samples not only exhibited clustering but that there were some differences in the tendency to cluster as well. Thus:

- The more hydrophilic samples exhibited relatively lower clustering tendencies while the more hydrophobic samples had higher clustering tendencies.

- Also, as the concentration of water in the polymer samples increased, the clustering function decreased, although, as already mentioned, the decrease was marginal.

- The fact that higher clustering was seemingly obtained at lower activity ranges rather than at the higher range would appear to be contradictory. However, it should be remembered that the clustering function does not measure the amount of clustering obtaining in the system, per se, but rather the tendency (or the "hunger") to cluster.

Thus, at the lower water activities (or RH, for that matter), the tendency for water molecules to segregate one from another was higher while at higher activities, the clustering obtaining was only sufficient to overcome the excluding effect of an isolated molecule. As Zimm and Lundberg (1956) stated, the first water molecules to enter into a polymer loosen up the structure making it easier for the subsequent molecules to enter in the neighbourhood of the first water molecule rather than go elsewhere. This is why the values of this parameter decrease with the RH.

In summary, the following were the main findings obtained from the study of equilibrium moisture sorption-desorption isotherms:

(i) **Equilibrium moisture content and Isotherms:** Equilibration with the different relative humidity conditions was apparent following prolonged exposure of the films in the DVS. The obtained profiles enabled the computation of the equilibrium moisture content (EMC), from which sorption-desorption isotherms were obtained. The isotherms were typically BET Type III. Thus, at low RH, there was observed a near linear variation of the EMC with the RH, while at high RH, moisture sorption was comparatively high. The effect of increasing the study temperature was a corresponding decrease in the extent of moisture sorption in the Eudragit L30 D-55, Opadry AMB and Sepifilm LP samples. An increase in sorption was observed in the Eudragit EPO film sample.

(ii) **Solubility coefficients:** The Sepifilm LP sample exhibited the highest solubility coefficients, demonstrating the preference of water vapour for this film. In a decreasing rank order, the solubility coefficients for the remaining film samples varied as follows: Opadry AMB film > Eudragit L30 D-55 film > Eudragit EPO film. The values of the solubility coefficient varied with the RH, which was in keeping with the non-ideal sorption characteristics of moisture within the samples. Two patterns were observed: In the first case, represented by Eudragit L30 D-55, Eudragit EPO Opadry AMB film, the solubility coefficients increased in a progressive fashion as the RH was increased. In the second case, typified by the Sepifilm LP film, an initial decrease in the values of the solubility coefficient which then increased with RH was seen. The effect of temperature on the solubility coefficients was a generalised decrease in the values of the solubility coefficients for all the film samples studied.

(iii) **The Zimm and Lundberg clustering function analysis:** It was established that the extent of clustering of the sorbed water molecules was generally lowest in the hypromellose film sample and highest in the Eudragit L30 D-55. The values for the Opadry AMB film sample were closer to the values for the Sepifilm LP sample. From this data, it was established that the tendency to cluster was greater in the Eudragit based films than in the Sepifilm LP or the Opadry AMB film samples.

3.4.4. Equilibrium Sorption-Desorption Kinetics

3.4.4.1 Sorption-Desorption Profiles

The experimental set-up whereby the relative humidity (RH) was varied from 0-25-0-50-0-75-0-90-0 % RH, with each step change lasting between 300-600 min enabled sorption-desorption profiles at different RH conditions and temperatures to be obtained. Typical plots of the profiles thus obtained are shown in Figure 3-14 through to Figure 3-17, respectively for the Eudragit L30 D-55, Eudragit EPO, Opadry AMB and Sepifilm LP film samples at 25 °C. The rest of the raw data, corresponding to 30 and 40 °C study temperatures, are presented in Appendix 2.

As in all previous cases where sorption-desorption profiles were plotted, the charts presented below also show the percentage dry basis (db) mass change on the primary y-axis versus time (min) on the x-axis as the RH was varied between 0-25-0, 0-50-0, 0-75-0 and 0-90-0 RH % (on the secondary y-axis). The exposure times were varied to allow for different equilibration times for the samples. It can also be seen that for most samples, equilibration times were fairly short and in all samples, the mass change curve levelled off, an indication that equilibration was achieved.

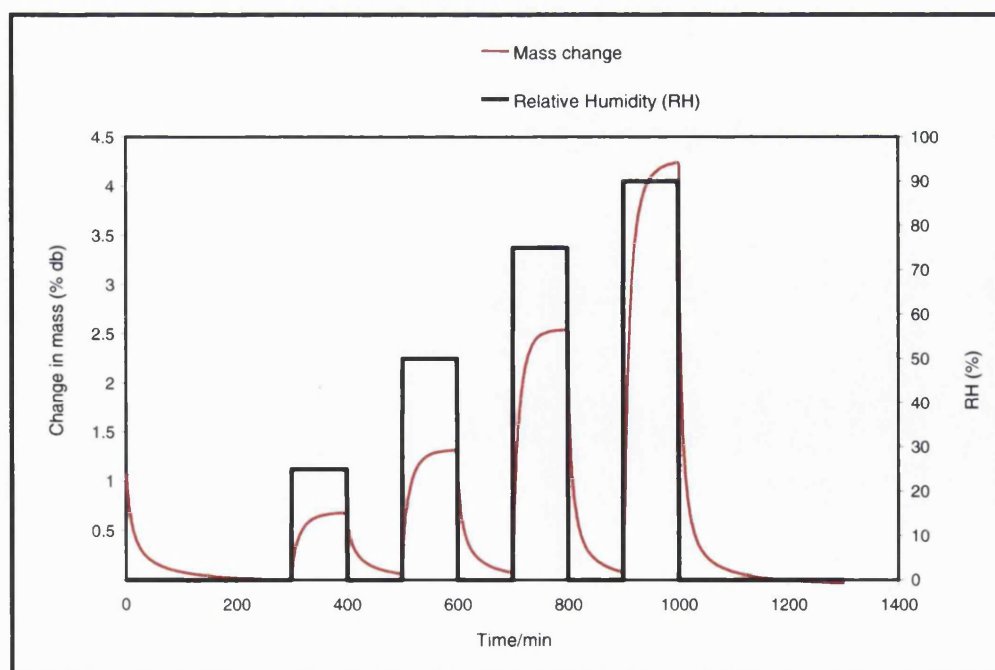


Figure 3-14. Step-wise Equilibrium Moisture Sorption-Desorption Profile of Eudragit L30 D-55 Film Exposed to 0-25-0-50-0-75-0-90-0 % RH Cycle (25.0 °C)

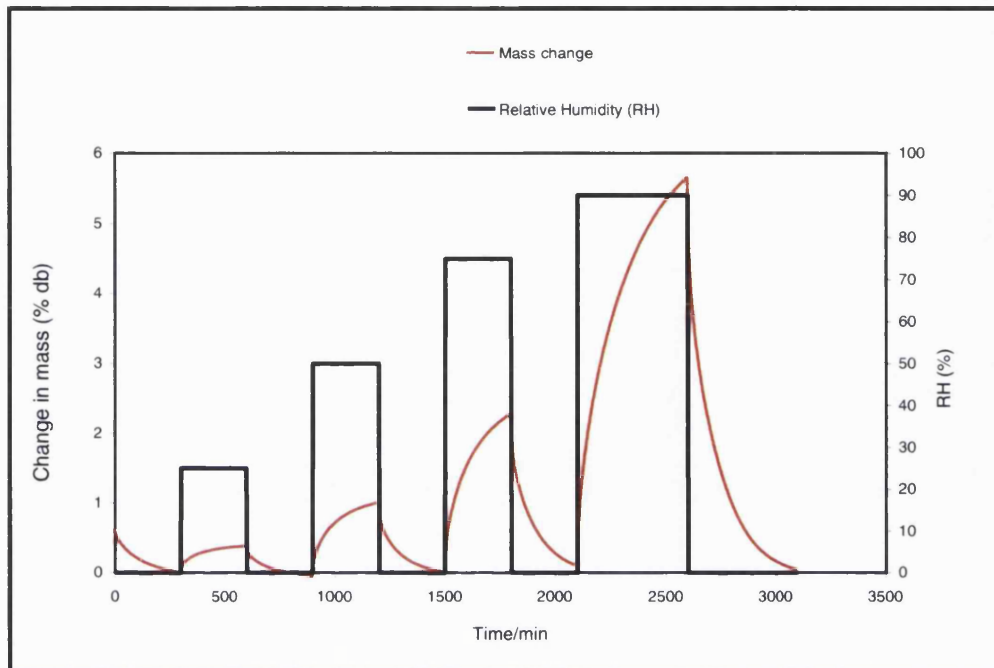


Figure 3-15. Step-wise Equilibrium Moisture Sorption-Desorption Profile of Eudragit EPO Film Exposed to 0-25-0-50-0-75-0-90-0 % RH Cycle (25.0 °C)

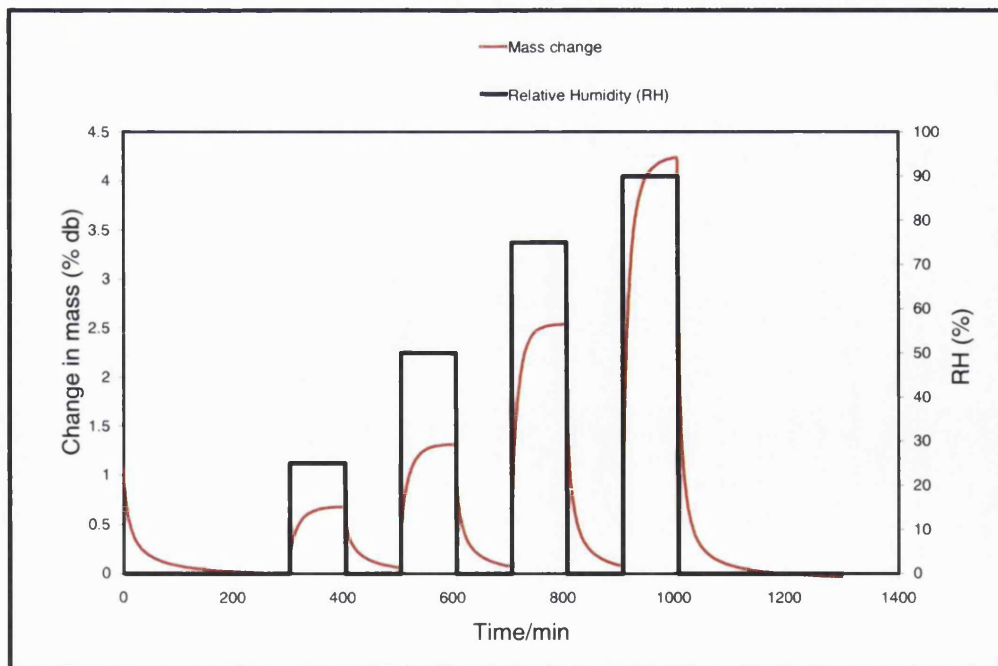


Figure 3-16. Step-wise Equilibrium Moisture Sorption-Desorption Profile of Opadry AMB Film Exposed to 0-25-0-50-0-75-0-90-0 % RH Cycle (25.0 °C)

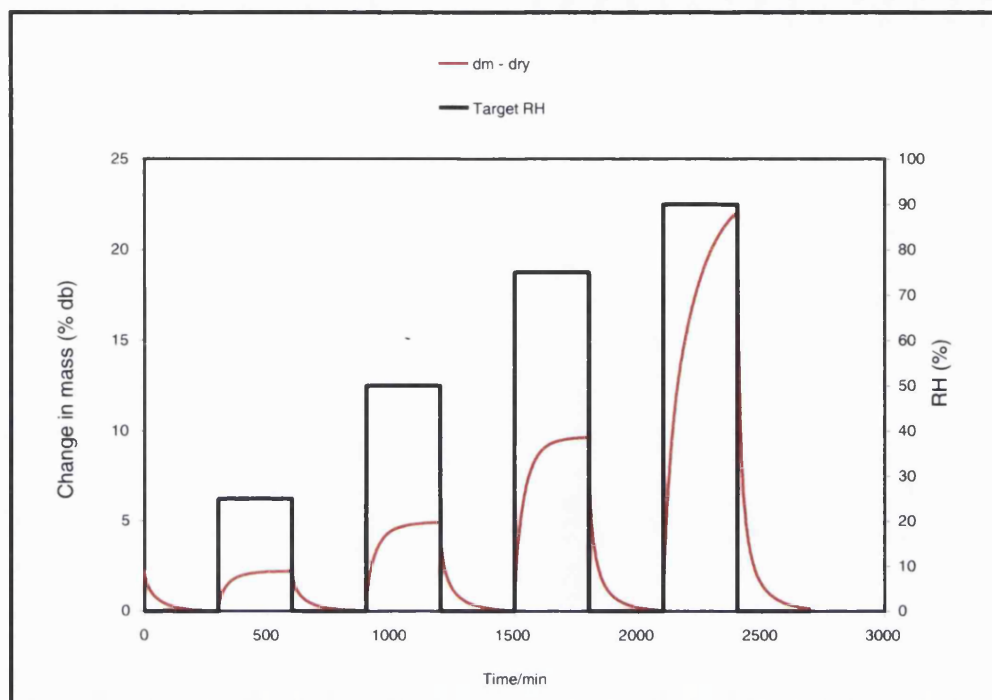


Figure 3-17. Step-wise Equilibrium Moisture Sorption-Desorption Profile of Sepifilm LP Film Exposed to 0-25-0-50-0-75-0-90-0 % RH Cycle (25.0 °C)

The results, as presented in Figures 3-14 to 3-17, for the step-wise equilibrium sorption-desorption studies reveal the responses of the different film samples to a step-wise increase in the RH. These curves are somewhat different from those shown in Figures 3-2 to 3-5, which were for the determination of isotherms. It was found necessary to use a step-wise protocol as this facilitated the study of the uptake/loss kinetics with one experiment. Thus, the initial RH step involved the variation of the RH from 0 to 25, which provided conditions to study a cycle for moisture uptake. By immediately reversing the cycle (to 25-0), it was then possible to generate data for the reverse (desorption) cycle. This pattern was then repeated for other RH gradients, i.e., 0-50 and 5-0, 0-75 and 75-0 and 0-90 and 90-0 % RH.

Owing to significant differences in the equilibration times among the film samples, it was not possible to plot all the curves on the same figure. This makes it difficult to see key differences in the sorption-desorption profiles exhibited by the different samples. If the equilibrium amount of moisture taken up at each of the RH conditions is considered, however, it will be seen that, in reality, the data have close similarity to the equilibrium sorption data obtained for the sorption-desorption isotherms in section 3.4.3.

3.4.4.2 Calculation of Diffusion Coefficients

Diffusion coefficients of moisture through the moisture barrier films were estimated from equilibrium sorption-desorption data using the Fickian diffusional model. The procedure involved fitting mass uptake data to Equation 3-4, from which the diffusion coefficient was estimated from the linear region of the plot.

The mass uptake data from the moisture sorption-desorption profiles (e.g., Figures 3-15 to 3-17) were utilised to obtain plots of M_t/M_∞ versus (\sqrt{t}/l^2) , otherwise known as kinetics plots. The plots, which show typical "S" curvature, are shown in Figure 3-18 to 3-21, respectively for Eudragit L30 D-55, Eudragit EPO, Opadry AMB and Sepifilm LP data obtained at 25 °C. Each chart corresponds to a given film sample.

The data obtained from the sorption-desorption profiles obtained at 30 and 40 °C are presented in Table 3-5. The solid lines in the charts refer to the kinetics plots corresponding to the sorption cycles (i.e., 0-25, 0-50, 0-75 or 0-90 % RH) while the dotted lines refer to the desorption cycles (i.e., 25-0, 50-0, 75-0 or 90-0 % RH).

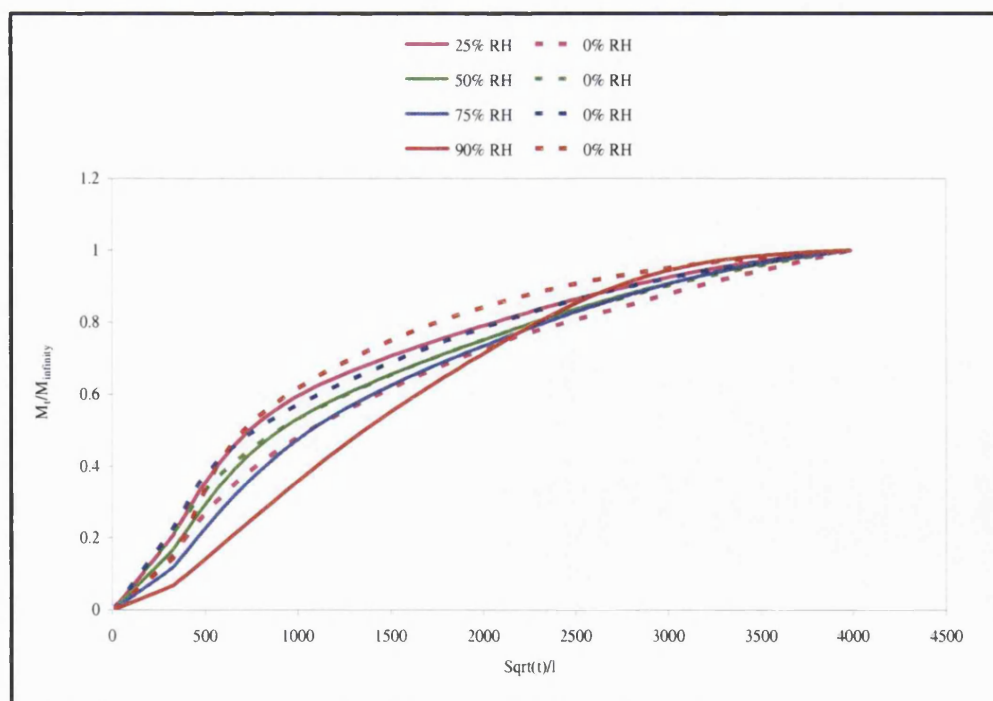


Figure 3-18. Plot of Fractional Uptake-Loss (M_t/M_∞) of Moisture versus Reduced Time (\sqrt{t}/l) for Eudragit L30 D-55 Film. Data for 25 °C.

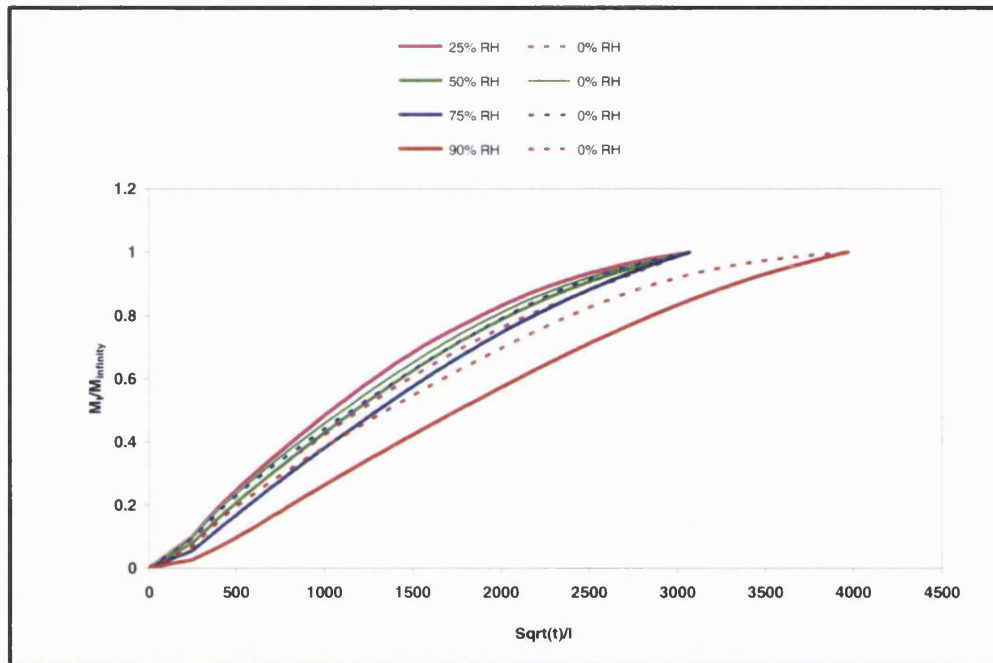


Figure 3-19. Plot of Fractional Uptake-Loss (M_t/M_{∞}) of Moisture versus Reduced Time (\sqrt{t}/l) for Eudragit EPO Film. Data for 25 °C.

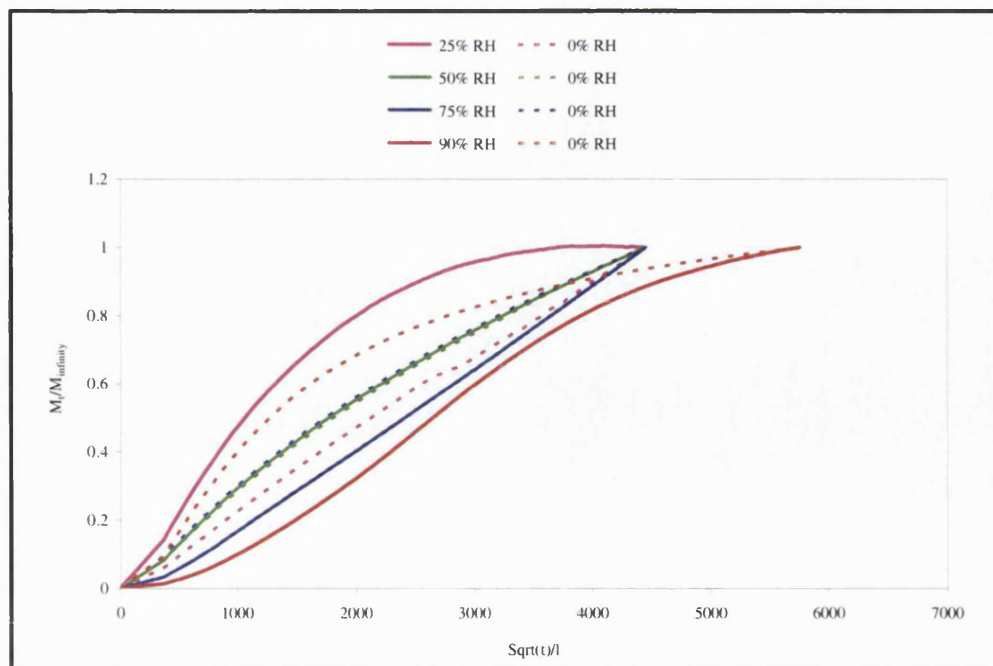


Figure 3-20. Plot of Fractional Uptake-Loss (M_t/M_{∞}) of Moisture versus Reduced Time (\sqrt{t}/l) for Opadry AMB Film. Data for 25 °C.

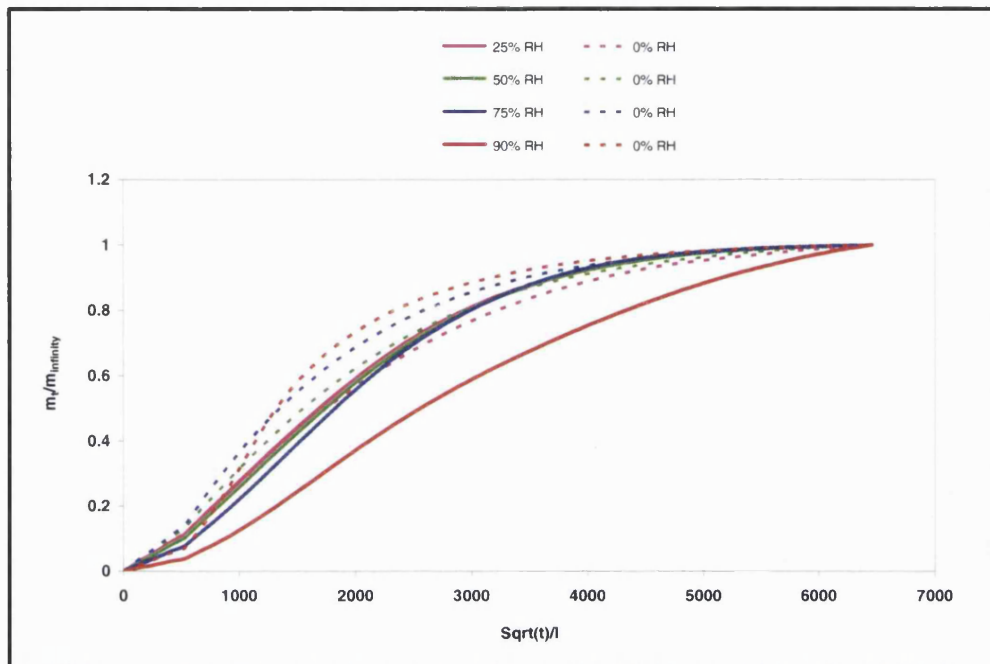


Figure 3-21. Plot of Fractional Uptake-Loss (M_t/M_∞) of Moisture versus Reduced Time (\sqrt{t}/l) for Sepifilm LP Film. Data for 25 °C.

All the curves in Figures 3-18 to 3-22 can be seen to display “S” shaped curvature. Also, the curves are generally fairly flatter in profile. This may imply that film samples did not instantaneously achieve saturation, which is in keeping with their role as moisture barriers. Although only data obtained at 25 °C are shown here, in reality, the curves at 30 and 40 °C exhibited similar behaviour.

With respect to the arrangement of the various curves corresponding to different step changes in RH, it can be seen that the sorption curve for the 0-25 % RH step change lies above the corresponding desorption curve. However, at the 0-50, 0-75, and 0-90 % RH step changes, this pattern can be seen to have reversed such that the sorption curves lie below the corresponding desorption curves. Irrespective of the sample or the temperature, the arrangement of the sorption curves showed no variation from this pattern, i.e., the curves for the 0-90 % RH step change lay below those for the 0-75 % RH step change which in turn lay below the 0-50 % RH step change. Except for the 25-0 % RH step change, desorption curves exhibited more variation in their arrangement.

To facilitate interpretation of the charts above, the early fractional sorption-desorption data (i.e., M_t/M_∞) were separately fitted to Equation 3-4. This procedure assumes that

diffusion coefficient; does not significantly change in this RH range, hence the nearly linear curve seen in Figures 3-16-3-19. For this work, a trial and error approach was used to establish the most suitable range that yielded the best fit. This was found to be $0.1 \geq M_t/M_\infty \geq 0.4$, which is slightly narrower than that reported in the literature. Nevertheless, there were sufficient data points within this narrower range that facilitated computation of the diffusion coefficients.

The obtained plots of M_t/M_∞ versus $(\sqrt{t}/l)^2$ for the reduced time are shown in Figure 3-22 and 3-23 for the Eudragit L30 D-55 sample, as an example. Although none of the regressions originated from zero, the intercepts were very close to zero and the goodness of fit values (R^2) were typically high. The diffusion coefficients thus obtained are summarized in Table 3-5.

It was not possible to calculate diffusion coefficients for the Eudragit L30 D-55 and the Opadry AMB film samples at 40 °C. Even though sorption-desorption profiles were successfully obtained at this condition, for reasons speculated later, the calculation of the diffusion coefficient was not possible using *Equation 3-4*.

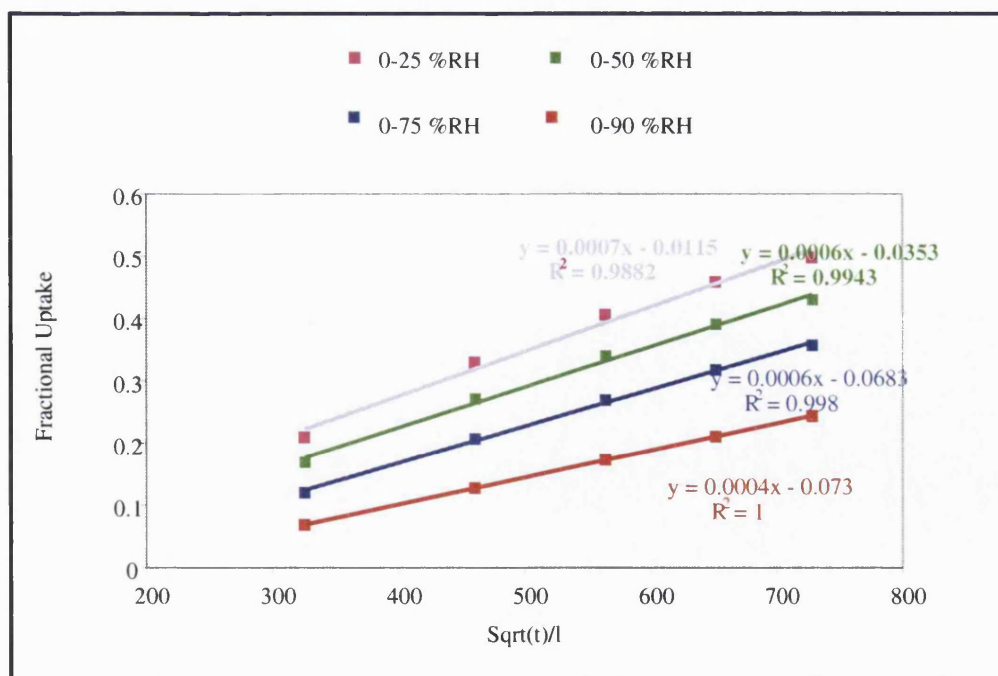


Figure 3-22. Early Time Linearization Plot of M_t/M_∞ versus \sqrt{t}/l for Eudragit L30 D-55 Film (For Sorption cycle Data Obtained at 25 °C)

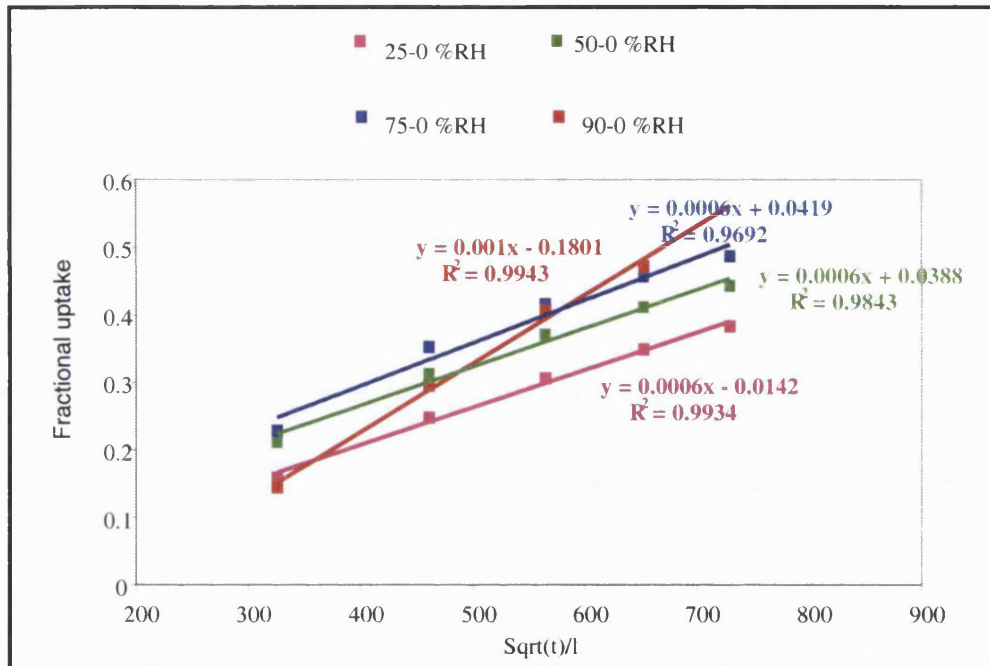


Figure 3-23. Early Time Linearization Plot of M_t/M_∞ versus \sqrt{t}/l for Eudragit L30 D-55 Film (For Desorption cycle Data Obtained at 25 °C)

For the diffusion coefficients of the films presented in Table 3-5, the data shows some key differences. For instance, the diffusion coefficients for Sepifilm LP, especially for the sorption cycles at low RH gradients, were generally the lowest, while the values for Eudragit L30 D-55 were surprisingly high, especially given the fact that this sample sorbed relatively little moisture. It is also of interest to note the apparently low diffusivity of Opadry AMB. Bearing in mind this sample exhibited comparable hygroscopicity to the Sepifilm LP film, the low diffusivity was somewhat unexpected.

The other key aspect of the data presented in Table 3-5 pertain to the effect of both the RH and temperature on the values of the diffusion coefficients obtained for the moisture barrier films studied. Inspection of data reveals a number of major trends. These trends are summarized in the following paragraphs below:

% RH Change	Eudragit L30 D-55	Eudragit EPO	Opadry AMB	Sepifilm LP
25 °C				
0-25	9.655	5.003	4.988	1.704
25-0	5.656	3.696	1.318	1.678
0-50	7.211	3.924	1.974	1.619
50-0	8.658	4.490	1.863	2.082
0-75	5.004	3.259	1.053	1.435
75-0	11.157	4.130	2.014	2.697
0-90	2.922	1.806	0.869	0.852
90-0	7.169	3.083	3.758	5.420
30 °C				
0-25	8.139	5.907	9.183	1.844
25-0	3.723	3.994	1.188	1.681
0-50	5.233	4.849	1.802	1.603
50-0	5.887	5.021	1.778	2.037
0-75	3.996	3.902	1.081	1.215
75-0	6.034	4.683	1.634	2.317
0-90	2.736	2.058	1.248	0.749
90-0	6.314	3.205	4.111	4.259
40 °C				
0-25	N/A	4.827	N/A	2.300
25-0	N/A	3.539	N/A	2.172
0-50	N/A	3.838	N/A	2.065
50-0	N/A	4.118	N/A	2.544
0-75	N/A	3.426	N/A	1.751
75-0	N/A	4.031	N/A	2.582
0-90	N/A	1.754	N/A	1.016
90-0	N/A	2.613	N/A	2.578

Table 3-5. Mean Moisture Diffusion Coefficients (D, cm²/s, x10⁻⁸) for Moisture Barrier Films. (Values averaged from n=3 Runs) N/A: Not Available

-Eudragit L30 D-55

For this film, increase in the RH gradient (i.e., from 0-25 to 0-90 % RH) resulted in a progressive decrease in the values of the diffusion coefficient. This was especially true for the sorption cycles. It can be seen that the highest diffusion coefficient value was obtained at the 0-25 % RH gradient while the lowest value was seen at the 0-90 %RH gradient. The data for the desorption cycles can also be seen to increase with RH, actually up to the 75-0 % RH gradient, there after, they appear to dip at the 90-0 % RH gradient. However, even at this condition, the value of the diffusion coefficient was still higher than the value for the sorption cycle (i.e., 0-90 % RH). Also, increase in temperature resulted in a decrease in the values of the diffusion coefficient, which is somewhat inconsistent with the general theory that temperature increases the speed of diffusing molecules. However, given that there were no data for this sample for the 40 °C condition, it is difficult to establish the overall effect of temperature for this sample.

-Eudragit EPO

The effect of RH on the diffusion coefficients for this sample largely followed the same pattern as for the Eudragit L30 D-55 sample described above. Thus, with increasing RH there was seen a decrease in the values of the diffusion coefficient corresponding to the sorption cycles while an increase in the diffusion coefficients was observed for the desorption cycles. The main difference with this sample, perhaps, is the nature in which the values of the diffusion coefficients changed for the desorption cycles. It appears that these values initially increased then started to dip such that at the 90-0 % RH gradient, the lowest values of the diffusion coefficient (for the desorption cycle) were obtained. The effect of temperature was also remarkable. For instance, as the temperature was raised from 25 to 30 °C, there was observed a corresponding increase in the values of the diffusion coefficients. Further increase in the temperature did not result in an increase but rather the obtained values of the diffusion coefficient were lower suggesting that at 40 °C the movement of the water molecules in this polymer film were somewhat more restricted than at the lower temperatures of 30 or 25 °C.

-Opadry AMB

The diffusion coefficient for this sample was seen to increase following an increase in the RH gradient for the sorption cycles but appeared to decrease for the desorption cycles. When the temperature was increased from 25 to 30 °C, similar patterns were seen. However, the values of the diffusion coefficients were slightly lower. The diffusion

coefficient for the 0-25 % RH gradient at 30 °C was much higher (i.e., 9×10^{-8} cm²/s). Whether this result reflects the effect of temperature rise or is an experimental error cannot be established because there are no data for the 40 °C to enable comparison. However, the trend obtained for the values of the diffusion coefficient for the desorption cycles at 30 °C is similar to the one seen for the data obtained at the lower temperature condition (i.e., 25 °C).

-Sepifilm LP

This sample generally yielded quite low values of the diffusion coefficient, especially for the sorption cycles. Also, for the sorption cycles, there was a progressive decrease in the values of the diffusion coefficient as the RH was increased. This pattern was observed at all the three study temperatures. For the desorption cycles, increase in RH resulted in an increase in the values of the diffusion coefficients. Generally, a rise in temperature was seen to increase the value of the diffusion coefficient, although the values obtained at 30 °C were slightly lower, perhaps suggesting that a five degree °C rise in temperature only had minimum effect. Otherwise, the influence of temperature is more visible if the data obtained at 40 °C are compared with those obtained at 25 °C.

In summary:

The data for the diffusion coefficients showed that there were wide differences amongst the different film samples. All samples exhibited diffusion coefficients that were dependent on the RH. This indicated a dependence of this parameter on the water content in the film samples. The Sepifilm LP film sample, especially for the sorption cycles at low RH gradients, exhibited the lowest diffusion coefficients. For instance, at the 0-50 % RH gradient (25 °C), a diffusion coefficient of 1.704×10^{-8} cm²/s was obtained. The diffusion coefficients for other samples were as follows: Eudragit L30 D-55 film = 9.655×10^{-8} cm²/s; Eudragit EPO film = 5.003×10^{-8} cm²/s; and Opadry AMB film 4.987×10^{-8} cm²/s.

Increasing the RH led to a decrease of the diffusion coefficient for the sorption cycle but resulted in an increase in the diffusion coefficient for desorption cycles. The effect of temperature, however, appeared to be mixed, with no clear trend emerging. As a rule, the diffusion coefficients for the 0-25 % sorption cycle were higher than the corresponding values for the desorption cycle. This showed that the rate of desorption at this condition was much slower than the rate of sorption.

3.4.5 Calculation of Permeability Coefficients

To cap this study, the permeability coefficients for the different moisture barrier polymer films were calculated, in accordance with the argument of the solution-diffusion mechanism, i.e., $P = [S][D]$ (Equation 1-5, Chapter 1). The values of the solubility coefficients (S) were those calculated from the sorption isotherms (as presented in Table 3-2). The diffusion coefficient employed in the calculation was the mean taken from the diffusion coefficients for the sorption and desorption cycles. The values shown are based on averaged values of $n=3$ determinations of the diffusion coefficients and solubility coefficients. The permeability coefficients P thus obtained are presented in Table 3-6 below.

RH Step Change	Eudragit L30 D-55	Eudragit EPO	Opadry AMB	Sepifilm LP
25 °C				
0-25	1.121	0.400	0.436	1.240
0-50	1.420	0.505	0.557	1.387
0-75	1.577	0.584	0.691	1.918
0-90	0.869	0.264	0.812	1.453
30 °C				
0-25	0.153	0.233	0.089	1.292
0-50	1.212	0.275	0.175	1.343
0-75	1.662	0.357	0.319	1.639
0-90	0.227	0.287	1.340	10.020
40 °C				
0-25	Not Calculated	0.204	Not Calculated	0.455
0-50	Not Calculated	0.213	Not Calculated	0.491
0-75	Not Calculated	0.302	Not Calculated	0.595
0-90	Not Calculated-	0.242	Not Calculated	3.064

Table 3-6. Calculated Permeability Coefficients $[(\text{cm}^3 (\text{STP}) \text{ cm})/(\text{cm}^2 \text{ s, cm Hg})]$ for Moisture Barrier films. °C [All Values are 10^{-6}]

The data presented in Table 3-6 above show a strong dependence on the RH. From the knowledge that the permeability is a property of a material, these coefficients should rightly be referred to as “apparent” permeability coefficients to emphasise this fact. Notwithstanding this fact, it can be seen that the Sepifilm LP film was the most permeable sample. This sample, it is worthy recalling, was the most hygroscopic moisture barrier coating. It is of interest to note that the permeability coefficients of the Eudragit L30 D-55 film are similar in magnitude to those of the Sepifilm LP sample,

although the differences between the values of the diffusion coefficient for the two film samples were statistically significant ($p > 0.05$). Given that this film sample exhibited relatively low hygroscopicity, it is clear that an inverse correlation of the permeability data with hygroscopicity exists for this sample. The permeability data for Opadry AMB and Eudragit EPO were similar in magnitude, especially at low RH gradients. It can also be seen that these two film samples were generally the least permeable. For the Eudragit EPO sample, the low permeability data was directly correlated with the hygroscopicity data. On the other hand, the Opadry AMB, the low permeability was inversely correlated with the hygroscopicity.

One other aspect worthy mentioning is in relation to the manner in which the permeability coefficients varied with the RH. Two generalized trends can be seen: In the first, the permeability coefficient increases steadily with the RH (from 0-25 % RH through to 0-75 % RH) but it then decreases at the 90 % RH gradient. This trend was exemplified by Eudragit L30 D-55, Eudragit EPO and the Sepifilm LP film samples. In the second group a progressive increase in the permeability coefficient as the RH was increased from 0-25 through to 0-90 % RH gradient was seen. This group was typified by the Opadry AMB film sample. Both trends appear to be in contrast with what most workers have observed previously, i.e., that glassy polymers show a typical trend of a decreasing permeability with increasing vapour pressure which then increases as the vapour pressure is further increased (Koros and Paul, 1976; Huvard et al., 1980; Barrie, 1986; Sanders, 1988; Bos et al., 1999, Ismael and Lorna, 2002). It is not clear what this outcome means to barrier functionality at this juncture. It is, perhaps, indicative of the possibility that the membranes studied were not in a glassy state.

3.5 DISCUSSION

3.5.1 Introduction

There are significant merits for studying sorption-desorption phenomenon under equilibrium regimes as opposed to fixed-time regimes. In a water-polymer system that has attained equilibrium, the water uptake (or loss) at each water activity (or the relative humidity RH) has been allowed to reach a steady state value at the end of the transient permeation regime. Thus, a state of thermodynamic balance exists between the polymer material and the water at the activity set in the vapour phase. This means that all the components of the system share the same energy/momentum. This facile balance, however, can hide important interactions which need to be determined. These interactions might not be visible under non-equilibrium conditions since for such system, the system components exist at different energy states at the same time.

The discussion presented below is for the equilibrium sorption-desorption studies undertaken to measure moisture sorption isotherms and permeation through the different film samples. For convenience, it is divided into three sections, i.e.: section 3.5.2 for the trends obtained from the sorption isotherms, section 3.5.3 discusses the modelling, while 3.5.4 discusses the data for sorption-desorption kinetic studies.

3.5.2 Equilibrium Moisture Sorption-Desorption Characteristics

3.5.2.1 Isotherms

Equilibrium sorption-desorption characteristics are best represented by the sorption-desorption isotherm. The isotherm, defined earlier as the relationship between the amount sorbed/desorbed at equilibrium and the relative humidity of the sorbate above the polymer, is determined by monitoring the weight of a sample until a constant value is obtained. The resulting profile of the sorption-desorption isotherm is a reflection of the nature of the water-polymer film interactions.

The uptake of water by a polymeric material is accompanied by two processes which take place depending on the nature of the polymer. These are polymer chain relaxation, and polymer matrix swelling. In hydrophilic polymers, the sorbed water may cause relaxation of the polymer chains as a result of plasticization. This increases the free volume of the polymer, resulting in dimensional changes in the polymer matrix, i.e., swelling. Swelling, together with the accompanying increase in sorption, manifests as

an up-turn in the sorption isotherm. On the basis of classification proposed for the different water fractions sorbed in polymers i.e., free water, freezable bound water and non-freezing bound water, it has been found that at low RH ranges of the isotherm, most of the sorbed water exists as non-freezing bound or freezing bound water. At high RH, the sorbed water mostly exists in the polymers as freezing bound water. The free and the freezable bound water species are characterised by high mobility and low plasticizing efficiency, while the freezing bound water molecules have much lower mobility and exhibit high plasticizing efficiency. Due to their high plasticizing ability, these water molecules are capable of disrupting interchain hydrogen bonding, and induce swelling (Musto et al., 2002). Thus, the nature of interaction of the sorbed water with the polymer chains determines which aspect, i.e., either relaxation or swelling, is operational at a particular point in the isotherm. The relative rates of polymer chain relaxation and sorption are important in directing the sorption equilibrium, and hence, the permeation characteristics of the membrane.

The isotherms obtained in this study were similar in profile to the Type III isotherms (BET classification). In the literature, Type II isotherms have been encountered in less hydrophilic polymers. The more highly hydrophilic polymers exhibit Type IV or V isotherms, while some less hydrophilic polymers, such as polydimethylsiloxane, and, unexpectedly, poly(vinyl alcohol), a very hydrophilic material, are reported to obey Flory–Huggins or Type III isotherms. Very hydrophobic polymers like polyethylene and polypropylene conform to the linear Henry's Law (Serad et al., 2001). For hydrophobic polymers, water-polymer interactions are minimal and the sorption process is near to ideal (random). Thus, from this "classification", it can probably be inferred that (i) the film samples studied were of the less hydrophilic category, and (ii) the sorption process was non-ideal, and was characterized by non-random distribution of the water molecules within the film samples.

Non-ideal sorption, such as that seen in this work, was first reported by Mathes (Vieth, 1991) who postulated that two competitive processes were occurring in the polymer, namely, dissolution, which obeyed Henry's law, and sorption, which followed Langmuir's isotherm. The total isotherm was, accordingly, the sum total of contributions from each of the two "sorption" modes. This is the basis for the dual-mode sorption model, which was reviewed in Chapter 2. This model has been used as a conceptual reference for water sorption in polymers, as follows:

At low water activities, the low extents of uptake correlate with the Langmuirian sorption. Here, the sorbed water molecules are “chemisorbed to specific polar sites (Stroeks and Dijkstra, 2001). Such a state is, therefore, characterized by the water molecules that are isolated from their neighbours and the water-water interactions are minimal. In this low activity region, the number of polar groups available on the polymer determined the extent of sorption. The more the number of polar sites, the higher will be the sorption. On the sorption-desorption isotherm, this low activity region corresponds well with the near-linear portion of the isotherm. With respect to the present study, examination of the isotherms reveals this region was possibly between $0-35 \pm 15$ % RH. The water existed in the samples as freezing bound water molecules. As the RH is increased above 50 % RH, sorption ceased to be limited to the Langmuirian mode. The water molecules then “spilled” out into the polymer matrix leading to Henrian sorption. This then gave rise to the exponential rise in sorption at high RH, reinforced by the preference of the water molecules for sorption into energetically favourable environments where the water molecules could easily collect. This water existed in the film samples either as the free water or freezing bound water.

In terms of the interrelationship between free energy, entropy and enthalpy of the water-polymer film system, Wolhfarth (2004) explained that the convex profile of the BET type III sorption isotherm was as such because the polymer-water interactions progressively became weaker (and hence the entropy) as the RH of the system increased. The increase in the entropy, however, compensated for the enthalpy loss, resulting into an overall decrease of the free energy. This gave rise to the convex nature of the isotherm. Since the sorbed water molecules are of the bound type at lower activities, the water-water interactions are negligible. However, at higher water activities, water-water interactions are no longer negligible and aggregation to form clusters becomes important. This results in an exponential increase in amount of water sorbed.

3.5.2.2 Sorption Hysteresis

It is known that for hysteresis to occur, more water must be held at the same water activity, a_w , during the desorption cycle than during the sorption cycle. From the definition of equilibrium and water activity, this occurrence should be considered a thermodynamic impossibility (Young and Nelson, 1967; Tvardovski et al., 1987). This is because at equilibrium the chemical potential of the water (μ_v) in the vapour above the

water in the polymer film. For this reason, film samples like Sepifilm LP and Opadry AMB exhibited higher solubility coefficients due similarity in polarity between the water and the polymer films. Conversely, samples like the Eudragit L30 D-55 and Eudragit EPO exhibited lower solubility coefficients. This was perhaps because these very samples were less polar. It is not, however, clear for now how factor (ii), i.e., the free volume, varied amongst the samples and how this could have influenced the extent of sorption in the samples studied as no specific studies were made to determine its role.

3.5.2.3.1 Effect of Temperature

In Chapter 2, the effect of temperature on the extent of sorption was not very clear. It was found that temperature led to an increase in the amount of moisture taken-up by the Eudragit EPO film sample. The other samples exhibited an apparent decrease in the extent of sorption, which, however, was marginal. This was perhaps due to the relatively short time the samples were exposed to the moisture stress in the DVS. However, under equilibrium sorption conditions, the picture was clearer, with two patterns emerging: The relatively hygroscopic films, as exemplified by Sepifilm LP and Opadry AMB, exhibited a substantial decrease in sorption as the temperature was increased. In contrast, the less hygroscopic films, exemplified by Eudragit L30 D-55 and Eudragit EPO, showed an increase in the extent of sorption with temperature. When the solubility coefficients were computed, however, the data unequivocally showed a decrease in the solubility coefficients as temperature was increased.

To understand this apparent anomaly, it is necessary to consider the variation of the solubility coefficients (and, thus, sorption) with temperature as described by the following Arrhenius relationship (Stannett, 1968):

$$S = S_0 \exp\left(\frac{-\Delta H_s}{RT}\right) \quad \text{Equation 3.8}$$

where ΔH_s is the enthalpy of sorption, S_0 is a pre-exponential factor. R and T are respectively the Universal Gas constant and absolute temperature. As ΔH_s is a negative value for vapours like water, it follows that sorption decreases with temperature. This would be consistent with the observations so far made. The author above makes mention of the fact that where interactions between the sorbed water and the polymer are existent, non-ideal behaviour in the above relationship may be observed due to the possibility for structural changes in the polymer samples as well as

changes in the polymer–water interactions as the temperature is increased. These could somewhat overshadow the effect of the increase in free volume leading to a solubility coefficient that may increase or decrease with temperature.

The discrepancy between the raw sorption data and the solubility coefficient data for Eudragit L30 D-55 and Eudragit EPO samples ought to be scrutinized in the context of the definition of the solubility coefficient. This parameter, as defined above, is a partition coefficient, which measures the concentration of water molecules in the air at a given temperature divided by the concentration in the polymer matrix. For an atmosphere maintained, say at a constant RH of 75 %, the saturated vapour density of water would increase from 17.3 g/m³ to 38.3 g/m³ as the temperature is raised from 25 to 40 °C. Thus, although the mass of the water in the films increases, in reality, the extent of sorption to specific sites in the samples would not be expected to change significantly since there are only a limited number of sites available for sorption in the films. Therefore, when the partition coefficient is obtained and compared for the samples at the two conditions, the result obtained at the higher temperatures would be less, giving a mirage effect of a reduction in the extent of sorption.

3.5.2.3.2 Effect of RH

Of greater significance is the manner in which the solubility coefficients varied with RH. In the first case (represented by Eudragit L30 D-55 and Eudragit EPO) the solubility coefficients increased steadily with RH. Compared with Sepifilm LP, the solubility coefficients first decreased, somewhat levelled at around the 35-50 % RH region, then increased again, peaking at the 90 % RH. The variation in the solubility coefficient for Opadry AMB sample was such that the solubility coefficient remained fairly constant until about the 35 % RH condition, thereafter, it increased steadily to comparatively high values. The pattern of variation in the values of the solubility coefficients described above could be interpreted as reflecting the manner in which water molecules interacted with the different polymer systems. Thus:

In the first category (i.e., Eudragit L30 D-55 and Eudragit EPO films), water-water interactions were more prominent owing to a fairly hostile environment in the polymeric matrix (i.e., comparatively hydrophobic). Therefore the solubility increased with an increase in the RH. The sorbed water molecules were mainly of the free water type and clustering was a key player in the solubility coefficient rather than plasticization. The pattern seen with Sepifilm LP would suggest that water molecules interacted strongly

with specific sorption sites, for instance, within the Langmuir-type sites at lower activities. As the RH was increased, plasticization of the films took place resulting into an increase in the solubility coefficient due to the accompanying increase in the free volume of the polymer films. The nearly constant sorption seen in Opadry AMB at low activities signified, perhaps, a coating surface related effect, whereby the coating offered initial resistance to the movement of the water front in this sample, which, however, once nullified, due to the solubilizing action of the water, resulted in an increase in the sorption. Such a physical barrier was speculated in Chapter 2.

3.5.3 Isotherm Modelling

3.5.3.1 BET Isotherm Model

The BET model is based on the concept that the sorbed water within the different polymer samples can exist in varying degrees of hydration. This arises because the sorption of the vapour can occur over a previously sorbed layer. Thus, unlike the Langmuir model, where it is assumed that sorption only takes place on unoccupied substrate sites, with the BET model, the initial sorption layer can act as a substrate for further sorption. Hence, instead of the isotherm levelling off to some unsaturated value (q.v Type II isotherm, BET classification), the uptake can be expected to rise indefinitely due to sorption taking place upon the second, third, fourth, etc., layers. The BET model has been the subject of renewed interest in recent years due to its simplicity and robustness, and is the principle behind the measurement of the surface area and pore size distribution in materials.

The BET model has therefore been widely utilised to interpret the experimentally measured sorption isotherm. For this purpose, a number of assumptions are made (Major and Blanchard, 2002):

- Sorption of the first layer occurs on sites of equivalent surface energy. This layer is represented by the “knee” of the sorption isotherm.
- The second layer sorbs on the first, the third on the second, etc and when the partial pressure p of the vapour is equal to the saturated vapour pressure p^0 the infinite layer is formed, i.e., equilibrium uptake is established.
- At equilibrium, the rates of condensation and evaporation are the same for each of the layers.

It is not clear why the BET models were selective in describing the isotherm data obtained in this work. Even where a description was possible, with the exception of the

solid and the chemical potential of the sorbed water in the polymer (μ_p) are equal. Nevertheless, some aspects of moisture sorption that are known to promote hysteresis have been discussed (e.g., Chou et al., 1973; Karel, 1989; Tvardovski et al., 1987). They include chemical changes in the polymer, steric factors, non-equilibrium of the processes and or swelling, surface tension, and wetting differences between the two cycles, and, irreversible sorption into micropores or capillaries. The conclusion by the authors above was that sorption hysteresis was associated with the relative speed with which the sorbate penetrated into and out of the sorbent. This is an important issue, for instance, the possibility for water molecules to be trapped and be held below the a_w when they would have otherwise been released, can be an important consideration for product stability but this requires inquiry at another opportunity.

3.5.2.3 Solubility Coefficients

The solubility coefficient, as explained earlier, also measures the amount of water dissolved in a polymer film sample under equilibrium conditions. Unlike the more familiar equilibrium moisture content, the solubility coefficient expresses the extent to which the water molecules partition between the polymer and the vapour phase above the polymer. Thus, it can be used to understand key differences between materials.

The data presented previously demonstrated some key differences. For instance, the Sepifilm LP sample, compared with the two Eudragit samples, and in some cases, the Opadry AMB film, had the highest solubility coefficients. This demonstrated the preference of water vapour for this film. Also, the values for the solubility coefficient were not constant for a given sample and temperature. This attests to the non-ideal sorption characteristics of the samples.

In order to understand the results of the solubility coefficient, it is worth reviewing some of the factors known to affect this coefficient. These include (i) the inherent condensability of the penetrant, (ii) the polymer–penetrant interactions, and (iii) the amount and distribution of excess free volume in the polymer (de Boer, 1968; Kontny, 1988). If the quantitative and qualitative differences in the solubility coefficients shown by the film samples could be accounted for, factors (ii) and (iii) would possibly be the main players since factor (i) can be taken to be constant.

Considering factor (ii), it can be inferred that to the extent the water molecule was similar in polarity to the polymer; the higher was the solubility coefficient of the sorbed

Sepifilm LP film, the activity range was quite narrow. Since the main statistical assumption of the BET model is that the influence of the solid material on the enthalpy and entropy of sorption extends only to the first sorbed layer and that the rest of the sorbed molecules, constituted as multilayers, possess properties of bulk water (Brunauer, et al, 1938), the general poor fit exhibited by the samples in this study, in part reflects the inadequacy of this assumption, and perhaps demonstrates that the sorption in the film samples was, perhaps, different from this generalised picture. Also, it is simplistic to expect the different sorption sites to be energetically equivalent, especially for heterogeneous materials like polymer coatings. It is reported that when the sites are not equivalent, the enthalpy of sorption changes as a function of coverage on the surface (Major and Blanchard, 2002).

Notwithstanding, some useful descriptions of the data were still obtained from the analysis offered by the BET model. Taking the monolayer values and the energy constant, for instance. The monolayer amount, as far as barrier coatings are concerned, should represent a key parameter. The monolayer amount has been defined as the moisture content at which a material is unaffected by moisture (Bell and Labuza, 1984). In the food technology, this value is highly revered. It is directly correlated with stability of food products in such a way that the higher this value the better the stability. The assumption being that the rate of deterioration at the M_0 content is zero because the water present in the material is not sufficient to act as a solvent (Salwin, 1963; Bell and Labuza, 1984). In this regard, the Sepifilm LP film should exhibit a greater degree of moisture binding, translating into better stability. The methacrylate film samples, on the other hand, would exhibit a poorer stability profile.

The energy constant, C_B , is related to the difference in the energy of sorption between the monolayer (ΔH_{m_0}) and the subsequent layers (ΔH_L). The greater this value, the higher the sorption in the lower activity region. Thus, if $C_B > 1$, $\Delta H_L < \Delta H_{m_0}$; If $C_B \leq 1$, $\Delta H_L > \Delta H_{m_0}$ (Kontny, 1988; Timmermann, 2001). This constant, thus, defines how pronounced the "knee" at the lower activity range of the isotherm is (see Figure 3-24 below). M_0 and C_B constants are known to be temperature dependent since, as mentioned above, they are related to the strength of interaction between water molecules and the polymer. Since an increase in temperature weakens the water-polymer binding forces, a corresponding decrease in the extent of sorption and hence the M_0 values should result. This trend exhibited by the Sepifilm LP data is consistent with the observations of van den Berg and Bruin (1982), who reported a decrease in

monolayer values for starch. The trend for Eudragit EPO, however, was the opposite of that seen for Sepifilm LP. As speculated earlier, an increase in temperature possibly provided the activation energy required to bring water molecules within the proximity of the polar groups, resulting into an increase in M_0 values and C_B values for this sample.

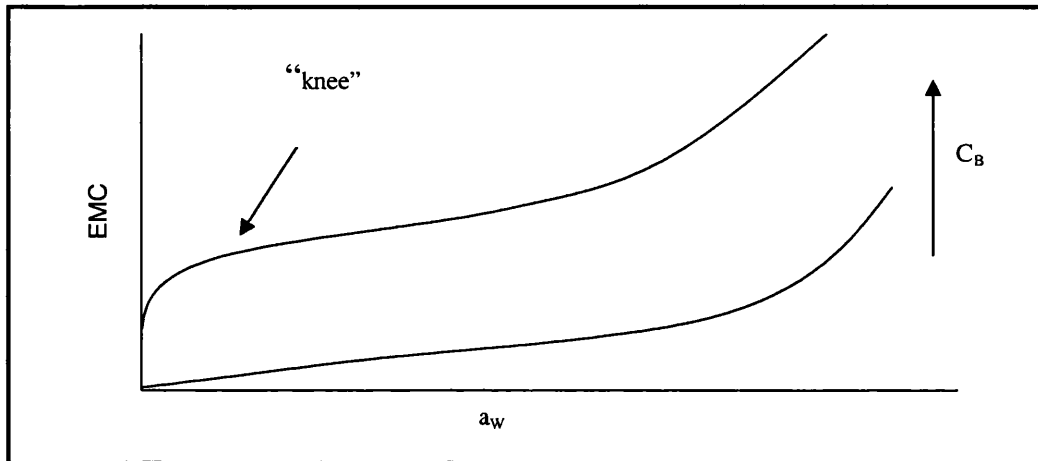


Figure 3-24. Illustration of the Influence of C_B on Sorption Profile

3.5.3.2 Clustering Function (G/v)

The data obtained from the analysis of the clustering tendency demonstrated distinct characteristics which are consistent with the speculations made above. It was shown that these samples not only exhibited clustering but that there were some differences in the tendency to cluster as well. The more hydrophilic samples exhibited relatively lower clustering functions while the more hydrophobic samples had higher clustering functions. Thus, in the relatively hydrophilic samples (Sepifilm LP and Opadry AMB film samples), by virtue of a greater level of polar groups, the sorption process was more energetic and binding of the sorbed water molecules stronger. In these samples, there was observed a lesser tendency to cluster. As a result, a greater proportion of sorbed water was in bound state for these samples. On the other hand, the comparatively hydrophobic films (i.e., Eudragit L30 D-55 and Eudragit EPO) are presumed to have had less polar groups available to which the water molecules could bind to. Consequently, the sorption process was less energetic and the extent of clustering greater. It is of interest to note that this description agrees well with the postulations made from the thermogravimetric data, as discussed in Chapter 2.

3.5.6 Sorption-Desorption Kinetics

3.5.6.1 Sorption-Desorption Kinetics

Diffusion, compared to sorption, is conceptually different. Diffusion is a kinetic phenomenon, characterised by movement within a space. Sorption, on the other hand, is thermodynamic, a “storing” kind of process. However, even though the two processes are conceptually different, the factors which influence sorption, in many respects, influence diffusion as well. One of these factors, clearly demonstrated for sorption, is the nature of water-polymer interactions, which defines the degree of polymer chain relaxation and swelling, hence the resulting equilibrium.

It is reported that degree of relaxation (and swelling) of the polymer chains, for instance, significantly determines the kinetics of the sorption-desorption process. Alfrey et al., (1966) showed that when the rate of relaxation was faster than the rate of diffusion, the polymeric material responded instantaneously to the penetrant and the kinetics observed were typically Fickian. This required the polymer matrix to have sufficient flexibility, a condition generally accepted to be the case in polymers above their glass transition temperature, T_g . On the other hand, if the rate of diffusion was more rapid than the rate of relaxation, the resulting transport behaviour was non-Fickian. In such a case, the diffusion process was not rate determining for sorption.

Arising from numerous studies about the transport of polar species (e.g., water, carbon dioxide, etc) through hydrophilic polymer films, four main typical transport mechanisms (herein designated as mechanism 1, 2, 3 and 4) have been described. The profiles accompanying these mechanisms as well as the variation of the diffusion coefficient D have been summarised by Piringer (2000). These patterns are shown in Figure 3-25 below. The sorption-desorption kinetics can be summarized as follows:

- Mechanism 1 is the classical Fickian transport. Both the sorption and desorption curves are perfectly interposed. Moreover, they all originate from zero.
- Mechanism 2, the diffusion coefficient increases with vapour concentration but the sorption curve is displaced above the desorption curve.
- In mechanism 3, D decreases with vapour concentration. The desorption curve is displaced above the corresponding sorption curve.
- Mechanism 4 is the anomalous type of behaviour characterised by significant swelling.

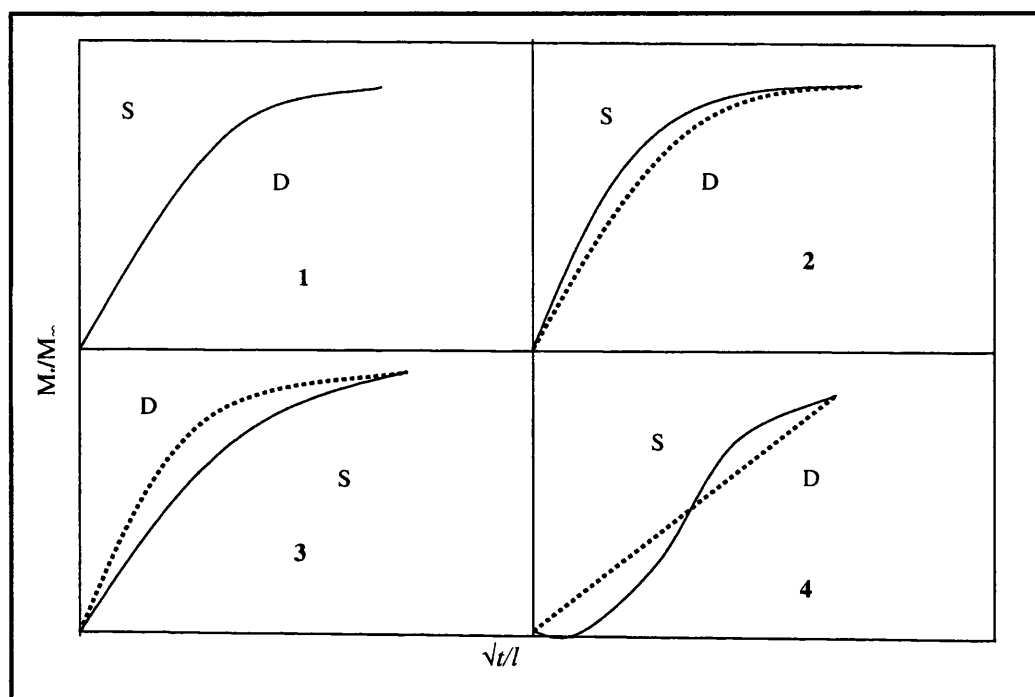


Figure 3-25. Typical Fractional Uptake/Loss (M_t/M_∞) Versus Reduced Time (\sqrt{t}/l) Curves For Different Transport Mechanisms (Piringer, 2000). (Full Lines Depict Sorption (S) Kinetics; Dotted Lines Depict Desorption (D) Kinetics)

The patterns described above not only give an indication of the relative rates of sorption and desorption as the RH was altered but also provide clues as to the nature of the sorption-desorption process obtaining in the samples studied. Thus, from the general shape of these curves, it can be stated that the diffusion process in the present study was essentially non-Fickian. The sorption process was faster than the corresponding desorption process at low water activities. At higher activities, the desorption rates become faster than the sorption rates, an indication of a change in kinetics.

Therefore it can be speculated that sorption of water led to some degree of swelling of the films, which manifested as non-Fickian kinetics. This is contrary to the expectation arising from the pertinent differences in the sorption exhibited by the films. In other words, despite the low amounts of moisture sorbed by the Eudragit samples, [and on the whole, by the Sepifilm LP and the Opadry AMB samples], the resulting sorption-desorption kinetics were essentially similar to those exhibited by the relatively highly sorbing Sepifilm LP and Opadry AMB samples.

3.5.6.2 Diffusion Coefficients

With specific reference to the results of the diffusion coefficients obtained in this study, it is worthy remembering an important dictum, i.e., that diffusion of water through polymers is influenced by the polarity of the polymer, as well as the plasticization and clustering of water molecules in the polymer matrix. The lower diffusivity in Sepifilm LP compared with that of Opadry AMB and the Eudragit films could be due to the higher polarity and the resulting cohesion. This would have translated into a polymer matrix with reduced free volume due to greater extents of intermolecular attractive forces between polymer segments. This aspect is discussed by Fava (1980), Debeaufort (1993), among others. The effect of reduced free volume would be a reduction in the mobility of sorbed water molecules, in which case, a negative correlation between sorption and diffusivity would be demonstrated. Also, the fact that there was observed a comparatively higher monolayer moisture content value with the Sepifilm LP sample suggests that a greater proportion of the sorbed water molecules could have been in a bound state rendering only a few of them available for diffusion.

For an explanation for the apparent decrease in the diffusion coefficients for the sorption cycle in response RH, one must refer to the evidence gathered from the clustering function as well as the possibility for plasticization in the respective samples. Thus, at lower activities, some of the water molecules were hydrogen bonded to the polymer segments and only the non-immobilised fractions participated in the diffusion process, as suggested above. The fact that the sorbed non-immobilised molecules existed as single entities, means that they were able to traverse the membranes faster. However, as the water activity increased, the tendency to form clusters increased. Cluster formation caused an increase in the average size of the diffusing species, which then reduced the diffusion coefficient.

Given that both plasticization and clustering were demonstrated, it is of interest to know which of the two phenomena was most prominent in influencing diffusion. This can be deduced from the behaviour of the diffusion coefficient, i.e., the extent of the reduction in the diffusion coefficient depended on which of the two factors was more prominent. Barrie (1986) and Ismael and Lorna (2002) state that in some polymers exhibiting Type II or Type III isotherms, a trend of an initially decreasing diffusivity with increasing RH which then increases after a certain pressure may be noted. This trend, where existent, has been attributed to plasticization, rather than clustering, as being the dominant

process, especially in the lower activity ranges up to 50 % RH. As shown in this work, there was a progressive decrease in the diffusion coefficient, suggesting that cluster formation, rather than plasticization, was the main factor influencing the variation of the diffusion coefficient with RH.

It is noteworthy to mention that the application of the Crank model to calculate diffusion coefficients of water through hydrophilic polymers can yield misleading results. In the first place, Fickian diffusional theory assumes that the molecules diffuse through the membrane freely without interactions. In this case, the polymer membrane is considered to be inert to the permeant. This assumption may not necessarily hold. Where polymer chain relaxation is in force, this can become significant, resulting into an apparently slower sorption process.

Two other features which can introduce errors in the calculation of the diffusion coefficients are (i) surface resistance and, (ii) sorption overshoot. In the former case, when the step change in RH is initiated, sorption does not instantaneously occur due to the surface of the film offering some form of resistance to the advancing sorbate front. This can, therefore, introduce a delay which would manifest as sigmoidal sorption when actually the kinetics are Fickian. For the sorption overshoot feature, a plot of the fractional uptake versus square root of time has a characteristic maximum before reaching an equilibrium value. This feature has been attributed to rearrangement of polymer chains subsequent to plasticization by the sorbate, among others (Rodriguez, et al, 2003). It is estimated that these can introduce an error as much as 10 % in the value of the diffusion coefficient. Because of these limitations, some workers have proposed alternative theories for analysing diffusion, which claim to provide more satisfying results (e.g., Long and Richman (1960) and Wilde and Shopov (1994).

3.5.6 Permeability Coefficients

The results for the permeability coefficients were not constant for a given sample but showed a variation with RH and or temperature. This was not unexpected, given the fact that both the solubility and diffusion coefficients obtained earlier had exhibited similar variation. Otherwise, the data shown demonstrated that at lower activities, the Sepifilm LP and the Eudragit L30 D-55 sample exhibited relatively higher permeability coefficients while the Eudragit EPO and Opadry AMB samples had lower permeabilities. Increase in the RH generally resulted in an increase in the permeability

coefficients. At the 0-90 % RH gradient, the increase in the permeability coefficients for the Eudragit L30 D-55 and the Opadry AMB samples was disproportionately high. Generally, an increase in temperature resulted in an increase in the permeability coefficients for all the film samples, although the trends were somewhat less straightforward.

There was no opportunity for verifying the validity of the above results as there are no published data in the literature for comparison purposes. With the availability of MVTR data (from Chapter 2) it would have been possible to determine the permeability coefficients by multiplying the MVTR data with the partial pressure gradient in the MVTR measuring cell. Unfortunately, this was also not possible as the equipment manufacturer (VTI Corporation) did not provide the dimensions of the cell. Nevertheless, comfort is taken in the fact that both the diffusion coefficients and solubility coefficients for Sepifilm LP are within the magnitudes reported previously (e.g., Okhamafe and York, 1983). Also, materials like leather and certain polymer composites are reported to have permeabilities in the regions of 10^{-5} to 10^{-8} [(cm³ (STP) cm)/(cm² s, cm Hg)] (Ulutan and Balkose, 1996). It can also be seen that the trends seen in the values of the permeability coefficients are very similar to moisture vapour transmission values. In addition, the increase in the permeability coefficients with RH is consistent with the many published reports in the literature on this subject, mention of which was made in Chapter 1. Otherwise, the permeability coefficients calculated for the moisture barrier film samples were of the order of 10^{-6} to 10^{-7} cm³ [(STP) cm/cm² s cm Hg)]. Compared with high density polyethylene (HDPE) or polyvinylidene chloride (i.e., cling film) which have water vapour permeabilities in the order of 10^{-10} to 10^{-11} (Morillon et al., 2002), moisture barrier coatings were clearly inferior barrier structures.

In order to comprehend these results, it is necessary review some key concepts on permeability, some of which were reviewed in Chapter 1. Firstly, it is necessary to state that permeation is a measure of the ability of a material to resist another to penetrate through its thickness. As can be judged from the many reviews on permeation of water in polymers, some of which have been already been highlighted, water permeability is a peculiar phenomenon because of its dependence on three main factors i.e., small size of the molecule, ease of condensation and ability for hydrogen bonding. Because of the highly polar nature of the water molecule, two kinds of permeation behaviour are reported depending upon the nature of the polymer: In hydrophilic polymers, due to

high affinity towards groups like $-OH$, $-COOH$, etc by the sorbed water, the permeability tends to be high due to intensive sorption onto high energy sites. Also, the cohesive forces between polymers and penetrating water molecules are greater than water-water interactive forces. For this reason, the solubility of water in such films is high resulting into high water permeability because of the contribution of the solubility term in the solution diffusion theory. In contrast, hydrophobic polymers can be expected to be less permeable to water molecules. The interaction of water molecules with hydrophobic polymers is minimal but the tendency to cluster is greater. Consequently those molecules, which are free to move in the hydrophobic polymers are somewhat hindered. The net or combined effect is a low diffusion coefficient and quite often a very low permeability.

If the four moisture barrier films studied are classified as either hydrophobic or hygroscopic/hydrophilic on the basis of the relative amounts of water sorbed, it can be seen from the results of permeability that the generalised pattern of variation of permeability with hydrophilic or hydrophobic polymers was not strictly followed, except, perhaps for the Sepifilm LP sample. It must be appreciated that these trends apply to pure polymers while the films studied were heterogeneous composites formulated from a whole variety of constituents, of which the polymer was one of the components.

Therefore, rather than discuss the results on the basis of the hydrophilicity/hydrophobicity of the film samples, the inclination is to interpret them in terms of the contribution of the diffusion coefficient and the solubility coefficient to the permeability coefficient. Thus, Sepifilm LP, which typically had lower diffusion coefficients (attributed to binding to the polymer segments by hydrogen bonding), also had very high solubility coefficients. This translated into permeability coefficients being comparatively high. Clearly, for this film, the solubility of the sorbed water in the film was the more important factor contributing to the permeability coefficient. The sudden decrease in the permeability at 90 % RH was, possibly, contributed to by a decrease in diffusivity, which could have arisen from an increase in the size of the clusters. It would be expected that at high RH, the membrane would be more fluid due to plasticization which would result into much higher diffusivity. As this is not the case, it means that the effect of plasticization on the permeation was less pronounced in this sample.

For Eudragit L30 D-55, this sample had relatively low solubility coefficients but relatively high diffusion coefficients. The result was that the permeability coefficient obtained was

comparable in magnitude to that of Sepifilm LP. The permeability coefficients for Eudragit EPO and Opadry AMB were comparable in magnitude despite the fact that the two samples exhibited different diffusion and solubility coefficients. The low permeability found in the former sample is attributed to low solubility and low diffusivity. Presumably, the low diffusivity was due to the presence of hydrophobic ingredients rather than the absence of polymer-water interactions. The same argument cannot, however, be applied to the Opadry AMB sample. It would appear that the general low diffusivity of this film, was due to immobilisation of the water by the polymer segments, in the same way as was for Sepifilm LP, coupled with the low solubility coefficients, obtained at the lower humidities. The reason for the apparent dip in permeability at the 90 % RH was possibly the same as for the Sepifilm LP sample.

Since there was no clear cut relationship between the amount of water sorbed and the resulting permeability, it can be argued, therefore, that rather than the amount of moisture sorbed, per se, the permeability of the films was dependent on the nature of penetrant-polymer interactions and their contribution to either the diffusion and or the solubility coefficients. In samples where little interaction was anticipated, the amount of water sorbed was small and the films did not undergo swelling or rearrangement. In such systems, the diffusion process governed the permeation process. In the case of systems where penetrant-polymer interactions were high, permeability appeared to be largely governed by solubility of the penetrant in polymer. Nivedita et al. (2004) arrived at similar conclusions for paint films and ascertained that for polymers that sorbed ≤ 5 % db of water, the diffusion coefficient was independent of the water content while for higher sorbing polymers, due to plasticizing action of water, increase in diffusion coefficient with water content was seen.

3.6 CONCLUSIONS

3.6.1 Introduction

The work undertaken in this chapter aimed to study equilibrium sorption-desorption of moisture by free film samples of moisture barrier coatings. Samples were subjected to a stepwise change in relative humidity (RH) from 0-90 % RH. Experiments were done at 25, 30 and 40 °C. The data obtained enabled the determination of sorption-desorption isotherms, sorption-desorption kinetics and permeability.

3.6.2 Moisture Sorption-Desorption Isotherms

Isotherms obtained were typically of the Type III according to the BET classification. In keeping with this type of isotherm, the films exhibited very little moisture uptake until a critical activity, speculated to be between 35- 50 % RH, had been reached. Further increase in the water activity resulted in an increase in the extent of sorption. As the main type of interaction between the polymer samples and the sorbed water was thought to be by hydrogen bonding, it was speculated that at the lower RH ranges, water molecules were directly hydrogen bonded to the polar groups within the films. The more the polar groups there were available, the greater was the sorption, and hence the resulting hygroscopicity exhibited by the films.

Polymer-water interactions were found to be very influential in patterns of sorption observed. In hydrophobic films (exemplified by Eudragit L30 D-55 and Eudragit EPO), low solubility coefficients were obtained. In addition, the values of the solubility coefficients increased with the RH in a progressive fashion. In contrast, the hygroscopic films yielded high solubility coefficients. Also, the solubility coefficients, and especially the Sepifilm LP sample, first decreased then increased again as the RH was increased. These patterns were ascribed to the way the polymer-sorbed water interacted with the films and the resulting plasticization/clustering.

3.6.3 Theoretical Analysis of Isotherms

The BET isotherm model was applied to the equilibrium sorption-desorption data to calculate the monolayer moisture content. A relationship between the hygroscopicity and the monolayer amounts was observed, i.e., films which sorbed more moisture yielded a higher value and vice versa. It was found that the applicability of the BET model to the data was quite limited. It was speculated that the sorption patterns within

the film samples was more complex than the simplistic monolayer-multi-layer dichotomy offered by the isotherm model. When the data was analysed according to the Zimm and Lundberg clustering theory, it was found that the clustering tendency was greater in the hydrophobic film samples than in the hygroscopic samples.

3.6.4 Sorption-Desorption Kinetics

Moisture sorption-desorption kinetics were found to be non-Fickian. Sorption was faster than desorption at low RH. As the RH was increased, desorption rates become greater. Uptake of water by the film samples was accompanied by swelling and polymer chain relaxation irrespective of their hygroscopicity. The hygroscopic films exhibited lower diffusion coefficients due to partial immobilisation of the water molecules and a more packed film structure, compared with the hydrophobic samples. It was established that although both plasticization and clustering phenomenon were existent, clustering was more important to the diffusion coefficients than plasticization.

3.6.5 Permeability Coefficients

The permeability coefficients calculated from the solubility and diffusion coefficients were of the order of 10^{-6} to 10^{-7} cm³ [(STP) cm/cm² s cm Hg)]. Compared with HDPE and Polyvinylidene chloride which have water vapour permeabilities in the order of 10^{-9} to 10^{-11} (Morillon et al., 2002), moisture barrier coatings were clearly inferior barrier structures. It was found that in hygroscopic films (notably Sepifilm LP), the high permeability was due to the high solubility coefficients of water in this film even though the diffusion coefficients were relatively small. Hydrophobic films, in contrast, exhibited high diffusion coefficients even though they had relatively low solubility coefficients (e.g., Eudragit L30 D-55). At high relative humidities, clustering and plasticization were observed to influence the permeability coefficients, as expected from their characteristic non-ideal sorption properties.

CHAPTER 4

Chapter 4

4.0 MOISTURE SORPTION AND DESORPTION BY TABLET CORES OF DISSIMILAR HYGROSCOPICITY

Outline

4.1	Introduction
4.2	Objectives
4.3	Materials and Methods
4.4	Results
4.5	Discussion
4.6	Conclusions

4.1 INTRODUCTION

Solid dosage forms may be exposed to water vapour during the process of manufacture, storage after being manufactured and even after the product has been finally dispensed to the end-user. Since many properties of the drug solid substances can be altered by the amount of moisture sorbed, it is in the interest of pharmaceutical formulators to know, not only to determine the amount of moisture that the dosage form can take up, but also the state in which the moisture is held within the dosage form. Such knowledge can aid the design of products with optimal stability and performance.

Compressed tablets, described as circular solid cylinders containing a single dose of active pharmaceutical ingredients (BP 2002), are the most common type of dosage form. They are obtained by compressing uniform volumes of particles of active substances in combination with a host of materials, commonly referred to as excipients. Compression is performed by two punches on a suitable tablet press.

Excipients are included in tablets because most active pharmaceutical ingredients are not easy to tablet on their own and/or are present in minute quantities. Thus, excipients provide the required fluidity, plasticity or bulkiness for the formulation. In addition, excipients influence other aspects of the dosage form, including functionality and stability. This influence is due to their chemical and physical characteristics, which are ultimately imparted to the formulations in which they are used.

In Table 4-1 below are listed some of the key properties of commonly used tablet excipients (Kottke and Rudnic, 2000). It can be seen that the properties of tablet excipients can be fairly diverse.

Excipient	Compaction	Flow	Solubility	Hygroscopicity	Lubricity
Lactose (Spray-dried)	3	5	4	1	2
Fast-Flo Lactose	4	4	4	1	2
Lactose (Anhydrous)	2	3	4	5	2
Maize Starch	2	1	0	3	3
Sucrose	4	3	5	4	1
Modified Starch (Pregelatinized)	3	2	2	3	2
Dicalcium phosphate	3	4	1	1	2
Microcrystalline cellulose	5	1	0	2	4

Table 4-1. Comparative Properties of Some Tablet Fillers Graded on a Scale of 5 (Good/High) to 1 (Poor/Low). 0 Means None (from Kottke and Rudnic, 2000)

Coating of compressed tablet provides a useful way of modifying the properties of the generic core. Thus, a great proportion of manufactured tablets are coated in some form or another. The British Pharmacopoeia (BP 2002) defines coated tablets as "Tablets covered with one or more layers of mixtures of various substances such as natural or synthetic resins, gums, insoluble inorganic fillers, plasticizers, polyhydric alcohols, waxes, authorized colouring matter and sometimes flavouring agents." The range of polymer coatings that can be used to film coat tablets was discussed in Chapter 1.

The most common technique for applying films onto tablets is spraying. This technique utilizes a pressure to break up the coating material into tiny droplets, a process known commonly as atomization. The atomized spray is then delivered to the surface of the tablet. Although spray application may be undertaken in a variety of coating equipment, it is most commonly carried out in a fluidized-bed coater. Typically, a fluidized-bed coater consists of a vertical cylindrical column with a perforated base plate through which an air stream flows upwards. A smaller inner column, the Wurster, may be inserted in the middle of the chamber. The coating dispersion is delivered from the bottom or top of the chamber. This is schematically depicted in Figure 4-1 below. The mechanism of fluidization is extensively reviewed elsewhere (e.g., Kulling and Simon, 1980) and will therefore not be repeated here.

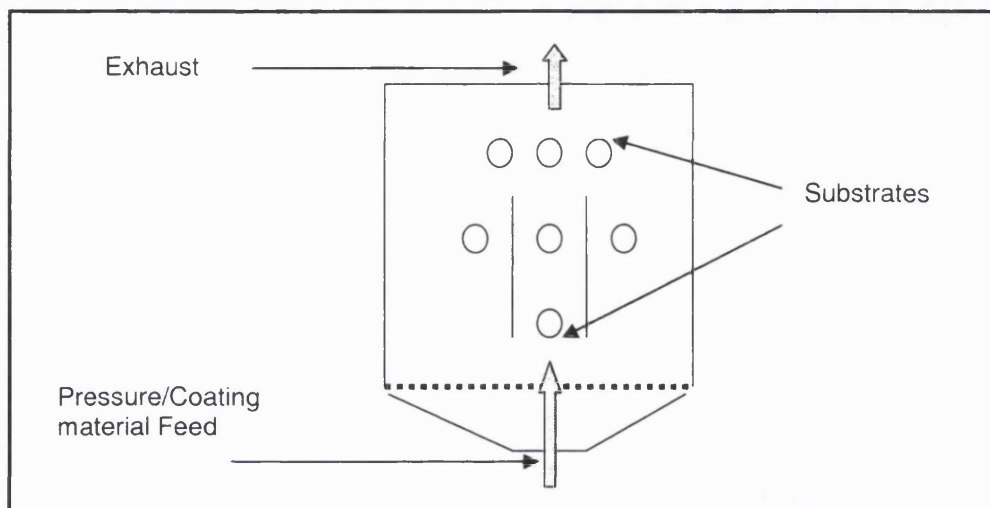


Figure 4-1. Schematic illustration of a Fluidized Bed Coater

4.2 SPECIFIC OBJECTIVES

The objectives of the work presented in this chapter were mainly two-fold: (i) To obtain moisture sorption and desorption profiles of uncoated model tablet cores of different hygroscopicity and the same cores coated with moisture barrier and enteric coatings, and (ii) to investigate the relationship between the type and quantity of coating and the core formulation on the extent of moisture sorption and desorption. Subsequently, it was desirable to determine the differences between moisture sorption properties and dissolution profiles of moisture barrier and enteric polymer coatings.

4.3 MATERIALS AND METHODS

4.3.1 Materials

The various materials used for the work described in this chapter comprised of excipients, from which the three different type of tablet core were prepared, a model drug substance, and the six different film coatings, which were prepared as described in section 2.2.1 and 2.2.2 of Chapter 2. In this chapter, the descriptions for the materials, as presented below, were, in general, adapted from the Handbook of Pharmaceutical Excipients, 3rd Edition, 2000. In some cases where other references were used, these are indicated accordingly.

4.3.1.1 Lactose

Lactose is a white, odourless and sweet-tasting naturally occurring disaccharide obtained from milk. Chemically, lactose is $O\text{-}\beta\text{-D galactopyranosyl-(1}\rightarrow\text{4)-}\alpha\text{-D glucopyranose}$. It exists in two isomeric forms, α -lactose and β -lactose. It is slightly soluble in water and non hygroscopic. Pharmaceutical-grade lactose is a highly purified material that is available in different grades. Each grade is characterised by different particle sizes and densities. For this study, the grade of lactose used was spray-dried lactose monohydrate NF (FastFlo, Batch No. 8599082161) which was purchased from Foremost Farms, Wisconsin, USA.

4.3.1.2 Microcrystalline cellulose

Microcrystalline cellulose (MCC) is partially depolymerized alpha cellulose derived from wood pulp. It is a white, odourless, tasteless, relatively free-flowing powder. Chemically, it is comprised of glucose units connected by a $1\text{-}4\ \beta$ glycosidic bond to form linear cellulose chains bundled together as micro fibrils in the walls of a plant cell. MCC is used as a tableting excipient for wet granulation and direct compression. With respect to moisture-sorbing properties, MCC is a hygroscopic material (Callahan et al, 1982). Various commercial grades are available in different particle sizes and moisture grades for different applications. For this work, MCC (Avicel PH 101, Batch No. 608233) was purchased from FMC International, Cork, Ireland.

4.3.1.3 Calcium dihydrogen Phosphate

Calcium dihydrogen phosphate (formula $\text{CaHPO}_4 \cdot n\text{H}_2\text{O}$ where $n = 0$ for anhydrous form; $n=2$ for dihydrate, molecular weight 136.06-172.09) is a white powder or crystalline material. It is insoluble in water and non-hygroscopic. It is stable at room temperature but loses its water of crystallisation at high temperature and humidity (Zografi, 1988). The material used for this study was a FOC sample of Calcium hydrogen phosphate, NF (Emcompress®, Batch No. 1029) from JRS Pharma GmbH, Rosenberg, Germany.

4.3.1.4 Starch

Starch (formula $(\text{C}_6\text{H}_{10}\text{O}_5)_n$, $n = 300\text{-}1000$) is a polysaccharide polymer based on α -glucose. It is mainly derived from the seeds of cereal plants. It is an odourless and tasteless fine, white-coloured powder made up of small spherical or ovoid granules. It is insoluble in ethanol and cold water. Starch is used in tablets and capsules as a filler,

binder, and disintegrating agent. Starch, like MCC is a hygroscopic excipient due to the presence of a high number of hydroxyl groups in the molecule (the equilibrium moisture content at 50 % RH is reported as 10 %) (Sakr, et al, 1974, Callahan et al., 1982). The material used in this study was partially pregelatinized maize starch NF (Starch 1500, Batch No. IN507558) and was purchased from Colorcon Limited, UK.

4.3.1.5. Carnauba wax

Carnauba wax occurs as hard and brittle pale yellow flakes or lumps of wax. It is mainly obtained from the leaves of *Copernicia cerifera* (Palmae). It consists of esters of a mixture of acids, hydroxyacids, oxypolyhydric alcohols, hydrocarbons and resinous matter. It is frequently used in the formulation of controlled release solid dosage forms (Walia et al., 1998). Carnauba wax, refined grade (Lot No. A014146801) was purchased from Fisher Scientific Supplies, Loughborough, UK. This material was supplied in the form of flakes. It was therefore ball-milled and sieved through a 125 µm sieve before being utilised in the tablet formulations.

4.3.1.6 Colloidal silicon dioxide

Colloidal silicon dioxide (formula SiO_2 , molecular weight 60.08) is a nano-size fumed silica. It is very light, bluish-white coloured odourless, non-gritty, powder that is practically insoluble in water. It also exhibits hygroscopic properties with very high water absorbency. In tablet formulations, colloidal silicone dioxide is mainly used as a glidant, but has also been employed as a disintegrant and adsorbent (Gore and Banker, 1979; Callahan et al., 1982). The material used in this work was Colloidal silicon dioxide (Cab-osil® -M-5, Lot 21510) and was purchased from Sigma Aldrich GmbH, Seelze, Germany.

4.3.1.7 Model Drug Substance (Diltiazem HCl)

Diltiazem hydrochloride was the model drug selected for this study. It normally occurs as a white to off-white crystalline powder with a bitter taste. Diltiazem, as the hydrochloride, is a calcium channel cellular influx inhibitor (slow channel blocker) and is used to treat various heart conditions (Kenny et al., 1985; Rabkin, 1992). It is known to be very soluble in water, methanol and chloroform. Commercial solid dosage preparations (tablets and capsules) contain diltiazem hydrochloride in doses of 60 mg or its multiples. Diltiazem (batch No. DIL 2197) for this study was purchased from Lusochemica spa, Milan, Italy.

4.3.1.8 Coating materials

The materials used to coat tablets were the same as those used to prepare free films. These were described in chapter 2 (section 2.2.1 and 2.2.2).

4.3.2 Methods

4.3.2.1 Tablet Formulation and Manufacture

Direct compaction was the method adopted to manufacture placebo and drug loaded tablet cores. The placebo cores were used for sorption and desorption studies. Diltiazem HCl, the model drug, was used as the marker compound for dissolution studies. It was included in the tablet cores at 30 % w/w by substituting the respective amount of lactose or calcium dihydrogen phosphate. Details of formulations from which the three different tablet types were manufactured are given in Table 4-2 below.

Ingredient	Tablet Core Formulation		
	Hygroscopic	Non-hygroscopic	Waxy
Lactose monohydrate	69.4	-	78.0
Pre-gelatinised maize starch	15.0	-	-
Microcrystalline cellulose	15.0	-	-
Calcium dihydrogen phosphate	-	99.5	-
Talc	-	-	3.0
Carnauba wax	-	-	14.0
Colloidal silicone dioxide	0.1	-	1.0
Magnesium stearate	0.5	0.5	4.0
Total (%)	100.0	100.0	100.0

Table 4-2. Details of Tablet Core Formulations (Quantities shown in % w/w)

The procedure for preparation of the tablet cores was as follows:

- (i). First, the powder ingredients of a given formulation were individually weighed on an appropriate balance. It was necessary to sift all weighed out powder to remove any foreign material. This was done using a 500 μ m sieve. The obtained powders were then placed in a large bowl of 3-4 kg capacity. Subsequently the materials were dry blended for 10 min in a Kenwood Chef planetary mixer Type KM400/410 (Kenwood, Hoban, UK).

- (ii). Midway through the mixing, the blending process was momentarily stopped and the edges of the bowl scraped using a spatula. The powder was manually mixed with a scoop for a few seconds after which the blending was then continued to the end.
- (iii). The powders obtained at the end of the blending operation were then compressed on a non-instrumented a Manesty Type F3 eccentric tablet press (Manesty Machines Ltd, Liverpool, UK) equipped with 7.0 mm plain standard concave tooling.
- (iv). Owing to the differences in the densities and compactibility of the different excipients, the target tablet fill weight and mean crushing strength were varied between 200-300 mg and 70-150 N to obtain tablets of identical surface area.

4.3.2.2 Tablet Coating

Coating of the tablets was undertaken in an Aeromatic Strea 1 laboratory scale fluidized bed coater (Aeromatic-Fielder AG, Bubendorf, Switzerland). This coater was equipped with a bottom spray pneumatic gun and a 1.2 mm nozzle but without a Wurster insert. A Gilson peristaltic pump (Type M312, Gilson, Gambetta, France) with speed variable capability was used to deliver material into the coating chamber.

Optimum coating conditions which yielded the highest efficiency and minimum agglomeration were established on coating trials performed with placebo tablets. These conditions are summarised in Table 4-3 below. After the predetermined coating time, tablets were removed from the coater, visually examined and weighed. Further drying was undertaken in a hot air oven for 6 hr. Thereafter, theoretical weight gain was calculated as follows:

$$\text{Theoretical Weight Gain (\%)} = \frac{\text{Weight of Tablets After Coating}}{\text{Weight of Tablets before Coating}} \times 100 \quad \text{Equation 4-1}$$

Dried tablets were then transferred into pre-labelled amber coloured glass bottles (1000 ml capacity), tightly sealed and stored in a large glass desiccator over silica gel at room temperature pending further tests.

Polymer Coating	Eudragit EPO	Eudragit L30 D-55	Shin Etus Acoat	Opadry AMB	Sureteric	Sepifilm LP
Pre-coating drying time, min	5.0	5.0	5.0	5.0	5.0	5.0
Atomizing pressure, bar	0.2	0.8	0.4	0.6	0.2	0.4
Spray rate, ml/min	5.0	3.0	2.5	1.5	3.0	3.0
Temperature						
In-let air temperature, °C	38	42	35	38	38	40
Bed temperature, °C	35	41	33	35	38	39
Out-let air temperature, °C	34	40	31	35	37	40
Coating time, min	55	12	45	75	20	35
Post-Coating drying time (min)	15.0	15.0	15.0	15.0	15.0	15.0
Target weight gain (%)	6.4	1.8	2.0	4.0	2.0	3.0

Table 4-3. Details of Coating Tablet Core Conditions Employed for Different Polymer Coatings

4.3.2.3. Evaluation of Uncoated and Coated Tablets

4.3.2.3.1 Uniformity of Weight

Uniformity of weight was evaluated using the BP methodology. To carry out this test, 20 tablets of a given batch were individually weighed and the mean weight, the standard deviation and the relative standard deviations were calculated in the usual way using MS Excel.

4.3.2.3.2 Tablet dimensions

Tablet thickness and diameter were measured using a digital micrometer gauge (Mitutoyo Corporation, Japan). Surface area (A_t) in mm^2 was calculated using the formula suggested by Munzel (1963):

$$A_t = 2\pi\{r.h + [r.c_r - \sqrt{c_r^2 - r^2}]\}^2 \quad \text{Equation 4-2}$$

where r is the tablet radius, h is the overall tablet height (or thickness) and c_r is the convex radius of the tablet punch (obtained from the tooling vendor (I-Holland Ltd, Nottingham, UK) as 9.5 mm).

4.3.2.3.3 Tablet breaking strength and friability

Tablet breaking force (F) was determined with the aid of the Eureka Automatic Hardness Tester (Type TBH 200, Eureka GmbH, Heusenstamm, Germany). Samples of ten tablets from each batch were individually tested. Friability was tested using a Roche Friabilator on a sample of five (5) tablets. The loss in weight after 4 min (100 drops) expressed as a percentage of the original weight was then calculated.

4.3.2.3.4 Tablet disintegration

Disintegration testing was performed in triplicate following the USP method on a Copley 4-Station Disintegration tester (Model DTG 4000, Copley Scientific, Nottingham, UK). The test medium was freshly distilled and deionised water which was maintained at $37 \pm 1^\circ\text{C}$. Six tablets of a given batch were placed into the baskets of the equipment which was then operated at a speed of 30 rpm with a stroke of 30 mm.

4.3.2.3.5 Tablet dissolution studies

Dissolution was conducted in triplicate using a USP 24 Apparatus 2 method. The equipment comprised a Pharma-Test automated dissolution bath (Type PTWS, Pharma Test GmbH, Hainburg, Germany) linked to a UV/VIS spectrophotometer

(Model CE2021, Cecil Instruments, Cambridge, UK). Distilled water (900 ml) maintained at 37.0 ± 0.5 °C was the dissolution medium. The absorbance wavelength was set at 235 nm. For each experimental run, six tablets were individually placed in the dissolution vessels. The sampling interval was set at 2.0 min through out the experiments. Data was processed by a pc with dissolution test software (IDIS, Icalis Data Systems, Berkshire, UK).

4.3.2.3.6 Calibration and validation of UV spectrometry

The analytical method for dissolution was calibrated by taking 0.5000 g of diltiazem HCl and dissolving it in 100 ml of water in a volumetric flask. Thereafter, 10 ml of this solution was diluted with water in a 100 ml volumetric. Standard solutions containing 10, 15, 20, 30, 40, and 50 mg/100 ml of diltiazem HCl were then prepared by taking appropriate aliquots with a glass pipette and diluting to 100 ml with water. Subsequently, UV absorbance values of standard solutions were measured ($n=3$) with a Varian double beam UV-Vis spectrophotometer (Type Cary 3E, Varian Inc., Palo Alto, CA, USA) at 235 nm using water as a blank. (The calibration curve and equipment performance report are shown in Appendix 3).

4.3.2.3.7 Scanning Electron Microscopy

Scanning electron microscopy (SEM) studies were performed using a Philips XL 20 scanning electron microscope (Philips, Cambridge, UK) on representative samples from each set. The specimens were coated with a gold palladium mixture and mounted on a sample holder. All the samples were examined at an accelerating voltage of 5–15 kV depending on the required magnification.

4.3.2.4 Moisture Sorption and Desorption Studies

Moisture sorption-desorption studies were undertaken in the dynamic vapour sorption (DVS) apparatus as previously described for the free films in Chapter 2. Two study protocols were used, i.e., fixed-time and equilibrium sorption-desorption. Fixed-time moisture sorption-desorption profiles of coated and uncoated tablet cores were obtained using three regimes, i.e., 0-50-0-50-0 %RH, 0-75-0-75-0 %RH, and 0-90-0-90-0 % RH with each step change lasting 300 min. Equilibrium sorption profiles were obtained only for uncoated and coated hygroscopic cores using a 0-90 % RH regime, which comprised a drying stage that lasted 2000 min and a wet stage that lasted 1000 min. All experiments were done in triplicate at 25 °C.

4.4 RESULTS

4.4.1 General Characteristics of Manufactured Tablet Cores

The tablet press used in this study was non-instrumented; therefore, it was not possible to obtain compression profiles of the three tablet core formulations. The following product properties were characterised as a way of measuring the tableability of the three formulations and establishing reference properties of the cores. The results are presented below under four sections, i.e., uniformity of weight, hardness, disintegration, uniformity of coating and dissolution profiles.

4.4.1.1 Uniformity of weight

The results for uniformity of weight are shown in Table 4-4. All three formulations exhibited low weight variations, typically below 1.0 %. The waxy tablets showed the lowest weight standard deviation.

Parameter	Hygroscopic	Non-Hygroscopic	Waxy
Mean weight, (g)	0.203	0.252	0.201
Standard deviation	0.002	0.001	0.001
RSD (%)	0.738	0.555	0.498

Table 4-4. Results of the Assessment of Tablet Weight Uniformity

In most pharmacopoeias, the uniformity of weight standard can also be used to monitor the uniformity of dosing of the active ingredient in the tablet. By taking a sample of tablets and calculating the mean, the compliance with the specified deviations can be then be established. In the BP, for instance, this standard requires that no more than two tablets differ from the mean by 5 %, and also, no single tablet differ by more than 10 %. As the results showed, all formulations had low weight variation. The waxy tablets showed the lowest weight variation, possibly due to the higher lubricant levels.

4.4.1.2 Tablet Strength

Tablet strength is described in terms of the breaking force and friability. Friability testing is an official test in the USP. It is undertaken to judge the ability of the tablets to withstand chipping, capping or breaking when subjected to friction or shock. The friability of the different samples was calculated as the per cent mass loss after 100 drops in the Roche Friabilator equipment. The results were as follows: 0.134%, 0.588 % and 0.613%, respectively for the hygroscopic, non-hygroscopic and waxy formulations.

The data for tablet hardness are shown in Table 4-5 below. The tablet breaking force is used to measure tablet resistance to bending, crushing, and impact stress or resistance to attrition. There is no official standard for tablet hardness; nevertheless, the minimum requirement for tablets to be film coated is unofficially set between 70-150 N by most pharmaceutical manufacturers.

Parameter	Formulation		
	Hygroscopic	Non hygroscopic	Waxy
Diameter (mm)	7.024 (0.0544)	7.022 (0.001)	7.014 (0.000)
Thickness (mm)	3.692 (0.012)	3.671 (0.141)	3.710 (0.094)
Breaking force (N)	118.8 (7.5)	78.2 (2.2)	72.6 (3.6)

Table 4-5. Results of the Tablet Breaking Force (N) (Std. Dev, n=5)

With respect to this work, the tablet strength and friability data showed that the hygroscopic formulation exhibited the highest strength and had the lowest friability. This is attributed to the inclusion of lactose. This material improves the mechanical strength of tablets (Rubinstein, 1988). The non-hygroscopic and waxy formulations exhibited slightly lower tablet strengths and higher friability, although neither formulation failed the minimum requirements.

For the waxy formulation, tablet strength was perhaps compromised by the large quantity of the hydrophobic substances. The slightly weaker cores seen in non-hygroscopic cores was an unexpected outcome, given the fact that calcium phosphate is reported to exhibit good compactibility. This was possibly due to overcompression.

4.4.1.3 Tablet disintegration

The results of the disintegration test are tabulated below in Table 4-6. Only the uncoated samples were evaluated for their disintegration properties.

	Hygroscopic	Non-Hygroscopic	Waxy
Min (min)	8.0	≥ 120	52.0
Max (min)	14.3	≥ 120	76.5
Mean (min)	10.7	-	64.9

Table 4-6. Results of the Tablet Disintegration Time (min)

The disintegration test is an empirical approach for simulating in-vivo performance of a tablet formulation. It is also an important quality assurance tool. The USP describes a disintegration test for uncoated tablets with up to 30 minutes as pass/fail criteria. Based on this criterion, therefore, only the hygroscopic formulation passed the disintegration test (≥ 30 min) while both the waxy and non-hygroscopic formulations failed. This is attributed to the inclusion of starch and microcrystalline cellulose in the hygroscopic formulation, which are well-known tablet disintegrants. Starch and microcrystalline cellulose act by drawing water into the tablet and swelling in the process which then causes the tablet core to break-up (Lowenthal, 1973; Rubinstein, 1988). Disintegrants were not included in the non-hygroscopic and waxy formulations.

Calcium dihydrogen phosphate, although capable of being rapidly penetrated by liquid due to its hydrophilicity and the characteristically high porosity of its tablets, it does not disintegrate on its own because of its insolubility in water (Jivraj et al., 2000). For the same reason, the slow disintegration in the waxy cores is attributed to the presence of lactose, the main filler in this formulation. Lactose is well known as having a relatively slow disintegration due to its limited solubility. It is also plausible that the inclusion of the magnesium stearate and talc compromised the disintegration of this core. These two materials have been shown to slow disintegration (Hussain, et al, 1992).

4.4.1.4 Tablet Coating

The tablets obtained after application of the coatings were visually inspected to find if there were any obvious discontinuities in the coatings. Once satisfied, the cores were then subjected to other tests. Even though it was desirable to carry out other tests, e.g., surface roughness, film adhesion and thickness, these tests were not done for lack of equipment. However, the variation of the dry weight gain was calculated and is shown in Table 4-7 below.

Name of coating	Tablet Formulations		
	Hygroscopic	Non-Hygroscopic	Waxy
Eudragit EPO	6.405±0.156	6.162±0.526	6.285±0.819
Eudragit L30 D-55	1.800±0.444	1.805±0.109	1.851±0.000
Shin-Etsu Aqoat	2.008±0.250	1.968±0.029	2.129±0.228
Opadry AMB	4.133±0.497	4.134±0.312	4.148±0.043
Sepifilm LP	3.254±0.624	3.036±0.409	3.189±0.008
Sureteric	2.183±0.155	1.997±0.217	2.040±0.044

Table 4-7. Dry Weight Gain (%) of Coated Tablet Cores (n=20, \pm Std Error, 95% Confidence Interval) Based on Means of the Dry Weight Gain for (n=3) Samples of 20 Coated Tablets

The fluidized bed coating process is extensively used in the pharmaceutical industry. This process involves precisely depositing a quantity of coating onto the surface of the tablet using a spray of the coating dispersion. For most functional coatings, the performance of the coating will depend on how uniformly the coating mass is deposited onto the surface of the dosage form. This also applies to barrier coatings; where by the integrity of the coating is critical to barrier performance.

The process requirements for depositing a uniform coating onto a solid dosage form are specific to properties of the substrate like weight, size, shape, and, perhaps density (Bauer et al., 1998). In most coating operations, especially at a scale of the present study, process optimization will be based on a black-box approach, i.e., the final product qualities are used to determine the success or failure of the coating process without understanding the exact dynamics of the process. For coating uniformity, various techniques are used, namely determination of weight uniformity, scanning electron microscopy (SEM), spectrometric techniques like NIR, and Raman, disintegration and/or dissolution testing, and measurement of the coating thickness with a micrometer (Nole et al., 2000; Silva et al., i.e., 2001; Romero-Torres, 2005).

In this study, the uniformity of the coating process was assessed by determining the variation of the weight gain among the tablet cores within the same batch and also between different batches coated with the same polymer. As the results in Table 4-7 demonstrate, variation was low. Furthermore, SEM micrographs of the coated tablet cores was also undertaken to assess the integrity of the applied coatings. An example of such micrographs is shown in Figure 4-2 below for the hygroscopic core coated with the Sepifilm LP coating dispersion. No evidence of major defects can be seen.

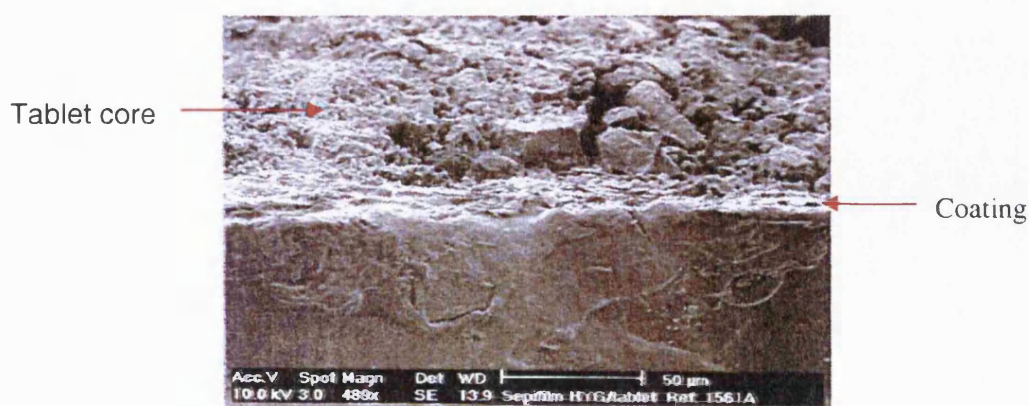


Figure 4-2a. Scanning Electron Micrograph of a Hygroscopic Tablet Core Coated With Sepifilm LP-Based Coating (magnification x 489)

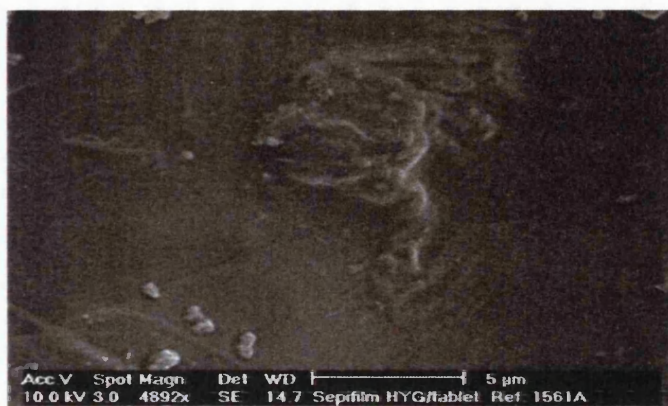


Figure 4-2b. Scanning Electron Micrograph of the Surface of a Hygroscopic Tablet Core Coated With Sepifilm LP Coating (magnification x 4900)

4.4.1.5 Dissolution Test Profiles

The dissolution profiles of uncoated and coated hygroscopic tablet cores are shown in Figure 4-3 below. The data are charted in terms of the cumulative amount of drug released versus time for the different coated hygroscopic products. Non-hygroscopic and waxy tablet cores were not subjected to the dissolution test because these formulations exhibited very poor disintegration times, as shown in Table 4-6.

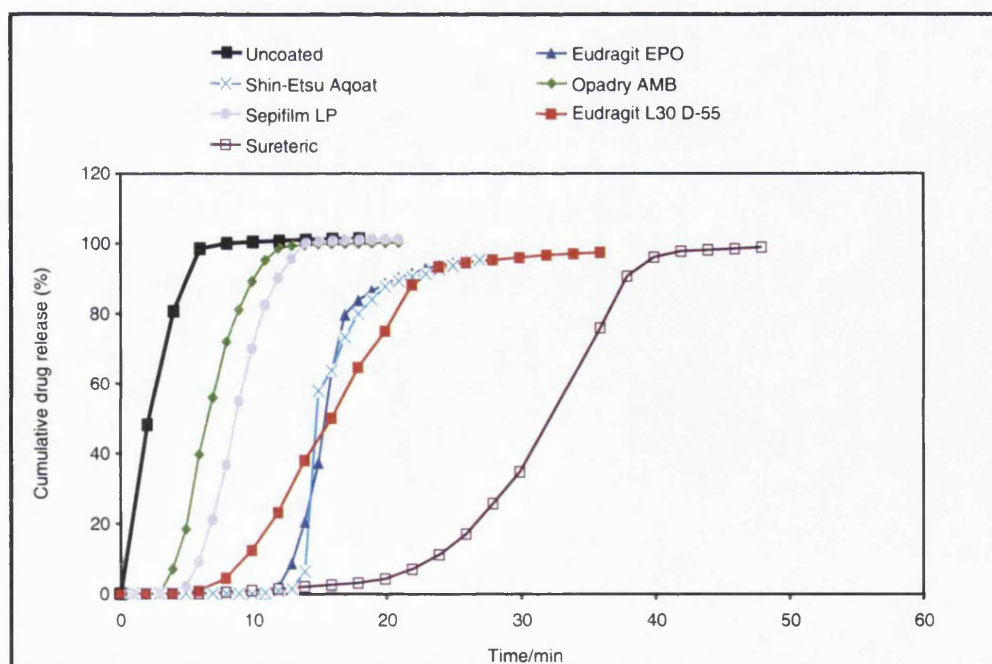


Figure 4-3. Dissolution Profiles of Diltiazem Uncoated Hygroscopic and the Same Tablet Cores Coated With Different Polymer Coatings.

Dissolution testing is extensively used during the development of new drug products, as well as routinely as a quality control tool during the production of tablets. Being an official test, the specifications, including the test media are usually stipulated by the pharmacopoeia. The most commonly used test media are 0.1 N HCl and phosphate buffer of pH 6.8 (Ashford et al., 1993; Karali et al., 1995; Fadda and Basit, 2005). However, other test media, such as distilled water, have also been used. During the course of the dissolution test, the active drug substance leaves the core and dissolves in the medium for it to be detected spectrometrically.

In this study, the dissolution test was undertaken in distilled water. The reason for choosing water was to enable the comparison of the degree of hydration of the different coatings to moisture uptake. Since diltiazem HCl, the model drug used in this study, is a high solubility molecule, the dissolution characteristics of the different coated cores reflect the speed with which the coatings “eroded”. In other words, it was the expectation that the dissolution of the drug was not the slowest step but rather the erosion of different coatings. Thus, the release of the active ingredient from the core was a reflection of the hydration characteristics of the coating.

From the dissolution profiles shown in Figure 4-3 above, it can be seen that tablet cores coated with the Opadry AMB and Sepifilm LP films showed only a slight slowing of dissolution of the drug from over the uncoated tablet core. For both of these specimens, hydration of the coatings was therefore very quick due to their pH independent solubility. The slightly longer time lag exhibited by the Sepifilm LP coated sample compared with the Opadry AMB coated sample was perhaps due to the presence of stearic acid in the former sample.

Tablet cores coated with the Eudragit L30 D-55, Eudragit EPO and Aqoat films exhibited intermediate release profiles, with a delay of up to 10 min before drug release was initiated. The Sureteric coated cores were, ultimately, the slowest releasing, taking ≈20 min before initiating drug release. Thus, these coatings can be considered slow-hydrating. It is of interest to note that the Eudragit EPO coated sample exhibited a much greater time lag, even though this coating is categorised as a conventional, non-functional coating. This coating is soluble at a pH below 5.5 and above the pH of 5, the Eudragit EPO coating becomes “soluble” by first swelling, which then increases the permeability before the drug molecules in the core can be released. The observed delay thus reflects the impediments of release via this mechanism as opposed to simple dissolution observed in Opadry AMB or Sepifilm LP coatings.

Also, despite the fact that dissolution testing was undertaken in media of neutral pH (i.e., distilled water, pH ≥ 6.5); which was higher than the minimum pH required for dissolution of the enteric films, it can be seen in Figure 4.3 that these samples exhibited a noticeable time lag in the dissolution profile. This “anomaly” is explained as follows: The factors relating to the medium which influence dissolution are the pH, buffer composition and buffer capacity, and ionic composition and strength (Ashford et al., 1993; Karali et al., 1995; Fadda and Basit, 2005). The ionic composition and strength of the dissolution media are understood to be key factors, as recently pointed out by Fadda and Basit (2005). Both factors directly contribute to the mechanism by which the enteric coat disintegrates. So, even if the distilled water used in this work had the required pH, the fact that the buffering capacity and ionic strength were insignificant could have resulted in the slow dissolution exhibited by the enteric coated samples.

4.4.1.6 Mean Dissolution Time

To facilitate quantitative comparison of the dissolution profiles presented in Figure 4-3 above, two parameters, the mean dissolution time MDT (min) and area under the curve (AUC) of the dissolution curve were selected as suitable parameters. The simplified mathematical definition of MDT is as follows (Riegelman and Collier, 1980; Tanigawara et al., 1982; Costa et al., 2003):

$$MDT = \frac{\int_0^{\infty} t \delta M_t}{\int_0^{\infty} \delta M_{\infty}} \quad \text{Equation 4.3}$$

where M_t is the mass of drug released in solution at time t . The denominator of Equation 4.3 corresponds to the total amount of drug released at t_{∞} . In Table 4-8 below are shown the values for the MDT and the AUC calculated for the data in Figure 4-2. The procedure for calculating both parameters was the same as that described by Pinto, et al., (1997) and involved integration of Equation 4.3 between the time t corresponding to 0 % drug release and t for 100 % release.

In line with the data shown in Figure 4-3, the uncoated tablet cores exhibited the lowest MDT and the AUC. This was followed by the Opadry AMB and Sepifilm LP coated samples which exhibited relatively low values. The Eudragit and Shin-Etsu Aqoat coated samples exhibited intermediate values while the Sureteric coated samples had the highest MDT and AUC. This confirms the categorization of the hydration characteristics of the different films presented in section 4.4.1.5 above.

Sample	MDT	AUC
Uncoated cores	2.13	213.28
Eudragit L30 D-55 coated core	12.53	946.84
Eudragit EPO coated core	15.86	1573.20
Hypromellose acetate coated core	16.30	1614.00
Opadry AMB coated core	6.88	689.56
Sepifilm LP coated core	8.71	869.11
Sureteric coated core	31.59	3129.23

Table 4-8. Mean Dissolution Time (MDT, min) and Area Under the Curve (AUC, %.min) for the Different Coated cores. The Constants were Calculated from the Dissolution Data in Figure 4-2

4.4.2 Moisture Sorption-Desorption Profiles of Tablet Cores

Moisture sorption-desorption studies were undertaken on uncoated and coated tablet cores of dissimilar hygroscopicity under fixed-time sorption-desorption regimes in the dynamic vapour sorption (DVS) apparatus. The objective being to determine the role played by the core hygroscopicity and the applied film on the extent of sorption and desorption of moisture from the cores. All experiments were performed at 25 °C as described in sections 4.3.2.4. Tablet cores were coated with the four moisture barrier films as well as the two enteric polymer films. The coating levels were in keeping with the minimum manufacturer's recommended levels. Details of the levels of coatings applied to the different cores are described in Table 4.7 above. Thus, the data are presented to reflect the objectives set out, i.e., moisture sorption-desorption characteristics of uncoated tablet cores of dissimilar hygroscopicity, and the same cores coated with the four different moisture barrier films. In addition, this section also presents the data for the hygroscopic cores coated with the two enteric polymer films.

4.4.2.1 Uncoated Tablet Cores

The sorption and desorption profiles for the uncoated hygroscopic, non-hygroscopic and Waxy tablet cores obtained following exposure to the 0-90-0-90-0 % RH protocol are shown in Figure 4-4 below. These profiles reflect trends seen in at least three experimental runs. As similar behaviour was seen at the 0-75-0-75-0 % RH and 0-50-50-0 % RH cycles, except for amounts moisture sorbed/desorbed (which were proportionately less) the data for these cycles are summarized in Table 4-9 in the form of mean moisture uptake/loss at the different conditions. For the convenience of comparison, the data at the 0-90-0-90-0 % RH protocol are also included in the table.

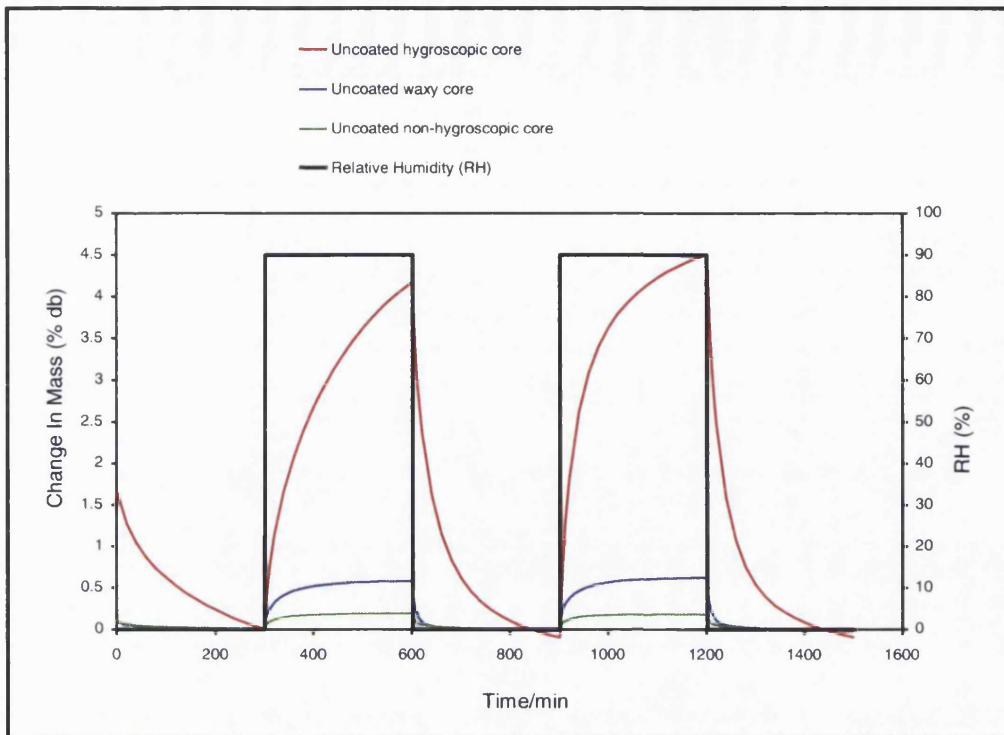


Figure 4-4. Fixed-Time Moisture Sorption-Desorption Profiles of Uncoated Hygroscopic, Non-hygroscopic and Waxy Tablet Cores Exposed to 0-90-0-90-0 % RH Cycle (25 °C)

RH Step Change	Core Type		
	Hygroscopic	Non-hygroscopic	Waxy
0-50 % RH	1.315 (0.001)	0.086 (0.050)	0.229 (0.003)
50-0 % RH	1.278 (0.006)	0.089 (0.004)	0.188 (0.021)
0-75 % RH	2.667 (0.044)	0.119 (0.006)	0.371 (0.018)
75-0 % RH	2.908 (0.011)	0.120 (0.022)	0.358 (0.002)
0-90 % RH	4.554 (0.008)	0.202 (0.015)	0.599 (0.010)
90-0 % RH	4.494 (0.005)	0.191 (0.010)	0.582 (0.114)

Table 4-9. Summary of Moisture Uptake-Loss Data for Uncoated Hygroscopic, Non-hygroscopic and Waxy Tablet Cores (at 25°C). (Std. Dev, n=3).

From the data presented in Table 4-9, it can be seen that hygroscopic cores sorbed more moisture than waxy cores, which in turn showed differences over non hygroscopic cores. Furthermore, hygroscopic cores exhibited an exponential rise in mass uptake and did not attain equilibrium in the 300 min exposure time. Also, the waxy and non-hygroscopic cores equilibrated fairly rapidly (~ 100 min of exposure). When cores were exposed to the drying cycles, all the three type of core returned to the original dry mass by the end of the experiment. However, while the hygroscopic core required about 250 min to loose all the moisture, the non-hygroscopic and Waxy cores achieved the dry state fairly rapidly (i.e., in about 50 min).

4.4.2.2 Coated Hygroscopic Tablet Cores

4.4.2.2.1 Hygroscopic cores coated with moisture barrier coatings

The sorption profiles for the hygroscopic cores coated with moisture barrier films (i.e., Eudragit L30 D-55, Eudragit EPO, Opadry AMB and Sepifilm LP) are presented in Figure 4-5 below. As was the case for the uncoated tablet cores above, the charted data show the moisture sorption-desorption profiles obtained at the 0-90-0-90-0 % RH protocol. The moisture sorption-desorption data corresponding to the 0-50-0-50-0 and 0-75-0-75-0 % RH are summarized in Table 4-10 below. For the ease of comparison, the data for the 0-90-0-90-0 % RH are also included therein Table 4-10.

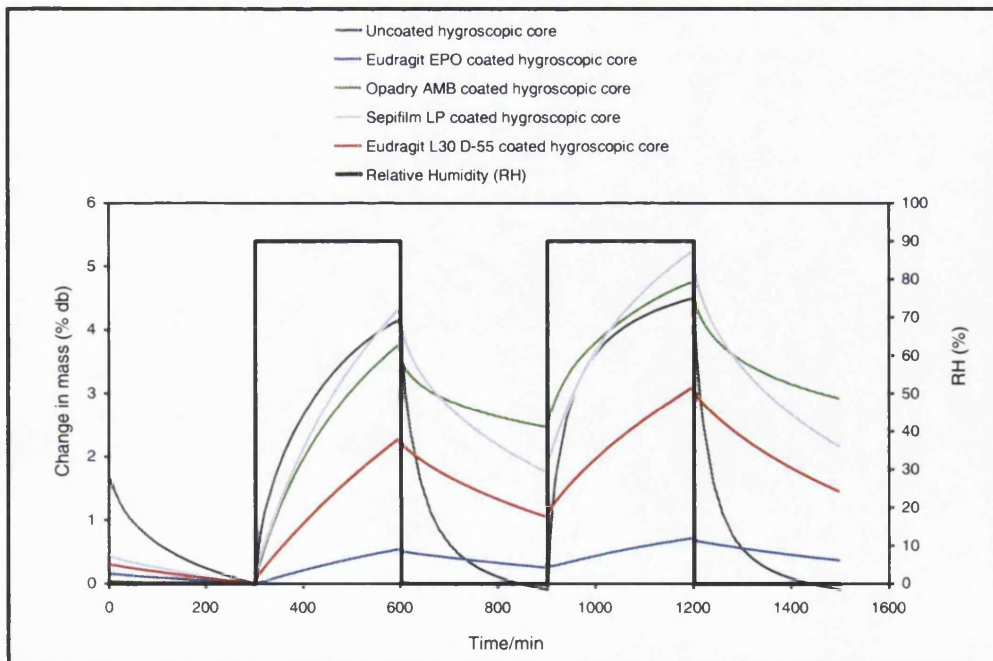


Figure 4-5. Fixed-Time Moisture Sorption-Desorption Profiles of Hygroscopic Tablet Cores Coated with Moisture Barrier Films. Samples Exposed to 0-90-0-90-0 %RH Cycle (25°C)

Sample	0-50 % RH/ 50-0 % RH	0-75 % RH/ 75-0 % RH	0-90 % RH/ 90-0 % RH
Eudragit L30 D-55 coated core	0.913 (0.066) 0.567 (0.015)	1.033 (0.051) 0.952 (0.031)	2.231 (0.011) 1.181 (0.072)
Eudragit EPO coated core	0.181 (0.014) 0.126 (0.017)	0.382 (0.001) 0.183 (0.027)	0.528 (0.024) 0.261 (0.004)
Opadry AMB coated core	1.087 (0.002) 0.085 (0.006)	1.418 (0.067) 0.404 (0.002)	3.777 (0.031) 1.312 (0.911)
Sepifilm LP coated core	1.213 (0.015) 1.090 (0.010)	2.175 (0.001) 1.784 (0.014)	4.258 (0.110) 2.474 (0.108)

Table 4-10. Summary of Moisture Uptake-Loss Data for Uncoated and Coated Hygroscopic Tablet Cores (at 25°C). (Std. Dev, n=3)

The data shows coated hygroscopic cores exhibited an exponential rise in mass and were not in equilibrium at the end of the experiment. Also, more or less a net reduction in the total amount of moisture sorbed over the uncoated sample was achieved. During the drying cycle, the samples did not return to their original dry mass. This behaviour was not apparent in the uncoated hygroscopic cores described above. Further descriptions for individual polymers are given in the following paragraphs:

Eudragit L30 D-55:

Coating of cores with Eudragit L30 D-55 resulted in a reduction of moisture sorbed over that seen in the uncoated core. This was probably due to the barrier effect of the coating and a possible change in sorption kinetics compared with the uncoated core or the free film. The Eudragit L30 D-55 free film itself was shown to have rapidly established an equilibrium mass gain and then rapidly desorbed this moisture when exposed to the drying cycle. The application of the coating on the tablet core however, resulted in a system that did not allow the tablet to equilibrate as rapidly as when it was uncoated. Despite the fact that both the Eudragit L30 D-55 film and the uncoated tablet core were able to lose moisture completely during desorption cycles, the coated core did not. Sorption and desorption for Eudragit L30 D-55 coated cores appeared to be pseudo zero order kinetic processes, although the sorption rate was marginally faster.

Eudragit EPO:

The Eudragit EPO coated samples sorbed the least moisture. Also, these samples did not attain equilibrium within the experimental time of 300 min by which the sorption process was stopped. On exposure to the drying cycle, only about 50 % of the sorbed moisture was lost by the coated sample. On repeat cycles, there was a modest

increase in the amount of moisture sorbed. However, the proportion of moisture lost was similar to that in the first cycle. It can be recalled that both the Eudragit EPO free film and uncoated hygroscopic core desorbed all the moisture sorbed within the 300 min drying time, however, the coated sample was able to retain a significant amount of moisture within itself. Therefore, a possible change in the sorption-desorption kinetics of the coated sample (slower) compared to either the free film or the uncoated tablet core can be anticipated.

Opadry AMB:

The Opadry AMB coated core achieved only a small reduction in the overall amount of moisture sorbed by the uncoated sample. Also, the sample did not achieve equilibrium. The Opadry AMB film was shown to possess some tendencies to retain moisture during desorption. This behaviour was manifested again although it was much more pronounced for the coated samples. For instance, during the first sorption process 3.7 % moisture was sorbed (the mass expected to be accommodated in the film if it behaved as a free film would be $13 \times 4 / 100 = 0.52\%$). Interestingly, this is approximately the mass that was desorbed rapidly at the start of the first desorption cycle. It is possible, therefore, that the mass of moisture that transferred into the core remained in the tablet core, whereas that in the film desorbed again. The second sorption process resulted in much less moisture uptake than the first, as if the process were moving toward a pseudo-equilibrium state.

Sepifilm LP:

The sorption process in the hygroscopic cores coated with Sepifilm LP also failed to reach equilibrium. Desorption showed substantial hysteresis and did not complete in the 300 minute window. The total mass of moisture sorbed was more or less that sorbed by the uncoated cores, but much more than could possibly be accommodated in the film alone (total uptake for the cast film was $\approx 21\%$, which for a 3% coating on the tablet cores would accommodate $21 \times 3 / 100 = 0.63\%$). Consequently (assuming the sorption of moisture in the coating to be similar to that seen with cast free films), the mass of moisture transferring to the tablet core was greater for this coat than for the methacrylates or the Opadry AMB coated samples.

4.4.2.2.2 Hygroscopic cores coated with enteric polymers

The sorption-desorption profiles of cores coated with hypromellose acetate phthalate and Sureteric were obtained only at the 0-90-0-90-0 % RH protocol due to time constraints. These data are presented in Figure 4-6. Eudragit L30 D-55 data are included for the ease of comparison with the moisture barrier films.

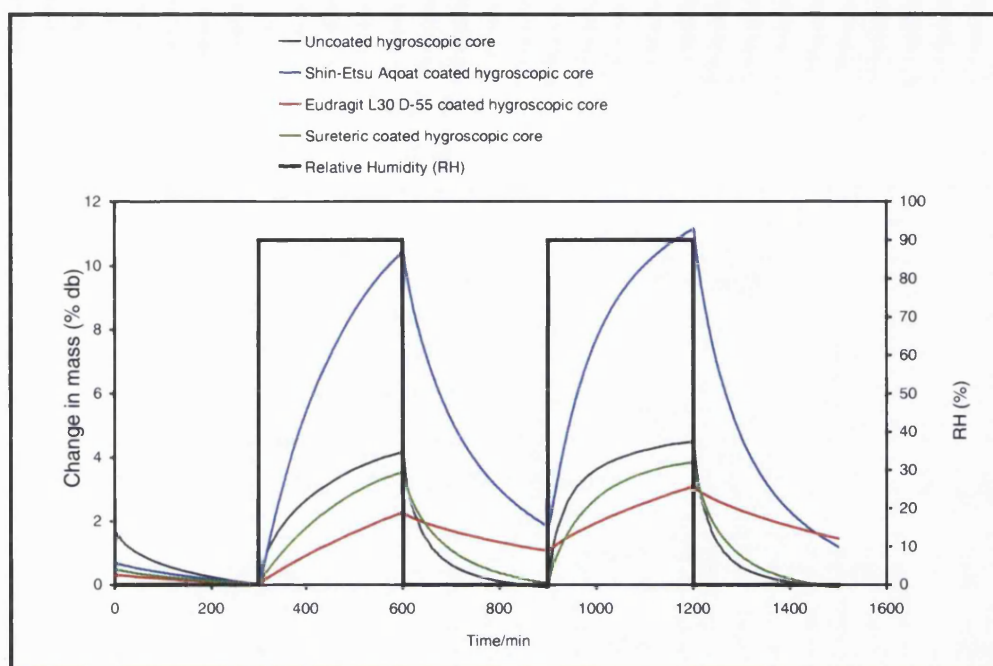


Figure 4-6. Fixed-Time Moisture Sorption-Desorption Profiles of Hygroscopic Tablet Cores Coated With Enteric Polymer Films. Samples Exposed to 0-90-0-90-0 % RH Cycle (25 °C)

Sureteric:

It can be seen from Figure 4-6 above that the Sureteric coated samples achieved only a marginal reduction in the moisture sorbed over the uncoated sample. Thus, the coated sample sorbed 3.465 (0.142) % db moisture compared with 4.585 (0.341) % db of the uncoated sample. Given the fact that Sureteric free film it self exhibited very low hygroscopicity, the result above was unexpected. Considering that the coating, applied at 2 % weight gain, was relatively thin, this result perhaps reflects the possibility that some moisture could have gained access to the core, trumping up the total amount of moisture taken by the sample.

Shin-Etsu Aqoat:

The data for Shin-Etsu Aqoat showed that these samples also failed to achieve a net reduction in the moisture sorbed over the uncoated hygroscopic core. Therefore, the low hygroscopicity of this film was also not imparted to the core to which it had been applied, in a similar way as the Sureteric coated core. Although there are no currently available literature reports on the moisture sorption characteristics of hypromellose acetate succinate, possibly because this is a relatively new polymer, nevertheless, similar expectations, as for the Sureteric, would not be far off. In consideration of the fact that the coating applied was only 2% weight gain, there is also a possibility that some moisture gained entry into the underlying core.

In summary, the results for moisture sorption-desorption studies exhibited by coated cores demonstrated very complex sorption-desorption patterns. Application of coatings to the cores resulted in systems which behaved more or less like the free films. In most cases, though, application of a barrier coating generally achieved a net reduction in the amount of moisture sorbed by the core. Importantly, under fixed sorption regimes, none of the samples achieved equilibration in the experimental time. In comparison, the cores coated with the two enteric polymers, viz., Sureteric and Aqoat, did not yield a clear-cut reduction in the extent of sorption like the cores coated with the moisture barrier films.

4.4.2.3 Coated Non-Hygroscopic Tablet Cores

The data for coated low hygroscopic cores are summarised in Figures 4-7 below. These charts show the sorption-desorption profiles of the different samples following exposure to the 0-90-0-90-0 % RH cycle. The data for 0-50-0-50-0 and 0-75-0-75-0% RH are summarised in Table 4-11 but as in the previous sections, the data for the 0-90-0-90-0 % RH cycle are included in the same table to facilitate comparison.

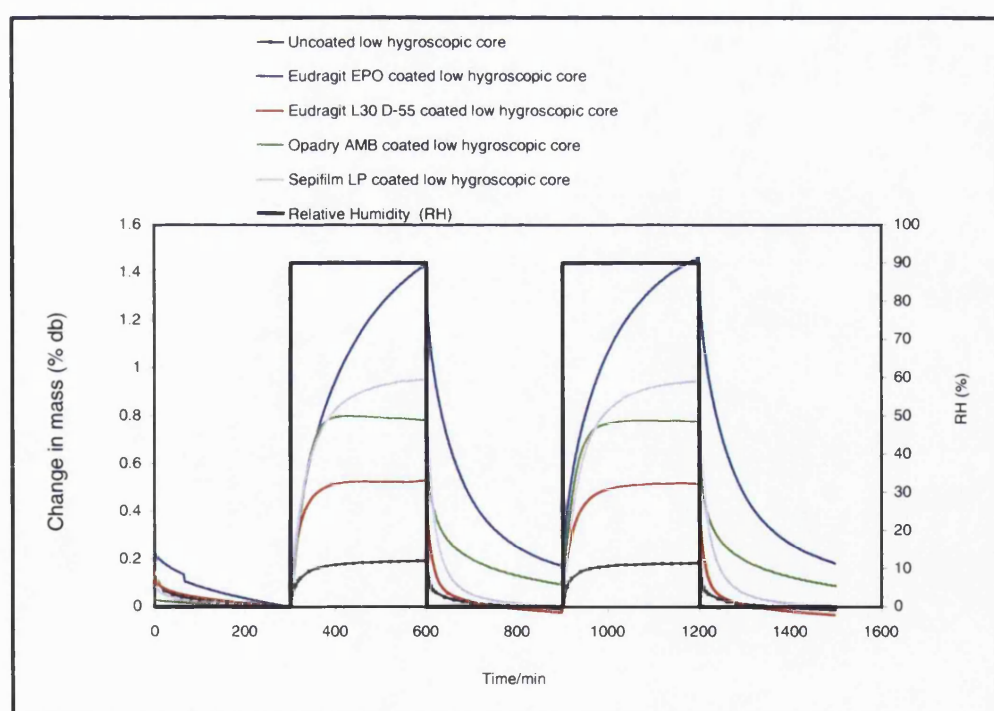


Figure 4-7. Fixed-Time Moisture Sorption-Desorption Profiles of Non-Hygroscopic Tablet Cores Coated With Moisture Barrier Films. Samples Exposed to 0-90-0-90-0 % RH Cycle (25 °C)

Sample	0-50/50-0	0-75/75-0	0-90/90-0
Eudragit L30 D-55 coated core	0.128 (0.001)	0.187 (0.001)	2.15 (0.001)
	0.111 (0.000)	0.186 (0.001)	1.88 (0.001)
Eudragit EPO coated core	0.498 (0.041)	0.756 (0.000)	1.433 (0.000)
	0.495 (0.001)	0.674 (0.001)	1.260 (0.001)
Opadry AMB coated core	0.191 (0.001)	0.348 (0.000)	0.783 (0.000)
	0.156 (0.000)	0.323 (0.000)	0.784 (0.000)
Sepifilm LP coated core	0.303 (0.003)	0.613 (0.009)	0.954 (0.001)
	0.268 (0.002)	0.607 (0.003)	0.952 (0.003)

Table 4-11. Summary of Moisture Uptake/Loss Data for Uncoated and Coated Non-hygroscopic Tablet Cores (at 25°C). (Std. Dev, n=3)

4.4.2.4 Coated Waxy Tablet Cores

The data for the waxy cores following exposure to the 0-90-0-90-0 % RH test condition are presented in Figure 4-8 below. Data for the 0-90-0-90-0 % RH are included to ease comparison. For other conditions, the data are summarised in Table 4-12.

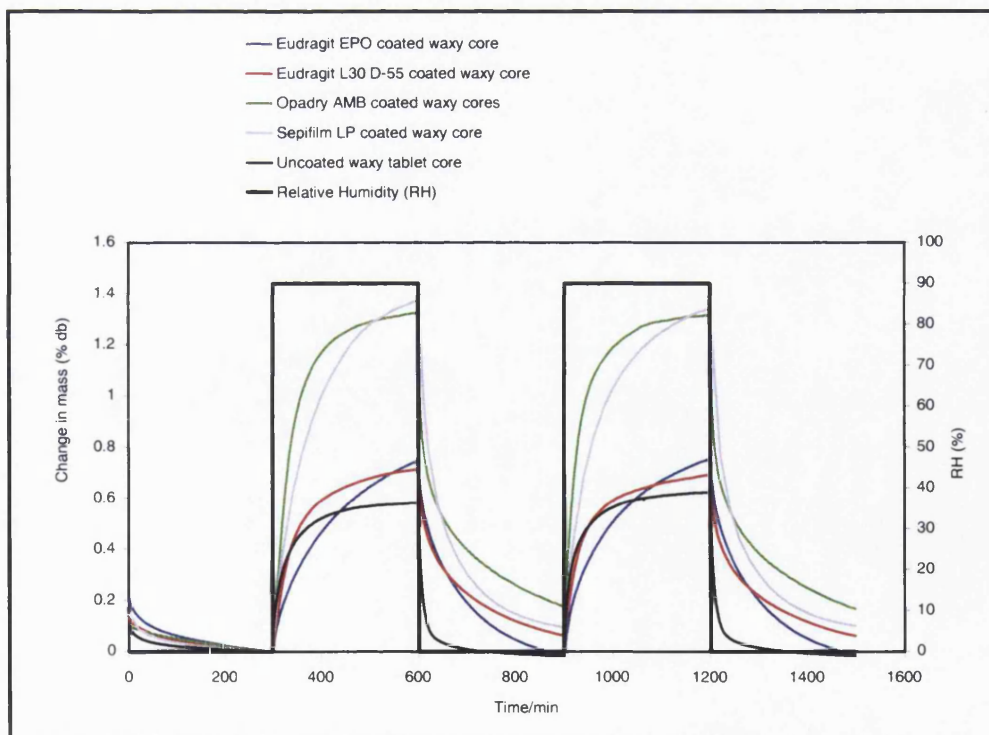


Figure 4-8. Fixed-Time Moisture Sorption-Desorption Profiles of Waxy Tablet Cores Coated With Moisture Barrier Films. Samples Exposed to 0-90-0-90-0 %RH Cycle (25 °C)

Core	0-50/50-0	0-75/75-0	0-90/90-0
Eudragit L30 D-55 coated	0.249 (0.003)	0.418 (0.001)	0.729 (0.010)
	0.238 (0.001)	0.389 (0.001)	0.669 (0.013)
Eudragit EPO coated	0.278 (0.024)	0.748 (0.000)	1.229 (0.001)
	0.282 (0.010)	0.763 (0.000)	0.995 (0.000)
Opadry AMB coated core	0.333 (0.001)	0.507 (0.023)	1.320 (0.018)
	0.297 (0.005)	0.420 (0.011)	1.146 (0.027)
Sepifilm LP coated	0.383 (0.006)	0.745 (0.005)	1.380 (0.013)
	0.362 (0.002)	0.751 (0.006)	1.286 (0.020)

Table 4-12. Summary of Moisture Uptake/Loss Data for Uncoated and Coated Waxy Tablet Cores (at 25°C). (Std. Dev, n=3)

The results for sorption and desorption of moisture by coated non-hygroscopic and waxy cores, as shown in section 4.4.2.3 and 4.4.2.4 above, demonstrate somewhat less complex behaviour. It can be seen that, except for the Eudragit EPO coated samples, all the coated samples belonging to this category more or less achieved equilibration. The behaviours of the coated samples were somehow simpler in that the water content of the coated samples appeared to be a sum-total of the moisture taken up by the core plus the film. Such trends would suggest that if the water content of the film or the core were known, the amount of moisture sorbed by the coated sample could then be predicted. This was not so for the hygroscopic samples. From the profiles of sorption, the apparent kinetics of sorption of the coated specimens were not so much different from those of the respective free films, which would suggest that for these samples, the sorption-desorption behaviour was largely a factor of the applied film coating, with little contribution from the core.

It is worthy stating at this juncture that the results described in this section (namely, section 4.4.2), with the exception of the data for Eudragit EPO, appear concurrently in the the publication by Mwesigwa et al. (2005). A copy of this publication is included in this thesis in Appendix 5.

4.4.3 Effect of Weight Gain on Moisture Uptake/Dissolution

The purpose of this work was to determine the effect of thicker film coatings on sorption-desorption profiles and dissolution. In section 4.4.2 the dissolution and moisture sorption-desorption characteristics of the tablet cores were studied on tablet cores coated at the minimum coating levels. In this undertaking, on top of the minimum levels obtained earlier, the non-drug and drug loaded hygroscopic cores were coated in such a way that the following weight gain outcomes were achieved: Eudragit L30 D-55 3.8 and 5.8 %; Eudragit EPO 8.4 and 10.4 %; Shin-Etsu Aqoat 4.0 and 6.0 %; Opadry AMB 8.0 and 12.0%; and Sureteric 4.0 and 6.0 %. Subsequently, the moisture sorption-desorption profiles and dissolution studies were undertaken on these cores. The results are presented in two sections: section 4.4.3.1 describes the moisture sorption-desorption characteristics of the cores, while section 4.4.3.2 describes the results for the dissolution test studies.

4.4.3.1 Moisture Sorption-Desorption Profiles

The sorption-desorption properties of the above-mentioned cores were studied at the 0-90-0-90-0 % RH protocol at 25 °C. The typical sorption-desorption profiles obtained are shown in Figure 4-9 through to Figure 4-14. The figures were charted in the same way as the figures presented previously.

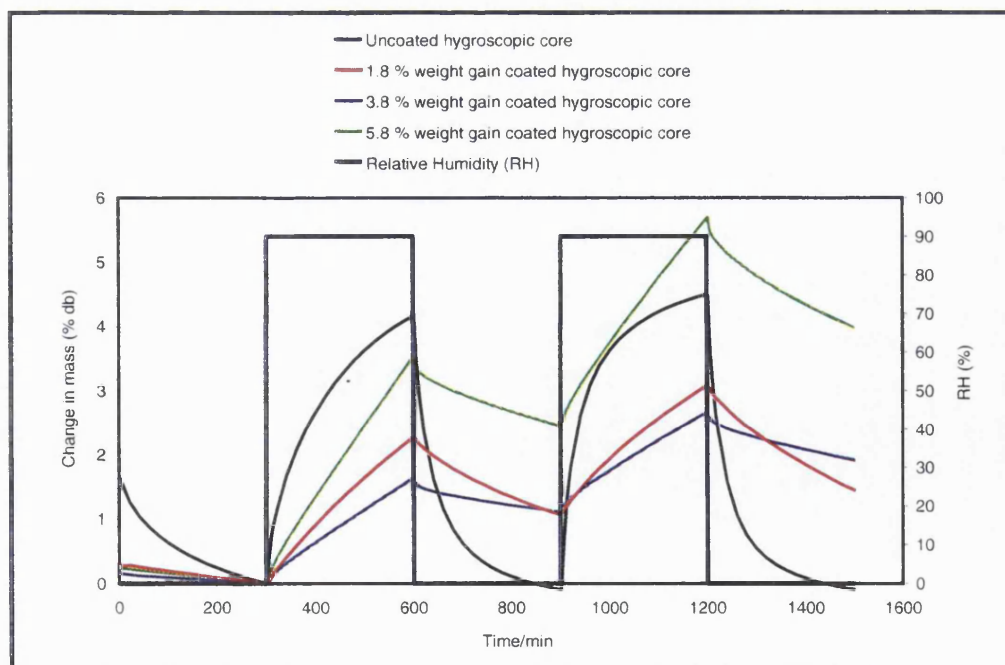


Figure 4-9. Fixed-Time Moisture Sorption-Desorption Profiles of Hygroscopic Tablet Cores Coated With Eudragit L30 D-55 Film at Increasing Weight Gain. Samples Exposed to 0-90-0-90-0% RH Cycle (25 °C)

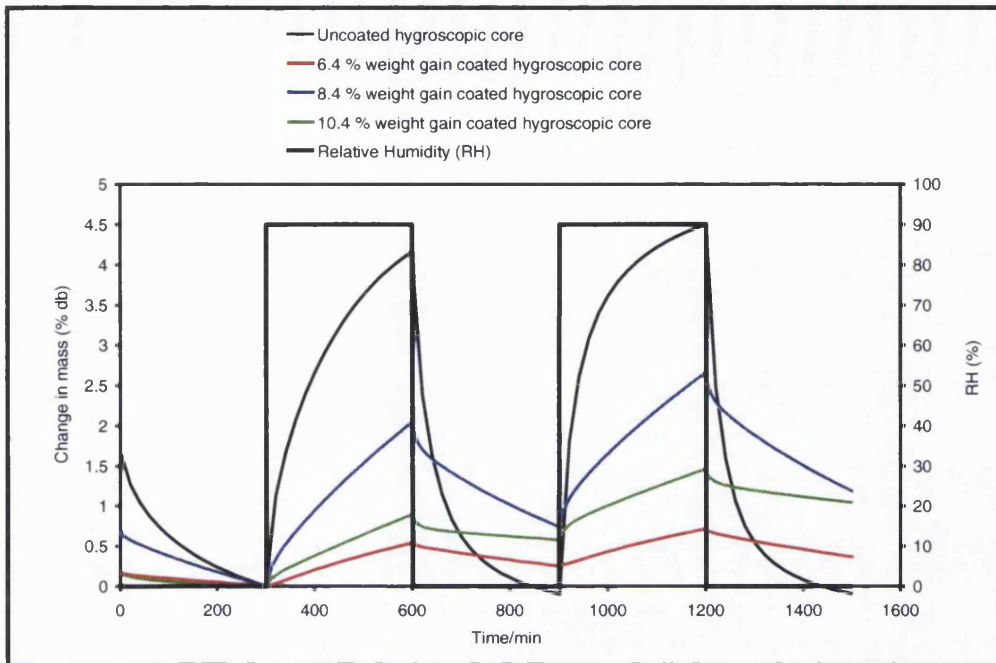


Figure 4-10. Fixed-Time Moisture Sorption-Desorption Profiles of Hygroscopic Tablet Cores Coated with Eudragit EPO Film at Increasing Weight Gain. Samples Exposed to 0-90-0-90-0% RH Cycle (25 °C)

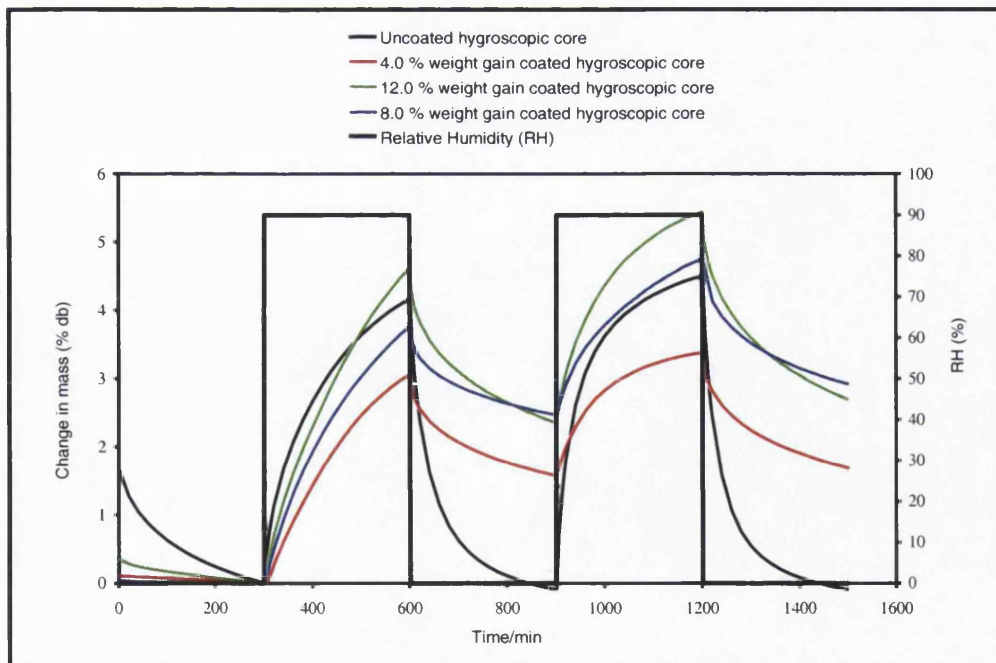


Figure 4-11. Fixed-Time Moisture Sorption-Desorption Profiles of Hygroscopic Tablet Cores Coated with Opadry AMB Film at Increasing Weight Gain. Samples Exposed to 0-90-0-90-0% RH Cycle (25 °C)

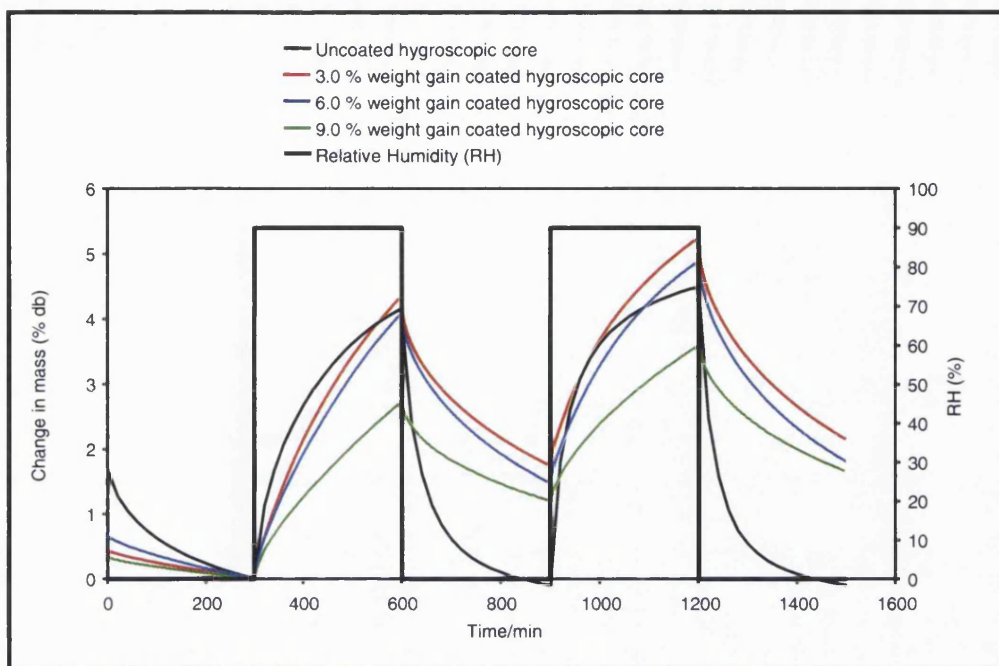


Figure 4-12. Fixed-Time Moisture Sorption-Desorption Profiles of Hygroscopic Tablet Cores Coated with Sepifilm LP Film at Increasing Weight Gain. Samples Exposed to 0-90-0-90-0% RH Cycle (25 °C)

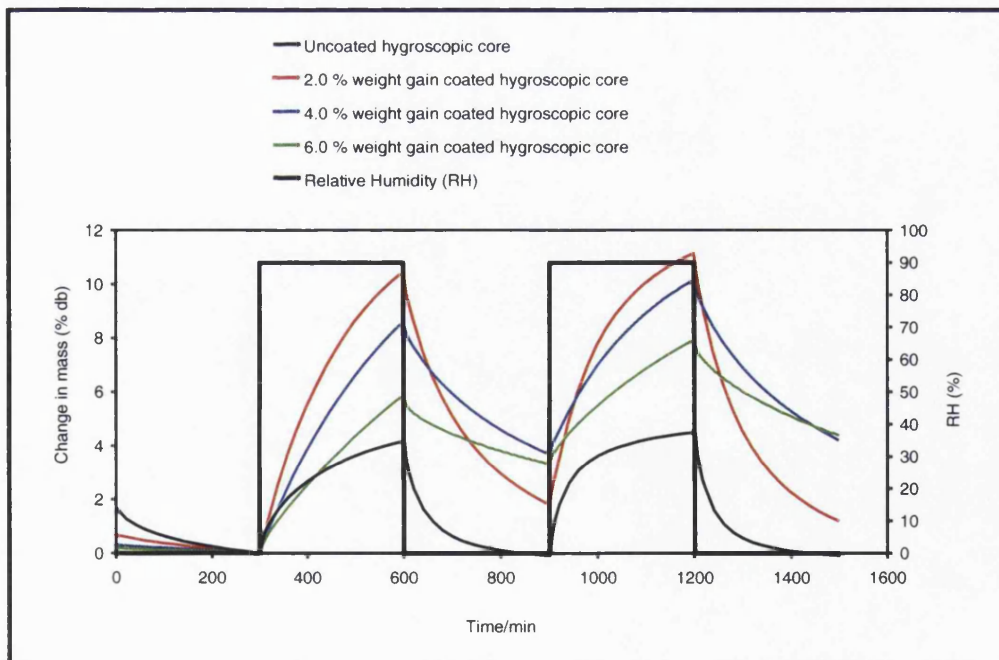


Figure 4-13. Fixed-Time Moisture Sorption-Desorption Profiles of Hygroscopic Tablet Cores Coated with Shin-Etsu Acoat Film at Increasing Weight gain. Samples Exposed to 0-90-0-90-0% RH Cycle (25 °C)

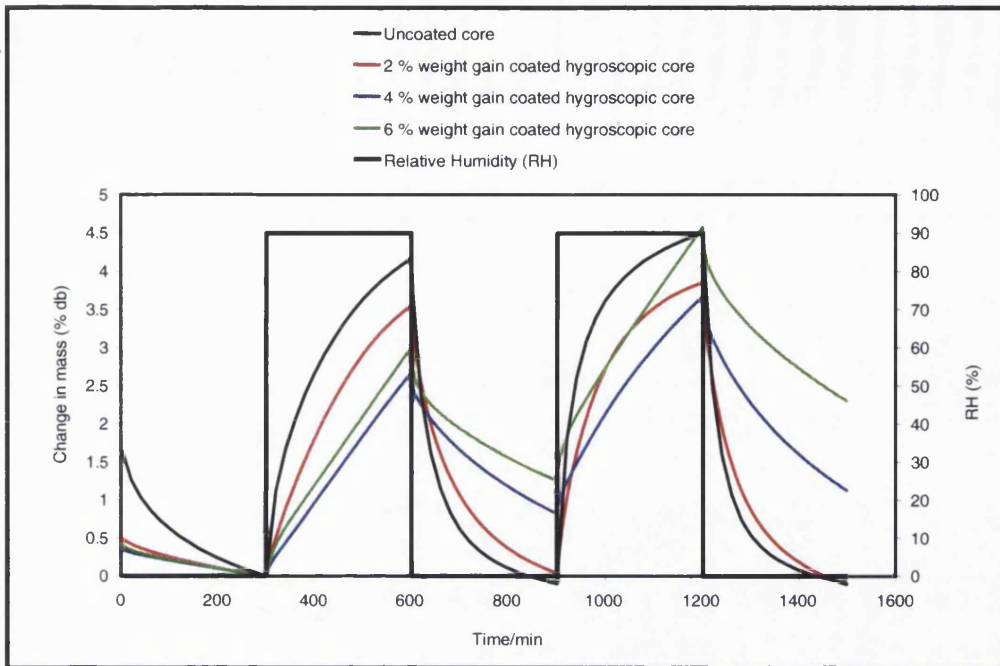


Figure 4-14. Fixed-Time Moisture Sorption-Desorption Profiles of Hygroscopic Tablet Cores Coated with Sureteric Film at Increasing Weight Gain. Samples Exposed to 0-90-0-90-0% RH Cycle (25 °C)

It can be seen from the profiles presented that major differences in sorption-desorption characteristics of the samples in relation to an increase in the thickness of the applied coating emerged. Thus, four general trends were identified:

- (i). In the first group, viz., Sepifilm LP and Aqoat coated cores, there was a progressive reduction in the moisture sorbed as the weight gain was increased.
- (ii). In the second group, i.e., Eudragit L30 D-55 and Sureteric coated samples, there was an initial decrease in the moisture sorbed which was followed by an increase in the sorbed moisture with weight gain increase.
- (iii). In the third category, exemplified by Eudragit EPO, increase in the weight gain resulted in an initial increase but as the weight gain was increased further, a reduction in the moisture sorbed was obtained.
- (iv). In the last category, i.e., the Opadry AMB coated sample, increase in the weight gain led to a progressive increase in the moisture sorbed.

Generally, the moisture sorption-desorption behaviour exhibited by the different cores was quite complex demonstrating the contribution of the core in some samples and the effect of the film coating in others on the extent of sorption-desorption by the coated samples.

4.4.3.2 Dissolution Profiles

Dissolution profiles (of coated tablet cores containing diltiazem HCl as the marker drug) were obtained in a similar way as for the cores coated at the minimum levels. These profiles are shown in Figure 4-15 to Figure 4-20 respectively for the Eudragit L30 D-55, Eudragit EPO, Opadry AMB, Sepifilm LP, Sureteric and Shin-Etsu Aqcoat coated cores. The charts show interlaid dissolution profiles for the uncoated core as well as the cores coated in increasing weight gain. As in previous cases, the per cent cumulative drug release is plotted on the y-axis while the time (in min) is plotted on the x-axis.

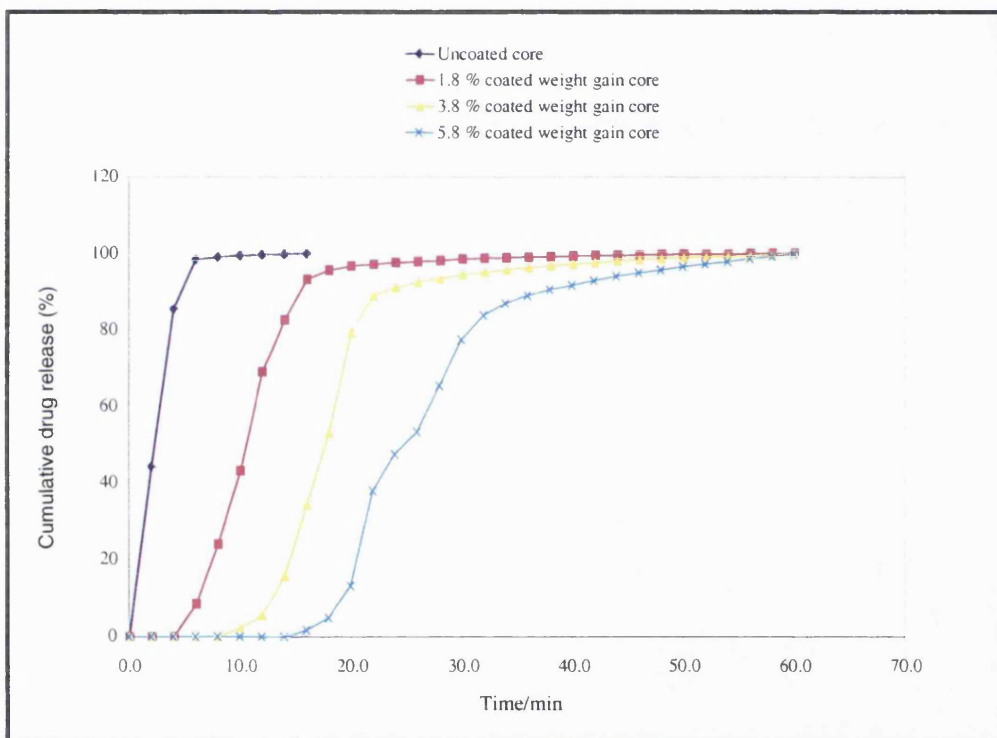


Figure 4-15. Dissolution profiles of Diltiazem from Hygroscopic Tablet Cores Coated with Eudragit L30 D-55 at Increasing Weight Gain

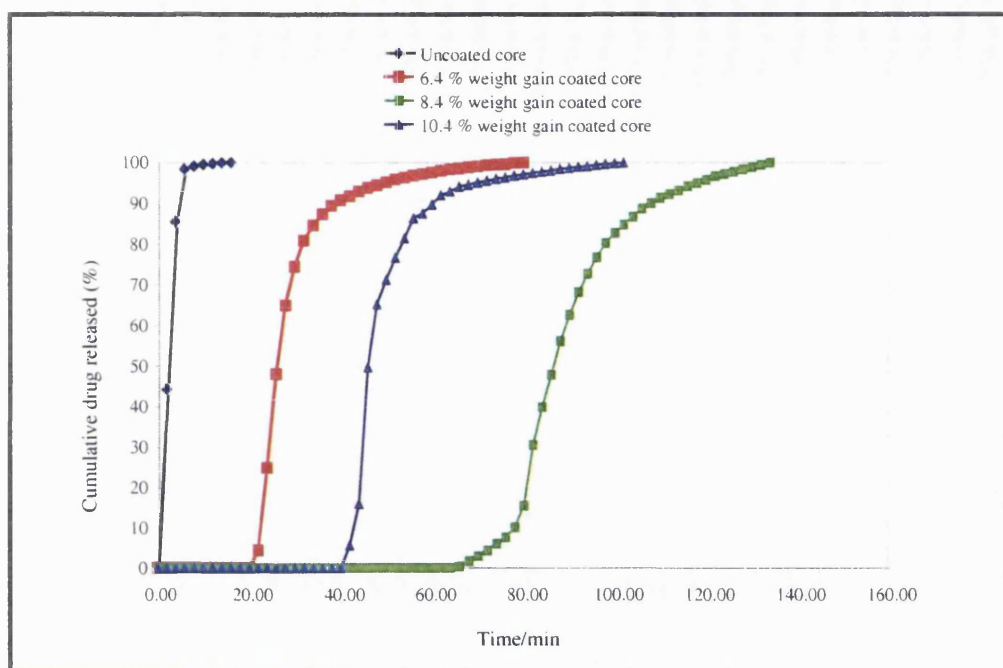


Figure 4-16. Dissolution Profiles of Diltiazem from Hygroscopic Tablet Cores Coated with Eudragit EPO at Increasing Weight Gain

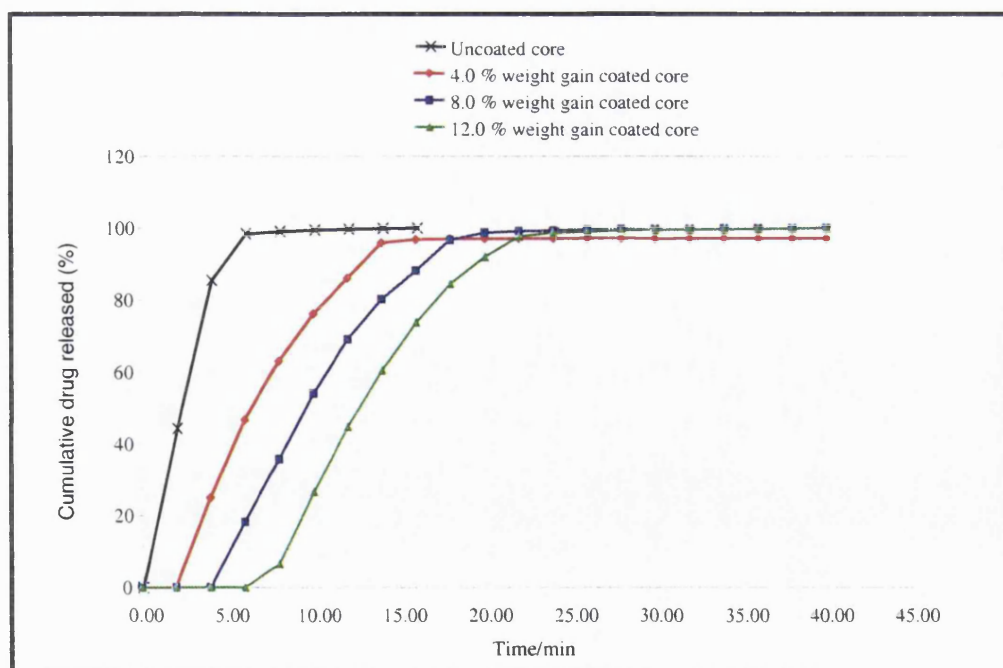


Figure 4-17. Dissolution Profiles of Diltiazem from Hygroscopic Tablet Cores Coated with Opadry AMB Film at Increasing Weight Gain

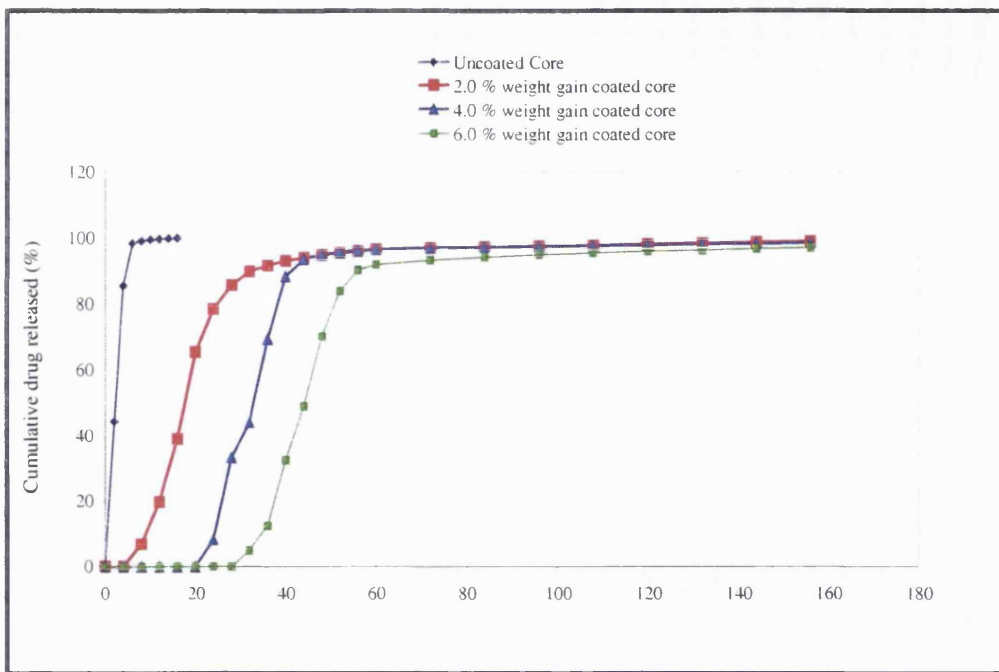


Figure 4-18. Dissolution Profiles of Diltiazem from Hygroscopic Tablet Cores Coated with Sepifilm LP Film at Increasing Weight Gain

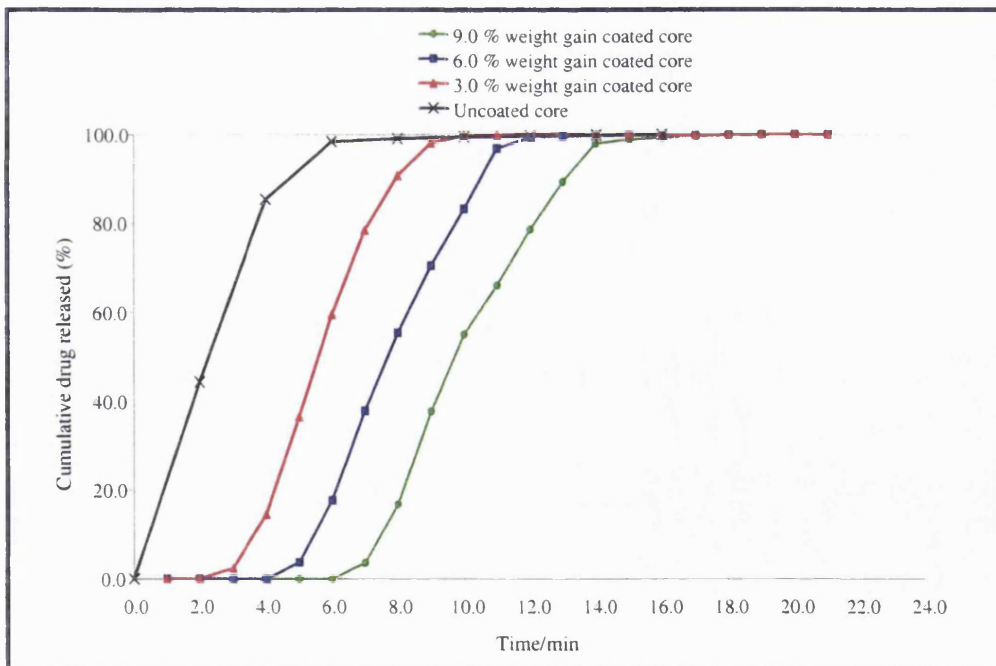


Figure 4-19. Dissolution Profiles of Diltiazem from Hygroscopic Tablet Cores Coated with Shin-Etsu Aqoat Film at Increasing Weight Gain

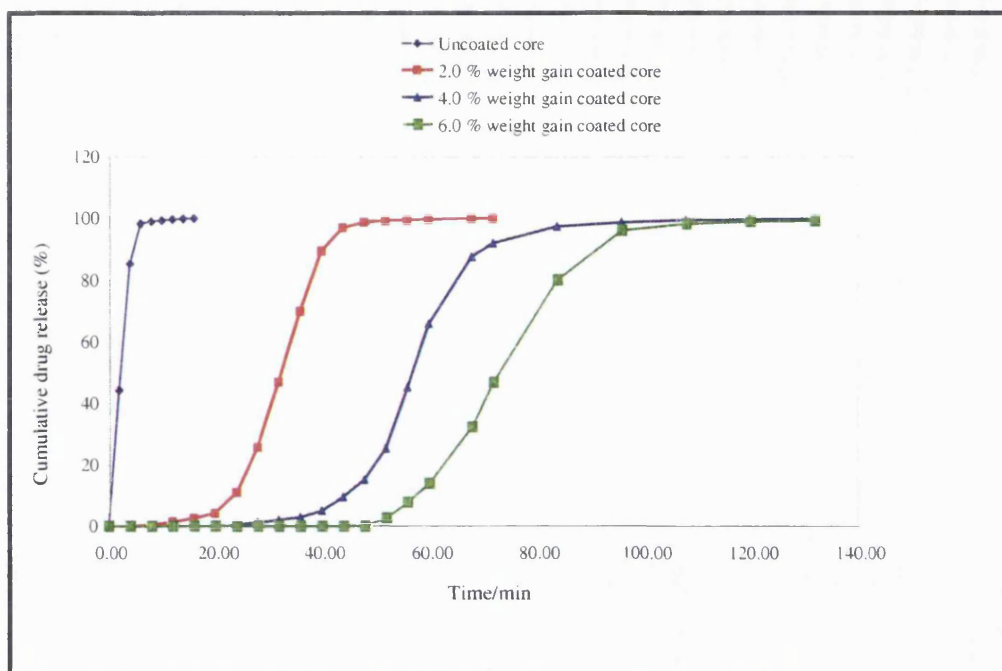


Figure 4-20. Dissolution Profiles of Diltiazem from Hygroscopic Tablet Cores Coated with Sureteric Film at Increasing Weight Gain

The charts show that increasing the thickness of the coating on the tablets resulted in an increase in the dissolution time. The effect was less dramatic with Opadry AMB and Sepifilm LP coated samples compared with Eudragit EPO, Eudragit L30 D-55 or the two enteric coated samples. With the enteric coated samples, the dissolution process was considerably delayed. It can be seen from the figures above that the dissolution characteristics of all the different coated tablet cores coated at increasing wet gains were more straightforward compared to the moisture sorption-desorption data. Thus, an increase in the polymer coating levels resulted in a corresponding increase in the time lag, which affected the initialisation of dissolution. The length of this time lag varied from sample to sample. For the Sepifilm LP and Opadry AMB coatings, the delay was the lowest. Both coatings are presumed to have simply dissolved away on contact with water via the usual process of bond annihilation and or erosion. This indicates that the effect of increasing the thickness of the coating only slightly affected dissolution in the two cases. This was not so for enteric coatings, since these coatings disintegrated via a different mechanism. The effect of increasing the thickness of the coating was therefore an important factor. Also, for coatings which released the drug via swelling (e.g., Eudragit EPO), the effect of coating thickness increased the diffusion path and consequently resulted in the observed time-lag in the dissolution profile.

In general, the outcome of these tests demonstrates that the different coatings can be grouped into three main classes, i.e., rapidly hydrating, comprising Opadry AMB and Sepifilm LP, intermediate hydrating, comprising Eudragit L30 D-55, Eudragit EPO and Shin-Etsu Acoat, and slowest hydrating, typified by Sureteric. This classification corroborates well with the qualitative observations made on the dissolution profiles presented earlier. Also, an interrelation with moisture sorption data can be seen. Thus, the more hygroscopic films also happened to hydrate and dissolve fastest. However, whether this similarity in the results obtained for the two phenomenon (i.e., sorption and dissolution) mean that the permeabilities of water vapour and liquid water were equivalent is not clear at this stage and remains a matter for debate. It would appear that, in the present case, different behaviours were found.

4.4.4 Equilibrium Sorption Profiles of Tablet Cores

The final aspect of this work involved evaluating the equilibrium sorption profiles hygroscopic cores coated with the respective moisture barrier coatings. Through trial and error, the following test protocol was found to deliver the required test conditions: 0-90 % RH with a prolonged dry stage lasting 2000 min and a wet phase lasting 1000 min. The obtained profiles are presented in Figure 4-21 below for Eudragit L30 D-55, Eudragit EPO, Opadry AMB and Sepifilm LP coated cores.

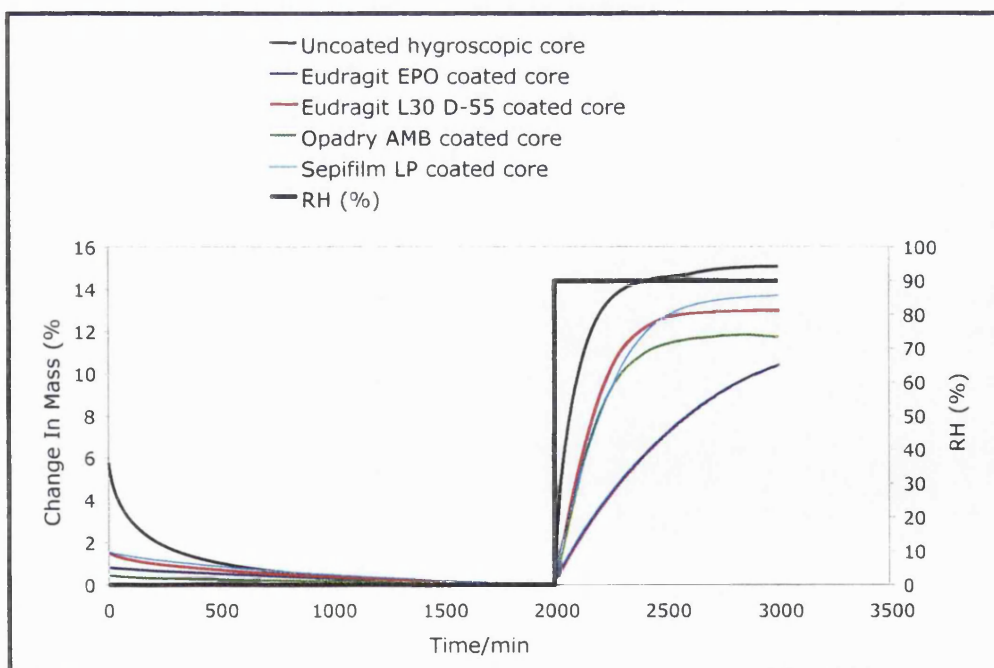


Figure 4-21. Equilibrium Moisture Sorption Profiles of Uncoated and Coated Hygroscopic Tablet Cores Exposed to 0-90 % RH Cycle (25 °C)

The sorption characteristics obtained after prolonged exposure of the tablet cores to moisture in the DVS yielded a picture which was clearer than that obtained under fixed-time sorption regimes. The least hygroscopic sample was the amino methacrylate coated sample, which sorbed 10.407 (0.755) % db moisture. For this sample, the amount of moisture reaching the core, assuming the film had sorbed moisture in the same way as the free film, was calculated as 10.245 % db. The Opadry AMB coated sample, the second least hygroscopic sample, sorbed 11.724 () % db of moisture, meaning that 11.184 % db moisture potentially reached the core. The amount similarly reaching the core for the Eudragit L30 D-55 and Sepifilm LP coated samples were, respectively 12.893 % db and 13.047 % db.

The other aspect relating to the response of the different coated samples following extended exposure to moisture include the fact that all samples were able to achieve equilibration, with the exception of those coated with the Eudragit EPO film. It is also apparent that the Opadry AMB coated core achieved a higher net reduction in the amount of water sorbed compared with the Eudragit L30 D-55 coated sample. Under fixed-time sorption regimes, this particular sample only achieved a marginal reduction in the amount of moisture taken up over the uncoated cores. With this clearer picture emerging, the amount of moisture taken by the different coated samples roughly varied between 60 % (for the Eudragit EPO coated sample) to about 90 % (for the Sepifilm LP coated sample) over the total amount sorbed by the uncoated core. Had the respective coatings been 100 % water proof, the amount of water taken by the coated samples would have been minimal. As this was not the case, the presumption is that this water was taken up by the sample, possibly redistributed between the coating and the core. Given the limited mass of coating in relation to the mass of the core for a given sample, the expectation was that the core bore the brunt of this uptake.

4.5 DISCUSSION

4.5.1 Introduction

Direct compression was the method used to make tablet cores in this study. This method is very straightforward and very easy to assemble. However, it can be problematic. One of the difficulties of direct compression is obtaining formulations that readily flow to ensure consistent and reproducible tablets. McCormick (2005) recently discussed the causes and solutions of problems commonly encountered in direct compression. Suffice to say, it was the intention of this work to obtain cores that were consistent from batch to batch, and as the results showed, this objective was achieved.

Many physicochemical properties of tablet formulations, such as strength, disintegration, and dissolution, are functions of the ingredients in the formulation on one part, and the method of manufacture, on the other. To determine if the manufactured tablet cores possessed the required qualities, several tests were performed, e.g., uniformity of fill weight, the tablet breaking force, and friability testing, disintegration and dissolution. Tablet strength is especially critical in direct compression because this process does not include a binder. As was demonstrated with the results from the different tests, the objective of ensuring that the manufactured tablet cores were consistent was achieved.

4.5.2 Tablet Core Formulation

No single excipient possesses all the properties ideal to make tablets, let alone for direct compression formulations. In most cases, it is necessary to use blends of different excipients. Thus, fillers provide the required bulk and compactibility, lubricants and glidants for lubricity, disintegrants for aiding tablet break-up, etc. Some properties of commonly used fillers for formulation of tablets, e.g., lactose, calcium phosphate, were listed earlier in the introduction to this chapter. Depending on the levels of use, these materials are capable of imparting their characteristics to the formulations in which they are used.

The rationale for using different materials and the levels was as follows: The hygroscopic formulation was designed with lactose as the main filler. This material, although non-hygroscopic, was selected to give this formulation the required mechanical strength and compactibility. Hygroscopicity was rendered by microcrystalline cellulose and pregelatinized starch. Magnesium stearate was the lubricant at minimal level of 0.5 % to minimise its hydrophobic effects. Colloidal silica was present at 0.1 % as a glidant.

The non-hygroscopic formulation was developed from calcium phosphate as the sole excipient. Due to its abrasive nature, it was necessary to include magnesium stearate as a lubricant to minimise sticking on punches. Lastly, the waxy formulation was designed from carnauba wax, talc and magnesium stearate, which were present at high concentrations. Lactose was chosen as the filler as it was not expected to influence hydrophobicity of the formulation. Colloidal silica (1.0%) was included as an adsorbent. The strategy of varying tablet weight and/ or compression pressure also made it possible to manufacture of tablets of identical dimensions.

4.5.4 Moisture Sorption-Desorption Characteristics of Tablet Cores

The moisture sorption-desorption characteristics of uncoated tablet cores of different hygroscopicity showed that the formulation containing lactose, microcrystalline cellulose, and starch was the most hygroscopic core, in line with the categorization set out in this work. This formulation exhibited the greatest tendency to take up water but did not attain equilibration within the time of the experiment. In comparison, the cores formulated from calcium phosphate or from lactose, carnauba wax and talc, exhibited a lesser tendency to take up water but equilibration was attained fairly quickly. Generally, the moisture sorption-desorption characteristics for coated cores demonstrated very complex sorption-desorption patterns. Application of the coatings to the cores resulted in systems which behaved more or less like free films. For hygroscopic cores application of the barrier coating generally achieved a net reduction in the amount of moisture sorbed by the core while the cores coated with the two enteric polymers, viz., polyvinyl acetate phthalate) and Shin-Etsu Aqoat did not yield a clear-cut reduction in the extent of sorption over the uncoated cores.

The uptake of moisture by an uncoated tablet core should be a straight forward affair that reflects the moisture sorptive properties of the constitutive excipients in the specimen in question. As pointed out elsewhere (Bryn, 1982; Hancock and Shamblin, 1998), the hygroscopicity of a material, from a physicochemical point of view, depends on its chemical composition, and possibly, its physical state. As there are no reports in the current literature which offer a direct comparison of the water sorbed by the tablet cores similarly formulated as described in this work, it is herein presumed that the water sorption characteristics of the respective cores reflect, to a large degree, the chemical and physical characteristics, and therefore the water sorption characteristics of the constituent excipients in the cores. Thus, the high hygroscopicity and the exponential rise in the amount water exhibited by the hygroscopic formulation (4.585 (0.341) % db) are attributed to the presence of starch and microcrystalline cellulose.

Being carbohydrates, these materials are hydrophilic, a property that was imparted to this formulation [the equilibrium moisture sorption of starch, cellulose and lactose are respectively reported as 10 %, 5 % and 2.0 %. Lactose, although a carbohydrate like starch and microcrystalline cellulose, was not expected to contribute to the hygroscopicity of this formulation due its low molecular weight and fewer -OH groups per monomer unit. The same reasons are given for the low sorptive capacity exhibited by the non-hygroscopic formulation (which sorbed a meagre 0.274 (0.110) % db moisture) and the waxy formulation (0.625 (0.152) % db), i.e., the presence, mainly of calcium phosphate and lactose, in the respective formulations. The slightly higher sorption shown by the waxy formulation compared with the non-hygroscopic formulation could have been contributed by colloidal silica, which is hygroscopic and also a moisture absorbent, as well as the lactose. These materials were included at levels of 1 % w/w and 78% w/w respectively.

The uptake of moisture by a coated tablet core is, however, not a straight forward affair as is the case for the uncoated samples. Since the applied films are not water-proof, there are potentially two or more factors that can impact on the sorption-desorption process. Thus, on one hand, there is the applied film coating, present on the outside of specimen, that will take-up, interact with (store) and transmit the moisture depending on its hydrophilicity and permeability characteristics. The film coating is by all means the first point of contact for the incident water vapour molecules. On the other hand, there is the inner tablet core, whose physicochemical properties, as explained above, may also somewhat influence the extent of moisture that the entire specimen takes up.

Until the present study, there have been no reports, at least from the examination of the main stream pharmaceutical literature, which investigated what aspect of a coated dosage form, determined the extent of moisture sorption by the dosage form and how the water molecules distributed between the coating and the core. From the evidence so far gathered, it would appear that this is no trivial matter. Just to recap the results of the present study, it was found that the mass gain for non-hygroscopic and waxy cores was a sum of that which would be expected to be sorbed by the moisture barrier films and that which was sorbed by the uncoated core, whereas for the hygroscopic cores, although the barrier coatings allowed substantial water sorption into the core, the extent of this was less and the rate of uptake lower than for the uncoated sample. The picture that emerged from coating hygroscopic cores with enteric films or at increasing weight gain was even more complex. For instance, uptake for the enteric coated samples was substantially above that of the uncoated core, which was unexpected given the low hygroscopicity of free films of the enteric polymers.

For the hygroscopic cores coated in such a way that thicker film coatings were applied on to the cores by increasing the weight gain, even more complex sorption-desorption behaviour was obtained. This was categorised into three, perhaps four groups. Thus:

-In the first group (i.e., the Sepifilm LP and Shin-Etsu Aqoat coated samples) increase in the thickness of coating resulted in a decrease in the extent of sorption. It would seem that for these samples, some level of moisture was reaching the inner core, especially at the first and probably the intermediate coating level. At the final coating level, the applied coating offered sufficient barrier action which restricted the amount of water reaching the core. Therefore, for these samples, increase in coating thickness led to better barrier performance. This is a logical conclusion, especially when the permeability characteristics of the Sepifilm LP film are considered. With this film, the results in Chapter 3 showed that the diffusion of water was much slower due to a more cohesive membrane matrix. It is, thus, speculated that increasing the thickness of the coating on the tablet core had the effect of increasing the diffusion path with the net result that the water reaching the core was progressively less.

-For the second category (viz., Eudragit L30 D-55 and Sureteric coated samples) increase in the thickness of the coating resulted in an initial decrease in the extent of sorption but as the coating thickness was increased further (e.g., at 5.4 % for Eudragit L30 D-55), there was observed an increase in the extent of sorption.. With a minimum coating level of 2 %, it is logical to suppose that there were present discontinuities in the coating such that a proportion of the moisture was reaching the core via this route. It would seem that the tablet core's participation in the sorption process then decreased progressively at the second and third level as the coating became more uniformly applied. The "unexpected" increase in sorption at the final coating level suggests that a good proportion of the sorbed moisture went into the extra layer of the coating rather than the tablet core underneath. It is thought that the effect of increasing the thickness of the coating on diffusion of the moisture was similar to that in group one above.

-The third category (Eudragit EPO coated samples) exhibited an initial increase in the extent of sorption as the weight gain was increased. However, further increase in the thickness of the coating resulted in a decrease in the extent of sorption. This may well mean that at the first level, some moisture gained entry into the core. At the intermediate level (8.4 %), however, the increase in the sorption was possibly due to effect of sorption into the core and the coating. For the highest level (12.4 % wg), the thickness of the coating rendered the sorption process to be restricted largely within the film, which manifested as a decrease in the extent of sorption. Certainly, this behaviour

was far more complex. If it is to be recalled, the Eudragit EPO film exhibited both a low moisture diffusion coefficient and a low solubility coefficient. It is possible to suppose that patterns exhibited by this film reflect the combined role of moisture diffusion and solubility influences within the film.

-The last category, exemplified by the Opadry AMB coated sample, was straightforward. Increase in the thickness of the applied coating resulted in a corresponding increase in the extent of sorption. Given that the quantity of moisture desorbed in the second cycle was greater than the first, it would appear that a greater mass of moisture was situated near the surface in an environment from which desorption was easy. This would imply that a good proportion of the water taken by the samples was possibly being retained within the films rather than leaching into the core underneath. The behaviour of this film is, thus, very intriguing.

Despite this apparent complexity, there are sufficient clues in the obtained results to enable one to hypothesize on the possible mechanism behind the moisture uptake and distribution patterns observed among the different samples studied. Thus, when the dosage form was placed in a humid environment, the expectation of the applied barrier coating would be to limit the entry of the water into the tablet core. There are four possible pathways by which the barrier coating could respond to moisture:

In mechanism I, the barrier coating can hold the moisture inside itself and not let it be transferred into the underlying core. Thus, there would be an increase in weight of the coated core that corresponds with that the expected maximum sorptive capacity of the applied film. It is unlikely that this mechanism was in operation in the present study, except perhaps, as suggested above, for the Opadry AMB samples coated at higher weight gains. In other samples, the total uptake by the coated samples was above that expected to be accommodated in the applied films alone.

In mechanism II, the barrier coating can bar any uptake of moisture, with the net result that neither the film nor the coating were able to sorb moisture. For this mechanism, the barrier coating must be 100 % water-proof. The mass change in a humid environment will be zero or very minimal. Although this would be the most desirable scenario, as explained in Chapter 1 (section 1.2, Definition of moisture barrier coatings), this approach would be unattainable for a conventional coating because of the simultaneous requirement for disintegration in gastric fluids.

In mechanism III, the barrier coating can transmit all the moisture into the underlying core without holding any amount within itself. The mass change exhibited by the

sample would reflect that of the uncoated core alone. Examination of the moisture sorption data for the coated samples indicates that the samples, with the exception of those hygroscopic cores coated with Sureteric and Shin-Etsu Acoat, exhibited more or less a net reduction in the amount of moisture sorbed over the uncoated samples. This indicates that this mechanism was unlikely.

In mechanism IV, the barrier coating holds some of the moisture within itself and transmits the "excess" into the core. For this mechanism, the amount of moisture initially available for sorption into the core would be largely dependent on the characteristics of the coating, i.e., the solubility of the water in the films while the amount that permeates into the core, would then be dependent on the coating permeability. It is also possible for the core to act as a wick, pulling the moisture into itself depending on which of the two specimens (i.e., the core or the coating) had the greater hygroscopicity. It is most probable that this was the main mechanism in operation. The question now is, what aspect of this mechanism is rate-limiting? Crucially, what determines whether the coated sample achieves a net reduction in the amount of moisture sorbed over the uncoated core? Both aspects are crucial in understanding the performance of the barrier films.

From the analysis of all the sorption-desorption patterns exhibited by the coated hygroscopic, non-hygroscopic and waxy tablet cores, it would appear that the "secret" perhaps lies in the relative differences in the hydrophilicity/hygroscopicity of the applied coating and that of the underlying tablet core. Thus, where the applied film coating was the more hydrophilic/hygroscopic specimen compared to the underlying core, there was observed no net reduction in the extent of sorption. The applied coating was the rate-limiting factor. Here, once the film became saturated with moisture (i.e., maximum uptake), there was nothing to stop the underlying core also becoming saturated with moisture. The net result was that the total amount taken up by the coated sample was a sum total of that taken by the film and the core. This scenario was what was seen in coated non-hygroscopic and waxy cores, as well as the hygroscopic cores coated with Sureteric and Shin-Etsu Acoat. On the other hand, where the applied film was the less hydrophilic/hygroscopic specimen, there was observed a net reduction in the extent of sorption because the tablet core was now the determinant factor influencing the sorption process. For this scenario, the core acted as a wick, pulling the moisture from the applied film into the core.

To understand what determined why only the coated hygroscopic samples achieved a net reduction in the extent of water taken up, a fundamental understanding of the

phenomenon of equilibration is necessary. The reason is that when the coated samples were investigated under prolonged exposure to moisture, that was when the coated hygroscopic cores were clearly observed to achieve a net reduction. Moreover, a net reduction in the extent of sorption was seen after equilibration had been attained. Thus, from the knowledge that under equilibrium sorption, no net exchange of moisture with its environment takes place, and that from the definition of this state, the equilibrium relative vapour pressure generated by the moisture within the product (referred to as the water activity) must equal that of the environment (the water activity, of course, reflects the part of the moisture that can be exchanged between the product and the environment or another specimen) it can be speculated that the observed reduction in the extent of sorption reflected how quickly the water activity within the specimens was able to equilibrate with that of the immediate environment. With the applied film coating making immediate contact with the environment, it was, perhaps, the free water within the film coatings that contributed to the attainment of this equilibration.

If the above theory was the case, it should be possible to correlate the free water content of a given film sample with equilibration kinetics and the ability to achieve a net reduction in the extent of sorption. That is to say, polymer films with a higher binding capacity (less free water) would achieve a less net reduction in the extent of sorption over the uncoated samples than films with less binding capacity (greater free water). This is because in the former category, the underlying core would be given greater opportunity to continue sorbing moisture because there was a less proportion of free water in this sample to contribute towards equilibration, while in the film samples with a greater proportion of free water, the equilibration with the environment would be relatively rapid. Confirmation of this theory is provided by the equilibrium sorption data in section 4.4.4 where it can be seen that the Sepifilm LP coated samples (less free water, higher moisture binding capacity) were able to achieve the least reduction in the extent of sorption over the uncoated samples, while the methacrylate coated samples (more free water, less binding capacity) achieved a greater reduction in the amount of moisture sorbed over the uncoated tablet core.

4.5.5.2 Relationship Between Dissolution and Moisture Sorption

The relationship between uptake of and dissolution in liquid water and moisture vapour for moisture barrier coatings was investigated to determine how the two phenomena might be related and also, how one affects the other. The following findings were made in respect to the performance of the samples:

For the Opadry AMB coating: this coating, from the evidence of the dissolution data, was of the highly soluble category, indicating, perhaps a greater permeability of the liquid form of water. However, the same coating exhibited low water vapour permeability (8.128×10^{-7} [cm³ (STP) cm/cm².s. cmHg, 0-90 % RH gradient/25 °C). The low water vapour permeability for this membrane was attributed to intermediate-to-low water solubility and a low diffusion coefficient. It was speculated that this outcome was a physically moderated barrier action, perhaps arising from the presence of crystalline regions in the membrane or possibly a more taut film structure due to polymer interpenetration. Therefore, this coating could perhaps represent the nearest to what an ideal moisture barrier coating should be, i.e., having good barrier properties to water vapour but also good solubility in liquid water.

The Eudragit EPO coating, on the hand, was not the most soluble coating, judging from the time lag exhibited during the dissolution tests. This coating also exhibited low water vapour transmission rates and permeability, which were attributed to low water solubility (from solubility coefficient data) and low diffusion coefficients. It was speculated that these attributes were related to the presence of a large proportion of hydrophobic ingredients, mainly magnesium stearate and stearic acid. This coating turned out to be the most sensitive to the presence of water (through plasticization) and temperature (conversion to rubbery state) perhaps due to a low glass transition temperature, T_g .

The Sepifilm LP coating exhibited high water vapour permeability mainly due to high water solubility even though the diffusion coefficients were generally lower due to binding of the water molecules in the membranes. For this coating, solubility and permeability to liquid water was also very high. The Eudragit L30 D-55 coating represented somewhat different behaviour: The permeability to water vapour was quite high, due to a comparatively high diffusion coefficient. The solubility to water vapour and to liquid water (from dissolution data) was, however, low.

Given the fact that the chemical potential of the vapour at unit water activity is the same as that of the liquid water, the permeability should be independent of the physical state, in which case, the equivalence of the permeability for the two water states would be the expectation. As demonstrated above, this appears to be the case for the Sepifilm LP polymer system since permeability to the liquid and vapour states of water seemed to be correlated. Further explanation in support of this line of argument is provided on the basis of the permeation mechanism outlined earlier in which molecules are required to move as individuals in order to permeate the polymer membrane. For molecules of a

liquid, this requires them to have sufficient energy to leave the liquid. At a given liquid–vapour interface at equilibrium, the number and energy distribution of molecules having sufficient energy to vaporize would be exactly equal in the two phases per unit area of interface. Thus, the liquid water and the saturated water vapour at the same temperature would be identical when only molecules capable of penetrating a polymer membrane are considered. Barrier (1968) has explained that the apparent differences between permeability of the two water states could be due to difficulties of maintaining vapour at unit activity.

On the other hand, it is perfectly possible for membranes to be water proof but still be permeable to the vapour form of water. In fact, certain silicone based membranes, for instance, are reported to be 100 % water proof to liquid water but capable of transmitting water vapour through them at the same time (Von Fraunhofer and Boxall, 1976). This example somewhat seems to mirror the behaviour exhibited by the Eudragit L30 D-55 film. For this sample, the permeability to liquid water was low while that to water vapour was high. The observed differences in permeation to liquid and vapour could be explained on the basis of the basic difference in kinetic energy of molecules in two states. Since water molecules in the liquid state have a very small kinetic energy while the same molecules in vapour form are in a constant motion at an average velocity of about 450 m/s (Nivedita et al., 2004), the high velocity of the vapour can lead to the penetration across the molecular gaps in films to be several orders of magnitude more than the liquid water. Thus, considering small path length across typical polymer films, penetration of water vapour across the films would be very high. Therefore, the relatively higher mobility of water molecule in gaseous phase, compared to the existence of liquid water molecules in un-associated states due to hydrogen bonding in liquid form facilitates the transport of water vapours through the polymers.

However, as the results of the present study have demonstrated, it is possible to fabricate a membrane that possesses a low water vapour permeability but at the same time also exhibit a high liquid water permeability. This scenario was exemplified by the Opadry AMB film system. On the other hand, a membrane with high permeability to water vapour permeability while also having a low permeability to liquid water is also possible, as exemplified by the Eudragit L30 D-55 film. These characteristics, as demonstrated above, were mainly dependent on the chemical and physical characteristics of the membranes in question, rather than difficulties in experimentally measuring the permeability, or differences in the kinetic energies of the water molecules in the two states, as suggested by Barrier (1968) above.

4.6 CONCLUSIONS

4.6.1 Introduction

The work undertaken in this chapter aimed to study the sorption-desorption characteristics of uncoated and coated tablets cores of dissimilar hygroscopicity. Samples were subjected to three sorption-desorption test regimes in which the RH was varied between 0 and 50, 75 or 90 % RH. In addition, the dissolution test was applied to the coated cores to understand the relationship between moisture sorption and hydration properties of the films.

4.6.2 Effect of Tablet Core Hygroscopicity on Sorption-Desorption

Uncoated and coated hygroscopic cores sorbed more moisture than the corresponding Waxy cores which in turn showed differences over the non-hygroscopic cores. In addition, hygroscopic cores exhibited an exponential rise in mass and did not attain equilibration in the 300 min exposure time. Desorption for these cores was characteristically slow. In comparison, uncoated and coated waxy and non-hygroscopic cores equilibrated and also returned to the dry mass much more rapidly than the hygroscopic cores.

Coated hygroscopic cores, with the exception of those coated with the Sureteric or the Shin-Etsu Aqoat, achieved a net reduction in the amount of moisture sorbed over the uncoated core. The Eudragit EPO coated sample was the least hygroscopic. This sample achieved the highest net reduction in the amount of moisture sorbed by the samples. The hygroscopicity of the other samples ranked as follows: the Eudragit L30 D-55 coated sample < Opadry AMB coated sample ≤ the Sureteric coated sample < the Sepifilm LP coated sample << the Shin-Etsu Aqoat coated sample. Therefore, in terms of the rate and extent of water transfer from the environment, the data obtained showed that application of a moisture barrier coating to the hygroscopic was beneficial.

Coated waxy and non-hygroscopic cores did not achieve a net reduction in the amount of moisture sorbed. From the sorption-desorption profiles, the total sorption was close to being the sum total of the amount of moisture sorbed by the free film and the core. Thus, application of a moisture barrier to the non-hygroscopic and waxy cores did not appear to be beneficial. Under extended sorption regimes, the moisture sorption characteristics of coated hygroscopic cores under equilibrium test conditions were slightly different from those obtained under fixed-time sorption regimes. Thus, the least sorbing sample was the Eudragit EPO coated cores closely followed by the Opadry AMB and the Eudragit L30 D-55 coated samples. The most hygroscopic coated sample

was the Sepifilm LP coated sample. All coated samples achieved an overall net reduction in the amounts of moisture taken over the uncoated core. The amounts of moisture sorbed varied between 60 and 90 % of that taken-up by the uncoated hygroscopic cores.

4.6.3 Effect of Increasing Weight Gain on Moisture Sorption-Desorption and Dissolution Characteristics

Increasing the thickness of the coating produced a very mixed picture. In the first category, i.e., Sepifilm LP and Shin-Etsu Acoat coated cores, the effect of increasing the weight gain was a decrease in the amount of moisture taken up. It was speculated that a thicker coating increased the diffusion path, which resulted in less moisture reaching the core. In the second category (Eudragit EPO, Eudragit L30 D-55 and Sureteric coated cores) increasing the thickness of the coating first resulted in a net reduction of sorption, but a further increase in the thickness of the core resulted in an increase of the extent of sorption above the amounts achieved by samples coated at the minimum and intermediate levels. The last category was exemplified by the Opadry AMB coated samples for which an increase in the thickness of the coating resulted in a progressive increase in the extent of sorption.

The effect of weight gain increase on dissolution of the cores coated at increasing weight gains was, however, straightforward as all the studied samples showed nearly similar trends. For the cores to which was applied pH-independent coatings [Opadry AMB and Sepifilm LP], the effect of increasing the weight gain was a marginal increase in the lag time for dissolution. For all other samples, increase in weight gain resulted in a major delay in initializing dissolution. The longest delay was seen with Sureteric.

4.6.4 Distribution of Water Between the Core and the Coating

The data obtained suggested that the factor which determined whether the coated samples attained equilibration was the difference in the hygroscopicity/hydrophilicity of the core and the coating applied on the core. Thus, in those samples where the core was the more hygroscopic specimen compared to the applied film, equilibration was attained much more slowly and a net reduction in the extent of sorption was achieved. For samples in which the applied coating was the more hygroscopic specimen, the coated sample achieved equilibration rapidly and no net reduction in the extent of sorption was recorded.

CHAPTER 5

Chapter 5

5.0 ASPIRIN HYDROLYSIS IN TABLET CORES OF DISSIMILAR HYGROSCOPICITY

Outline

- 5.1 Introduction
 - 5.2 Study Objective
 - 5.3 Experimental Methodology
 - 5.4 Results and Discussion
 - 5.5 Discussion and Conclusions
-

5.1 INTRODUCTION

For some tablet formulations, sorption of moisture from the environment is undesirable. This is because of the potential for physical and/or chemical instability. Chemical instability is perhaps the most undesirable outcome for a drug product taking up moisture. This is mainly because the underlying processes accompanying chemical instability are often irreversible, and may result into production of by-products that are toxic or therapeutically inactive (Ahlneck and Zografis, 1990; Wu and Fassih, 2005).

Chemical-related decomposition of drug molecules may be effected via a number of pathways. These include hydrolysis, oxidation, reduction, photolysis, deamidation, racemization, isomerization, etc. Of these pathways, hydrolysis is probably the most important. This process usually involves the breakage of bonds, mainly an ester or an amide bond, when the drug molecules react with water.

In most solid dosage forms, including tablets, the active drug substance is present in a smaller proportion compared to the excipients. Thus, the excipients can play a key role in influencing the amount of water sorbed and therefore the stability profile of the drug product. This aspect was clearly demonstrated in the previous chapter (Chapter 4). For instance, differences in the extents of sorption of different excipients were seen. In the same chapter, it was also shown that moisture barrier coatings can reduce the amount of water sorbed into certain formulations. The challenge, therefore, of moisture barrier coatings is to demonstrate stability of a moisture sensitive drug substance under conditions of high humidity. Of interest is how the sorption and permeability data of the moisture barrier coatings relate to the stability profile of a moisture sensitive drug substance formulated in the tablet cores. The other issue of interest relates to viability of applying the coatings using the aqueous film coating process, given the typically high humidity and temperatures that exist in the coating chamber.

A method where by dry powder is layered onto pellets has been reported as a viable alternative to conventional coating methods (Cerea et al., 2004). Whether this approach could be used in combination with a moisture barrier coating to minimise the effect of atmospheric moisture requires to be investigated.

5.2 SPECIFIC OBJECTIVES

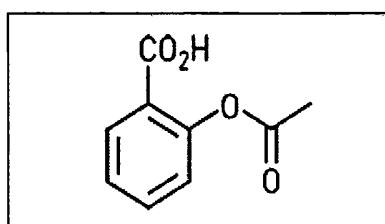
The main aim of the work presented in this chapter was to investigate the relationship between moisture sorption and stability of a moisture sensitive compound formulated in uncoated and coated tablet cores of dissimilar hygroscopicity (details of which were described in Chapter 4). Two tablet core formulation systems were studied, i.e.: (i) conventional tablet cores, which were subsequently coated with moisture barrier coatings, and (ii) powder-layered (by compression) hygroscopic cores consisting of powder coated cores to which moisture barrier coatings were subsequently applied. Aspirin, a classic moisture sensitive compound, was the model drug chosen for study. Thus, aspirin hydrolysis in the aforementioned cores was quantitatively determined following exposure to conditions of high humidity. The goal was to establish the viability of applying a moisture barrier coating onto a core of a moisture sensitive compound and the effectiveness of such a system in reducing the chemical instability of a model moisture sensitive compound.

5.3 MATERIALS AND METHODS

5.3.1 Materials

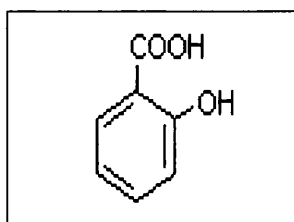
5.3.1.1 Aspirin

Aspirin (*O*-Acetoxybenzoic acid, formula $C_6H_4(OCOCH_3)CO_2H$, molecular weight 180.2, see chemical structure below) occurs mainly as a white crystalline solid or granular powder. It is freely soluble in water and ethanol. In the solid state, aspirin is stable, it undergoes hydrolysis in the presence of moisture to produce acetic acid and salicylic acid (Leeson and Mattocks, 1958; Carstensen and Attarchi, 1988). The material used in this work was Aspirin USP grade (Lot 30K0935) and was of a crystalline type. It was purchased from Sigma Aldrich Co.



5.3.1.2 Salicylic acid

Salicylic acid ($C_6H_4(OH)CO_2H$, 2-hydroxybenzoic acid, m.w. 138.1, see chemical structure below) is a fine white or colourless powder or crystalline solid. As mentioned above, it is a by-product of aspirin hydrolysis although this is not necessarily the method by which it is produced commercially. It is slightly soluble in water. It has a melting point of 159 °C and sublimates readily at ≤ 76 °C (Gore et al., 1968). Salicylic acid (Lot 60K0127), used in this study as a standard, was purchased from Sigma Aldrich.



5.3.1.3 Reagents and Solvents

A list of solvents, reagents and other miscellaneous materials used in this study is shown below:

Solvents:

1. Acetonitrile, HPLC Grade, Lot No. 0417304, purchased from Fisher Scientific, Loughborough, UK.
2. Distilled Water, HPLC Grade, Lot No. 0552202, purchased from Fisher Scientific, Loughborough, UK.
3. Methanol, HPLC Grade, Lot No. 0380995, purchased from Fisher Scientific, Loughborough, UK.

Chemical Reagents

1. Phosphoric acid 85% w/w, HPLC Grade, Lot No. A017945901, purchased from Fisher Scientific, Loughborough, UK.
2. Phosphorus pentoxide, Extra Pure, Batch No. 13190, purchased from Sigma Aldrich, Inc., St. Louis, MO, USA.
3. Sodium chloride, Analar, Batch No. K264781330939, purchased from BDH Laboratory Supplies, Poole, UK.

Consumables

1. HPLC Column (Zorbax Eclipse XDB –C8 46x150 mm, 5 μ m), Lot. No. B03082, from Agilent Inc., USA.

5.3.2. Methods

5.3.2.1 Manufacture and Coating of Conventional Tablet Cores

Conventional aspirin tablets were prepared by the direct compression technique. The procedure for preparing and testing these tablets was similar to the one described for neat cores (in Chapter 4). Details of the formulations used in the manufacture of the tablet cores are shown in Table 5-1 below. Stearic acid was the lubricant used in the place of magnesium stearate to prevent the interaction with the aspirin.

Ingredient	Quantity in Tablet (%)		
	Hygroscopic cores	Non-hygroscopic cores	Waxy cores
Aspirin	30.0	30.0	30.0
Lactose monohydrate	44.4	-	43.0
Pre-gelatinised maize starch	15.0	-	-
Microcrystalline cellulose	15.0	-	-
Dicalcium phosphate	-	64.5	-
Talc	-	-	3.0
Carnauba wax	-	-	14.0
Colloidal silicone dioxide	0.1	-	1.0
Stearic acid	0.5	0.5	4.0
Total	100.0	100.0	100.0

Table 5-1. Details for Aspirin Tablet Core Formulations

As much as was possible, the aspirin tablet cores prepared for this study were made to be similar in weight and dimensions as the non-drug loaded tablet cores used in Chapter 4. Thus, the target tablet weight was 200 mg for hygroscopic and waxy tablets, and 250 mg for non-hygroscopic tablets. Tests to determine the thickness, diameter, breaking force, and friability of the manufactured tablets were subsequently undertaken similarly as previously described in Chapter 4.

Before coating was undertaken, tablet cores were first dried in a vacuum oven at 40 °C for 6 hr. This step was taken for the purpose of driving off any loose moisture from the tablet cores. The procedure for coating and evaluating the tablets was the same as that described in Chapter 4. The coating levels were in keeping with the minimum recommended levels required for moisture protection, reference to which was also made in the same chapter. After coating, the tablet cores were placed into amber coloured glass bottles, tightly sealed and stored in an air tight desiccator over phosphorus pentoxide until required at a later time.

5.3.2.2 Manufacture and Coating of Powder-Layered Tablet Cores

Powder-layered tablet cores were based on the hygroscopic formulation. The inner cores (average weight 200 mg) consisted of aspirin (60 mg), lactose (78.8 mg), microcrystalline cellulose (30 mg), starch (30 mg), colloidal silicone dioxide (0.2 mg) and magnesium stearate (1.0 mg). Tablets were prepared by compressing the powders using 7.0 mm round, standard flat-faced punches on a Manesty eccentric tablet press. The target thickness was 3.50 mm. The breaking force strength was 150-200 N.

The obtained cores were subsequently powder coated (by compression) with a separate non-drug loaded formulation consisting of lactose (69.4% w/w), microcrystalline cellulose (MCC, 15 % w/w), starch (15 % w/w), colloidal silicone dioxide (0.1 % w/w) and magnesium stearate (0.5 % w/w). The procedure was as follows: half the quantity of the powder coating material for each individual tablet was placed into the die cavity using a spatula. The pre-formed tablet core was then carefully positioned in the centre of the die cavity on top of the powder using a pair of tweezers. The remaining half of the coating material was then added. The powder coating material plus the embedded tablet core were then compressed. Further tests such as weight variation, crushing strength, friability, and thickness were subsequently performed on the obtained tablet cores. Coating of the tablet cores was undertaken in a fluidized bed with Eudragit L30 D-55, aminomethacrylate, Opadry AMB, and Sepifilm LP polymer coatings in the same way as described for the conventional cores. The coating levels were in keeping with the recommended minimum levels required for moisture protection.

5.3.2.3 Stability Testing Conditions and Sampling

The International Conference on Harmonization (ICH Q1A) Guideline lists three main conditions by which stability of pharmaceutical products may be evaluated, i.e.: (i) long-term conditions: 25 °C at 60 % RH for 12 months; (ii) intermediate conditions: 30 °C at 65 % RH for 6 months, and (iii) accelerated conditions: 40 °C at 75 % RH for 6 months (ICH Steering Committee, 1998). For this work, however, the following conditions were utilised, i.e., 75 % RH/25 °C. All samples were exposed for a total period of three months. The reason for adopting a lower temperature of 25 °C as opposed to 40 °C was to minimise the effect/contribution of temperature on the decomposition of aspirin. This allowed the investigation of moisture-related effects alone. Temperature stability was provided by a Gallenkamp thermostatted incubator Type 100-230E (Sanyo Gallenkamp, Loughborough, UK). The required relative humidity conditions were provided by sodium chloride salt slurries in glass desiccators (Nyqvist, 1983).

Desiccators were first cleaned and allowed to dry before use. Saturated salt slurries were prepared by taking an excess quantity of sodium chloride and dissolving it in hot water (with a temperature of about 65 °C). Once the sodium chloride dissolved, a generous amount of additional sodium chloride was again added to the solution. The obtained slurry was then allowed to cool to room temperature and subsequently transferred to the desiccator. Desiccators were validated by (i) measuring the relative humidity inside the desiccator using a digital hygrometer, and (ii) monitoring the weight of empty pre-labelled glass containers placed in the desiccators for a period of two weeks. The desiccator RH was established as 74.8 per cent, while the weight gain of non-sample loaded containers was found to be < 0.1 per cent.

In total, 21 samples, each containing 80 tablets randomly picked from each of the three uncoated and coated hygroscopic, low hygroscopic and waxy formulations, were placed into tared pre-labelled open glass containers (150 ml capacity). After the weight of the tablets was recorded, the containers were topped with loose cotton wool to prevent condensation making direct contact with the tablets (while in the incubators). The samples were then placed into the desiccators prepared as described above and subsequently transferred into the incubators maintained at constant temperature (25 °C or 40 °C). Tablets were sampled on day 0, 7, 14, 30, 60, and 90 to determine weight gain due to sorption. For each time point, ten tablets were removed for analysis.

5.3.2.4 Assay Method

5.3.2.4.1 Sample preparation

Samples for analysis by HPLC were prepared by taking five tablets from a given batch and carefully grinding them in a clean and dry glass mortar with the aid of a dedicated pestle. Thereafter, about 40 ml of the extraction solvent [comprising acetonitrile-methanol-phosphoric acid (92:8: 0.5)] was added to the powdered material in the mortar. The resulting mixture was transferred into a dry 100 ml volumetric flask and made to volume with the extraction solvent. The flask was subsequently sonicated for a further 10 minutes at 25 °C. The flask was then quickly removed from the bath, shaken briefly and a portion of the mixture (about 40 ml) transferred into a clean glass centrifuge tube. Centrifugation of the contents was then undertaken at 10000 rpm for 10 minutes at 5.0 °C. The centrifuge tubes (+ contents) were removed from the equipment whereupon 5 ml of the supernatant was removed with a clean 10 ml syringe. This solution was transferred into 2 ml glass vial via a 0.45 µm Nylon Acrodisc syringe filter (Pall Gelman Sciences Corporation, MI, USA).

5.3.2.4.2 Sample analysis

Samples were assayed for aspirin and salicylic acid content using a previously validated reverse phase/isocratic HPLC method (Fogel et al, 1984). The equipment consisted of an integrated HP 1050 Series HPLC system comprising an HP 1050 autosampler, set at 10 μ l, an HP 1050 pump and an HP1050 multiple wavelength detector system. The detector was interfaced with a pc with PC/Chrome Software (H & A Scientific Inc., Greenville, NC, USA).

5.3.2.4.3 Chromatographic conditions

The mobile phase consisted of water-acetonitrile-phosphoric acid (75:25:05) filtered through a 0.45- μ m GHP HPLC mobile phase filtration membrane (Pall Gelman Sciences Corporation, Ann Arbo, MI, USA) prior to use. The chromatographic column was an Agilent Zorbax Exclipse XDB-C8 46x150 mm, 5 μ m internal phase (Agilent Technologies, supplied by Hichrome Limited, Theale, Berks, UK). Other details were: Injection Volume: 10 μ l; Flow Rate: 1.5 mL/min; Maximum Run Time: 14.0 min; Assay wavelength: 295 nm; Pressure: 2 bar; and Column temperature 40 °C.

5.3.2.4.4 Calibration of HPLC assay method

A stock solution was prepared by dissolving 2.0000 g of pure aspirin (i.e., 20 mg/ml) and 0.0200 g of pure salicylic acid (i.e., 0.02 mg/ml, which was 1.0 % relative to aspirin) in 100 ml of the extracting solution. Five standard solutions containing 1.0, 1.5, 2.0, 3.0, 4.0 and 5.0 mg/ml aspirin and 0.01, 0.02, 0.03, 0.04, 0.05 mg/ml salicylic acid were then prepared from the stock solution by taking appropriate aliquots of the stock solution and diluting with the extracting solution. These standards were injected using the above conditions. From the obtained peak areas, a five-point calibration curve was obtained (See Appendix 4 for the calibration curves obtained).

5.3.2.4.4 Validation of HPLC assay method

The assay was firstly validated by spiking pure aspirin (4.0 mg/ml) with salicylic acid (0.04 mg/ml) and obtaining the chromatograms. The procedure was repeated with placebo tablet formulations which were spiked with pure aspirin (concentration range 75.0-125.0 %, equivalent to the combined "label" claim of five tablets) and pure salicylic acid (1.0-3.0 % of respective quantity of aspirin). The aspirin and salicylic acid concentrations in each sample were subsequently measured under the same conditions as above. The assay was also evaluated for specificity, accuracy, precision, detection limit, linearity and robustness.

5.3.2.5 Statistical Analysis

Differences in the experimental results were examined using either the student t-test or one-way analysis of variance (ANOVA) if there were more than two data sets. Fixed level testing was used to measure statistical significance. A p value of less than 0.05 was taken as indicative of statistical significance.

5.4 RESULTS

5.4.1 HPLC Assay Validation

HPLC assay is the method of choice in the USP for determining limits of salicylic acid, the main degradation product of aspirin, in dosage forms. The USP also recommends an HPLC methodology for quantification of aspirin and salicylic acid in a whole variety of dosage forms. However, other equally suitable methods are widely documented in the literature. To ensure robustness of the assay method, the analytical procedure must be validated for accuracy, repeatability, linearity, precision and reproducibility.

For the present study, chromatograms were recorded for pure aspirin and after spiking it with salicylic acid. The analytical wavelength of 295 nm was found to be effective and enabled the separation and detection of both aspirin and salicylic at the same sensitivity. A typical chromatogram of aspirin spiked with salicylic acid in the extraction solvent is shown in Figure 5.1 below.

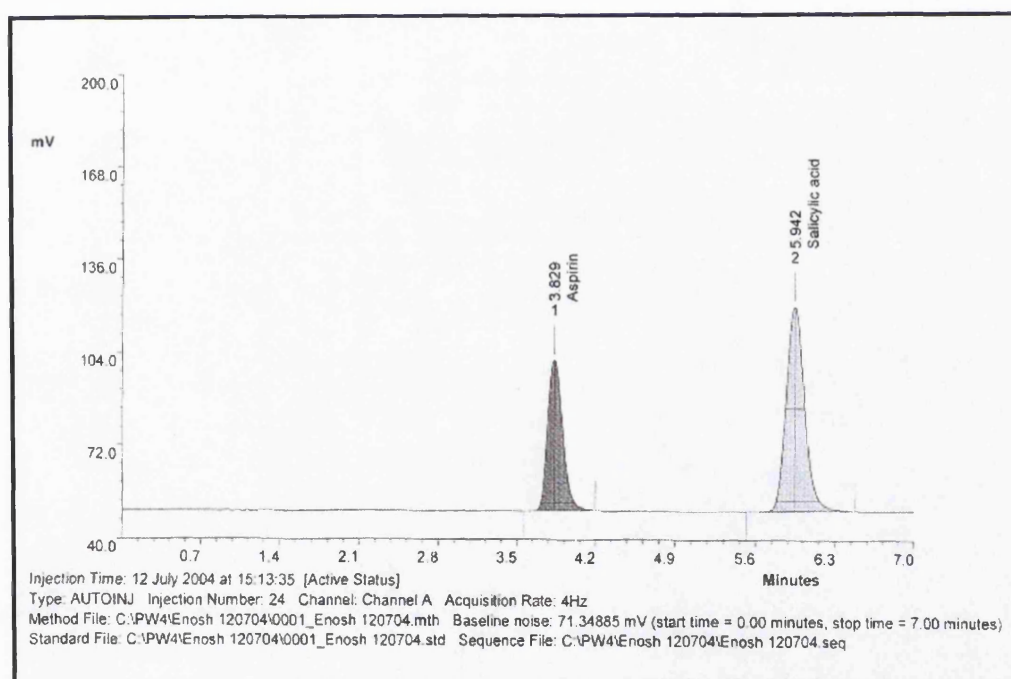


Figure 5-1. Typical Chromatograms of Aspirin and Salicylic in the Extraction Solvent

The assay produced a stable baseline with resolved peaks after approximately 3.8 min (aspirin) and 5.9 min (salicylic acid). The assay was reproducible with a typical coefficient of variation of 0.519 per cent and 0.741 per cent, respectively for aspirin and salicylic acid. Calibration curves plotted for aspirin and salicylic acid showed that the

detector response (peak area) was linear for the standards with the concentration ranges of 1.0-5.0 mg/ml of aspirin and 0.01-0.05 mg/ml of salicylic acid injected. A regression analysis of the data (n=5) resulted in a correlation coefficient of 0.9999 for aspirin and 0.9998 for salicylic acid (see Appendix 4).

The limit of detection (3 times the noise level) was 0.00393 $\mu\text{g/ml}$ for aspirin and 0.00248 $\mu\text{g/ml}$ for salicylic acid. The limit of quantitation was 0.0130 $\mu\text{g/ml}$ for aspirin and 0.0083 $\mu\text{g/ml}$ for salicylic acid (10 times the noise level). The accuracy of the assay was checked by analyzing aspirin and salicylic acid in the three formulations. A typical chromatogram for the hygroscopic formulation is shown in Figure 5-2 below.

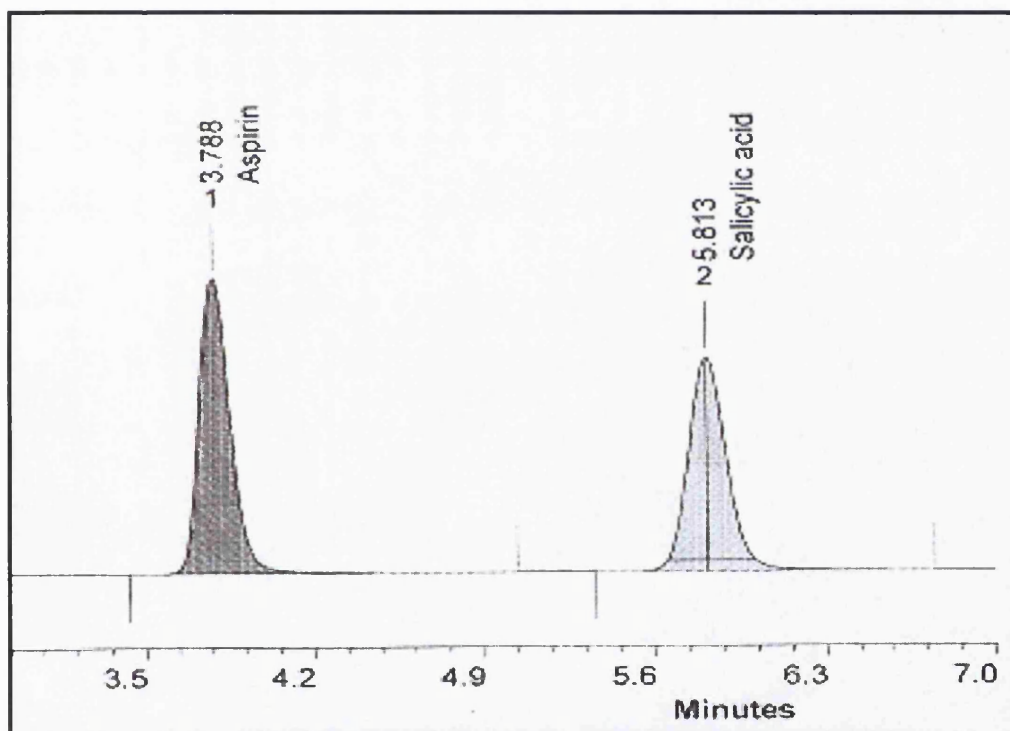


Figure 5-2. Typical Chromatograms of Aspirin and Salicylic in the Mobile Phase

It can be seen in Figure 5-2 above that the assay was specific to aspirin and salicylic acid molecules in the mobile phase. No interference between the aspirin and salicylic acid or with any other components, such as the excipients, is evident in the chromatogram at the two retention times. Furthermore, the typical mean percentage recovery was 99.78 ± 3.3 determined from hygroscopic cores.

5.4.2 Results for Conventional Tablet Cores

This section describes the results for conventional tablet cores. The term conventional here in means cores ordinarily compressed on the tablet machine, as described in section 5.3.2. The results are presented as follows, i.e., section 5.4.2.1 describes the physical characteristics while 5.4.2.2 presents the data for aspirin hydrolysis.

5.4.2.1 Physical Characteristics of Uncoated Tablet Cores

Physical characteristics of the tablet cores, i.e., mean weight and weight uniformity, tablet breaking force and friability, diameter and thickness, used in the work presented in this section were assessed as described previously (Chapter 4). The aim was to determine, respectively, dose uniformity, robustness (i.e., the ability to withstand the shock of coating), and to determine the surface area so as to ensure that the applied coatings were similar in thickness to the non-drug loaded tablet cores in Chapter 4.

The results for the physical characteristics of aspirin tablets are shown in Table 5-2 below. The tablets manufactured in this study were similar in many respects (e.g., tablet weight) to those described in Chapter 4. Also, the other measured characteristics (i.e., tablet breaking force, friability) were satisfactory.

Parameter	Hygroscopic	Non-Hygroscopic	Waxy
Mean weight (mg)	200.201	249.546	203.954
Std. dev.	3.413	1.557	3.332
RSD (%)	1.126	1.115	0.956
Diameter (mm)	7.005	7.108	6.996
Thickness (mm)	3.581	3.625	3.602
Breaking Force (N)	127.2 (3.2)	95.7 (6.6)	88.9 (5.2)
Friability (%)	0.125	0.328	0.149

Table 5-2. Physical Characteristics of Aspirin Tablets

5.4.2.2 Aspirin Hydrolysis in Uncoated Tablet Cores After Exposure to 75% RH/25 °C

The purpose of this work was to determine the extent of aspirin hydrolysis in uncoated conventional tablet cores of dissimilar hygroscopicity. The goal was to understand if the stability profiles of aspirin within these cores were correlated with the moisture sorptive characteristics exhibited by the three types of tablet core.

In this study, the assay results for the three uncoated formulations following exposure to 75 % RH/25 °C are shown in Figures 5-3 and 5-4 below. These figures show the amount of aspirin remaining in the tablets (i.e., retained strength, expressed as a percent) as well the salicylic acid generated during three months of exposure.

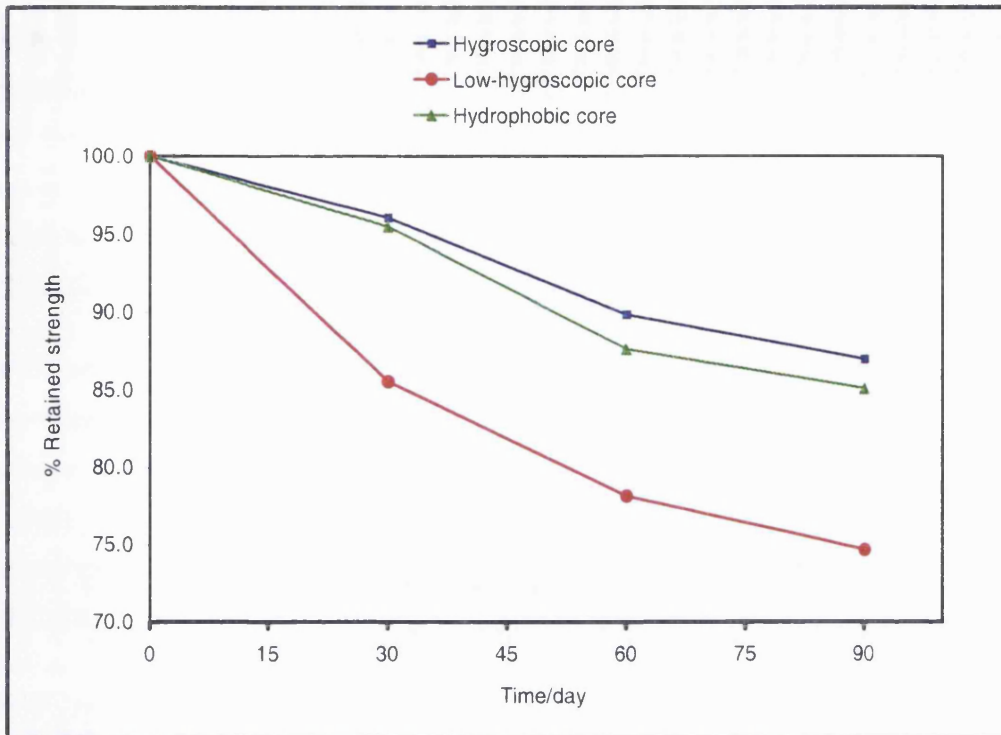


Figure 5-3. Aspirin Hydrolysis in Uncoated Hygroscopic, Non-Hygroscopic and waxy Tablet Cores exposed to 75 % RH/25 °C

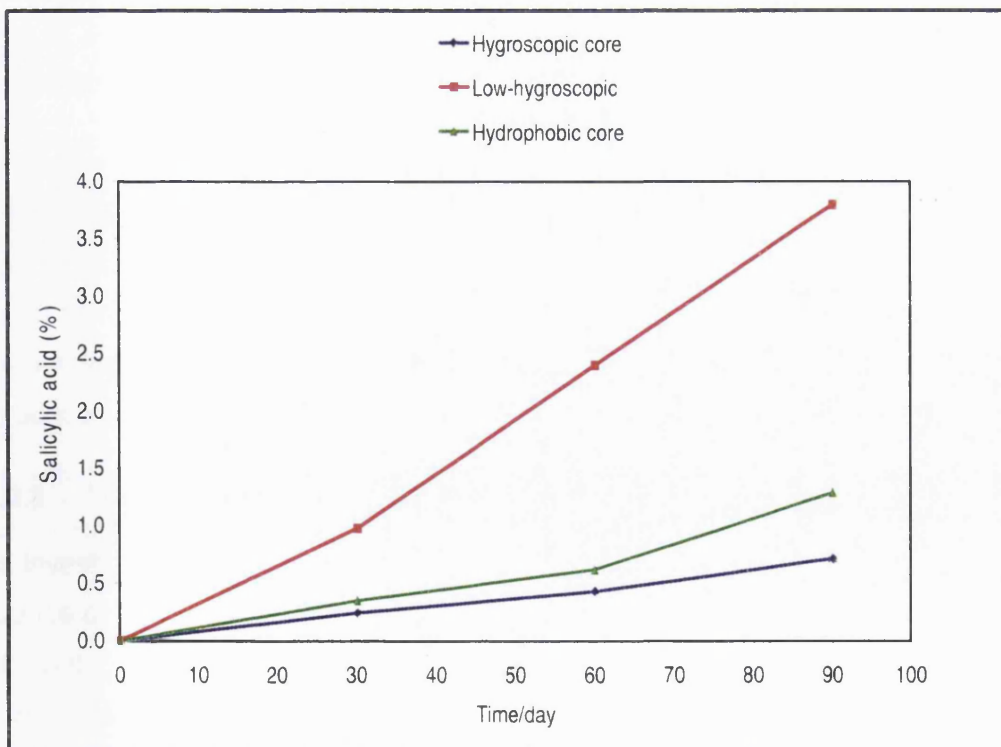


Figure 5-4. Salicylic acid Generated in Uncoated Hygroscopic, Non-Hygroscopic and Waxy Tablet Cores exposed to 75 % RH/25 °C

The non-hygroscopic cores exhibited the highest hydrolysis of aspirin (after three months, the salicylic acid=11.39 (0.561) mg/tablet) while hygroscopic cores showed the least (salicylic acid=1.421 (0.024) mg/tablet). Hydrolysis in waxy cores was only slightly higher than in the hygroscopic cores (i.e., 2.574 (0.301) mg/tablet). Tablets were also observed to have salicylic acid (whiskers) on their surfaces, presumably from the hydrolysis of aspirin. This phenomenon was observed to be highest in the non-hygroscopic cores and lowest on the hygroscopic cores.

Salicylic acid is known to undergo sublimation under ambient conditions. The fact that it was present on the surface of the tablets (in form of characteristic “whiskers”) meant that there was a possibility that the quantities of salicylic detected by the assay were less than actually generated by hydrolysis. Because of this, it was considered more accurate to monitor the extent of decomposition from the amount of aspirin remaining in the core rather than the amount of salicylic acid generated.

Another issue of interest which was noted with uncoated tablets was that the extent of aspirin hydrolysis immediately shot up in non-hygroscopic cores well before exposure to relative humidity and or temperature (i.e., at $t=0$). Although the extent of hydrolysis was still very low (typically $<0.001\%$), nevertheless, it was higher than what was observed with hygroscopic cores or waxy cores. Over the three months, however, the levels of aspirin or salicylic acid detected in uncoated tablet cores that were not exposed to the stress conditions were observed to have remained fairly constant.

In summary, the results above showed that the hygroscopic formulation exhibited the better stability profile for aspirin. This was closely followed by the waxy formulation, which in turn exhibited a better profile over the non-hygroscopic formulation. It is of interest to note that in spite of the hygroscopic formulation sorbing significantly more moisture than either the waxy or non-hygroscopic formulations, the extent of aspirin degradation was far less in the hygroscopic cores.

5.4.2.3 Coated Conventional Tablet Cores

This investigation was undertaken in order to assess two different factors, i.e., (i) the influence of the coating process on the degradation of aspirin within the three types of core, and (ii) subsequently, to determine the effectiveness of the applied moisture barrier coatings in preventing the hydrolysis of aspirin after exposure of the coated tablet cores to conditions of high humidity (i.e., 75 % RH). The results are presented below to reflect these two objectives, i.e., section 5.4.2.3.1 shows the data for the influence of coating, while 5.4.2.3.2 is for the stability data.

5.4.2.3.1 Influence of coating process on aspirin hydrolysis

In Table 5-3 below are shown results of the quantities of aspirin retained in tablet cores before and after coating with different polymers. The data reflect the average aspirin content per individual coated tablet for the three types of core.

Coating	Hygroscopic	Non-hygroscopic	Waxy
Uncoated	59.803 (0.503)	74.966 (0.297)	59.547 (0.554)
Eudragit L30 D-55	58.384 (0.245)	74.517 (0.187)	59.281 (0.066)
Eudragit EPO	59.255 (0.672)	73.726 (0.353)	58.677 (0.441)
Opadry AMB	57.541 (0.113)	72.181 (0.476)	57.798 (0.725)
Sepifilm LP	58.803 (0.455)	73.207 (0.913)	59.254 (1.211)

Table 5-3. Mean Amount of Aspirin (mg) Remaining in Tablet Cores after Coating with Different Coatings (\pm Std. Dev, n = 5)

As can be seen, the differences between the data for the uncoated samples and the coated samples were not significant. It can be stated that the data presented in Table 5-3 above do not provide the evidence to suggest that the coating process resulted in major differences in aspirin hydrolysis in the coated cores, even though the data for the Opadry AMB coated samples appear to somewhat suggest that the hydrolysis in these cores during the application of this coating may have been slightly higher. The slightly lower aspirin content in these samples probably reflects the slightly longer coating time required during the application of the Opadry AMB samples.

5.4.2.3.2 Aspirin hydrolysis in coated tablet cores after exposure to 75% RH/25 °C

The results for the assay of aspirin in samples coated with different moisture barrier coatings following exposure to 75% RH/ 25 °C are shown in Figures 5-5 through to 5-7. These figures also show the amount of aspirin remaining in the tablets (i.e., retained strength, expressed as a percent) during three months of exposure.

The role of the core formulation and, in some respects, the coating, on the extent of aspirin hydrolysis can be seen. The major point of reference appears to relate to the differences among the different core types, the effect of the type of coating and the resulting differentiation with respect to the hydrolysis obtained. It is clearly visible from the results presented in Figures 5-4, 5-5 and 5-6 that in all the uncoated tablet cores, the extent of aspirin degradation was significantly less than in the coated samples. It was the expectation that the tablet cores coated with a barrier coating would perform better than the uncoated sample. However, the results above do suggest the contrary.

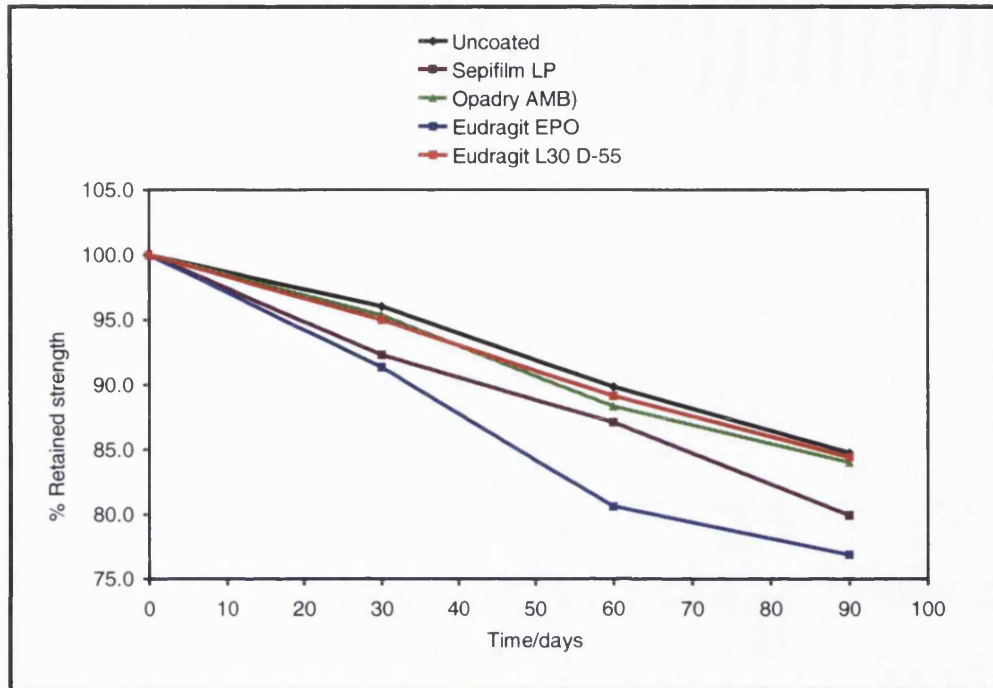


Figure 5-5. Aspirin hydrolysis in Uncoated and Coated Hygroscopic Tablet Cores Exposed to 75 % RH/25 °C for 3 Months

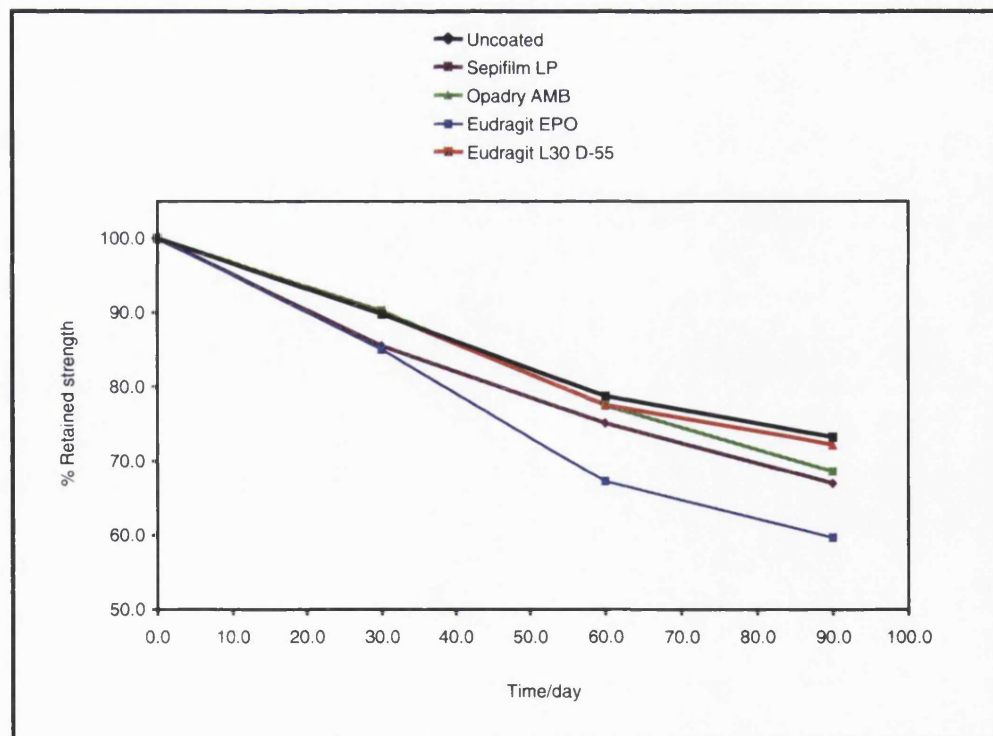


Figure 5-6. Aspirin Hydrolysis in Uncoated and Coated non-Hygroscopic Tablet Cores Exposed to 75 % RH/25 °C for 3 months

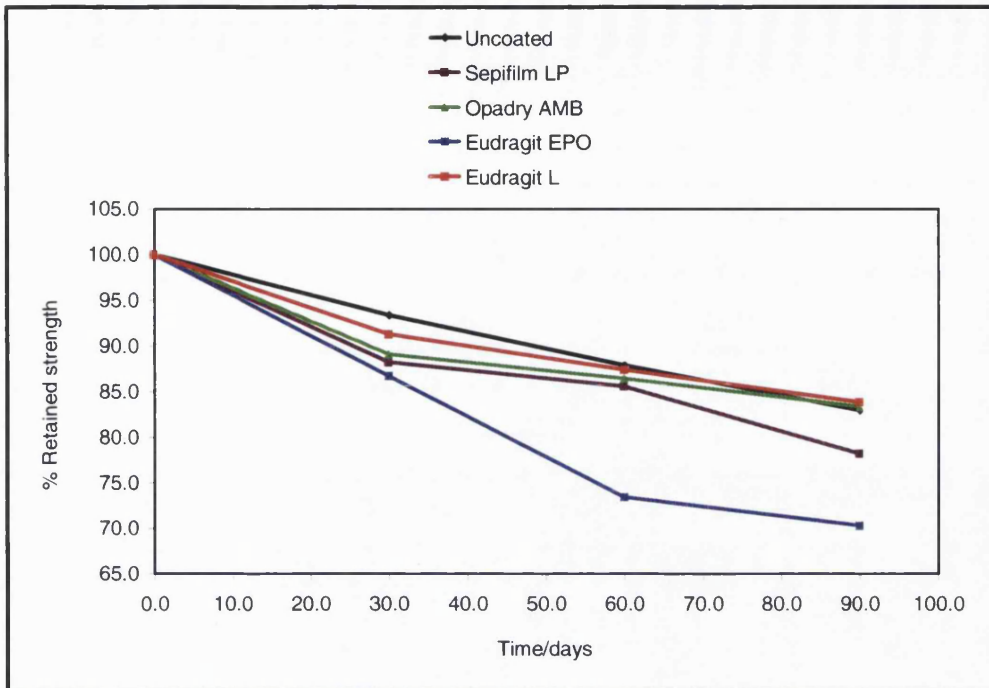


Figure 5-7. Aspirin hydrolysis in Uncoated and Coated waxy Tablet Cores exposed to 75 % RH/25 °C for three months

Also, it is of interest to note the consistently poor stability profile exhibited by the tablet cores coated with the Eudragit EPO films. In fact, it can be seen that all the three types of tablet core the extent of aspirin breakdown followed the following pattern: Uncoated cores < Eudragit L30 D-55 coated cores \leq Opadry AMB coated cores \leq Sepifilm LP coated cores \ll Eudragit EPO coated samples. The extent of aspirin degradation in all samples appeared to increase with time. Thus, initially, there was rapid hydrolysis which then gradually slowed down with time. Using an analysis of variance, the differences between the retained strength of aspirin in the uncoated and the coated samples were, on the whole, as follows: not significant ($p < 0.05$) for the differences between the uncoated tablet cores and cores coated with Eudragit L30 D-55 and the Opadry AMB films but significant ($p > 0.05$) for the Sepifilm LP and Eudragit EPO.

In summary, it was found that aspirin hydrolysis in tablet cores was significantly higher in coated samples than in the uncoated cores. Among the three core formulation types, Eudragit EPO coated samples exhibited the highest instability. The differences in the hydrolysis of aspirin among the other coated samples were not so wide in relation to the amount of water sorbed by the samples meaning that the barrier functionality of the coatings was not the important factor.

5.4.3 Powder-Layered Tablet Cores

This work was undertaken in order to investigate if the stability of aspirin within the cores, and subsequently, if the effectiveness of the applied moisture barrier coatings, could be improved by applying a separate powder coat, sandwiched between the main aspirin-loaded tablet core and the applied film coating. Details of how these cores were manufactured were presented in section 5.3.2. The results below are presented, first to describe the physical characteristics of these cores, and secondly, the extent of aspirin degradation in the powder-layered cores during the coating operation and following exposure to conditions of high humidity.

5.4.3.1 Physical Characteristics of Uncoated Powder-Layered Tablet Cores

The physical characteristics, namely, thickness, diameter, breaking force and friability, of the powder layered tablet cores are given in Table 5-4 below.

Physical property	Measurement
Mean weight (mg) (\pm std dev)	435.453 (1.569)
RSV (%)	0.360
Thickness (mm)	5.514 (0.018)
Diameter (mm)	12.028 (0.046)
Breaking force (N)	186.614 (8.013)
Friability (%)	0.655

Table 5-4. Physical Characteristics of Uncoated Powder-Layered Tablet Cores

Powder-layered tablet cores were manually manufactured by hand-rolling the tablet press. As such, it was much more difficult to ensure consistency of the obtained tablet cores. However, as the results for the weight uniformity show, the obtained cores were satisfactory. The results for tablet breaking force show that these cores were of a much stronger hardness. This result reflects, in part, the larger size of the specimen, otherwise, it was necessary to use much higher compression pressure in order for the powder coat to adequately adhere to the underlying core.

5.4.3.2 Aspirin Hydrolysis in Powder-Layered Tablet Cores Coated with Moisture Barrier Coatings and Exposed to 75 %RH/25 °C

The data shown in Table 5-5 demonstrate the effect of the coating process on aspirin hydrolysis in powder-layered tablet cores. The retained strengths of aspirin in the uncoated powder layered tablet cores and the same cores to which different moisture barrier coatings had been applied are compared.

Sample Name	Hygroscopic
Uncoated Core	59.953 (0.523)
Eudragit L30 D-55	59.117 (1.581)
Eudragit EPO	61.015 (0.576)
Opadry AMB	59.455 (0.718)
Sepifilm LP	60.003 (0.591)

Table 5-5. Mean amount of Aspirin Remaining in Powder-Layered Tablet Cores Before and after Coating with Moisture Barrier Films (\pm Std. Dev, n = 3)

Generally, the data shows that there was minimal degradation of aspirin during the coating process. Analysis of variance showed that there were no significant differences between the aspirin content in uncoated and coated tablet cores.

The data in Figure 5-8 compares the amounts of aspirin remaining in the uncoated powder layered tablet cores and the same cores to which different moisture barrier coatings had been applied following exposure to conditions of moisture stress.

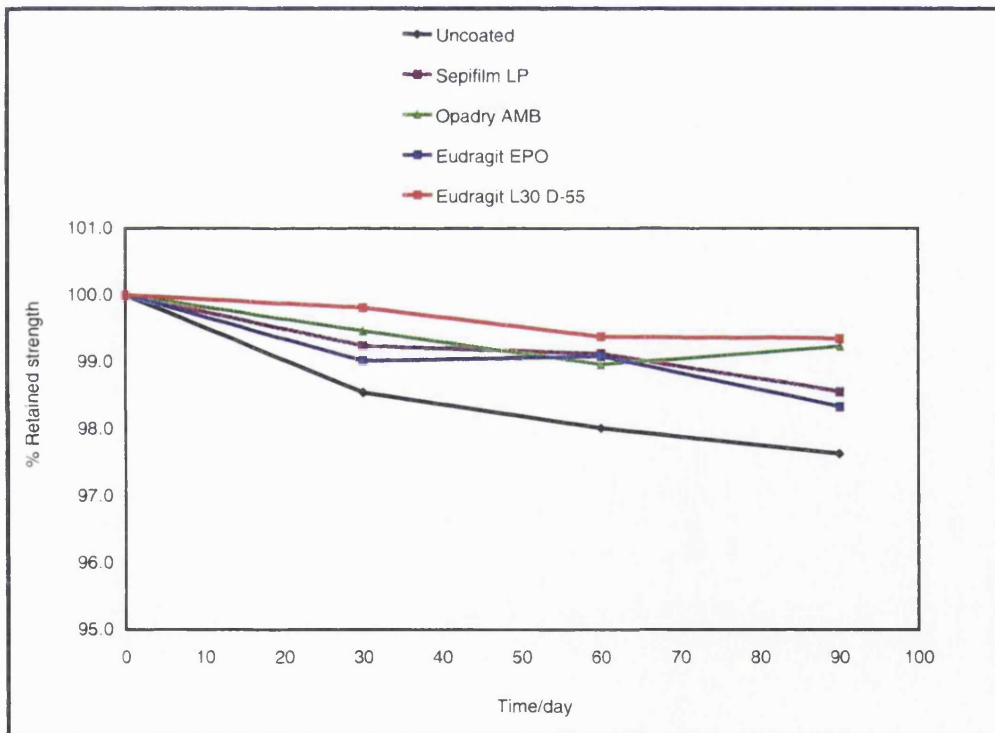


Figure 5-8. Aspirin hydrolysis in Powder-Layered Hygroscopic Tablet Cores at 75 % RH/25 °C to which Moisture Barrier Films were Applied. Samples Exposed for 3 Months

The results shown in Figure 5-7 above for the powder-layered tablet cores show that there was far less decomposition of aspirin in these cores, whether during coating or after exposure at conditions of high relative humidity. Also, the differences between the different samples coated with the moisture barrier films on one hand and the powder coated sample without a moisture barrier coating were not statistically significant. This suggests that the powder coating perhaps, enhanced the performance of the applied moisture barrier coating. Since the uncoated powder-layered cores exhibited significantly more hydrolysis compared to the same cores to which moisture barrier coatings had been applied, these results further suggest that this effect was not necessarily related to the powder layer, per se., but perhaps a combination of the moisture barrier coating and the powder layer.

5.5 DISCUSSION

5.5.1 Introduction

Aspirin is probably one of the most investigated drug molecule as far as solid state stability of drug molecules is concerned. The literature on aspirin is vast, hence quite a lot is known about the degradation pathways of this substance. For instance, it is reported that the hydrolysis of aspirin is influenced by hydrogen ions, the type and particle size of the excipient used (Ahlneck and Alderborn, 1988; Landín et al., 1994; Du and Hoag, 2000); compression pressure (Lee et al, 1965), formulation additives (Maulding and Zoglio, 1969); form of the drug (Ahlneck and Lundgren, 1985); coatings (Okhamafe and York, 1986; Ruotsalainen, 2003) as well as the storage conditions (Kornblum and Zoglio, 1967; Carstensen and Attarchi, 1988). The intention of this discussion is, therefore, to use the existing understanding to interpret the results presented in this chapter.

5.5.2 Uncoated Conventional Cores

The results of this study showed that there were major differences in the extent of aspirin hydrolysis in uncoated cores. Thus, although the hygroscopic cores sorbed the highest amounts of water, the extent of hydrolysis of aspirin was lowest with this sample. The non-hygroscopic cores exhibited the highest hydrolysis of aspirin while the extent of hydrolysis was intermediate in the Waxy samples. Thus, the amount of water sorbed was not directly correlated with the extent of aspirin decomposition.

For the majority of solid dosage forms, the active drug substance is present in smaller proportions compared to the excipients. Thus, excipients play a key role in determining the amount of water sorbed and therefore the stability profile of the product. The fact that excipients may influence the sorptive properties of a tablet core was also demonstrated in Chapter 4 of this thesis. In addition, several other studies, some of which are pointed out in the paragraph above, have demonstrated the participation of other factors. Lee et al., (1965), for instance, studied the effect of water vapour pressure, moisture sorption and tablet hardness on the stability of aspirin. The authors showed that the stability of aspirin was related to the moisture sorptive capacity and hardness of tablets. Harder tablets sorbed less moisture and exhibited better stability. This is not difficult to comprehend. The harder tablets tend to be less porous than the soft tablets, hence, the ability for moisture to penetrate into the interior is much reduced with the former than the latter. Therefore, tablet hardness can, by itself, have a significant influence on the stability of the active ingredients.

With regard to this work, on the evidence of tablet hardness alone, it is possible, on one hand, to say that tablet hardness was important since the formulation which yielded the hardest tablets also had the best stability profile. However, as this was also the same formulation that happened to sorb the greatest quantities of moisture, it cannot be concluded that a correlation between aspirin stability and tablet hardness existed since the non-hygroscopic cores, which had intermediate hardness, exhibited the worst stability profile and also sorbed the least moisture (see Table 5-6 below).

	Hygroscopic core	Non-hygroscopic core	Waxy core
% aspirin decomposition	13.016	25.321	16.123
Total moisture sorbed (%)	9.6	0.11	0.37
Mean tablet hardness (N)	127.2	95.7	88.9

Table 5-6. Aspirin Decomposition, Moisture Sorbed (at 75 % RH/25 °C) and Mean Tablet Breaking Force of Uncoated Tablet Cores

It can be stated that for tablets formulated with the same excipients, the core hardness may be an important influence. Where different excipients were used, hardness and other mitigating factors may play part in the stability profile of the active ingredient. An alternative explanation is to consider the concept of “free” and “bound” water. Water in the presence of solids is known to exist in different thermodynamic states, i.e., either in bound or solvent like state. Thus, for a solid dosage form, the total moisture sorbed in the core is a combination of free water and bound water. The former species exists in an unbound or loosely bound state, while the latter is tightly bound, either (i) as hydrate in the crystalline structure, (ii) hydrogen-bonded to polar groups, or (iii) entrapped within the amorphous structure of the constituent excipients. Bound water does not participate in reactions, like hydrolysis whereas free water is highly mobile and is available for chemical reactions (Adamson, 1982; Zografi, 1988).

Carstensen (1988), Zografi and Kontny (1988) and Zografi (1988) explained that it was the availability of “free water” and the rate at which the water activity of the dosage form reached the humidity of the environment that were the determining factors for solid state drug stability, rather than simply the total moisture sorbed. Thus, solids which equilibrated rapidly with the RH were observed to exhibit a poor stability profile than those which took a longer time to attain equilibrium. In accordance with the Leeson and Mattocks model (Leeson and Mattocks 1958) the drug hydrolysis reaction is understood to take place with water molecules loosely bound on the surface of the drug

crystals. These water molecules, behave like bulk liquid water, and have the ability to solubilize drug molecules (Carstensen, 1988).

With regard to the above results, therefore, it can be speculated that the sorbed moisture in the hygroscopic formulation was able to interact with the polar groups of starch and microcrystalline cellulose through hydrogen bonding rendering a greater proportion of the sorbed water to be in bound form. The non-hygroscopic formulation, in contrast, had little binding capability and most of the sorbed moisture, even though considerably much less, was in the form of free water capable of hydrolysing aspirin. This could account for the lower hydrolysis that was observed in the hygroscopic cores than in the non-hygroscopic formulation. The better than expected stability observed with the waxy formulation could be attributed to the presence of colloidal silicone dioxide, which, as well as being used as a glidant, is also a well known water adsorbent. Its inclusion in this formulation might have restricted the availability of free water leading to better than expected stability of aspirin.

5.5.3 Application of Moisture Barrier Coatings

This aspect of this study was done to enable a comparison of the performance of the different moisture barrier coatings following application onto cores of different hygroscopicity. As mentioned earlier, the challenge of a barrier coating is to prevent moisture sorption into the core and offer protection to those active substances that are hydrolysed by water. The expectation, therefore, was that for a given formulation, the coated cores would demonstrate less hydrolysis than their uncoated equivalents.

To recap the results, it was established that application of a moisture barrier coating did not enhance the stability of aspirin in the tablet cores. However, by sandwiching a powder layer between the inner drug-loaded tablet core and the film coating, it was found that the extent of aspirin hydrolysis was much curtailed. Significantly, the differences in the hydrolysis of aspirin among the coated samples were not so wide in relation to the amount of water sorbed by the samples meaning that the barrier functionality of the coatings was not the important factor. Thus, the results for the conventional tablet cores were clearly unexpected.

For a molecule as widely investigated (that is, as far as moisture related instability is concerned) as aspirin is, it is surprising that the literature on the hydrolysis of aspirin in coated tablets is very limited. Survey of the current pharmaceutical literature on this subject did not yield any studies which were undertaken to compare the stability of aspirin in uncoated and coated tablets. It is inconceivable, nevertheless, that the

present study is the first of its kind that has specifically looked at this problem. This somewhat makes it difficult to rationalise the present results with what is already known or what is to be expected from the perspective of the protective function of moisture barrier coatings.

The closest reported analogy to the present work is the study by Canefe and Duman (1993), who investigated the stability of aspirin and ascorbic acid in coated micropellets. The authors reported higher degradation in coated micropellets than in the uncoated samples. It was suggested that the unusual result was due to, what the authors called, microhumidity, in the coated samples. Otherwise, the work of Plaizier and De Neve (1993) avoids the direct comparison between the uncoated and coated samples, preferring, in stead, to concentrate on deterioration in the physical parameters, such as hardness and disintegration. Other than these two specific reports, there does not appear any other reported work relating to the decomposition of aspirin in coated tablet cores.

The “microhumidity” hypothesis proposed by Canefe and Duman is an interesting proposition that deserves further examination. There is a genuine chance that moisture can be trapped inside the tablet core by the applied film coating. It is not incomprehensible to see why the moisture barrier coating should not restrict the escape of moisture from within the core in the same way as it restricts the entry of moisture from the external environment. This matter was therefore investigated by subjecting the aspirin tablet cores to a slightly different regime. First, the uncoated tablet cores were thoroughly dried at 40 °C (under vacuum 1000mbar, 6 hrs) before application of the moisture barrier coatings. After coating, the tablets were again dried under the same conditions. These steps were undertaken to minimise the chances of moisture being trapped into the tablet cores before exposure to high humidity. The tablet cores were then exposed to a slightly different temperature regime consisting 40 °C/75 % RH for one month. It was anticipated that the higher temperature should further prevent the trapping of moisture in the tablet cores by facilitating “evaporation”.

The results (not shown) revealed similar patterns in the decomposition of aspirin to those obtained at 25 °C/75 % RH, namely, there was lower aspirin decomposition in uncoated samples and higher decomposition in coated samples. Thus, it was shown that the idea of “microhumidity” was probably not valid. Also, given the relatively high permeability of the moisture barrier coatings, and also from consideration of the moisture sorption-desorption profiles (data presented in Chapter 4) of the tablet cores, it can be inferred that although the coated tablet cores were capable of retaining

moisture within themselves, the resulting hysteresis was not a result of the barrier coatings stopping the escape of the sorbed water but perhaps entrapment or repacking of the cores in response to the moisture. Furthermore, for a system that has equilibrated with the external relative humidity, there is no reason to expect that some of the free water molecules within one part of this system (the core) would have limited mobility while others (in the film) would be free to escape. Clearly, the results obtained above should be due to some other factors, hitherto not reported.

It is widely reported that the adhesion of coatings is decreased when the coated samples take up moisture (e.g., Okhamafe and York, 1986). This would be expected given the fact that the sorbed moisture would be capable of distorting the bonding between the coating and the core. It is possible to assume that the results, whereby the coated samples exhibited higher hydrolysis than the uncoated samples, were perhaps related to the boundary between the coating- and the tablet core. This is schematically illustrated in Figure 5-9 below showing the coating and the core.

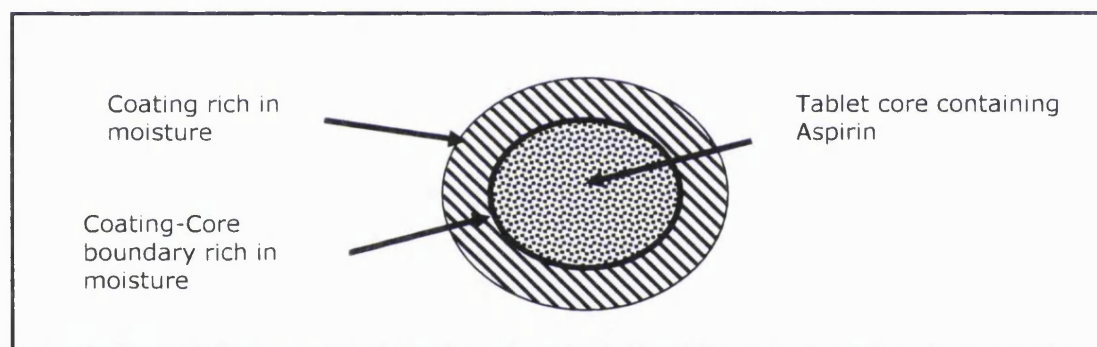


Figure 5-9. Schematic Diagram Illustrating the Coating-Core Boundary where Aspirin Hydrolysis Possibly Takes Place

As demonstrated in the previous chapters, the moisture barrier coatings utilised were not water proof structures. On interaction with moisture, it is possible that a portion of the moisture taken up by coated samples probably became trapped at the core-coating boundary forming a film of water. Such a scenario could result from a possible destruction of the adhesion of the coating to the core by the same sorbed moisture, a phenomenon that is well documented (Klages et al., 1996; Barranco et al., 2004). Thus, this boundary film, representing a region rich in moisture, could have been the region where the aspirin molecules were degraded. The extent of the hydrolysis in this film could have depended on the availability of free, unbound water in the coating capable of diffusing into this boundary film. Thus, if this was the case, a differentiation

in the extent of aspirin hydrolysis would emerge interrelated with amount of free water in the coatings as well as the decrease in the adhesion to the cores.

It can be seen that, to an extent, the speculations above are roughly consistent with the thermogravimetric analysis (TGA) data obtained in Chapter 2. The adhesion hypothesis is supported further by the data obtained from applying a separate powder layer between the inner core and applied moisture barrier coating where an improvement in the stability profile of the cores was observed. This suggests that the powder coating prevented the direct contact of the drug loaded core with water during the coating operation. When exposed to high humidity, the loose water molecules which would have come from the polymer film coating, were no longer available to make direct contact with the inner core as was the case with conventional coatings.

Further examination of the stability data for Eudragit EPO coated samples lends support to the assertion made above. It was observed that the decomposition data for these samples were out of the ordinary given the low hygroscopicity of Eudragit EPO coated samples and expectation for a much better aspirin stability profile. In fact, it was noticed that the Eudragit EPO coated samples were unique in being the only ones that changed colour (from white to dark brown) during the study and coating lost its adhesion and could easily be peeled off from the cores. Typical sample pictures of tablets obtained are shown in Figure 5-10 below.

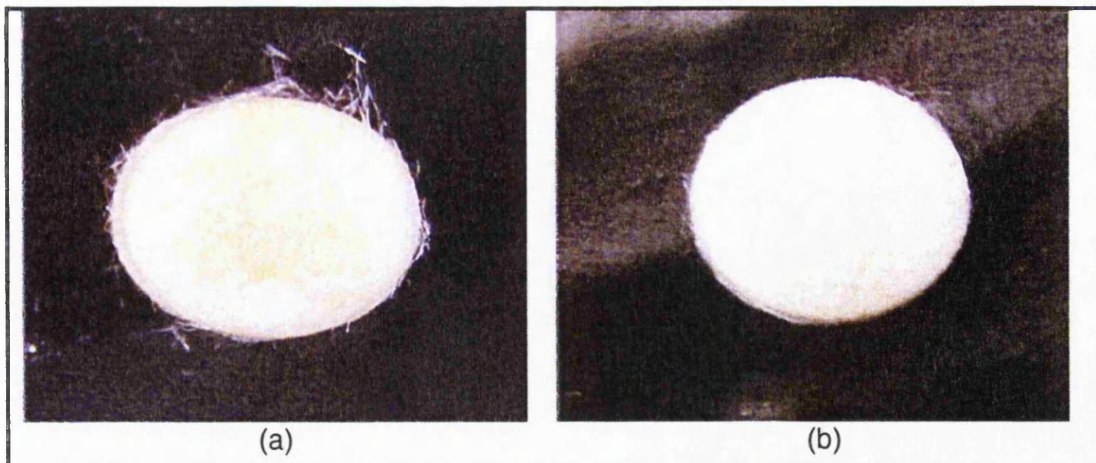


Figure 5-10. Photographs of Eudragit EPO Coated Hygroscopic Tablets. (a) Coating Without Magnesium stearate (b) Coating With Magnesium stearate. (Salicylic acid Whiskers on Tablets Surfaces are Evident in Both Cases)

Initially, it was thought that these unusual results were due to the presence of magnesium stearate, a key ingredient in the coating formulation, which compromised

the adhesion of the coating to the cores, which encouraged the formation of the hypothesized water film. A coating formulation that did not include magnesium stearate in the formulation was similarly evaluated. Aspirin tablets were prepared and coated in the same manner as before. Samples were removed and examined after one month. It was noted that no improvement in the performance of the coating was evident as free salicylic acid whiskers could still be seen on the outside of the samples. However, there was subjective evidence that suggested more aspirin hydrolysis in the samples with magnesium stearate in the formulation.

In conclusion, while the hygroscopicity of the tablet cores was found to be a very influential factor in determining the extent of aspirin hydrolysis among the uncoated samples, the role of the applied moisture barrier coating could not be appreciated.

5.6 CONCLUSIONS

5.6.1 Introduction

The purpose of this work was to determine the extent of aspirin hydrolysis in uncoated and coated tablets cores formulated to exhibit different moisture sorbing characteristics. Tablets were exposed to high humidity (i.e., 75 % RH) at room temperature in a constant temperature incubator. The coatings evaluated were Eudragit L30 D-55, Eudragit EPO, Opadry AMB and Sepifilm LP. Tablets were removed for assay after 0, 30, 60 and 90 days. Retained strength assay of aspirin and salicylic acid were determined by a stability indicating HPLC method.

5.6.2 Role of Tablet Core Hygroscopicity

It was found that uncoated non-hygroscopic cores exhibited the highest hydrolysis of aspirin (after 3 months, salicylic acid content = 11.39 ± 0.562 mg/tablet) while the hygroscopic cores showed the least hydrolysis (salicylic acid content = 1.418 ± 0.344 mg/tablet). Aspirin hydrolysis the Waxy cores was marginally higher than in the hygroscopic (salicylic acid content = 4.572 ± 1.301 mg/tablet). The differences in the extents of hydrolysis were attributed to the differences in the rates at which free water equilibrated to the environmental relative humidity rather than the extent of sorption, per se. Thus, even though the hygroscopic core had sorbed the most quantities of water, it was hypothesized that the rate of equilibration of this core was slower resulting in the amount of water available for hydrolysis to be less in this core.

5.6.3 Effect of Application of Moisture Barrier Coatings

Aspirin hydrolysis in coated tablet cores was found to be significantly higher in coated samples than in the uncoated cores. Among the three core formulation types, Eudragit EPO coated samples exhibited the highest instability. The differences in the hydrolysis of aspirin among the other coated samples were not so wide in relation to the amount of water sorbed by the samples meaning that the barrier functionality of the coatings was not the important factor. Because of this, it was hypothesized that the higher extent of aspirin hydrolysis in the coated samples was due to the presence of moisture at the coating-tablet core boundary. This was confirmed by the performance of powder-layered tablet cores which exhibited better aspirin stability.

CHAPTER 6

Chapter 6

6.0 GENERAL CONCLUSIONS AND SUGGESTED FUTURE WORK

Outline

6.1	General Conclusions
6.2	Suggested Future Work

6.1 GENERAL CONCLUSIONS

6.1.1 Moisture Barrier Polymer Films

6.1.1.1 Sorption-Desorption Characteristics of Cast Polymer Films

The moisture sorption and permeability characteristics of the four moisture barrier coatings experimentally studied in this work revealed very complex behaviour. The anomalous equilibrium and kinetic behaviour was attributed to the highly polar nature of the water molecule and the associated and/or resulting polymer-water interactions. The polarity of the polymer was hypothesized to be a key factor in determining the rate and extent of sorption. Thus, systems in which the constituent polymers had polar groups exhibited high moisture uptake, and vice versa.

It was demonstrated with the aid of thermogravimetric analysis and near-infrared spectroscopy that the water-polymer interactions were mainly through hydrogen bonding leading in moisture fractions that were tightly bound to the polymer segments and moisture existing as loosely bound or un-bound water. The resulting high solubility and/or the high diffusivity, coupled with the plasticizing effects and or the clustering of the sorbed water, resulted in fairly high water vapour permeabilities.

The relative humidity (RH) and temperature were observed to be important determinants of the extent of sorption in the free films. An increase in RH resulted in an increase in sorption. At high RH, all samples exhibited a disproportionately high moisture sorption. This was attributed to plasticization of the polymer matrix, yielding membranes which were more fluid. Increase in temperature resulted in a decrease in sorption for Sepifilm LP, Eudragit L30 D-55 and Opadry AMB but resulted in an increase in moisture sorption in Eudragit EPO. The increase in sorption in the Eudragit EPO sample was unexpected, but was attributed to plasticization of the matrix of this membrane, which transformed the polymer from a glassy to a rubbery state. It was speculated that plasticization opened up the film structure, further facilitating the access of water molecules to the polymer matrix.

6.1.1.2 Permeability Characteristics of Cast Polymer Films

Knowledge of both the solubility coefficient from sorption isotherms and the diffusion coefficient from sorption kinetics facilitated the calculation of the permeability coefficients, in accordance with the solution-diffusion model. The solubility and diffusion coefficients thus obtained enabled the characterization of the permeation behaviour in the film samples. Permeability coefficients thus determined were of the order of 10^{-6} to 10^{-7} cm^3 [(STP) cm/cm^2 s cm Hg)]. Compared with barriers like HDPE and Polyvinylidene chloride with reported moisture permeabilities in the order of 10^{-9} to 10^{-11} (Morillon et al., 2002), moisture barrier coatings were judged as inferior barriers.

It was found that in more hygroscopic films (notably Sepifilm LP), the high permeability was due to the high solubility coefficients of water in this film even though the diffusion coefficients were relatively low. Hydrophobic films (e.g., Eudragit L30 D-55), in contrast, exhibited high diffusion coefficients even though they had relatively low solubility coefficients. In some samples, e.g., Opadry AMB, the permeability rates for moisture were comparatively low even though the sample was adjudged as being highly hydrophilic. This behaviour was attributed to more compact polymer membranes which resulted in low diffusion coefficients. For the Eudragit EPO sample, low permeability was attributed to the presence of hydrophobic additives which restricted the sorption and movement of water through the membranes.

At high relative humidities, clustering and plasticization were observed to influence the permeability coefficients. However, no direct relationship was found between the amount of water sorbed and the amount of water that permeated the free films, or the stability profiles exhibited by the different coated samples. The reason for these results was attributed to the fact that the sorption process was thermodynamic process, governed by hydrophilicity of the film, while permeation was a rate phenomenon, dependent on the concentration differential on the two sides of the films.

6.1.2 Moisture Sorption-Desorption Characteristics of Tablet Cores

When the moisture barrier coatings were applied to cores of different hygroscopicities, only the hygroscopic core achieved the net effect of reducing the extent of sorption while the non-hygroscopic and waxy cores showed no net reduction in the extent of sorption. The net reduction in the amount of moisture sorbed by the coated hygroscopic cores varied between 60-90 per cent of that sorbed by the uncoated hygroscopic core. Ideally, the barrier coatings should be independent of the nature of the substrate to which they have been applied, and also, be able to achieve a zero per

cent moisture uptake. It was speculated that the behaviour of the coated core (comprising the core and the barrier membrane) in response to the moisture stress depended on the relative differences between the hygroscopicity of the core and the film. This influenced the rate at which the water activity in the core equilibrated against the equilibrium relative humidity of the environment. Thus, the benefits of moisture barrier films, in terms of rate and extent of water transfer from an environment with abundant water vapour, were limited to formulations with hygroscopic tablet cores coated at the minimum and the intermediate levels.

6.1.3 Aspirin Hydrolysis in Tablet Cores

When the barrier coatings were applied to the different core types containing aspirin as a model drug, the stability profile of the drug exhibited by the tablet core types demonstrated that the hygroscopicity of the core was a key factor compared to the nature of the barrier coating. There was no strong evidence linking the effect of film type on aspirin hydrolysis. In fact, except for the Eudragit EPO copolymer, there was little differentiation between the extents of aspirin in the different coated samples. It was speculated that the protection offered by moisture barrier coatings was not the result of a barrier action against water permeation but rather of the ability to prevent the hydrolytic chemical reactions that occurred in the water at the coating-core boundary. This proposition was confirmed by investigations undertaken on powder-layered hygroscopic tablet cores to which moisture barrier coatings were subsequently applied. It was established that in these tablet, the extent of aspirin hydrolysis was significantly much less. Thus, the powder coating was able to prevent direct contact between the aspirin containing core and the film of moisture formed as a result of loss of adhesion due to sorption of moisture.

6.1.4 Conclusion

This study showed that the moisture barrier coatings investigated were not able to completely seal the tablet cores from moisture when placed under conditions of high humidity. This does not mean that moisture barrier coatings are completely irrelevant. In fact, there might be some merit in using moisture barrier coatings when combined with other measures, e.g., inclusion of a desiccant to limit the RH in the package to low values ($\leq 35\%$ RH) since below this value, the films sorbed relatively little moisture. Otherwise, if better barrier performance is to be attained at high relative humidity, the ability to prevent the collection of water molecules at the boundary region between the coating and the core is essential. It is anticipated that the ability of the moisture barrier coating to form a tight bond with the core would be an advantage.

6.2 SUGGESTED FUTURE WORK

The work undertaken in this thesis was limited to four moisture barrier coatings. Even though these samples covered a fairly broad range of hydrophilicity and hydrophobicity characteristics, it is worthy investigating other systems as well. For instance, Ethylcellulose (Aquacoat ECD[®], FMC Biopolymer) and Cellulose acetate phthalate (Aquacoat CPD[®], FMC Biopolymer) are also marketed as moisture protective coatings while a new system based on a co-polymerised polyvinyl-polyethylene glycol system (Kollicoat Protect[®], BASF) has recently been launched. It is not clear whether cellulose acetate and ethyl cellulose, being water insoluble polymers, might lead to different barrier performance from systems investigated in this work.

Another aspect that might be of interest in future is to investigate the role played by different formulation components on barrier performance. This work was limited to ready-to-use systems. For instance, it is not clear from this study what the overall role of additives like talc or titanium dioxide is. It is known that these materials can affect film properties, including mechanical properties but how they affect permeability of moisture barrier films is not yet reported.

The role of polymer crystallinity in barrier performance needs to be explored. It is known that crystalline regions in a polymer membrane are resistant to water sorption and permeation. There are no reports that link the two phenomena yet. Likewise, controlled introduction of crystallinity into the polymer could be explored as a way of enhancing barrier action, perhaps with the aim of fabricating films which are resistant to water vapour but soluble in liquid water.

The possible relationship between barrier properties and a tightly packed, ordered hydrogen bonded polymer network structure needs to be explored. In this study, it was hypothesised that this was possibly the reason for the low permeability of the Opadry AMB system. McHugh and Krotcha (1994) arrived at similar conclusions for a starch acetate film system. Already, systems, known as Intepenetrating networks (IPNs) are showing promise in parallel technologies. As a future direction for formulating moisture barrier coatings, IPNs could be very promising. Future investigations, especially those aimed at optimizing barrier performance, could explore this line.

There will be a need for investigations about powder coatings. Cerea et al (2004) recently reported a novel method for applying Eudragit EPO coatings on to substrates that did not need solvents. Whether this system offers better barrier activity compared to coatings applied conventionally needs to be established.

Finally, the technique of plasma treatment of the coatings to improve barrier performance needs to be explored. This technique is already being used for moisture barrier coatings used in parallel industries but has yet to be reported in the pharmaceutical sector.

REFERENCES

- Abrams, D. S., Prausnitz., 1975. Statistical thermodynamics of liquid mixtures: A new expression for the excess Gibbs energy of partly or completely miscible systems. *AIChE J.*, 21, 116-127.
- Achanta, A. S., Adusumili, P. S., James, P. S., Rhodes, C. T., 2001a. Thermodynamic analysis of water interaction with excipient films. *Drug Dev. Ind. Pharm.*, 27, 227-240.
- Achanta, A. S., Adusumili, P. S., James, P. S., Rhodes, C. T., 2001b. Hot melt coating: water sorption behaviour of excipient films. *Drug Dev. Ind. Pharm.*, 27, 241-250.
- Aguilar-Vega, M., Paul, D. R., 1993. Gas transport properties of polyphenylene ethers. *J. Polymer Sci.*, 31, 1577-1589.
- Ahlnock, C., Alderborn, G., 1989., Moisture adsorption and tableting. I. Effect on volume reduction properties and tablet strength for some crystalline materials. *Int. J. Pharm.* 54, 131-141.
- Ahlnock, C., Lundgren, P. 1985. Methods for the evaluation of solid state stability and compatibility between drug and excipient. *Acta Pharm Suec.*, 22, 305-314.
- Ahlnock, C., Zografi, G., 1990. The molecular basis of moisture effects on the physical and chemical stability of drugs in the solid state. *Int. J. Pharm.*, 62, 87-95.
- Alfrey, T., Gurnee, E. F., Lloyd, W. G. 1966. Diffusion in glassy polymers. *J. Polymer Sci., Part C* 12, 249-261.
- Allinson, J. G., Dansereau, R., Sakr, A., 2001. The effects of packaging on the stability of a moisture sensitive compound. *Int. J. Pharm.*, 221, 49-56.
- Altinkaya, S. A., Yenil, H., Ozbas, B. 2005. Membrane formation by dry-cast process. Model validation through morphological studies. *J. Membr. Sci.*, 94, 249-255.
- Alvarez-Lorenzo, C., Gómez-Amoza, J. L., Martínez-Pacheco, R., Souto, C., Concheiro, A., 2000. Interactions between hydroxypropylcelluloses and vapour/liquid water. *Eur. J. Pharm. Biopharm.*, 50, 307-318.
- Anderson, R. B., 1946. Modifications of the Brunauer, Emmett and Teller equation. *J. American Chem Soc.*, 68, 686-691.
- Ashford, M., Fell, J., Attwood, D., Woodhead, P. J., 1993. An in vitro investigation into the suitability of pH-dependent polymers for colonic targeting. *Int. J. Pharm.*, 91, 241-245.
- ASTM E96-93 (1993). Standard Test Method for Water Vapour Transmission of Materials. In: Annual Book of ASTM Standards. Philadelphia, PA. American Society for Testing and Materials.
- ASTM F-1249-90 (1990). Standard Test Method for Water Vapour Transmission of Materials. In: Annual Book of ASTM Standards. Philadelphia, PA. American Society for Testing and Materials.

- Aulton, M. E., 1995. Mechanical properties of film coats. In: Cole, G., Hogan, J., Aulton, M. E., (Eds.), *Pharmaceutical coating technology*. Taylor and Francis Ltd., London, pp. 306.
- Aulton, M. E., Abdul-Razzak, M. H., Hogan, J. E., 1984. Mechanical properties of hydroxypropylmethylcellulose films derived from aqueous systems: Part 1. The influence of plasticizers. *Drug Dev. Ind. Pharm.*, 7, 649-668.
- Bair, H. E., 1981. Thermal analysis of adhesives in polymers. In: Turi, E. A., (Ed.), *Thermal characterization of polymeric materials*. Academic Press, San Diego, pp. 845-909.
- Banker, 1966. Film coating theory and practice. *J. Pharm. Sci.*, 55, 81-89.
- Barranco, V., Carpentier, J., Grundmeier, 2004. Correlation of morphology and barrier properties of thin microwave plasma polymer films on metal substrates. *Electrochimica Acta*, 49, 1999-2013.
- Barrer R. M. 1984. Diffusivities in Glassy Polymers for the Dual Mode Sorption Model. *Journal of Membrane Science* 1984;18:25-35.
- Barrer R. M: Activated Diffusion in Membranes. *Trans. Faraday Society* 1939;35:644-656.
- Barrer R. M: Permeation, Diffusion and Solution of Gases in Organic Polymers. *Trans. Faraday Society* 1934;35:628-643.
- Barrer, R. M., 1939. Activated Diffusion in Membranes. *Trans. Faraday Society*, 35:644-656.
- Barrer, R. M., 1968. In: Crank, J., Park, G. S., (Ed.), *Diffusion in Polymers*, Academic Press, New York, pp 165-217.
- Barrer, R. M., 1975. In: Hopfenberg, H. B., (Ed.), *Permeability of Plastic Films and Coatings*, Plenum Press, New York, pp. 113-124.
- Barrer, R. M., 1984. Diffusivities in glassy polymers for the dual mode sorption model. *J. Membr. Sci.*, 18, 25-35.
- Barrer, R. M., Barrie, J. A., Slater, J. 1958. Sorption and diffusion in ethylcellulose. Part III. Comparison between ethylcellulose and rubber. *J. Polym. Sci. Polym. Phys. Ed.* 27, 177-185.
- Barrie, J. A., 1968. Water in Polymers. In: Crank J., Park, G. S. (Eds.), *Diffusion in Polymers*, Academic Press, London, pp. 259.
- Basit, A. W., 2005. Advances in colonic drug delivery. *Drugs*. 65, 1991-2007.
- Baudoux, M., Dechesne, J. P., Delattre, L., 1990. Film coating with enteric polymers from aqueous dispersions. *Pharm. Technol. Int.*, 2, 20-26.

- Bauer, K. H., Lehmann, K., Osterwald, H., Rothgang, G. 1998a. Coated dosage forms. Fundamentals, manufacturing techniques, biopharmaceutical aspects, test methods, and raw materials. CRC Press, Stuttgart, Germany, pp. 65-119.
- Bauer, K. H., Lehmann, K., Osterwald, H., Rothgang, G. 1998b. Coated dosage forms. Fundamentals, manufacturing techniques, biopharmaceutical aspects, test methods, and raw materials. CRC Press, Stuttgart, Germany, pp. 200.
- Bell, L.N., Labuza, T.P. 1984. Moisture sorption: Practical aspects of Isotherm Measurement and Use. American association of Cereal Chemists, Inc. MN. USA. First edition.
- Berens A R, Hophenberg H B (1982). Diffusion of organic vapours at low concentrations in glassy PVC, polystyrene and PMMA. *J. Membr. Sci.*, 10, 283-303.
- Bergren, M. S, 1994. An automated controlled atmosphere microbalance for the measurement of moisture sorption. *Int. J. Pharm.* 103: 103-114.
- Bhaskar, G., Ford, J. L., Hollingsbee, D. A., 1998. Thermal analysis of the water uptake by hydrocolloids. *Thermochimica Acta*, 322, 153-165.
- Biquet, B., Labuza, T. P., 1988. Evaluation of the moisture permeability characteristics of chocolate films as an edible moisture barrier. *J. Food Sci.*, 53, 989-998.
- Bos, A., Pünt, I. G. M., Wessling, M., Strathmann, H. 1998. Suppression of CO₂ induced plasticization by semi-interpenetrating polymer network formation. *J. Polym. Sci., Phys. Ed.*, 36, 1547-1556.
- Bradford, E. B., Vanderhoff, J. W., 1972. A study of morphological changes in latex films. *J. Macromol. Sci.*, 6, 671-694.
- Bravo-Osuna, I., Ferrero, C., Junénez-Castellanos, M. R., 2005. Water sorption-desorption behaviour of mEudragit L30 D-55-starch copolymers : effect of hydrophobic graft and drying method. *Eur. J. Pharm. Biopharm.*, 59, 537-548.
- Brittain, H. G., Bugay, D. E., Bogdanowich, S. J., DeVincentis, J., 1988. Spectral methods for determination of water. *Drug Dev. Ind. Pharm.*, 14, 2029-2046.
- Brunauer, S., Emmett, P. H., Teller, E., 1938. Adsorption of gases in multimolecular layers. *J. Am. Chem. Soc.*, 60, 309-319.
- Buckton, G., Darcy, P. 1995 Assessment of disorder in crystalline powders-a review of analytical techniques and their application. *Int. J. Pharm.*, 179, 141-158.
- Byrn, S. R., 1982. *Solid State Chemistry of Drugs*. 1st Ed., Academic Press, New York, pp 156.
- Callaha, J. C., Cleary, G. W., Elefant, M., Kaplan, G., Kensler, T., Nash, R. A., 1982. Equilibrium moisture content of pharmaceutical excipients. *Drug Dev. Ind. Pharm.*, 8, 355-369.
- Campbell, R., Sackett, G., 1999. Film Coating. In: Avis, K., Shukla, A.J., Chang, R.J., (Eds.), *Pharmaceutical Unit Operations Coating*, Interpharm/CRC Press, Boca Raton, Florida, pp. 69.

- Canafe, K., Duman, G., 1993. Studies on the formulation parameters and stabilities of micropellets containing salicylic acid and ascorbic acid. *Pharmazie*, 48, 935-937.
- Carstensen, J. T., 1988. Effect of moisture on the stability of solid dosage forms. *Drug Dev. Ind. Pharm.*, 14, 1927-1969.
- Carstensen, J. T., 1993. *Pharmaceutical Principles of Solid Dosage Forms*. Technomic Publishing, Lancaster, PA.
- Catlow, C. R. A., Parker, S. C., Allen, M. P., (Eds.), 1990. *Computer simulation of fluids, polymers and solids*, Kluwer, Dordrecht, pp
- Cerea, M., Zheng, W., Young, C. R., McGinnity, J. W., 2004. A novel powder coating process for attaining taste masking and moisture protective films applied to tablets. *Int. J. Pharm.*, 279, 127-139.
- Cerofolini, G. F., Rudzinski, W. 1997. Theoretical principles of single and mixed gas adsorption equilibria in heterogeneous solid surfaces. In: Rudzinski, W., Steele, W. A., Zgrablich, G., (Eds.), *Equilibria and Dynamics of Gas Adsorption on Heterogeneous Solid Surfaces*, Elsevier, Amsterdam. Pp. 1-55.
- Cervera, M. F., Karjalainen, M., Airaksinen, S., Rantanen, J., Krogars, K., Heinämäki, J., Colarte, A. I., Yliruusi, J., 2004. Physical stability and moisture sorption of aqueous chitosan-amylose starch films plasticized with polyols. *Eur. J. Pharm. Biopharm.*, 58, 69-76.
- Chalkykh, A. E., 1983. Diffusion in Polymers. In: Malkin A, Ya., Ashadsky, A. A., Kovriga, V. V., Chalykh, A. E., *Experimental Methods of Polymer Physics*. MIR Publishers, Moscow, pp. 431-513.
- Chou, H. E., Acott, K. M., Labuza, T. P. 1973. Sorption hysteresis and chemical reactivity: lipid oxidation. *J. Food Sci.* 38, 316-319.
- Ciurczak, E. W., 2001. Principles of Near-Infrared Spectroscopy. In: Burns, D. A., Ciurczak, E. W., (Eds.), *Handbook of Near-Infrared Analysis*. Marcel Dekker, New York, pp. 7-18.
- Ciurczak, E. W., Drennan, J., 2001. Near-Infrared Spectroscopy in Pharmaceutical Applications. In: Burns, D. A., Ciurczak, E. W., (Eds.), *Handbook of Near-Infrared Analysis*. Marcel Dekker, New York, pp. 609-632.
- Coma, V., Sebti, I., Pardon, P., Deschamps, A., Pichavant, F. H., 2001. Antimicrobial edible packaging based on cellulosic ethers, fatty acids and nisin incorporation to inhibit *Listeria innocua* and *Staphylococcus aureus*. *J. Food Protection*, 64, 470-475.
- Cornejo-Bravo, J. M., Siegel, R. A., 1996. Water vapour sorption behaviour of copolymers of N,N-diethylaminoethyl methacrylate and methyl methacrylate. *Biomaterials* 17, 1187-1193.
- Costa, F. O., Sousa, J. J. S., Pais, A. A. C. C., Formosinho, S. J., 2003. Comparison of dissolution profiles of ibuprofen pellets, *J. Control. Release* 89, 199-212.
- Coyle, F. M., Martin, S. J., McBrierty, V. J., 1996. Dynamics of water molecules in polymers. *J. Molecular Liquids*, 69, 95-116.
- Crank, J. *The Mathematics of Diffusion*, 2nd Ed., Clarendon Press, Oxford, 1975.

- Dawoodbhai, S., Rhodes, C. T., 1989. The effect of moisture on powder flow and on compaction and physical stability of tablets. *Drug Dev. Ind. Pharm.*, 15, 1577-1600.
- de Boer, J. H., 1968. *The Dynamic Character of Adsorption*, 2nd Ed., Clarendon Press, Oxford.
- de Wilde, W. P., Shopov, P. J., 1984. A simple model for moisture sorption in epoxies with sigmoidal and two-stage sorption effects. *Composite Structures* 27, 243-252.
- Dean, D. A., 1988. Packs for Pharmaceutical Products. In: Aulton, M. E., (Ed.), *Pharmaceutics The science of dosage form design*, Churchill Livingstone, Edinburgh, pp. 215-222.
- Debeaufort, F., Martín-Polo, M., Voilley, A. 1993. Polarity homogeneity and structure affect water vapor permeability of model edible films. *J. Food Sci.*, 58, 426-434.
- Debeuafort, F., Voilley, A., Meares, P., 1994. Water vapour permeability and diffusivity through methylcellulose edible films . *J. Membr. Sci.* 91, 125-133.
- Detallante, V., Langevin, D., Chappey, C., Métayer, M., Mercier, R., Pinéri, M., 2002. Water vapour sorption in naphthalenic sulfonated polyimide membranes. *J. Membr. Sci.*, 190, 227-241.
- DiBenedetto, A. T., Paul, D. R., 1964. An interpretation of gaseous diffusion through polymers using fluctuation theory. *J. Polym. Sci., Part-A2*, 1001-1010.
- Demertzis, P. G., Kontominas, M., 1988. Study of water sorption of egg powders by inverse gas chromatography. *Eur. Food Res. Technol.*, 186, 213-217.
- Donhowe, G., Fennema, O., 1994. Edible films and coatings: Characteristics, Formation, Definitions, and Testing Methods. In: Krochta, J. M., Baldwin, E. A., Nisperos-Carriedo, M., (Eds.), *Edible Coatings and Films to Improve Food Quality*. Technomic Publishing Co., Inc., Pa, USA, pp. 1-24.
- Du, H., Hoag, S. W., 2001. The influence of excipients on the stability of the moisture sensitive drugs aspirin and niacinamide: comparison of tablets containing lactose monohydrate with tablets containing anhydrous lactose. *Pharm. Dev. Technol.*, 6, 159-166.
- Duckworth, R. B., 1984., The water-vapour sorption isotherms of microcrystalline cellulose and purified potato starch. Results of a collaborative study. *J. Food Engineering*, 3, 51-73.
- Ellis, J. R., Brillig, E. B., Endicott, C., 1970. Tablet Coating. In: Lachman, L., Lieberman, H. A., Kanig, J. L., (Eds.), *The Theory and Practice of Industrial Pharmacy*, Lea and Fabinger, Philadelphia, USA, pp. 197-225.
- Evans, R. B., Watson, G. M., 1961. Gaseous diffusion in porous media at uniform pressure. *J. Chem. Phys.*, 35, 2076-2083.
- Fadda, H. M., Basit, A. W., 2005. Dissolution of pH responsive formulations in media resembling intestinal fluids: bicarbonate versus phosphate buffers. *J. Drug Del. Sci. Tech.*, 15, 273-279.

Fassihi, R. A., mcPhillips, A. M., Uraizee, S. A., Sakr, A. M., 1994. Potential use of magnesium stearate and talc as dissolution retardants in the development of controlled release drug delivery systems. *Pharm., Ind.*, 56, 579-583.

Fava, R. A., 1980., *Polymers: Physical Properties*. In: Felder, R. M., Huward, G. S., (Eds.), *Methods of Experimental Physics*, Vol. 16, Part C, Academic Press, New York, (Chapter 17).

Favre, E., Nguyen, Q. T., Clément, R., Néel, J., 1996a. The engaged species induced clustering (ENSIC) model: A unified mechanistic approach of sorption phenomena in polymers. *J. Membrane Sc.*, 117, 227-236.

Favre, E., Nguyen, Q. T., Clément, R., Néel, J., 1996b. Clustering of solvents in membranes and its influence on membrane transport properties. *J. Membrane Sci.*, 113, 137-150.

Felder, R. M., Huvard, G. S., 1980. Permeation, Diffusion and Sorption of Gases and Vapours, *Methods of Experimental Physics*, Vol. 16c, Academic Press, New York. pp. 315-377.

Felton, L. A., McGinity, J. W. 1997. Influence of plasticizers on the adhesive properties of an acrylic resin copolymer to hydrophilic and hydrophobic tablet compacts. *Int. J. Pharm.*, 154, 167-178.

Finney, J. L., 1982. Towards a molecular picture of liquid water. In: Franks, F., Mathias, S. F., (Eds.), *Biophysics of Water*, John Wiley & Sons, Salisbury, pp. 73-96.

Flaconnéche, B., Martin, J., Klopffer, M. H. 2001. Transport properties of gases in polymers. *Experimental methods. Oil Gas Sc Technol.*, 56, 245-259.

Flory, P. J., 1941. Thermodynamics of high polymer solutions. *J. Chem. Phys.* 9, 660-661.

Flynn G.L., Yalkowsky S.H., Roseman T.J. 1974. Mass Transport Phenomena and Models: Theoretical Concepts. *J. Pharm. Sci.* 63, 479-510.

Food and Drug Administration, 1998. *Stability Testing of Drug Substances and Drug Products. Guidance for Industry*. U.S Department of Health and Human Services, Food and Drug Administration, Centre for Drug Evaluation and Research.

Ford, J. L., 1999. Thermal analysis of hydroxypropyl methylcellulose and methylcellulose. Powders, gels and matrix tablets. *Int. J. Pharm.*, 179, 209-228.

Ford, J. L., Rubinstein, M. H., 1980. Formulation and ageing of tablets prepared from indomethacin-polyethylene glycol 6000 solid dispersions. *Pharm Acta Helv.*, 55, 1-7.

Ford, J. L., Timmins, P. 1989. *Pharmaceutical Thermal Analysis Techniques and Applications*. Ellis Horwood, Chichester, pp. 25-68.

Forssell, P. M., Mikkila, J. M., Moates, G. K., Parker, R., 1998. Phase and glass transition behaviour of concentrated barley-starch-glycerol-water mixtures: a model for thermoplastic starch. *Carbohydrate Polymers* 34, 275-282.

Franks, F., 1997. Phase changes and chemical reactions in solid aqueous solutions: science and technology. *Pure Appl. Chem.*, 69, 915-920.

Franson, N. M., Peppas, N. A., 1983. Influence of copolymer composition on non-Fickian water transport through glassy copolymers. *J. Appl. Polymer Sci.*, 28, 1299-1310.

Freundslund, R. L., Jones, J. M., Prausnitz., 1975. Group-contribution estimation of activity coefficients in non-ideal liquid mixtures. *AIChE J.* 21, 1086-1099.

Frisch, H. L., 1980. Sorption and Transport in glassy polymers. A review. *Polymer Eng. Sci.*, 20, 2-13.

Fujita H. 1961. Diffusion In Polymer Diluent Systems, *Adv. Polymer Sci.* 3, 1-47.

Fujita, H. 1968. Organic vapours above the glass transition temperature. In: Crank, J., Park, J. S., *Diffusion in Polymers*, Academic Press, New York.

Fukuda, M., Kawai, H., Yagi, N., Kimura, O., Ohta, T., 1990. FTIR study on the nature of water sorbed in poly(ethylene terephthalate) film. *Polymer*, 31, 295-302.

Fukuda, M., Ochi, M., Miyagawa, M. and Kawai, H., 1991. Fundamental-studies on the interaction between moisture and textiles 12. Moisture sorption mechanism of aromatic polyamide fibers—stoichiometry of the water sorbed in poly(para-phenylene terephthalamide) fibers. *Textile Research Journal* 61, 668–680.

Giron, D. 1997. Thermal Analysis of Drugs and Drug Products. In: Boylan, C., Swarbrick, J., (Eds.), *Encyclopedia of Pharmaceutical Technology*, Marcel Dekker, New York, pp. 1-80.

Gore, A. Y., Banker, G. S., 1979. Surface chemistry of colloidal silica and a possible application to stabilize aspirin in solid matrixes. *J. Pharm. Sci.*, 68, 197-202.

Gore, A. Y., Naik, K. B., Kildsig, D. O., Peck, G. E., Smollen, V. F., Banker, G. S., 1968. Significance of salicylic acid sublimation in stability testing of aspirin-containing solids. *J. Pharm. Sci.*, 57, 1850-1854.

Gucluyildiz, H., Banker, G. S., Peck, G. E. 1977. Determination of porosity and pore size distribution of aspirin tablets relevant to drug stability. *J. Pharm. Sci.*, 66, 407-414.

Guggenheim, E. A., 1966. *Applications of Statistical Mechanics*, Clarendon Press, Oxford, p. 186.

Guilbert, S., 1986., *Technology and Application of Edible Protective Films.*, In: Mathlouthi, M., (Ed.). *Food Packaging and Preservation: Theory and Practice*. Elsevier, London, pp. 371-393.

Guilbert, S., Biquet, B. 2000. Edible Films and Coatings. In: Bureau, G., Moulton, J. L., (eds.), *Food Packaging Technology*, Vol. 1., Wiley-VCH Verlag GmbH, Weinheim, pp. 315-353.

Guo, J., Robertson, J. E., Amidon, G. L. 1993. An investigation into the mechanical and transport properties of aqueous latex films. A new hypothesis for the film forming mechanism of aqueous dispersions. *Pharm. Res.*, 10, 405-410.

Gutierrez-Rocca, J. C., McGinity, J. W. 1994. Influence of water soluble and insoluble plasticizers on the physical and mechanical properties of acrylic resin copolymers. *Int. J. Pharm.*, 103, 293-301.

H. Fujita, A. Kishimoto and K. Matsumoto. Concentration and temperature dependence of diffusion for systems PMA and n-alkylacetates *Trans Faraday Soc* 56 (1967), p. 424.

Hagenmaier, R. D., Shaw, P. E., 1991. Permeability of shellac coatings to gases and water vapour. *J. Agricultural Food Chem.*, 38, 1799-1803.

Hancock, B. C., Zografi, G. 1993. The use of solution theories for predicting water vapour absorption by amorphous pharmaceutical solids. A test of the Flory-Huggins and Vrentas models. *Pharm. Res.*, 10, 1262-1267.

Hancock, B. C., Zografi, G. 1994. The relationship between the glass transition temperature and the water content of amorphous pharmaceutical solids. *Pharm. Res.*, 11, 4471-4477.

Hancock, B. C., Zografi, G., 1993. Use of solution theories for predicting water vapour absorption by amorphous pharmaceutical solids: test of the Flory-Huggins and Vrentas models. *Pharm. Res.*, 10, 1262-1267.

Hancock, B. C., Zografi, G., 1994. The relationship between the glass transition temperature and the water content of amorphous pharmaceutical solids. *Pharm. Res.* 11, 471-477.

Hancock, B. C., Zografi, G., 1996. Effects of solid state processing on water vapour sorption by aspirin. *J. Pharm. Sc.*, 85, 246-248.

Handbook of Pharmaceutical Excipients, 3rd Ed. 2000, Pharmaceutical Press, London, UK.

Handbook of Tables for Applied Engineering Science. Bolz, R. A., Tuve, G. L., (Eds.), 1973. 2nd Ed., CRC Press, Boca Raton FL., pp 548-549.

Hansen, L. D., Crawford, J. W., Keiser, D. R., Wood, R. W. 1996. Calorimetric method for rapid determination of critical water vapor pressure and kinetics of water sorption on hygroscopic compounds. *Int. J. Pharm.* 135, 31-42.

Hartley, L., Chevance, f., Hill, S.E., Mitchell, J.R., Blanshard, J.M.V. 1995. Partitioning of water in binary biopolymer mixtures at low water content. *Carbohydrate Polymers* 28, 83- 89.

Hatakeyama, H., Hatakeyam, T., 1998. Interaction between water and hydrophilic polymers. *Thermochimica Acta*, 308, 3-22.

Heal, G. R. 2002. Thermogravimetry and Derivative Thermogravimetry. In: Haines, P. J., (Ed.), *Principles of Thermal Analysis and Calorimetry*. The Royal Society of Chemistry, Cambridge, pp. 10-53.

Heidemann, D. R., Jarosz, P. J., 1991. Preformulation studies involving moisture uptake in solid dosage forms. *Pharm. Res.*, 8, 292-297.

- Hernandez, R. J., 1994. Effect of water vapour on the transport properties of oxygen through polyamides. *J. Food Eng.*, 22, 495-507.
- Higuchi A., Fushimi H., Iijima T. 1985., Gas Permeation Through Hydrogels II. Poly(Vinyl Alcohol-Co-Itaconic Acid) Membranes. *J. Membr. Sci.*, 25, 171-180.
- Hodge, R. M., Edward, G. H., Simon, G. P. 1996. Water absorption and states of water in semicrystalline poly(vinyl alcohol) films. *Polymer*, 37, 1371-1376.
- Hogan, J. E., 1982. Aqueous versus organic solvent film coating. *Int. J. Pharm. Tech. Prod. Mfr.*, 3, 17-20.
- Hogan, J. E., 1983. Additive effects on aqueous film coatings. *Manuf. Chem.*, 54, 43-47.
- Hogan, J. E., 1995. Film coating materials and their properties. In: Cole, G., Hogan, J. E., Aulton, M. , (Eds.), *Pharmaceutical Coating Technology*, Taylor and Francis Ltd, London, pp. 6-50.
- Hoy, K. L., 1973. Estimating the effectiveness of latex coalescing aids. *J. Paint Technol.*, 45, 51-56.
- Hu, Y., Topolkaev, V., Hiltner, A., Baer, E. 2001. Measurement of water vapour transmission rate in highly permeable films. *J. Appl. Polymer Sci.*, 81, 1624-1633.
- Huggins, M., 1942. Thermodynamic properties of solutions of long-chain compounds. *Ann. N. Y. Acad. Sci.*, 43, 1-32
- Hussain, M. S. H., York, P., Timmins, P., 1992. Effect of commercial and high purity magnesium stearates on in-vitro dissolution of paracetamol DC tablets . *Int. J. Pharm.*, 78, 203-207.
- Huvar, G. S., Stannett, W. J., Koros, H. B., Hopfenberg, H. B., 1980. The pressure dependence of CO₂ sorption and permeation in poly(acrylonitrile). *J. Membr. Sci.*, 6, 185.
- Hyland, R. W., Wexler, A. 1983. Formulations for the thermodynamic properties of the saturated phases of water from 173.15K to 473.15K. *ASHRAE Trans.*, 89-2A, 500-519.
- ICH Steering Committee, Draft ICH Harmonized Tripartite Guideline, 1998. *Stability Testing of New Drug Substances and Products*.
- Ismael, A. F., Lorna, W., 2002. Penetrant-induced plasticization phenomenon in glassy polymers for gas separation membrane. *Separation and Purification Technology*, 27, 173-194.
- Jivraj, M., Martini, L. G., Thomson, C. M., 2000. An overview of the different excipients useful for the direct compression of tablets. *Pharm. Sci. Technol. Today*, 3, 58-63.
- Jones, F. R., 1994. Moisture absorption-anomalous effects. In: Jones, F. R., (Ed.), *handbook of polymer-fibre composites*, 1st Ed., Longman Scientific, Harlow, Essex.
- Jonquières, A., Perrin, L., Arnold, S., Lonchon, P., 1998. Comparison of the UNIQUAC with related models for modeling vapour sorption in polar materials. *J. Membr. Sci.*, 150, 125-141.

- Joshi, N. H., Topp, E. M., 1992. Hydration in hyaluronic acid and its esters using differential scanning calorimetry. *Int. J. Pharm.*, 80, 213-225.
- Kamper, S. L., Fennema, O. R., 1984. Water vapour permeability of an edible fatty acid bilayer film. *J. Food Sci.*, 49, 1482-1485.
- Kararli, T. T., Kirchoff, C. F., Truelove, J. E., 1995. Ionic Strength Dependence of Dissolution for Eudragit S-100 Coated Pellets. *Pharm. Res.*, 12, 1813-1816.
- Karel, M., 1989. Role of water activity. In: Singh, R. P., Medina, A. G., (Eds.), *In Food Properties and Computer-Aided Engineering of Food Processing Systems*. Kluwer Academic Publishers, Norwell, MA., pp. 135-155.
- Kast, W., Hohenthanner, C. R., 2000. Mass transfer within the gas-phase of porous media. *Int. J. Heat Mass Transfer*, 43, 807-823.
- Kellaway, I. W., Marriott, C., 1975. Correlations between physical and drug release characteristics of polyethylene glycol suppositories. *J. Pharm. Sci.*, 64, 1162-1166.
- Kenny, J., Kiff, D., Holmes, J. et al., 1985. Beneficial effects of diltiazem and propranolol, alone and in combination, in patients with stable angina pectoris. *Br. Heart J.*, 53, 43-46.
- Kesting, R. E., Fritzche, A. K., 1993. Theory of Gas Transport in Membranes. In: *Polymeric Gas Separation Membranes*, Wiley Science, New York., pp.
- Kim, D. Caruthers, J. M., Peppas, N. A. 1993. Penetrant transport in crosslinked polystyrene *Macromolecules* 26, 1841-1847.
- Kim, S. J., Lee, K. J., Kim, S. I., 2003. Water sorption of poly(propylene glycol)/poly(acrylic acid) interpenetrating polymer network hydrogels. *Reactive and Functional Polymers*, 53, 69-73.
- Kim, S. J., Yoon, S. G, Lee, Y. M., An, K. H., Kim, S. I., 2003. Water sorption of poly(vinyl alcohol)/poly(diallyldimethylammonium chloride) interpenetrating polymer network hydrogels. *J. Applied Polymer Sci.*, 90, 1389-1392.
- Kim, T. K., Koros, W. J., Husk, G. R., O'Brien, K. C., 1988. Relationship between gas separation properties and chemical structure in a series of aromatic polyimides. *J. Membr. Sci.*, 37, 45-62.
- Klages, C. P., Dietz, A., Höing, T., Thyen, R., Weber, A., Willich, P., 1996. Deposition and properties of carbon-based amorphous protective coatings. *Surface and Coatings Technology*, 80, 121-128.
- Knight, F. B., 1981. *Essentials of Brownian motion and diffusion*. American Mathematical Society, Rhode Island, USA., pp. 5.
- Kontny, M. J., 1988. Distribution of water in solid pharmaceutical systems. *Drug Dev. Ind. Pharm.*, 14, 1991-2027.
- Kornblum, S., Zoglio, M. A., 1967. Pharmaceutical heterogeneous systems. I. Hydrolysis of aspirin in combination with tablet lubricants. *J. Pharm. Sci.*, 1569-1575.

- Koros, W. J., 1990. Barrier polymers and structures: Overview. ACS Symposium Series. No. 43, pp. 1-21.
- Koros, W. J., Chern, R. T., 1987. Separation of gaseous mixtures using polymer membranes. In: Rousseau, R. W., (Ed.), Handbook of Separation Process Technology, Wiley Intersciences, New York, pp. 862-953.
- Koros, W. J., Paul, D. R., Rocha, A. A., 1976. Carbon dioxide sorption and transport in polycarbonate. *J. Polym. Sci., Polym. Phys. Ed.*, 14, 675-688.
- Kottke, M. K., Rudnic, E. M., 2000. Tablet Dosage Forms. In: Banker, G. S., Rhodes, C. T., (Eds.), *Modern Pharmaceutics*, 4th Ed., Marcel Dekker, New York., pp287-333.
- Krogars, K., Heinamaki, J., Karjalainen, M., Niskanen, A., Leskela, M., Yliruusi, J., 2003. Enhanced stability of rubbery amylose-rich maize starch films plasticized with a combination of sorbitol and glycerol. *Int. J. Pharm.*, 251, 205-208.
- Kulling, W., Simon, E. J., 1980. Fluid-bed technology applied to pharmaceuticals. *Pharm. Tech.*, 3, 79-83.
- Kyritsis, A., Pissis, P., Gómez Ribelles, L., Monleón, M., 1995. Polymer-water interactions in poly(hydroxyethyl acrylate) hydrogels studied by dielectric, calorimetric and sorption isotherm measurements. *Polymer Gels and Networks*, 3, 445-469.
- Lagaron, J.M., Gimenez, E., Gavara, R., Saura, J.J., 2001. Study of the influence of water sorption in pure components and binary blends of high barrier ethylene-vinyl alcohol copolymer and amorphous polyamid and nylon-containing ionomer. *Polymer* 42, 9531-9540.
- Landín, M., Casalderrey, M., Martínez-Pacheco, R., Gómez-Amoza, J. L., Souto, C., Concheiro, A., Rowe, R. C., 1995. Chemical stability of acetylsalicylic acid in tablets prepared with different particle size fractions of a commercial brand of dicalcium phosphate dihydrate. *Int. J. Pharm.*, 123, 143-144.
- Lane, R., A., Buckton, G., 2000. The novel combination of dynamic vapour sorption gravimetric analysis and near infra-red spectroscopy as a hyphenated technique. *Int. J. Pharm.*, 207, 49-56.
- Langmuir, I., 1918. The sorption of gases on plane surfaces of glass, mica and platinum. *J. Am. Chem. Soc.*, 40, 1361-1402.
- Lee, S., De Kay, H. E., Banker, G. S. 1965. Effect of water vapour pressure on moisture sorption and the stability of aspirin and ascorbic acid in tablet matrices. *J. Pharm. Sci.*, 54, 1153-1158.
- Leeson, L., Mattocks, A. 1958. Decomposition of Aspirin in the Solid State. *J. Am. Pharm. Assoc., Sci. Ed.* 1958, 47, 392.
- Legras, M., Hirata, Y., Nguyen, Q. T., Langevin, D., Métayer, M., 2002. Sorption and diffusion behaviors of water in Nafion 117 membranes with different counter ions. *Desalination* 147, 351-357.

Lehmann, K. O. R., 1997. Chemistry and Application Properties of Polymethacrylate Coating Systems. In: McGinity, J. W. (Ed.), *Aqueous Polymeric Coatings for Pharmaceutical Dosage Forms*, vol. 7, 2nd Ed., Dekker, New York.

Lehto, V., Lankinen, T., 2004. Moisture transfer into medicament chambers equipped with a double barrier-desiccant system. *Int. J. Pharm.*, 275, 155-164.

Li, L. C., Peck, G. E., 1989. Water based silicone elastomer controlled release tablet film coating III-Drug release mechanisms. *Drug Dev. Ind. Pharm.*, 15, 1943-1968.

Lin, H., Freeman, D. 2003. Gas solubility, diffusivity and permeability in poly(ethylene oxide). *J. Membr. Sci.*, 239, 105-117.

Lin, S., Chen, K., Run-Chu, L., 2000. Organic esters of plasticizers affecting the water absorption, adhesive property, glass transition temperature and plasticizer permanence of Eudragit acrylic films. *J. Control. Rel.*, 68, 343-350.

Long, F. A., Richaman, D., 1960. Concentration gradients for diffusion of vapours in glassy polymers and their relations to time dependent diffusion phenomenon. *J. Am. Chem. Soc.*, 82, 513-519.

Lourdin, D., Coignard, L., Bizot, H., Colonna, P., 1997. Influence of equilibrium relative humidity and plasticizer concentration on the water content and glass transition of starch materials. *Carbohydrate Polymers* 36, 5401-5406.

Lowenthal, W., 1973. Mechanism of action of tablet disintegrants. *Pharm. Acta Helv.*, 48, 589-609.

Luck, W. A. P. 1974. In Luck, W. A. P., (Ed.), *Structure of water and aqueous solutions*. Verlag Chemie, Weinheim, Germany, pp. 248-284.

Lundberg, J. L., 1972. Molecular clustering and segregation in sorption systems. *Pure Appl. Chem.*, 31, 261-281.

Lundberg, J. L., 1972. Molecular clustering and segregation in sorption systems. *Pure Appl. Chem.*, 31, 261-281.

Lundberg, J.L., 1972. Molecular clustering and segregation in sorption systems. *Pure Appl. Chem.*, 31, 261-281.

Maeda, H., Ozaki, Y., Tanaka, M., Hayashi, N., Kojima, T., 1995. Near infrared spectroscopy and chemometrics studies of temperature-dependent spectral variations of water: relationship between spectral changes and hydrogen bonds. *J. Near Infrared Spectrosc.*, 3, 191-201.

Maeda, Y., Paul, D. R., 1987. Effect of antiplasticization on gas separation and transport. II. Poly(phenylene oxide). *J. Polym. Sci. Ed.* 25, 981-1003.

Major, J. S., Blanchard, G. S., 2002. Adsorption behaviour of polymer modified interfaces. *Langmuir*, 18, 6548-6553.

Mamaliga, I., Schabel, W., Kind, M., 2004. Measurements of sorption isotherms and diffusion coefficients by means of a magnetic suspension balance. *Chem. Eng. Processing*, 43, 753-763.

- Marais S, Metayer M, Nguyen, T. Q., Labbé, M., Perrin, L., Saiter, J. M., 2000. Permeometric and microgravimetric studies of sorption and diffusion of water vapour in an unsaturated polyester. *Polymer*, 41, 2667-2676.
- Martin, A.N., 1993. *Physical Pharmacy, Physical Chemical Principles in the Pharmaceutical Sciences*, 4th Ed., Williams & Wilkins, Baltimore, USA, pp. 53-76.
- Martin-Paulo, M., Voilley, A., Blond, G., Colas, B., Mesnier, M., Floquet, N. 1992. Hydrophobic films and their efficiency against moisture transfer. 2. Influence of the physical state. *J. Agricultural and Food Chemistry*, 40, 407-412.
- McBain, J. W., 1932. *The Sorption of Gases and Vapours by Solids*. George Routledge, London.
- McCormick, D., 2005. Evolutions in direct compression. *Pharmaceutical Technology*, April, 52-62.
- McCrystal, C. B., Ford, J. T., Rajabi-Siahboomi, A. R., 1999. Water distribution studies within cellulose ethers using differential scanning calorimetry. 1. Effect of polymer molecular weight and drug addition. *J. Pharm. Sci.*, 88, 792-796.
- McGinniss, 1996. Advances in environmentally benign coatings and adhesives. *Prog. Organic Coatings*, 27, 153-161.
- McHugh, T. H., Krotcha, J. M., 1994. Permeability properties of edible films. In: Krotcha, J. M., Baldwin, E. A., Nisperos-Carriedo, M. (Eds.), *Edible Coatings and Films to Improve Food Quality*, Lancaster Technomic Publishing Company, pp139-183.
- Meares P: Diffusion of Allyl Chloride in Polyvinyl Acetate. Part I. The Steady State of Permeation. *Journal of Polymer Science* 1958;27:391-404.
- Meares, P. 1954. The diffusion of gases through poly(vinyl acetate). *J. Am. Chem.* 76, 3415-3420.
- Mercea, P., 2000. Models for diffusion in Polymers. In: *Plastic Packaging Materials for Food: Barrier Function, Mass Transport, Quality Assurance and Legislation*. Verlag GmbH, Weinheim, pp. 125-157.
- Merten, U., 1966. *Transport properties of osmotic membranes. Desalination by reverse osmosis*, MIT Press, Cambridge, MA.
- Modesti, M., Dall'Acqua, C., Lorenzetti, A., Florian, E., 2004. Mathematical model and experimental validation of the water cluster influence upon vapour permeation through hydrophilic dense membrane. *J. Membr. Sci.*, 229, 211-223.
- Morgan, R. J., O'Neal, J. E., Fanter, D. L. 1980. The effect of moisture on the physical and mechanical integrity of epoxies. *J. Mater. Sci.*, 15, 751-753.
- Morillon, V., Debeaufort, F., Blond, G., Capelle, M., Voilley, A., 2002. Factors affecting the moisture permeability of lipid based edible films: a review. *Crit. Rev. Food Sci. Nutrition*, 42, 67-89.

- Mroso P.V., Li Wan Po A., Irwin W. J. 1972. Solid-state stability of aspirin in the presence of excipients: Kinetic interpretation, modeling, and prediction. *J. Pharm. Sci.*, 71, 1096-1101.
- Munzel, K. 1963. Recent advances in pharmaceutical coating. *Pharm. Acta. Helv.*, 38, 65-85 and 129-146.
- Musto, P., Ragosta, G., Scarinza, G., Mascia, L. 2002. Probing the molecular interactions in diffusion of water through epoxy and epoxy-bismaleimide networks, *J Polym Sci Part B: Polym Phys* 40, 922-938.
- Nagai, T., Obara, S., Kokubo, H., Hoshi, N., 1997. Application of HPMC and HPMCAS to aqueous film coatings of pharmaceutical dosage forms. In: McGinnity, J. W., (Ed.), *Aqueous Polymeric Coatings for Pharmaceutical Dosage Forms*, vol. 7, 2nd Ed., Dekker, New York.
- Nielsen, L. E., 1974. *Mechanical properties of polymers and composites*. Vol. 1 and 2., Marcel Dekker, New York.
- Nivedita, S., Sangai, V., Malshe, C. 2004. Permeability of polymers in protective organic coatings. *Progressive in Organic Coatings* 50, 28-39.
- Nyqvist, H. 1983. Saturated salt solutions for maintaining specified relative humidities. *Int. J. Pharm. Technol. Prod. Manuf.*, 4, 47-48.
- Okhamafe, A. O., York, P. 1983. Analysis of the permeation and mechanical characteristics of some aqueous-based film coating systems. *J. Pharm. Pharmacol.* 35, 409-415.
- Okhamafe, A. O., York, P. 1985. Adhesion characteristics of some pigmented and unpigmented aqueous based film coatings applied to aspirin tablets. *J. Pharm. Pharmacol.*, 37, 849-853.
- Okhamafe, A. O., York, P. 1986. Mechanical properties of some pigmented and unpigmented aqueous based film coatings applied to aspirin tablets. *J. Pharm. Pharmacol.*, 38, 414-419.
- Pace, R. J., Datyner, A., 1979. Statistical mechanism model for diffusion of simple penetrants in polymers. I. Theory. *J. Polym. Sci.*, 17, 437-
- Park G. S. 1952. The Determination of the Concentration Dependent Diffusion Coefficient for Methylene Chloride in Polystyrene by a Steady State Method. *Trans. Faraday Society* 48:11-21.
- Pascat, B., 1986. Study of some factors affecting permeability. In: Mathlouthi, M., (Ed.), *Food Packaging and Preservation: Theory and Practice*, Elsevier, London, pp. 7-24.
- Patel, N. K., Patel, I. J., Cutie, A. J., Wadhe, D. A., Monkhouse, D. C., Reier, G. E. 1988. The effect of selected direct compression excipients on the stability of aspirin as a model hydrolysable drug. *Drug Devt. Ind. Pharm.* 14, 77-98.

- Paul, D. R., 1976. The solution diffusion model for swollen membranes. *Sep. Purif. Methods*, 5, 33.
- Paul, D. R., Koros, W. J., 1976. Effect of partially immobilising sorption on permeability and the diffusion time lag. *J. Polym. Sci., Polym. Phys. Ed.*, 14, 675-686.
- Paul, D. R., Koros, W. J., 1976. Effect of partially immobilizing sorption on permeability and the diffusion time lag. *J. Polym. Sci.*, 14, 675-685.
- Pearnchob, N., Siepmann, J., Bodmeir, R., 2003. Pharmaceutical applications of shellac: Moisture-protective and taste-masking coatings and extended-release matrix tablets. *Drug Dev. Ind. Pharm.*, 29, 925-938.
- Petereit, H. U., Assmus, M., Lehmann, K., 1995. Glyceryl monostearate as a glidant in aqueous film coating formulations. *Eur. J. Pharm. Biopharm.*, 41, 219-228.
- Petereit, H., Weisbrod, W., 1999. Formulation and process considerations affecting the stability of solid dosage forms formulated with methacrylate copolymers. *Eur. J. Pharm. Biopharm.*, 47, 15-25.
- Petropoulos J. H., 1989. Macroscopic and microscopic descriptions of penetrant transport in membranes and their physical significance. In: Mika, A. W., Winnicki, T. Z., (Eds.), *Advances in Membrane Phenomenon, Processes*, Wroclaw Technical University Press, pp. 45-65.
- Petropoulos, H., 1994. Mechanisms and theories for sorption and diffusion in polymers. In: Paul, D. R., Yampol'skii, Y. P., (Eds.), *Polymeric Gas Separation Membranes*, CRC Press, Boca Raton, FL., pp. 17-82.
- Pickard J. F., Rees, J. E., 1974. Film coating: 1 Formulation and process considerations. *Manuf. Chemist & Aerosol News*, 4, 19-22.
- Pinto, J. F., Podczek, F., Newton, J M., 1997. The use of statistical moment analysis to elucidate the mechanism of release of a model drug from pellets produced by extrusion and spheronisation. *Chem. Pharm. Bull.*, 45, 171-180.
- Piringer G. Permeation of water vapour and volatile organic compounds. In: Piringer, G., Baner, A. L. (Eds.), *Plastic Packaging Materials for Food: Barrier Function, Mass Transport, Quality Assurance and Legislation*, Wiley/VCH, Weinheim, Germany, pp239-286.
- Plazier-Vercammen, J. A., DeNeve R. E., 1993. Evaluation of water and organic coating formulations for the protection of tablets against humidity. *Pharmazie*, 48, 441-446.
- Prager, S., Bagley, E., Long, F.A. 1953. Diffusion of Hydrocarbon Vapours into Polyiso-butylene *J Am Chem Soc* 75, 1255-1256.
- Prager, S., Long, F. A. 1951. Diffusion of hydrocarbons in polyisobutylene. *J. Am. Chem. Soc.* 73:4072-4075.
- Prinderre, P., Cature, E., Piccerelle, Ph., Kalantzis, G., Kaloustian, J., Joachim, J. 1997. Evaluation of some protective agents on stability and controlled release of oral pharmaceutical forms by fluid bed technique. *Drug Dev. Ind. Pharm.*, 23, 817-826.

- Quinn, F. X., Kampff, E., Smyth, G., McBrierty, V. J. 1988. Water in hydrogels. 1. A Study of Water in Poly(N-Vinyl-2-pyrrolidone/methylmethacrylate) Copolymer. *Macromolecules*, 21, 3191-3198.
- Rabatin, J. G., Gale, R. H., Newkirck, A. T. 1960. The mechanism and kinetics of dehydration of calcium hydrogen phosphate dihydrate. *J. Phys. Chem.*, 64, 491-493.
- Rabkin, S. W. 1992. The calcium antagonist diltiazem has antiarrhythmic effects which are mediated in the brain through endogenous opioids. *Neuropharmacology*, 31, 487-496.
- Rezac, M. E., Schöberl, B., 1999. Transport and thermal properties of poly(ether imide) / acetylene-terminated monomer blends. *J. Membr. Sci.*, 156, 211-222.
- Rhodes, C. T., Porter, S. C., 1998. Coatings for controlled-release drug delivery systems. *Drug Dev. Ind. Pharm.*, 34, 1139-1154.
- Richards, J. H., Aulton, M. E., 1988. Kinetics and Stability Testing., In: Aulton, M. E., (Ed.). *Pharmaceutics The science of dosage form design*, Churchill Livingstone, Edinburgh, pp. 125-128.
- Riegelman, S., Collier, P., 1980. The application of statistical moment theory to the evaluation of in vivo dissolution time and absorption time. *J. Pharmacokinet. Biopharm.*, 8, 509-534.
- Rodriguez, O., Fornasiero, F., Arce, A., Radke, C. J., Prausnitz, J. M. 2003. Solubilities and diffusivities of water vapor in poly(methylmethacrylate), poly(2-hydroxyethylmethacrylate), poly(N-vinyl-2-pyrrolidone) and poly(acrylonitrile). *Polymer* 44, 6323–6333.
- Roe, R. J., 1991. *Computer simulations of polymers*, Prentice Hall, Eaglewood Cliffs, pp.
- Romero-Torres, S., Pérez-Ramos, R., Morris K. R., Grant, G. R., 2005. Raman spectroscopic measurement of tablet-to-tablet coating variability *J. Pharm., Biomed. Anal*, 38, 270-274
- Rowe, R. C., 1984., *Materials Used in the Film Coating of Oral Dosage Forms*. In: Florence, A. T., (Ed.), *Materials Used in Pharmaceutical Formulation*, Blackwell Scientific Publications, Oxford, pp. 1-36.
- Rowe, R.C., 1985. Film coating-ideal process for the production of modified release oral dosage forms. *Pharm. Int.*, 6, 14-17.
- Rubinstein, M. H., 1988. Tablets. In: Aulton, M. E., (Ed.). *Pharmaceutics The science of dosage form design*, Churchill Livingstone, Edinburgh, pp. 304-321.
- Ruotsalainen, M., Heinamaki, J., Taipale, K., Yliruusi, J., 2003. Influence of the aqueous film coating process on the properties and stability of tablets containing a moisture-labile drug. *Pharm. Devt Technol.*, 8, 443-451.
- Rutherford, S. W., 2001. Polymer permeability and time lag at high concentrations of sorbate. *J. Membr. Sci.*, 183, 101-107.

- Ruthven, D. M., 1984., Principles of Adsorption and Adsorption Processes, John Wiley and Sons, Inc., New York, pp. 1-60.
- Sakr, A. M., Elsabbagh, H. M., Emara, K. M., 1974. Sta-Rx 1500 starch: a new vehicle for the direct compression of tablets. *Arch. Pharm. Chem. Sci.*, 2, 14-24.
- Salame, M. 1986. Prediction of gas barrier properties of high polymers. *Polymer Engineering and Science*, 26, 1543-1546.
- Salwin, H., 1963., Moisture levels required for stability in dehydrated foods. *Food Technology*, 8, 58-61.
- Sanders, E. S., 1988. Penetrant-induced plasticization and gas permeation in glassy polymers. *J. Membr. Sci.*, 37, 63-80.
- Sastry, S. V., Wilber, W., Reddy, I. K., Khan, M. A. 1998. Aqueous-based polymeric dispersion: preparation and characterization of cellulose acetate pseudolatex *Int. J. Pharm.*, 165, 175-189.
- Serad, G. E., Freeman, B. D., Stewart, M. E., Hill, A. J. 2001. Gas and vapour sorption and diffusion in poly(ethylene terephthalate). *Polymer* 42, 6926-6943.
- Shelukar, S., Ho, J., Zega, J., Roland, E., Yeh, N., Quiram, D., Nole, A., Katdare A., Reynolds, S. 2000. Identification and characterization of factors controlling tablet coating uniformity in a Wurster coating process. *Powder Technology*, 110, 29-36
- Slade, L., Levine, H., 1993. Water relationships in starch transitions. *Carbohydrate Polymers* 21, 105-131.
- Smith, B. 1973. Basic Thermodynamics. Imperial College Press, pp. 36-62.
- Soles, C. L., Chang, F. T., Gidley, D. W., Yee, A. F., 2000. Contributions of the nanovoid structure to the kinetics of moisture transport in epoxy resins. *J. Polymer Sci.*, 38, 776-791.
- Soney, C. G., Sabu, T., 2001. Transport phenomenon through polymeric systems. *Progr. Polym. Sci.*, 26, 985-1017.
- Spitael, J., Kinget, R., 1977. Preparation and evaluation of free films. *Pharm. Acta. Helv.*, 52, 47-50.
- Srinivasa, P. C., Ramesh, M. N., Kumar, K. R., Tharanathan, R. N., 2003. Properties and sorption studies of chitosan-poly(vinyl alcohol) blend films. *Carbohydrate Polymers*, 53, 431-438.
- Stading, M., Rindlav-Westling, A., Gatenholm, P. 2001. Humidity-induced structural transitions in amylose and amylopectin films. *Carbohydrate Polymers* 45, 209-217.
- Stannett, V. T., 1968. Simple gasses. In: Crank J., Park, G. S., (Eds.). *Diffusion in polymers*, Academic Press, London, pp. 41-73.
- Stannett, V. T., 1978, The transport of gases in synthetic polymeric membranes-an Historic perspective. *J. Membr. Sci.*, 3, 97.
- Stannett, V. T., Hopfenberg, H. B., Petropoulos, J. H., 1972. In: Bawn, C. E. H., (Ed.), *MTP International Reviews of Science*, Vol. 8, Butterworths, London. pp. 329-369.

Stannett, V. T., Koros W. J., Paul D. R., Lonsdale H.K., Baker R.W. 1979. Recent advances in polymer membrane science technology and technology. *Adv. In Polymer Sci.* 32, 69-121.

Stannett, V. T., Koros, W. J., Paul, D. R., Lonsdale, H. K., Baker, R. W., 1970. Recent advances in membrane science and technology. In: Flinn, J. E, (Ed.), *Membrane science and technology: Industrial, Biological and Waste Treatment*, Plenum Press, pp. 71-121.

Stern S. A., Trohalaki, S., 1990. Fundamentals of Gas Diffusion in Rubbery and Glassy Polymers. In: Koros, W. J., (Ed.), *Barrier Polymers and Structures*, ACS Symposium Series, No. 43, pp. 22-59.

Stern, S. A., Frisch, H. L., 1981. The selective permeation of gases through polymers. *Ann. Rev. Mat. Sci.*, 11, 523-550.

Stuart, B., 2004. *Infrared Spectroscopy: Fundamentals and Applications*. John Wiley and Sons, West Sussex, England, pp. 113-135; 168.

Stubberud, L., Arwidsson, H. G., Graffner, C., 1995. Water-solid interactions. Part 1. Techniques for studying moisture sorption/desorption. *Int. J. Pharm.*, 114, 55-64.

Sun, Y., Lee, H., 1996. Sorption/desorption properties of water vapour in poly (2-hydroxyethyl methacrylate): 1. Experimental and preliminary analysis. *Polymer*, 37, 3915–3919.

Surana, R. K., Danner, R. P., Tihnuinhiogi, F., Duda, J. L., 1997. Evaluation of inverse gas chromatography for prediction of and measurement of diffusion coefficients. *J. Polym. Sci., Part B* 35, 1233-1240.

Tanaka, K., Kita, H., Okano, M., Okamoto, K. 1992. Permeability and permeaselectivity of gases in fluorinated and non-fluorinated polyimides. *Polymer* 33, 585-582.

Tanigawara, Y., Yamaoka, K., Nakagawa, T., Uno, T., 1982. New method for the evaluation of an in vitro dissolution and disintegration time. *Chem. Pharm. Bull.*, 30, 1088-1090.

Theodorou, D. N., 1996. In: Neogi, P., (Ed.), *Diffusion in polymers*, Marcel Dekker, New York. Pp. 67-142.

Thielmann, F. 2004. Introduction into the characterization of porous materials by IGC. *J. Chromatography A*. 1037, 175-123.

Thoma, K, Bechtold, K., 1999. Influence of aqueous coatings on the stability of enteric coated pellets and tablets. *Eur. J. Pharm. Biopharm.*, 47, 39-50.

Thrasher, S. R., Rezac, E. M., 2004. Transport of water and methanol vapours in alkyl substituted poly(norisomane). *Polymer*, 45, 2641-2649.

Ticehurst, M. D., York, P., Rowe, R. C., Dwivendi, S. K., 1996. Characterization of the surface properties of lactose with IGC, used to detect batch variation. *Int. J. Pharm.*, 141, 93-99.

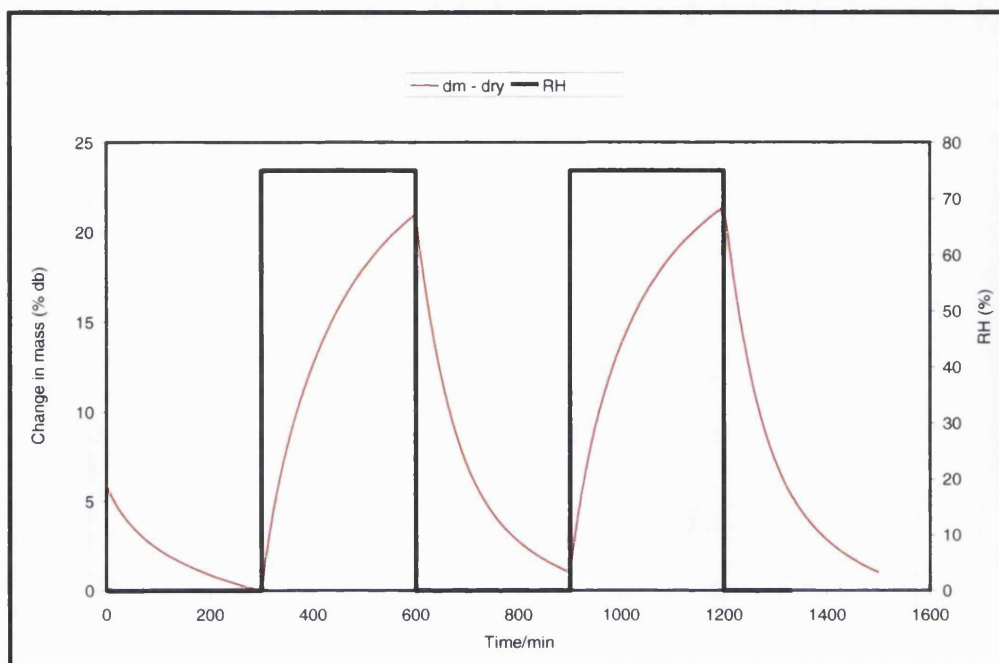
Timmermann, E. O. 2003., Multilayer sorption parameters: BET or GAB values?. *Colloids and Surfaces A: Physicochem. Eng. Aspects*, 220, 235-260.

- Tishmack, P. A. Bugay, D. E. Byrn, S. R., 2003. Solid-state nuclear magnetic resonance spectroscopy - pharmaceutical applications. *J. Pharm. Sci.*, 92, 441-474.
- Tsujita, Y. 2003. Gas sorption and permeation of glossy polymers with microvoids. *Prog. Polym. Sci* 28, 1377-1401.
- Tvardovski, A. V., Fomkin, A. A., Tarasevich, Yu. I., Zhukova, A. I., 1997. Hysteresis phenomenon in the study of sorptive deformation of sorbents. *J. Colloids and Interfaces*, 191, 117-119.
- Ulutan, S., Balkose, D. 1996. Diffusivity, solubility and permeability of water vapor in flexible PVC/silica composite membranes. *Journal of Membrane Science* 115, 217-224.
- Umprayn, K., Mendes, R. W., 1987., Hygroscopicity and moisture adsorption kinetics of pharmaceutical solids: A review. *Drug Dev. Ind. Pharm.*, 13, 653-693.
- US Pharmacopeia 24 and National Formulary 18, 2000. United States Pharmacopeial Convention, Inc., 1840, Rockville, MD.
- van Campen, L., Zografi, G., Carstensen, J. T., 1980. Approach to the evaluation of hygroscopicity for pharmaceutical solids. *Int. J. Pharm.*, 5, 1-18.
- van Den Berg, C., Bruin, S., 1981. Water Activity and its Estimation in Food Systems: Theoretical Aspects. In: Rockland, L. B., Stewart, G. F., (Eds.), *Water Activity: Influences on Food Quality*.
- van der Wel, G.K., Adan, O.C.G., 1999. Moisture in organic coatings – a review. *Progress in Organic Coatings* 37, 1-14.
- van Krevelen, D. W., 1990. Properties of Polymers, Their correlation with chemical structure, their numerical estimation and prediction from additive group contributions, 3rd Ed., Elsevier, Amsterdam.
- van Savage, G, Rhodes, C. T., 1995. Sustained release coating of solid dosage forms: historical review. *Drug Dev. Ind. Pharm.*, 21, 93-118.
- Vieth, W. R., 1988. *Membrane Systems: Analysis and Design*: Hanser Publishers, New York.
- Vieth, W. R., 1991. Diffusion In and Through Polymers. Principles and Applications. Carl Hanser Verlag, Munich. pp. 200-214.
- Villalobos, R., Hernandez-Munoz, P., Chiralt, A. 2005. Effect of surfactants on water sorption and barrier properties of hydroxypropyl methylcellulose films. *Food Hydrocolloids* xx, 1-8.
- Vogt, M., Hauptmann, R. 1995. Plasma-deposited passivation layers for moisture and water protection . *Surface and Coatings Technol.*, 74-75, 676-681.
- von Fraunhofer, J. A., Boxall, J., 1976. *Protective paint coatings for metals.*, Portcallis Press, London, pp.
- Vrentas, J. S., Duda, J. L., 1977. Diffusion in polymer-solvent systems I, *J. Polym. Sci., Polym. Phys. Ed.* 15, 403-452.

- Walia, P. S., Stout, P. J., Turton, R., 1998. Preliminary evaluation of an aqueous wax emulsion for controlled-release coating. *Pharm Dev Technol.*, 3, 103-113.
- Wanchai, S., Craig, D. Q. M., Newton, J. M., 1996. The use of dielectric analysis as a means of characterizing the effects of moisture uptake by pharmaceutical glyceride bases. *Int. J. Pharm.*, 132, 1-8.
- Weinkauff, D. H., Paul, D. R., 1990., Effects of structure order on barrier properties, In: Koros, W. J., *Barriers Polymers and Structures*. ACS Symposium Series, 423. pp.
- Wessling, M., Schoeman, S., van den Boomgaard, Th., Smolders, C. A., 1991. Plasticization of gas separation membranes. *Gas Sep. Purif.* 5, 222-228.
- Wijmans, H., Baker, R. W., 1995. The solution-diffusion model: a review. *J. Membr. Sci.*, 107, 1-21.
- Wolffarth, C., 2004. Enthalpy changes in polymer solutions at elevated temperatures. In: Wolffarth, C., (Ed.), *Handbook of thermodynamic data of polymer solutions at elevated temperatures*, CRC Press, pp. 377-424.
- Wu, C., McGinity, J. W., 2000. Influence of relative humidity on the mechanical and drug release properties of theophylline pellets coated with an acrylic polymer containing methylparaben as a non-traditional plasticizer. *Eur. J. Pharm. Biopharm.*, 50, 277-284.
- Wu, Y., Fassihi, R. 2005. Stability of metronidazole, tetracycline HCl and famotidine alone and in combinations. *Int. J. Pharm.*, 290, 1-13.
- Yi-Yan, R.M. Felder and W.J. Koros. Selective permeation of hydrocarbon gases in poly(tetrafluoroethylene) and poly(fluoroethylene-propylene) copolymer *J Appl Polym Sci* 25 (1980), p. 1755 - 1774.
- Young, J. H., Nelson, G. H., 1967. Theory of hysteresis between sorption and desorption isotherms in biological materials. *Trans. Am. Soc. Agricultural Eng.*, 10, 260-263.
- Zimm, B.H., Lundberg, J. L., 1956. Sorption of vapours by high polymers. *J. Phys. Chem.* 60, 425-428.
- Zimmerman, C. M., Koros, W. J., 1999. Comparison of gas transport and sorption in the ladder polymer BBL and some semi-ladder polymers. *Polymer*, 40, 5655-5664.
- Zograf, G., 1988. States of water associated with solids. *Drug Dev. Ind. Pharm.*, 14, 1905-1919.
- Zograf, G., Kontny, M. J., 1986. The interaction of water with cellulose and starch-derived pharmaceutical excipients. *Pharm. Res.*, 3, 187-194.

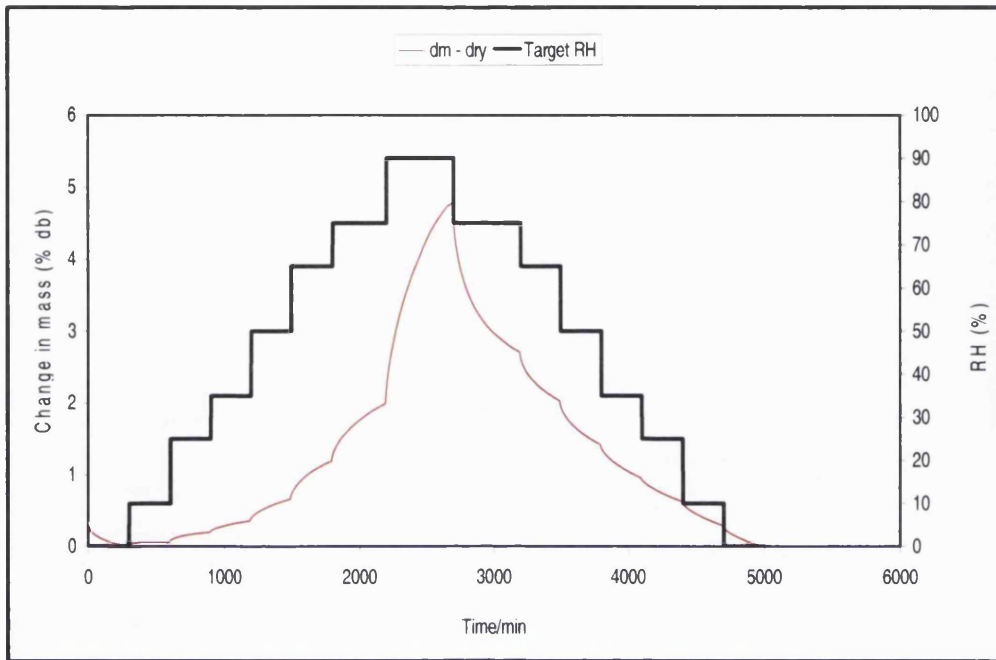
APPENDICES

APPENDIX 1

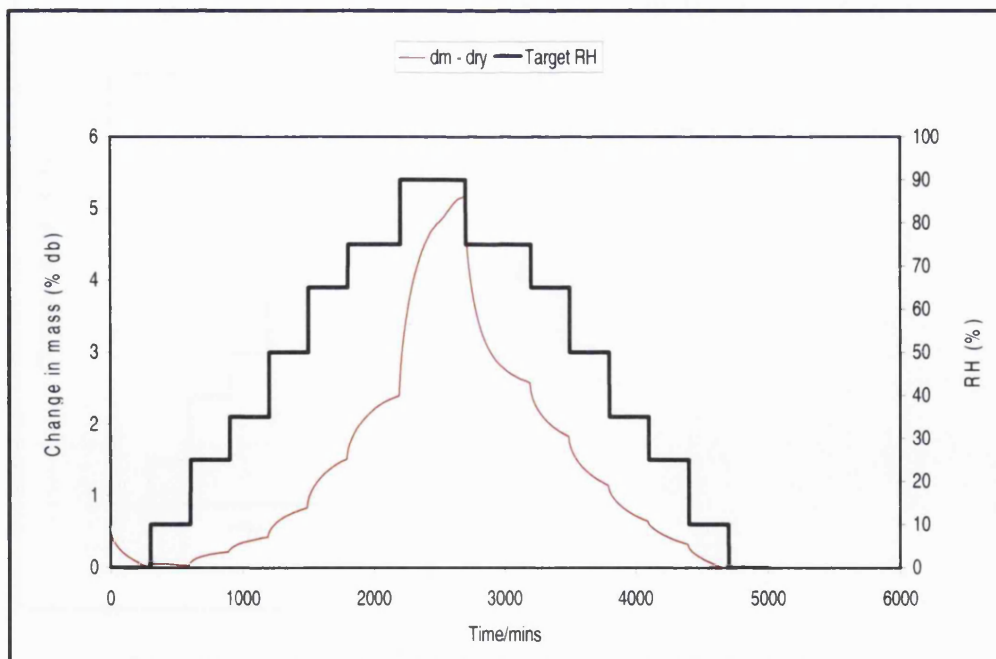


Typical Fixed-Time Moisture Sorption-Desorption Profile of Xanthan gum Exposed to 0-75-0-75-0 %RH Cycle (25 °C)

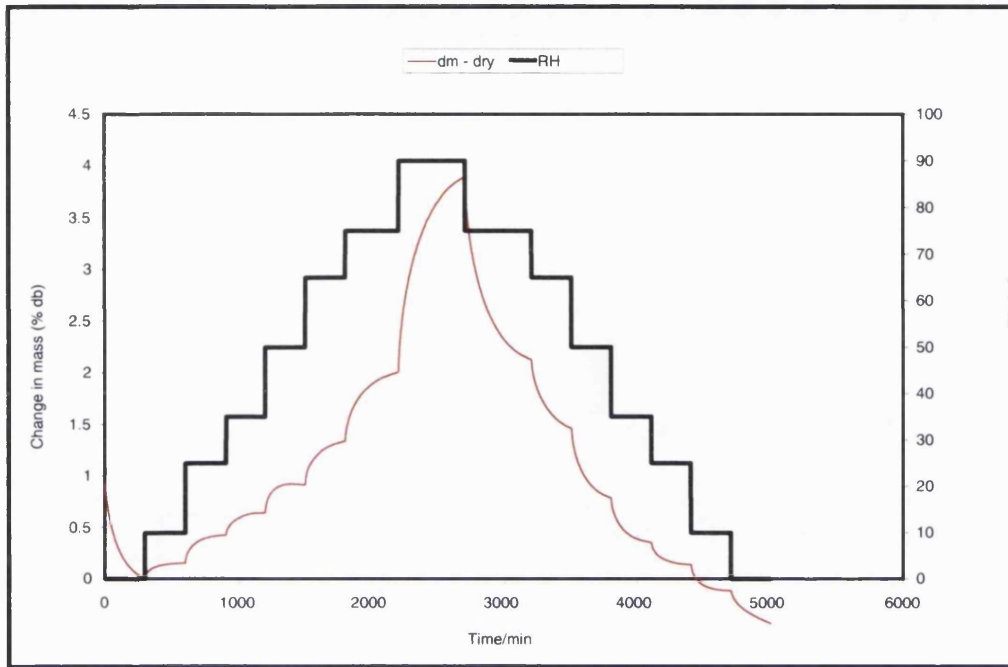
APPENDIX 2



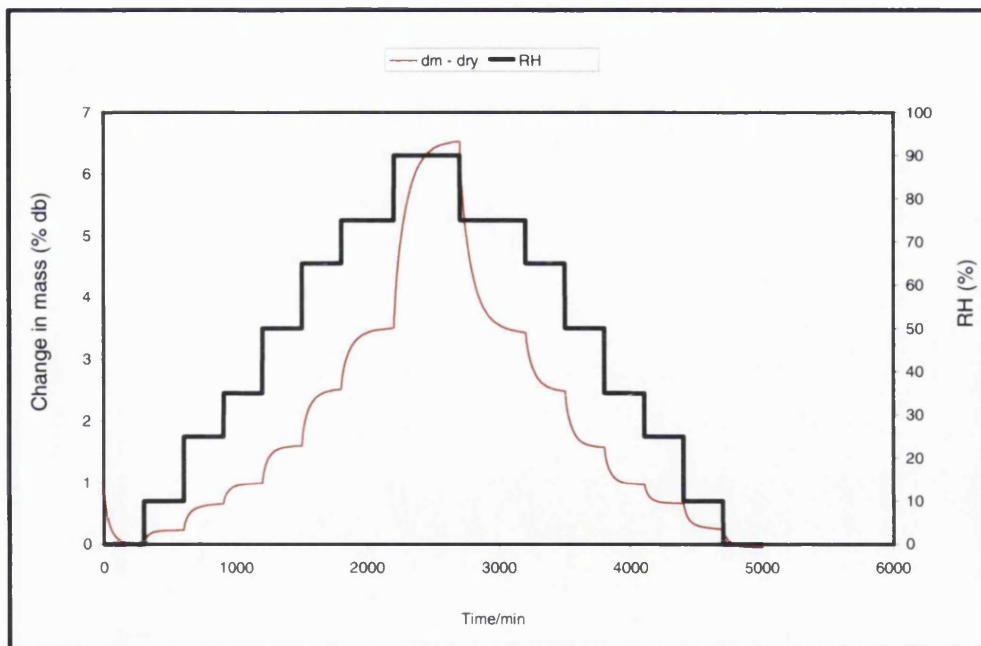
Typical Equilibrium Moisture Sorption-Desorption Profile of Ethyl methacrylate Film Exposed to 0-10-25-35-50-65-75-90-75-65-50-35-25-10-0 %RH Cycle (30 °C)



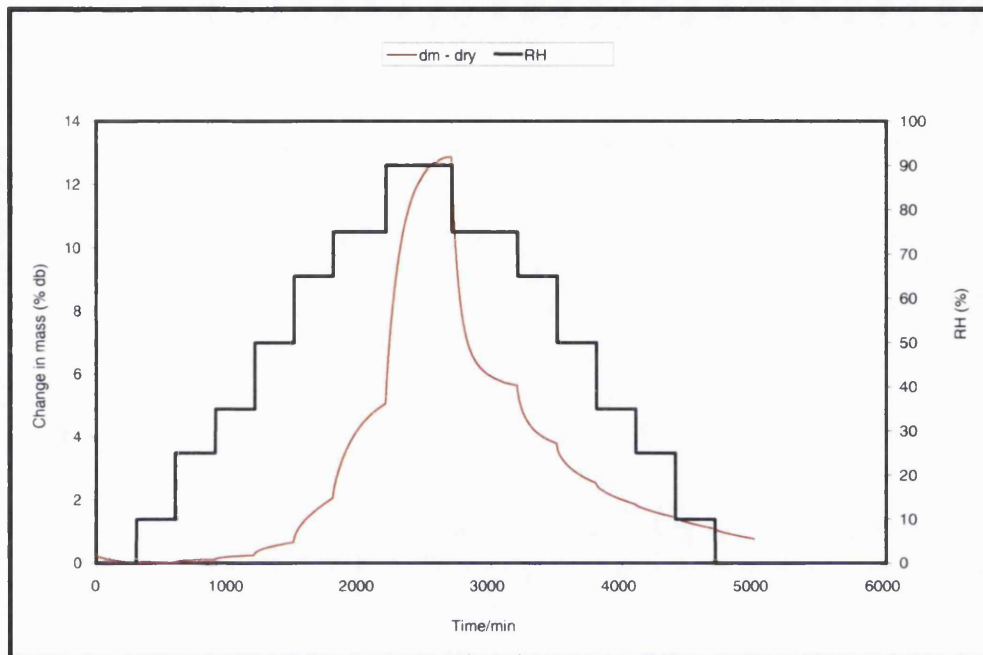
Typical Equilibrium Moisture Sorption-Desorption Profile of Ethyl methacrylate Film Exposed to 0-10-25-35-50-65-75-90-75-65-50-35-25-10-0 %RH Cycle (40 °C)



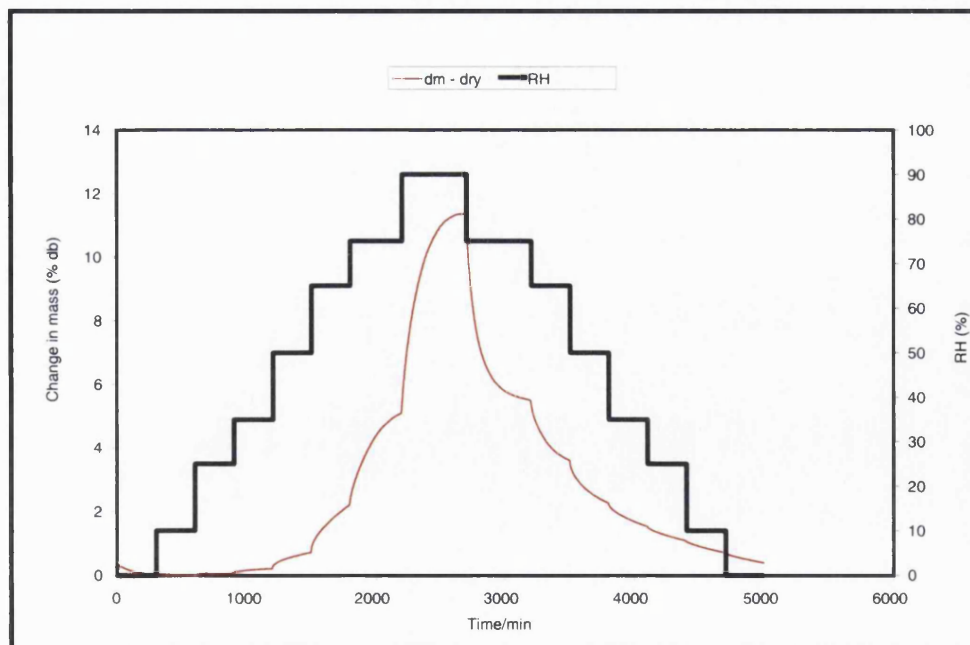
Typical Equilibrium Moisture Sorption-Desorption Profile of Eudragit EPO Film Exposed to 0-10-25-35-50-65-75-90-75-65-50-35-25-10-0 %RH Cycle (30 °C)



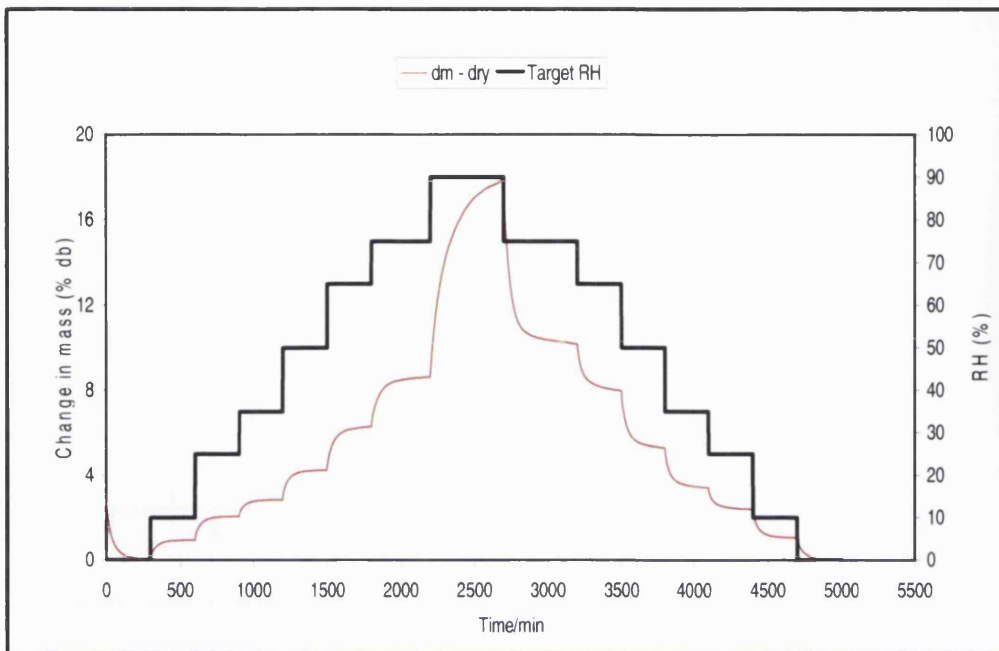
Typical Equilibrium Moisture Sorption-Desorption Profile of Eudragit EPO Film Exposed to 0-10-25-35-50-65-75-90-75-65-50-35-25-10-0 %RH Cycle (40 °C)



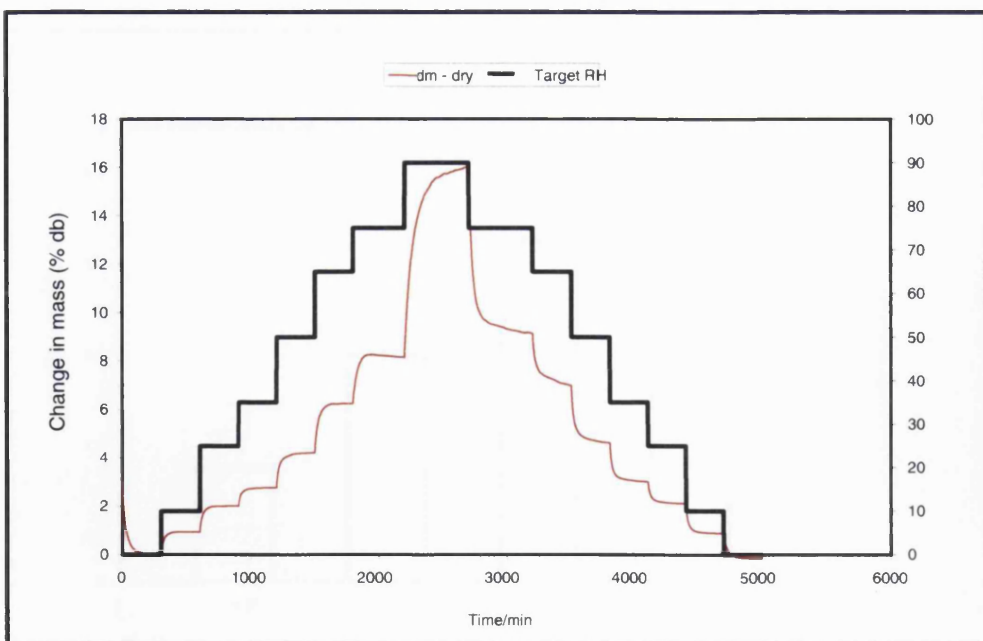
Typical Equilibrium Moisture Sorption-Desorption Profile of Opadry AMB Film Exposed to 0-10-25-35-50-65-75-90-75-65-50-35-25-10-0 %RH Cycle (30 °C)



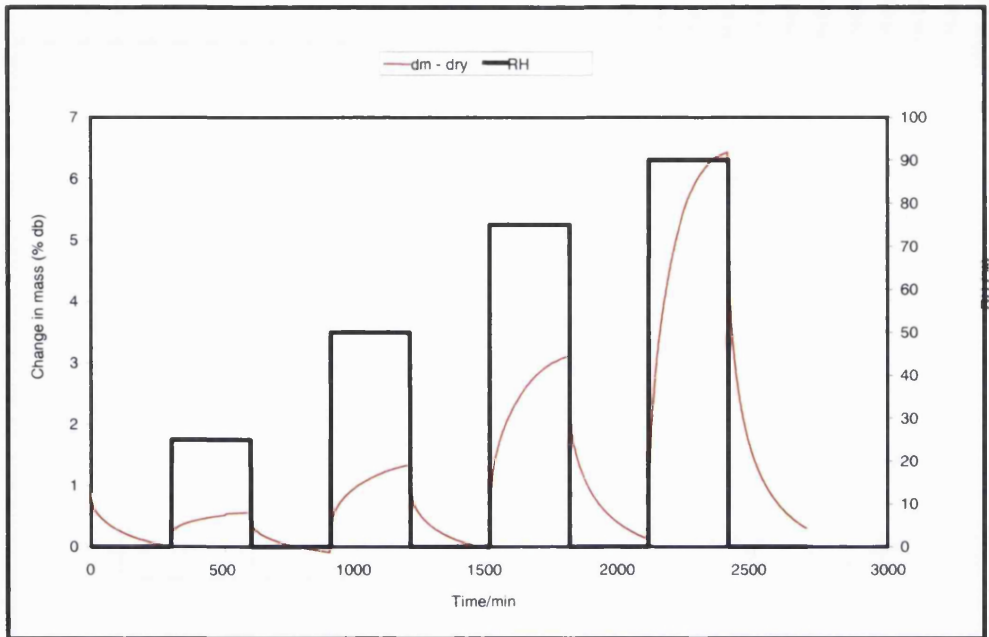
Typical Equilibrium Moisture Sorption-Desorption Profile of Poly(vinyl alcohol) Film Exposed to 0-10-25-35-50-65-75-90-75-65-50-35-25-10-0 %RH Cycle (40 °C)



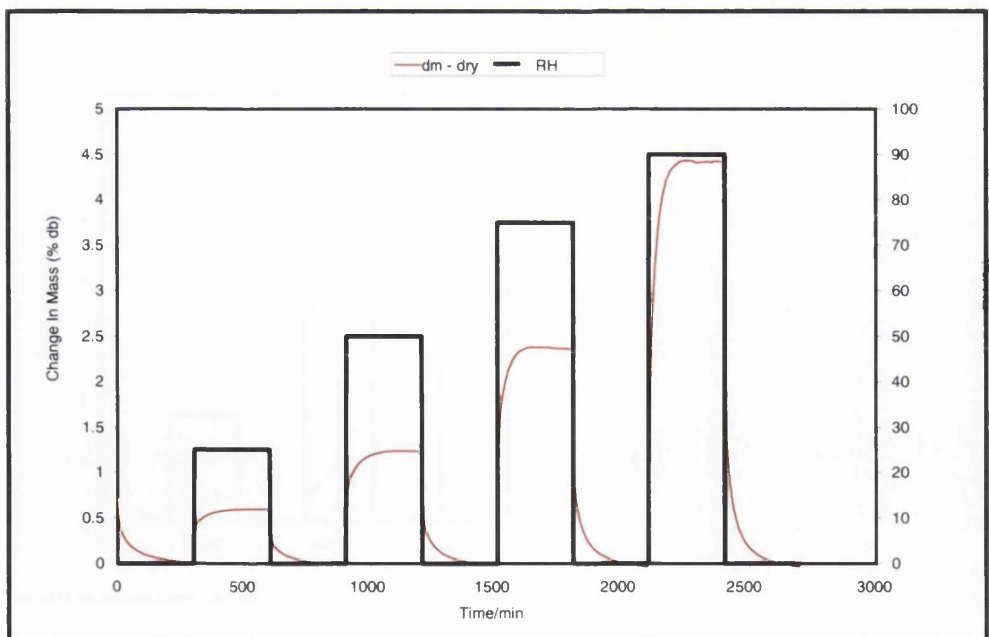
Typical Equilibrium Moisture Sorption-Desorption Profile of Sepifilm LP Film Exposed to 0-10-25-35-50-65-75-90-75-65-50-35-25-10-0 %RH Cycle (30 °C)



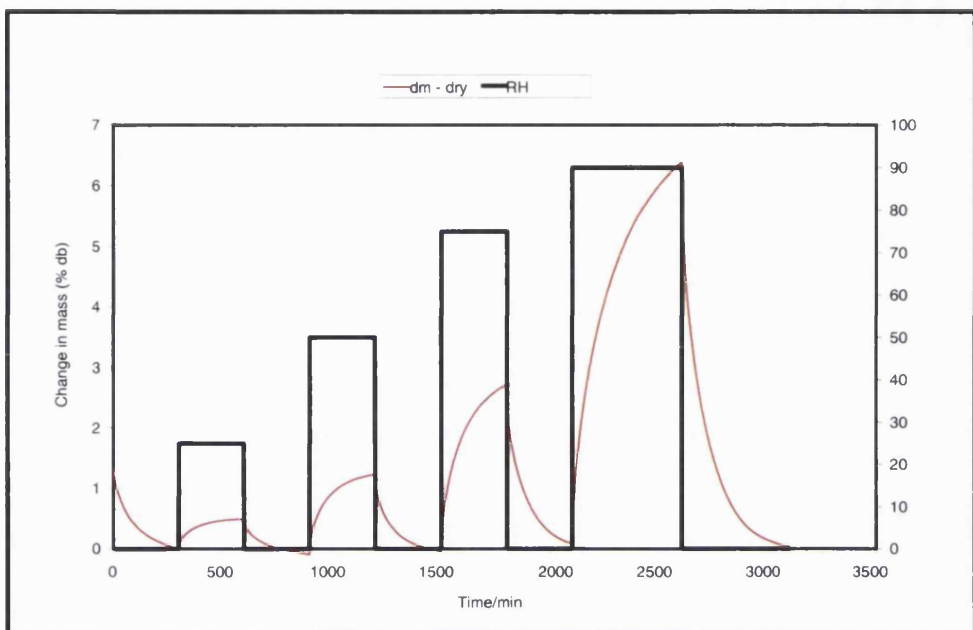
Typical Equilibrium Moisture Sorption-Desorption Profile of Sepifilm LP Film Exposed to 0-10-25-35-50-65-75-90-75-65-50-35-25-10-0 %RH Cycle (40 °C)



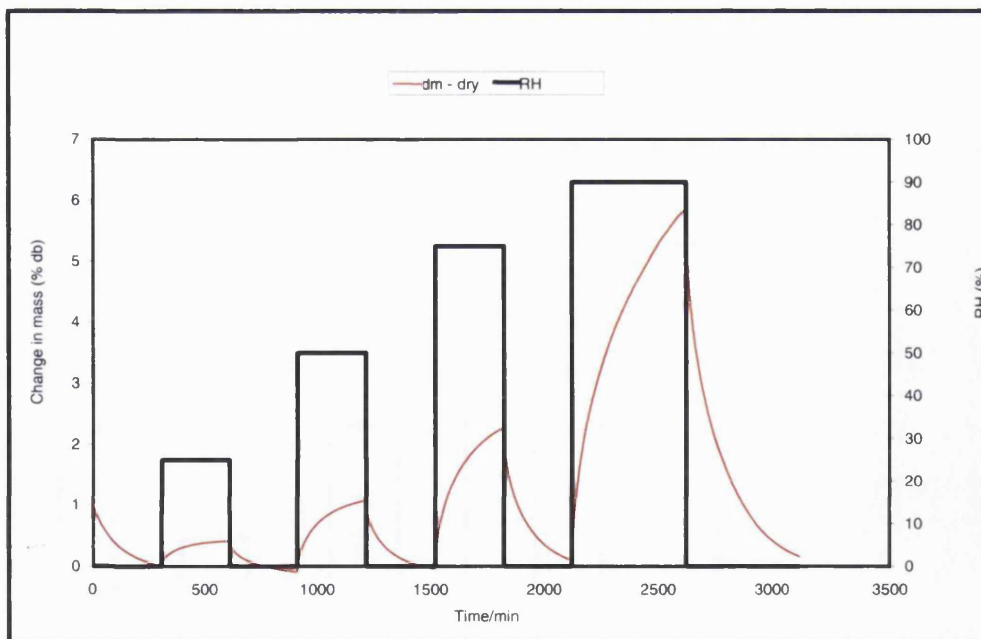
Typical Step-wise Equilibrium Moisture Sorption-Desorption Profile of Ethyl methacrylate Film Exposed to 0-25-0-50-0-75-0-90-0 %RH Cycle (30 °C)



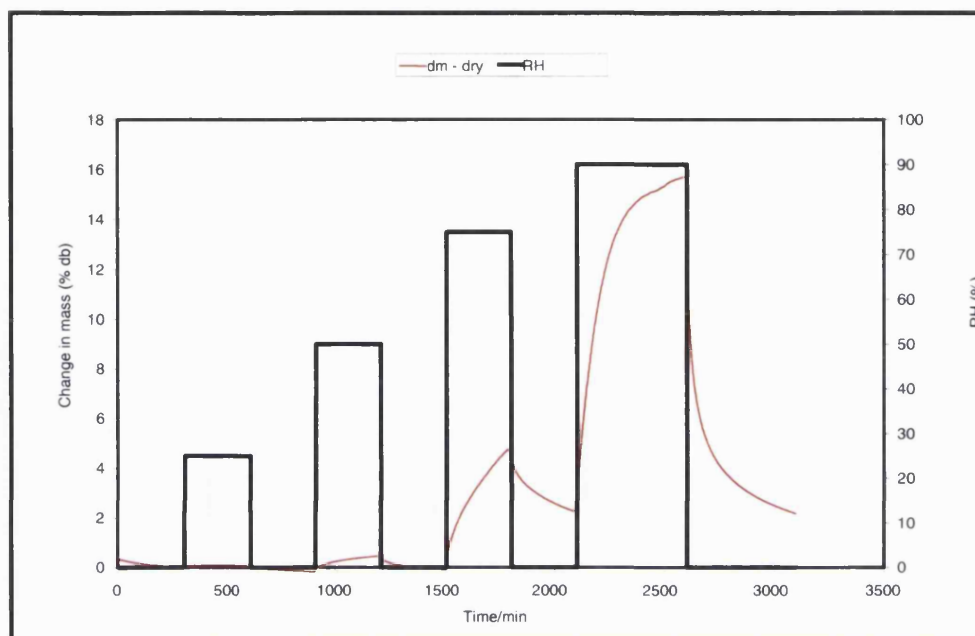
Typical Step-wise Equilibrium Moisture Sorption-Desorption Profile of Ethyl methacrylate Film Exposed to 0-25-0-50-0-75-0-90-0 %RH Cycle (40 °C)



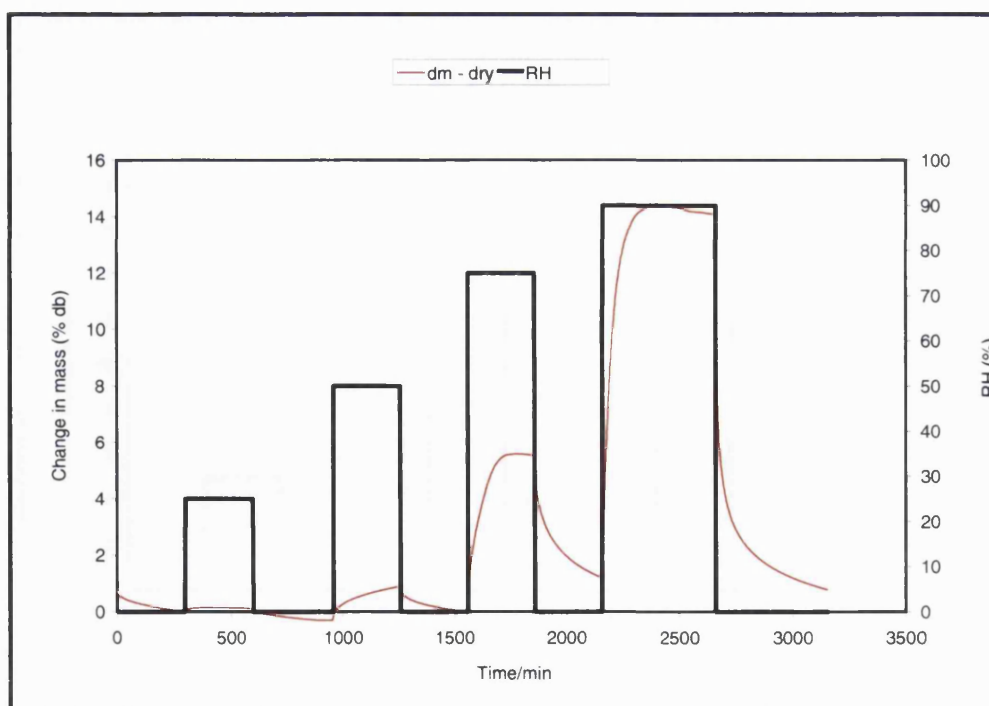
Typical Step-wise Equilibrium Moisture Sorption-Desorption Profile of Eudragit EPO Film Exposed to 0-25-0-50-0-75-0-90-0 %RH Cycle (30 °C)



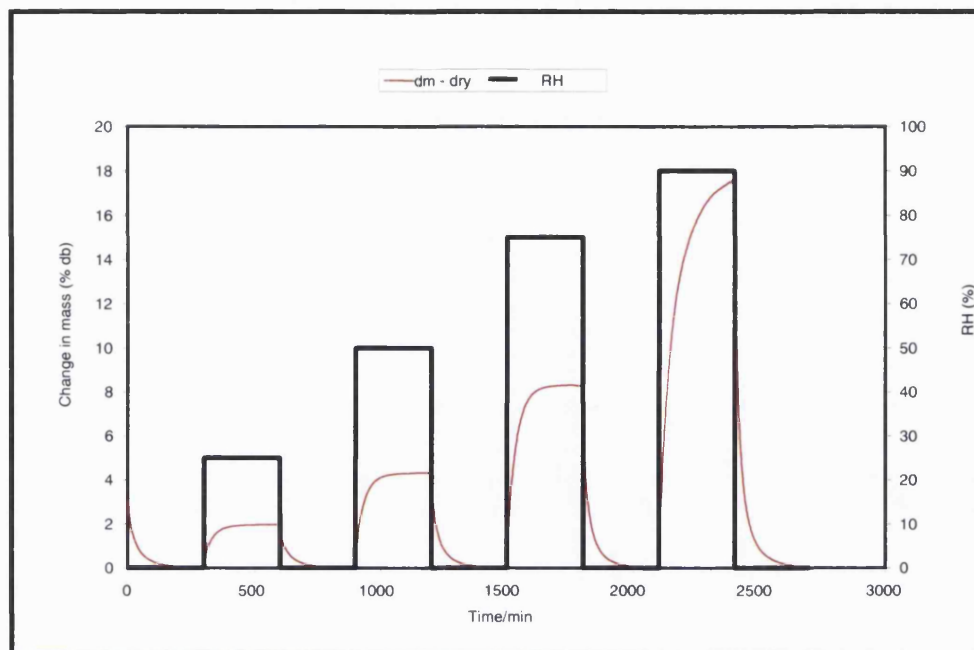
Typical Step-wise Equilibrium Moisture Sorption-Desorption Profile of Eudragit EPO Film Exposed to 0-25-0-50-0-75-0-90-0 %RH Cycle (40 °C)



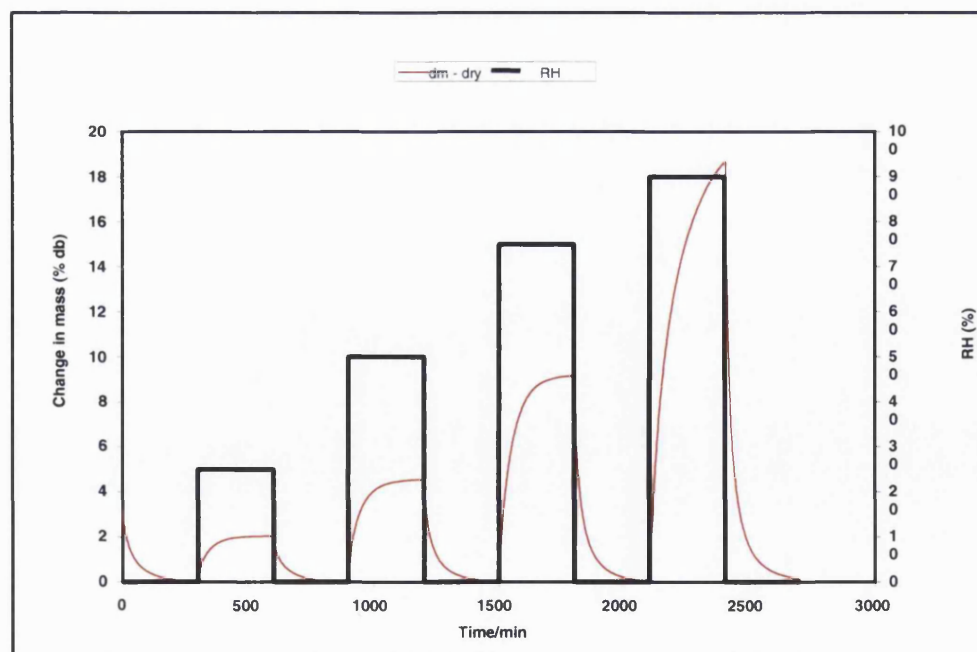
Typical Step-wise Equilibrium Moisture Sorption-Desorption Profile of Opadry AMB Film Exposed to 0-25-0-50-0-75-0-90-0 %RH Cycle (30 °C)



Typical Step-wise Equilibrium Moisture Sorption-Desorption Profile of Opadry AMB Film Exposed to 0-25-0-50-0-75-0-90-0 %RH Cycle (40 °C)

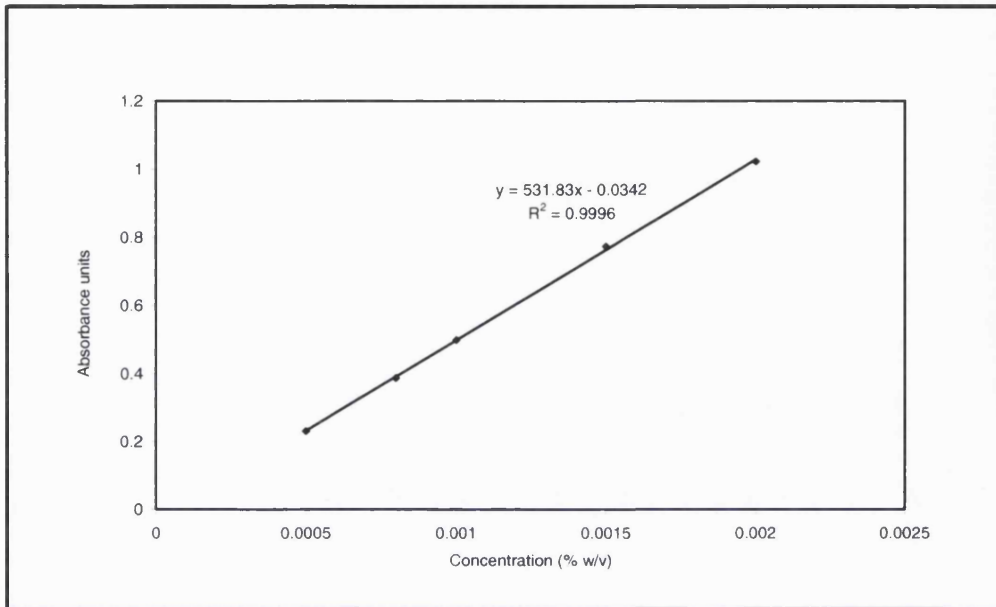


Typical Step-wise Equilibrium Moisture Sorption-Desorption Profile of Sepifilm LP Film Exposed to 0-25-0-50-0-75-0-90-0 %RH Cycle (30 °C)

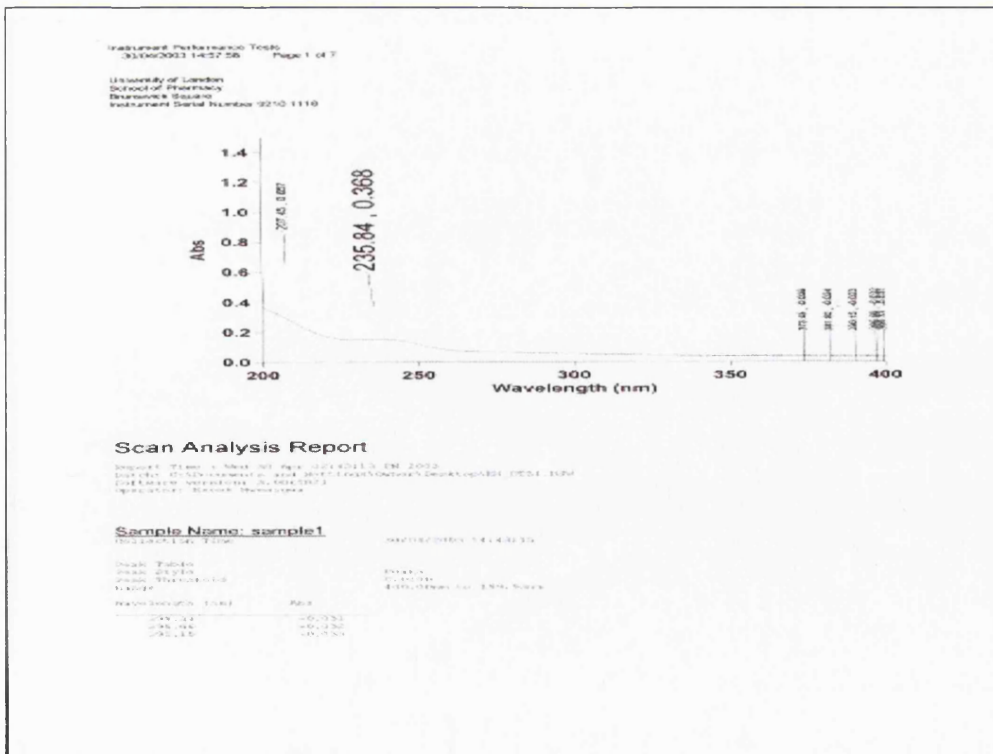


Typical Step-wise Equilibrium Moisture Sorption-Desorption Profile of Sepifilm LP Film Exposed to 0-25-0-50-0-75-0-90-0 %RH Cycle (40 °C)

APPENDIX 3

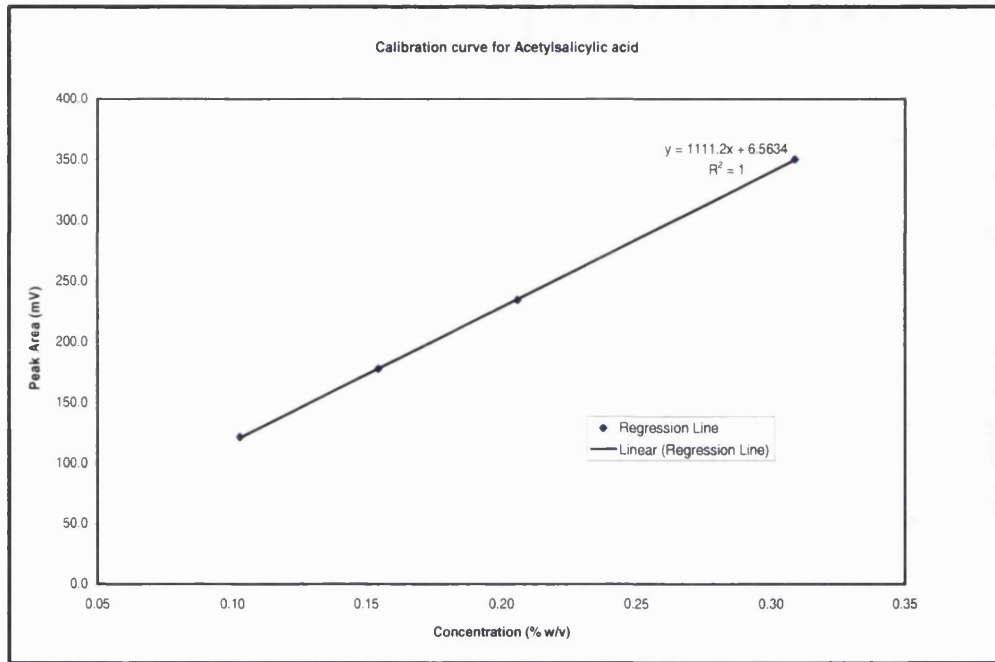


Calibration Curve for the Quantitative Analysis of Diltiazem HCl by UV-Vis Spectroscopy

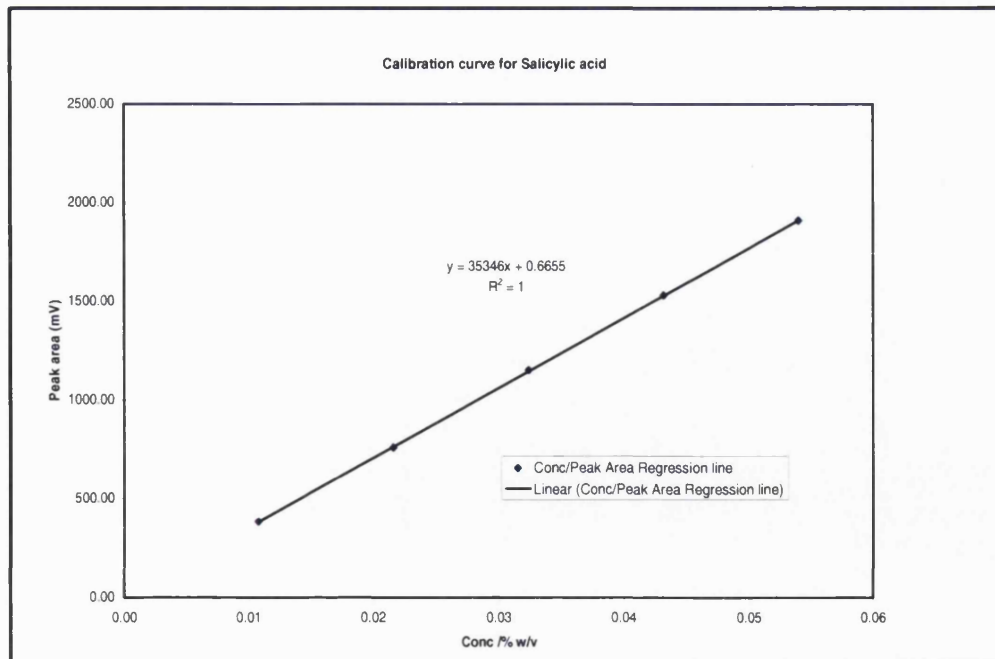


UV-Vis Spectrophotometer Scan Analysis Summary Report Showing the Peak of Maximum Absorption for Diltiazem HCl

APPENDIX 4



Calibration Curve for the Quantitative Analysis of aspirin by acid by HPLC



Calibration Curve for the Quantitative Analysis of Salicylic Acid by Reverse Phase HPLC

APPENDIX 5

(Reprint of article where part of this work has been previously published)

The Hygroscopicity of Moisture Barrier Film Coatings

Enosh Mwesigwa, Graham Buckton, and Abdul W. Basit

Department of Pharmaceutics,
The School of Pharmacy,
University of London, 29-39
Brunswick Square, London
WC1N 1AX, UK

ABSTRACT The hygroscopicity of three commercial moisture-barrier film coatings, namely, Eudragit L30 D-55 (methacrylic acid-ethyl acrylate copolymer), Opadry AMB (polyvinyl alcohol based system), and Sepifilm LP 014 (hypromellose, microcrystalline cellulose, and stearic acid based formulation), was investigated using a dynamic vapor sorption apparatus. Moisture uptake by cast films and uncoated and coated tablet cores, which were designed to be hygroscopic, low hygroscopic, and waxy, was measured following exposure to repeat relative humidity (RH) cycles of 0-50-0-50-0%, 0-75-0-75-0%, and 0-90-0-90-0% RH at 25°C. Eudragit cast film exhibited the fastest equilibration but was also the least hygroscopic. Sepifilm had the fastest sorption and took up the greatest mass of water. The rate of uptake for Opadry film was similar to Sepifilm. However, this film continued to sorb moisture for a longer period. When returned to 0% RH it retained moisture in the film showing that it had a high affinity for moisture within the film. The data for the different cores indicated that there was very little benefit in using a moisture barrier film on cores with low hygroscopicity, the mass gain being a sum of that which would be expected to sorb to the film and that which sorbs to the uncoated core. There was, however, some advantage for hygroscopic cores where, even though the barrier coatings allowed substantial water sorption into the core, the extent of this was less and the rate of uptake lower than for the uncoated sample.

KEYWORDS Moisture sorption, Film coating, Moisture barrier, Eudragit, Opadry, Sepifilm

INTRODUCTION

Moisture is an important factor in the deterioration of medicinal products. Sorption of moisture must therefore be prevented or at least minimized for products that are susceptible to hydrolysis. This can be achieved by careful formulation, e.g., the selection of the appropriate excipients for tablets (Carstensen, 1993; Zografi & Hancock, 1994), and/or through the use of more efficient packaging (Allinson et al., 2001). For certain formulations of solid dosage forms, it is preferable to apply a polymer coating with moisture-barrier properties (Prinderre et al., 1997). This approach is appealing because polymers

Address correspondence to Graham Buckton, Department of Pharmaceutics, The School of Pharmacy, University of London, 29-39 Brunswick Square, London WC1N 1AX, UK; Fax: +44-(0)-20-7753-5858; E-mail: graham.buckton@ulsop.ac.uk

afford coatings that are mechanically strong and their permeability can be tailored to meet specific formulation needs.

The functional qualities of polymer films can be profoundly affected by the presence of moisture (Alvarez-Lorenzo et al., 2000; Cervera et al., 2004; Morillon et al., 2000). Sorbed moisture interacts with hydrophilic polymers disrupting inter- and intramolecular hydrogen bonds. This reduces chain cohesion and mechanical integrity, increases the free volume of the polymer, and may enhance permeation through the polymer (Cervera et al., 2004; Morillon et al., 2000). This is of particular significance to the functionality of moisture barrier coatings. Thus, the role of environmental conditions, particularly humidity, on moisture uptake by moisture barrier coatings and how such conditions affect barrier performance must be examined.

Moisture uptake and permeation through polymers is commonly analyzed in terms of the solution-diffusion mechanism. The basic assumption of this mechanism is that the permeants partition ("dissolve") in the polymer membrane at the upstream side and then travel down a concentration gradient to the downstream side where they subsequently desorb ("desolve"). The quantitative measure of the amount of permeant transported through the membrane is the permeability coefficient, P , which is a product of the sorption coefficient S , and the diffusion coefficient D (Debeaufort et al., 1994; Vieth & Sladek, 1965):

$$P = [S][D] \quad (1)$$

The solubility coefficient S is a measure of the amount of penetrant sorbed by the polymer while the diffusion coefficient D characterizes the ability of the permeant to move within the polymer. Experimentally, the diffusion coefficient is obtained from sorption kinetics plots while S is obtained from the linear portion of the sorption isotherm where it is assumed Henry's law applies (Debeaufort et al., 1994; Rodríguez et al., 2003; Ruthven, 2004; Vieth & Sladek, 1965).

Data on the utility of moisture barrier coatings is very limited. Although the general consensus for formulation of moisture sensitive drug substances is to use excipients of low hygroscopicity and/or low water activity (Ahlneck & Zografi, 1990; Zografi & Hancock, 1994), it is not clear whether the nature of the tablet

formulation influences the performance of barrier coatings. To the authors' knowledge, no work has previously evaluated the sorption properties of barrier coatings, especially after application to tablet cores of different hygroscopicities. This study, therefore, aimed to evaluate the sorption and desorption properties of three moisture barrier coatings, i.e., Eudragit L30 D-55 (a methacrylic acid-ethyl acrylate copolymer), Opadry AMB (polyvinyl alcohol based system), and Sepifilm LP 014 (hypromellose, microcrystalline cellulose, and stearic acid based formulation) after application onto tablet cores designed to be highly hygroscopic, low hygroscopic, and waxy. Dynamic vapor sorption technique was adopted as the method of choice as it has been demonstrated a suitable technique for studying sorption phenomenon in pharmaceutical materials (Begren, 1994; Lane & Buckton, 2000).

MATERIALS AND METHODS

Materials

Eudragit L30 D-55, Opadry AMB, and Sepifilm LP 014 were free samples from Rohm GmbH (Darmstadt, Germany), Colorcon Limited (Dartford, UK), and Seppic UK Ltd. (Hounslow, London, UK), respectively. Tablet excipients were lactose monohydrate NF (Fastflow, Foremost, Wisconsin, USA), dibasic calcium phosphate dihydrate, BP (Emcompress, Penwest, Patterson, New York, USA), pregelatinized starch (Starch 1500, Colorcon Limited, Dartford, UK), and microcrystalline cellulose (Avicel PH101, FMC Corporation). All other materials were from Sigma-Aldrich and were of analytical grade.

METHODS

Preparation of Coating Dispersions

Opadry AMB and Sepifilm LP are proprietary ready-to-use systems that are supplied in powder form for reconstitution in water. The Opadry AMB system consists of partly hydrolyzed polyvinyl alcohol, titanium dioxide, talc, lecithin soya, and xanthan gum. It is recommended for use as a 25% w/v aqueous dispersion. Sepifilm LP is comprised of hypromellose, microcrystalline cellulose, stearic acid, and titanium

TABLE 1 Formula for Preparing Eudragit L30 D-55 Coating Dispersion

Ingredient	Quantity (g)
<i>Polymer solution</i>	
Eudragit L 30 D-55	333
Triethyl citrate	10
Water	267
<i>Pigment suspension</i>	
Talc	168
Titanium dioxide	100
Polyethylene glycol 6000	17
Sodium carboxymethylcellulose	5
Water	700

dioxide for use as a 12% w/v aqueous dispersion. Eudragit L30 D-55 is an anionic polymer supplied as a 30% w/v aqueous dispersion. Although it is mainly used for enteric coatings, it is also recommended for moisture barrier coatings where it is used as a 15% w/v aqueous dispersion. The manufacturer's recommended formula for such coatings is shown in Table 1 (Rohm GmbH). The coating dispersion was prepared by mixing a specified amount of Eudragit L30 D-55 and triethyl citrate with part of the water. In a separate container, polyethylene glycol was dissolved in the remaining amount of water, to which talc and sodium carboxymethylcellulose were added. The mixture was then homogenized with a high speed stirrer for 10 min. The polymer suspension and the pigment suspension were then combined with gentle stirring which was continued during coating.

Cast Film Preparation

Cast films were prepared by dispensing respective coating dispersions onto shallow teflon molds. Dispersions were then evenly spread with the aid of a draw down bar. Molds were subsequently transferred into a hot air oven and dried at 40°C for eight hours. After cooling, films were removed from molds and stored at room temperature over silica gel. Film thickness was measured to the nearest 0.001 mm by a digital micrometer (Mitutoyo Corporation, Japan).

Tablet Manufacture and Coating

Tablet cores were manufactured by direct compression using a Manesty Type F3 single stage tablet press (Manesty Machines Ltd., Liverpool, UK) equipped

with 8.0mm standard concave tooling. Details of the three tablet formulations used were: lactose monohydrate (69.4%), microcrystalline cellulose (15.0%), pre-gelatinized starch (15.0%), magnesium stearate (0.5%), and colloidal silica (0.1%) for hygroscopic cores; dibasic calcium phosphate dihydrate (99.5%) and magnesium stearate (0.5%) for low hygroscopic cores; and lactose monohydrate (78.0%), carnauba wax (14.0%), talc (3%), magnesium stearate (4.0%), and colloidal silica (1.0%) for waxy cores. The target tablet fill weight and mean crushing strength were 200 mg and 125 N, respectively.

Coating was undertaken in an Aeromatic Strea 1 (Aeromatic-Fielder AG, Bubendorf, Switzerland) fluidized bed coater. Coating conditions were: charge 100 g, inlet temperature 40±2°C, drying temperature 38±2°C, spray rate 5 mL/min, and atomizing air pressure of 0.2 bar. Coating levels were in keeping with dry weight gains recommended by the respective manufacturers, i.e., Eudragit L 30 D-55 1.8% (or a polymer loading of 1.0 mg/cm²), Opadry AMB 4%, and Sepifilm LP 3%.

Vapor Sorption Studies

Moisture sorption/desorption of cast films and uncoated and coated tablet cores was studied in a Dynamic Vapour Sorption apparatus (DVS 1, Surface Measurement Systems, London, UK) equipped with a Cahn D-200 digital recording balance, a moisture sorption analyzer, and an IBM compatible PC with DVSWIN software that allowed pre-programming of sorption/desorption regimes. A description and applicability of the dynamic vapor sorption technique has been made by (Begren, 1994). In this study, the following relative humidity (RH) cycles were employed, i.e., 0-50-0-50-0% RH, 0-75-0-75-0% RH, and 0-90-0-90-0% RH. The temperature was maintained at 25°C with the help of an incubator. All reported experiments were performed in triplicate unless otherwise stated.

RESULTS AND DISCUSSION

Moisture Sorption Profiles of Cast Films

The sorption and desorption profiles of the films following exposure at the 0-90-0-90-0% RH cycle are

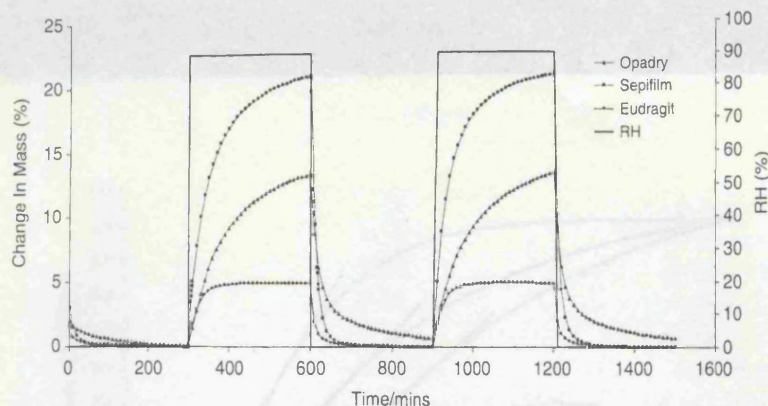


FIGURE 1 Moisture Sorption Profiles After Exposure to 0-90-0-90-0% RH Holding at Each Stage for 300 min at 25°C for Cast Films.

shown in Fig. 1. Data for the mean moisture uptake or loss, $M_{(t)}$ at 0-90-0-90-0% RH, 0-75-0-75-0% RH, and 0-50-0-50-0% RH is summarized in Table 2. These values were calculated from the weight, $W_{(t)}$, recorded at time $t=600$ min or 1200 min and the weight, $W_{(d)}$, of the dried sample at time $t=300$ min, 900 min, or 1500 min (refer to Eq. 2):

$$M_{(t)} = W_{(t)} - W_{(d)} / W_{(d)} \times 100 \quad (2)$$

The results show that Eudragit has the fastest equilibration and sorbs only a limited amount of moisture. Sepifilm has the fastest sorption and takes up the greatest amount of moisture but does not reach equilibrium within the experimental time. The rate of sorption for Opadry is similar to that of Eudragit, but Opadry continues to sorb moisture for a longer period and is not at equilibrium when the sorption process is stopped.

Desorption from the Eudragit film appears to be equal and opposite to the sorption response, with very rapid equilibration to the dry state. Sepifilm shows very rapid desorption, equilibrating to the dry state

much more rapidly than during sorption. The behavior of Opadry films is quite different with desorption seeming to be a two-step kinetic processes, a rapid event followed by a very slow desorption resulting in incomplete moisture loss. Although Sepifilm is the most hygroscopic film (presumably due to the hydrophilic nature of the hypromellose and microcrystalline cellulose), it loses moisture much more easily than it gains.

Sorption and Desorption Kinetics

The kinetics of sorption or desorption in polymer coatings are commonly interpreted in terms of the diffusion coefficient which characterizes the rate of diffusion of penetrant molecules in the polymer (Debeaufort et al., 1994; Ruthven, 2004; Vieth & Sladek, 1965). Crank (1968) proposed a model for calculating diffusion coefficients in polymer films. This model is basically a differential solution to Fick's second law applied to a homogenous film with a

TABLE 2 Amount of Moisture [$M_{(t)}$] Sorbed or Desorbed by Eudragit L30, Opadry AMB and Sepifilm LP Cast Films Following Exposure to 0-50-0-50-0% RH, 0-75-0-75-0% RH, and 0-90-0-90-0% RH Cycles

RH cycle/coating	$M_{(t)}$ (std. dev)		
	Eudragit L 30	Opadry AMB	Sepifilm LP
0-50	1.26 (0.0035)	1.96 (0.058)	4.59 (0.011)
50-0	1.26 (0.001)	1.79 (0.020)	4.59 (0.020)
0-75	2.74 (0.004)	5.46 (0.010)	9.17 (0.015)
75-0	2.74 (0.031)	4.55 (0.020)	9.17 (0.007)
0-90	4.90 (0.015)	12.26 (0.012)	21.84 (0.014)
90-0	4.87 (0.010)	10.43 (0.020)	21.85 (0.233)

Values (% dry basis) computed from means of both cycles for $n=3$ runs.

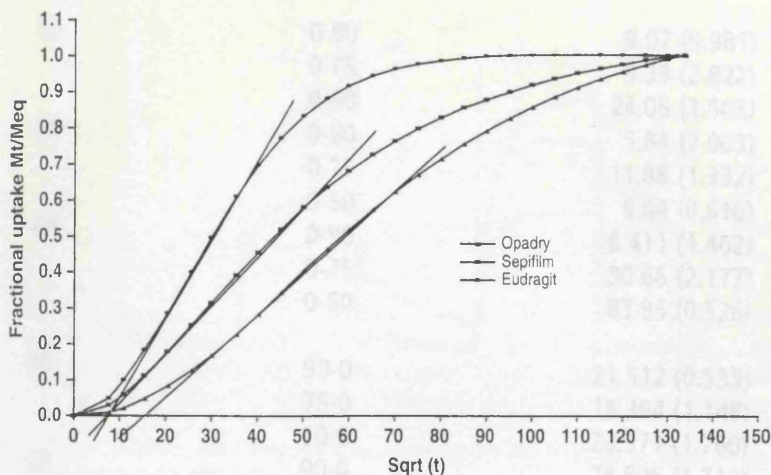


FIGURE 2 Fractional Uptake, $M(t)/M_{(eq)}$ Versus Square Root of Time Plot Showing the Kinetics of Moisture Sorption for Cast Films at 0-90% RH Gradient.

constant diffusion coefficient. The simplified form of this model is as follows:

$$M(t)/M_{(eq)} = 4(Dt/\pi L^2)^{1/2} \quad (3)$$

where $M(t)$ is the moisture uptake at time, t (s), and $M_{(eq)}$ is the uptake at saturation for a film of thickness L , with diffusion coefficient D (cm^2/s) subjected to a step change in surface concentration of permeant (e.g., a change in RH). A plot of the fractional uptake, $M(t)/M_{(eq)}$ versus $(t)^{1/2}$ is initially linear but levels off as $M(t)/M_{(eq)}$ approaches 1. Kinetics such as these are known as Fickian. The coefficient D is calculated from the gradient of the linear portion of the curve, i.e., $D = \pi S^2 L^2 / 4$.

Figures 2 and 3 show the fractional uptake versus the square root of time plots for sorption and

desorption at the 0-90% RH and 90-0% RH gradients (for 0-90-0-90-0% RH cycle). The plots show sigmoidal curvature and are consistent with published reports for other polymer systems displaying the so-called non-Fickian kinetics (Debeaufort et al., 1994; Vieth & Sladek, 1965). In Fig. 2, sorption curves are displaced towards the time coordinate and are consistently below the corresponding desorption curves (Fig. 3) indicating significantly higher desorption rates in the films. Although the sorption profile (in Fig. 1) shows that Sepifilm has the fastest sorption rates and the highest moisture uptake, the kinetics plot indicates that overall, Eudragit has the fastest kinetics. The kinetics for Opadry suggest significantly slower sorption and desorption processes pointing to a possible slowing up of the diffusion process by this film.

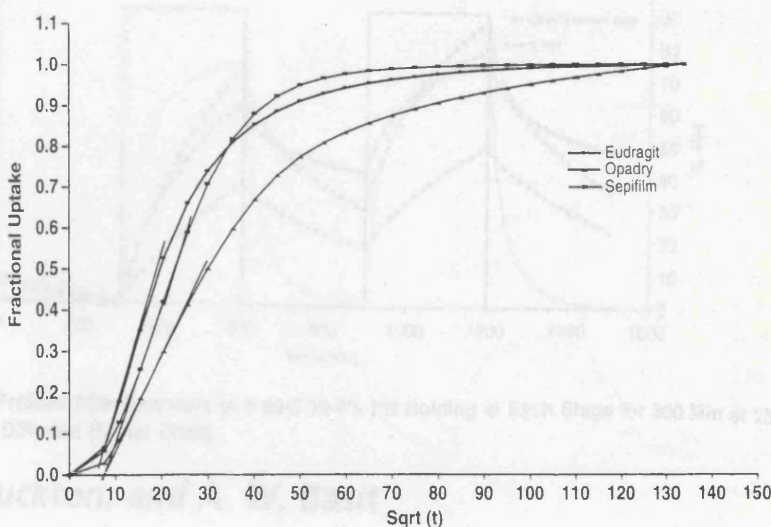


FIGURE 3 Fractional Uptake, $M(t)/M_{(eq)}$ Versus Square Root of Time Plot Showing the Kinetics of Moisture Desorption for Cast Films at 90-0% RH Gradient.

TABLE 3 Diffusion Coefficients, D (cm/s) of Cast Films for Sorption and Desorption Cycles Following Exposure to 0-50-0-50-0% RH, 0-75-0-75-0% RH, and 0-90-0-90-0% RH

Polymer	Thickness L (μm)	% RH gradient	D ($\times 10^{-8}$) cm/s (std. dev)	R^2
<i>Sorption</i>				
Eudragit L	50	0-90	9.07 (0.981)	0.995
		0-75	9.33 (2.022)	0.991
		0-50	24.05 (3.505)	0.987
Opadry	80	0-90	5.84 (2.003)	0.986
		0-75	11.88 (1.332)	0.985
		0-50	5.64 (0.616)	0.989
Sepifilm	60	0-90	6.411 (1.462)	0.994
		0-75	30.66 (2.177)	0.993
		0-50	83.95 (0.526)	0.988
<i>Desorption</i>				
Eudragit L	50	90-0	21.512 (0.535)	0.975
		75-0	15.394 (1.148)	0.986
		50-0	23.371 (1.760)	0.997
Opadry	80	90-0	24.606 (1.712)	0.978
		75-0	15.284 (0.524)	0.999
		50-0	66.380 (0.589)	0.996
Sepifilm	60	90-0	50.990 (0.534)	0.999
		75-0	76.454 (0.603)	0.988
		50-0	108.950 (0.585)	0.977

Film thickness approximated to the nearest decimal. R^2 shown for fitted and experimental values between $0.1 \geq M_t/M_\infty \leq 0.6$.

Values of D obtained from a least squares line of best fit for $0.1 \geq M_t/M_\infty \leq 0.5$ are tabulated in Table 3. The data corroborate well with the interpretation above. It is apparent that D increases with RH but not by a big magnitude suggesting that D is not strongly dependent on the amount of moisture in the films. When the kinetics are Fickian, diffusion is the rate limiting step as the rate of diffusion is slower than the rate of polymer chain relaxation (Rodríguez et al., 2003; Ruthven, 2004).

The corresponding diffusion coefficient is proportional to the concentration of moisture. However, when the kinetics of sorption are also influenced by rate of relaxation of polymer chains in response to the presence of moisture, the amount sorbed or desorbed increases gradually with time, resulting in apparent slow kinetics. The latter scenario might be the reason for the observed trends in the diffusion coefficients, but given the limited information at our disposal, it is impossible to make firm conclusions

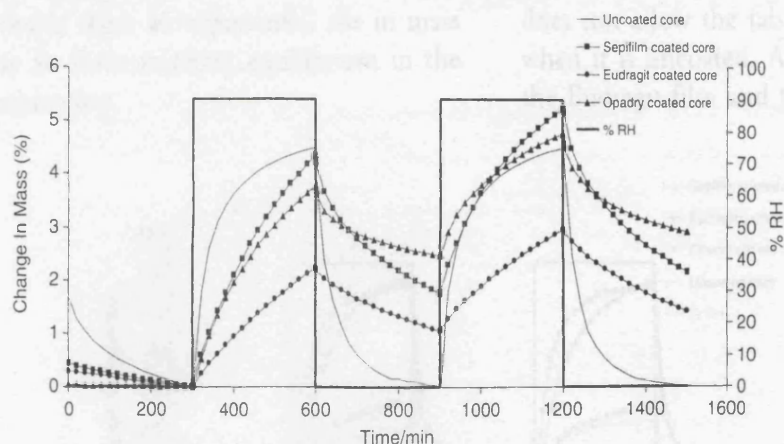


FIGURE 4 Moisture Sorption Profiles After Exposure to 0-90-0-90-0% RH Holding at Each Stage for 300 Min at 25°C for Hygroscopic Cores Without Coating and With Different Barrier Coats.

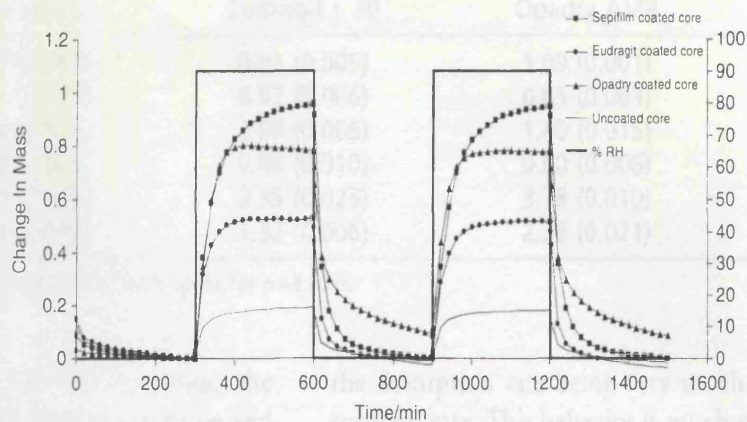


FIGURE 5 Moisture Sorption Profiles After Exposure to 0-90-0-90-0% RH Holding at Each Stage for 300 Min at 25°C for Low Hygroscopic Cores Without Coating and With Different Barrier Coats.

on the behavior of the films at this juncture without further investigations.

Moisture Sorption by Coated and Uncoated Tablet Cores

The data for moisture sorption to the different tablet cores at 0-90-0-90-0% RH cycle are shown in Figs. 4, 5, and 6. Data at other RH cycles is summarized in Tables 4, 5, and 6. It is clear that the nature of the tablet core has a substantial influence on the extent of moisture sorption. Uncoated and coated hygroscopic cores sorb more moisture than the uncoated and coated waxy cores which in turn have some differences over the sorption to the uncoated and coated low hygroscopic cores. Uncoated hygroscopic cores clearly show an exponential rise in mass uptake and are far from reaching equilibrium in the 300 min exposure time.

The desorption cycle of uncoated hygroscopic core shows a return to the original dry mass. For coated hygroscopic cores, the second exposure to RH results in more uptake than the first. It is not clear whether this is a function of the core or the barrier coating. In any case, it may be that following contact with moisture during the first sorption cycle barrier integrity is somewhat compromised. This might result in more moisture reaching the cores. Alternatively, the hygroscopicity of the films might be increasing as a result of moisture destroying polymer crystallinity.

Coating of the hygroscopic cores with Eudragit results in a reduction of total moisture sorbed, clearly due to a change in sorption kinetics. The Eudragit free film itself rapidly established an equilibrium mass gain and then rapidly desorbed moisture on drying. The coating on the tablet however, results in a system that does not allow the tablet to equilibrate as rapidly as when it is uncoated. Also, despite the fact that both the Eudragit film and the tablet core are able to lose

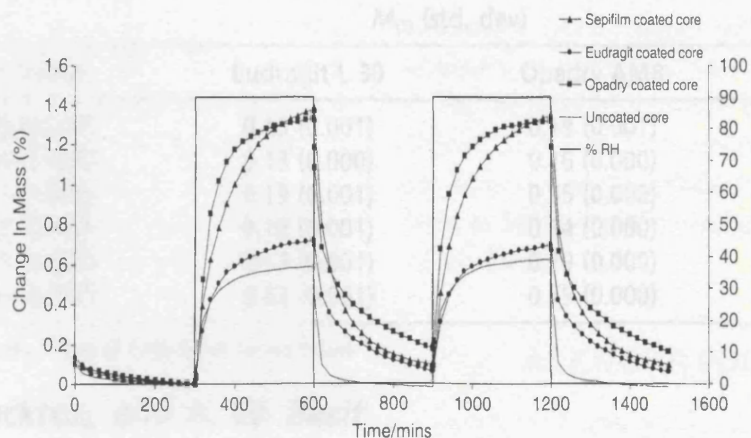


FIGURE 6 Moisture Sorption Profiles After Exposure to 0-90-0-90-0% RH Holding at Each Stage for 300 Min at 25°C for Waxy Cores Without Coating and With Different Barrier Coats.

TABLE 4 Amount of Moisture [$M_{(t)}$] Sorbed or Desorbed by Uncoated and Coated Hygroscopic Tablet Cores Following Exposure to 0-50-0-50-0% RH, 0-75-0-75-0% RH, and 0-90-0-90-0% RH Cycles

RH cycle/core	$M_{(t)}$ (std. dev)			
	Uncoated	Eudragit L 30	Opadry AMB	Sepifilm LP
0-50%	1.57 (0.010)	0.91 (0.005)	1.09 (0.001)	1.21 (0.006)
50-0%	1.57 (0.011)	0.57 (0.006)	0.85 (0.003)	0.98 (0.006)
0-75%	2.40 (0.021)	1.00 (0.066)	1.40 (0.015)	2.17 (0.000)
75-0%	2.40 (0.023)	0.69 (0.010)	0.60 (0.006)	1.47 (0.001)
0-90%	0.25 (0.006)	2.35 (0.025)	3.78 (0.010)	3.56 (0.012)
90-0%	4.25 (0.003)	1.32 (0.006)	2.36 (0.021)	2.56 (0.005)

Values (% dry basis) computed from means of both cycles for $n=3$ runs.

moisture completely during desorption cycles, the Eudragit coated tablet does not. Both the sorption and desorption are pseudo zero order kinetic processes, but with much faster rate of sorption than desorption. Presumably the slower desorption relates to the geometry of the diffusion path which is a typical cause of hysteresis.

For Sepifilm coated hygroscopic cores, the process again failed to reach equilibrium and showed substantial hysteresis, such that desorption did not complete in the 300 min window. The total mass of moisture sorbed was slightly less than that sorbed by the uncoated cores, but much more than could possibly be accommodated in the film (total uptake for the cast film was $\approx 21\%$, which for a 3% coating on the tablet cores would accommodate $21 \times 3/100 = 0.63\%$). Consequently (assuming the retention of moisture in the film to be similar to that seen with cast films), the mass of moisture transferring to the tablet core is greater for this coat.

The Opadry film, which has already shown a tendency to retain moisture during desorption, shows a somewhat similar pattern for coated cores but with

the desorption rate being very much different to the sorption rate. This behavior is much more extreme for the coated hygroscopic tablets. In the first sorption process, 3.7% moisture was sorbed (the mass expected to be accommodated in the film if it behaved as a free film would be $13 \times 4/100 = 0.52\%$). Interestingly, this is approximately the mass that was desorbed rapidly at the start of the first desorption cycle. It is possible, therefore, that the mass of moisture that is transferred remains in the tablet core, whereas that in the film desorbs again. The second sorption process results in much less moisture uptake than the first, as if the process were moving toward a pseudo-equilibrium state. The quantity of moisture desorbed after the second sorption process is greater than that for the first, indicating a greater mass of moisture that is situated near the surface in an environment from which desorption is easy.

The extent of sorption to the cores with low hygroscopicity (Fig. 5) is much less than for the hygroscopic cores (Fig. 4). The data for the low hygroscopicity are close to being a sum of the mass of moisture that is sorbed by the uncoated core and the mass that is

TABLE 5 Amount of Moisture [$M_{(t)}$] Sorbed or Desorbed by Uncoated and Coated Low Hygroscopic Tablet Cores Following Exposure to 0-50-0-50-0% RH, 0-75-0-75-0% RH, and 0-90-0-90-0% RH Cycles

RH cycle/core	$M_{(t)}$ (std. dev)			
	Uncoated	Eudragit L 30	Opadry AMB	Sepifilm LP
0-50%	0.08 (0.001)	0.13 (0.001)	0.19 (0.001)	0.27 (0.003)
50-0%	0.08 (0.006)	0.13 (0.000)	0.16 (0.000)	0.26 (0.002)
0-75%	0.11 (0.006)	0.19 (0.001)	0.35 (0.000)	0.26 (0.009)
75-0%	0.12 (0.000)	0.18 (0.001)	0.14 (0.000)	0.27 (0.003)
0-90%	0.19 (0.006)	0.53 (0.001)	0.79 (0.000)	0.95 (0.009)
90-0%	0.19 (0.000)	0.53 (0.001)	0.69 (0.000)	0.27 (0.003)

Values (% dry basis) computed from means of both cycles for $n=3$ runs.

TABLE 6 Amount of Moisture [$M(t)$] Sorbed or Desorbed by Uncoated and Coated Waxy Tablet Cores Following Exposure to 0-50-0-50-0% RH, 0-75-0-75-0% RH, and 0-90-0-90-0% RH Cycles

RH cycle/core	$M(t)$ (std. dev)			
	Uncoated	Eudragit L 30	Opadry AMB	Sepifilm LP
0-50%	0.23 (0.003)	0.25 (0.001)	0.33 (0.001)	0.38 (0.006)
50-0%	0.19 (0.001)	0.25 (0.000)	0.30 (0.005)	0.36 (0.002)
0-75%	0.37 (0.018)	0.40 (0.01)	0.52 (0.023)	0.75 (0.005)
75-0%	0.35 (0.002)	0.40 (0.012)	0.14 (0.011)	0.75 (0.006)
0-90%	0.63 (0.017)	0.71 (0.010)	1.32 (0.018)	1.36 (0.011)
90-0%	0.58 (0.030)	0.65 (0.013)	1.10 (0.027)	0.65 (0.020)

Values (% dry basis) computed from means of both cycles for $n=3$ runs.

taken up by the free film (refer to the previous example above for this mass corrected to tablet weight gain of coat). For example, the Sepifilm coat is expected to take up ca 0.63%, the core 0.2%, and the Sepifilm coated core takes up 0.9% (which is close to expected given the inevitable differences between the coat on the tablet and the cast film; Fig. 1). Equally, the Opadry coated low hygroscopic cores have a mass gain that is only slightly above that which would be expected from the sum of uptakes on the uncoated core and the cast film. The coated low hygroscopic cores all lose their mass in a similar way to that seen for the cast films, with only the Opadry coated sample retaining moisture in a similar way to Opadry free film (Fig. 1). It is reasonable to assume that the coatings on low hygroscopic cores perform in a similar way to free films, with little sign of excess moisture transfer to the cores, but equally with little sign of protection to the core over that seen for the uncoated tablets.

The data for the waxy cores (Fig. 6) are interesting in comparison to Figs. 4 and 5. For instance, the difference between the uncoated sample and the Eudragit coated core is smaller than that seen for the low hygroscopic cores (Fig. 5). The Sepifilm coated samples show a displacement above the core mass uptake that is in keeping with the data in Fig. 5 and which would indicate that the response here is a sum of the moisture held in the film (ca that expected from the cast film results) and the mass of moisture taken up by the uncoated core. As previously, there is modest accumulation of moisture in the Opadry coat.

The data for the low hygroscopic and waxy cores indicate that there is no real benefit of using a moisture barrier for these formulations, as the final result is essentially a sum of the mass of moisture that

would be expected to be taken up by the free film and the uncoated tablets. For the hygroscopic cores, all of the coats did limit the total mass of moisture in the system in comparison with the uncoated cores. Eudragit was the most effective coating for limiting moisture sorption but equally the most effective in limiting desorption from the core, which could be a disadvantage.

CONCLUSIONS

Moisture-barrier film coatings slowed moisture sorption into hygroscopic tablet cores. However, the extent and rate of moisture sorption was influenced by the tablet core formulation and there was no discernible benefit for cores which sorbed limited mass of moisture when uncoated.

On the basis of the amount of moisture sorbed, Sepifilm and Opadry films were more hygroscopic than the Eudragit film. The moisture sorption-desorption behavior of the films was very complex, and films exhibited different rates and extents of sorption and desorption. The Opadry film showed a tendency to retain moisture within the film which was attributed to a high moisture binding capacity.

The benefits of moisture barrier films, in terms of rate and extent of moisture transfer from an environment with abundant water vapor, would seem to be limited to formulations with hygroscopic tablet cores.

ACKNOWLEDGMENTS

Enosh Mwesigwa would like to acknowledge the financial support from the Commonwealth Scholarship Commission of the United Kingdom.

REFERENCES

- Ahnebeck, C., & Zografi, G. (1990). The molecular basis of the effects of moisture on the physical and chemical stability of drugs in the solid state. *International Journal of Pharmaceutics*, 62, 87–95.
- Allinson, J. G., Dausereau, R. J., & Sakr, A. (2001). The effects of packaging on the stability of a moisture sensitive compound. *International Journal of Pharmaceutics*, 221, 49–56.
- Alvarez-Lorenzo, C., Gomez-Amoza, J. L., Martinez-Pacheco, R., Conde, S., & Concheiro, A. (2000). Interactions between hydroxypropylcelluloses and vapour/liquid water. *European Journal of Pharmaceutics and Biopharmaceutics*, 50, 307–318.
- Begren, M. S. (1994). An automated controlled atmosphere microbalance for the measurement of moisture sorption. *International Journal of Pharmaceutics*, 103, 103–114.
- Carstensen, J. T. (1993). *Pharmaceutical Principles of Solid Dosage Forms*. Lancaster, PA: Technomic, 180.
- Cervera, F. M., Karjalainen, M., Airaksinen, S., Rantanen, J., Krogars, K., Heinamaki, J., Colarte, A. I., & Yliruusi, J. (2004). Physical stability and moisture sorption of aqueous chitosan-amylose starch films plasticized with polyols. *European Journal of Pharmaceutics and Biopharmaceutics*, 58, 69–76.
- Crank, J. (1968). *The Mathematics of Diffusion* (2nd Ed.). Oxford: Clarendon Press.
- Debeaufort, F., Voilley, A., & Meares, P. (1994). Water vapor permeability and diffusivity through methylcellulose edible films. *Journal of Membrane Science*, 91, 125–133.
- Lane, R. A., & Buckton, G. (2000). The novel combination of dynamic vapor sorption gravimetric analysis and near infra-red spectroscopy as a hyphenated technique. *International Journal of Pharmaceutics*, 207, 49–56.
- Morillon, V., Debeaufort, F., Blond, G., & Voilley, A. (2000). Temperature influence on moisture transfer through synthetic films. *Journal of Membrane Science*, 168, 223–231.
- Prinderre, P., Cauture, E., Piccerelle, Ph., Kalantzis, G., Kaloustian, J., & Joachim, J. (1997). Evaluation of some protective agents on stability and controlled release of oral pharmaceutical forms by fluid bed technique. *Drug Development and Industrial Pharmacy*, 23, 817–826.
- Rodriguez, O., Fornasiero, F., Arce, A., Radke, C. J., & Prausnitz, J. M. (2003). Solubilities and diffusivities of water vapor in poly(methylmethacrylate), poly(2-hydroxyethylmethacrylate), poly(N-vinyl-2-pyrrolidone) and poly(acrylonitrile). *Polymer*, 44, 6323–6333.
- Rohm GmbH (1965). Rapidly disintegrating coatings with Eudragit L30 D-55 from aqueous dispersions. Applications Technology Sheet. No. 1.5, 2001, Rohm GmbH, Chemische Fabrik, D-64275 Darmstadt, Germany.
- Ruthven, D. M. (2004). Sorption kinetics for diffusion-controlled systems with a strongly concentration-dependent diffusivity. *Chemical Engineering Science*, 59, 4531–4545.
- Vieth, W. R., & Sladek, K. J. (1965). A model for diffusion in a glassy polymer. *Journal of Colloid Science*, 20, 1014.
- Zografi, G., & Hancock, B. C. (1994). Water-solid interactions in pharmaceutical systems. In: D. J. A. Crommelin, K. K. Midha, T. Nagai (Eds.), *Topics in Pharmaceutical Sciences*. Stuttgart: Medpharm Scientific Publishers, 405–419.